5-2012

# Time Dependence of Bathymetric Effects on Hurricane Storm Surge

Christopher Dupuis

**Time Dependence of Bathymetric Effects on Hurricane Storm Surge**

By

Christopher Dupuis

A Thesis Presented to

The LSU Honors College

In Partial Fulfillment

Of the Requirements

For the Degree of

**Bachelor of Science**

in

**Physics**

Louisiana State University

May 2012

# Table of Contents

# INTRODUCTION

Hurricanes have long been one of the most destructive natural disasters known to society, and the storm surge generated often causes the most damage and loss of life out of several processes involved. Storm surges have been blamed for 90% of the fatalities caused by hurricanes in the United States as recently as 1973 (AMS 1973). In November 1970, a cyclone struck Bangladesh, creating a surge that killed approximately 300,000 (Dube 1997). More recently, Cyclone Nargis (2008) left at least 130,000 dead in Myanmar, although the death toll is thought to be underestimated. Over 80% of the deaths were attributed to the storm surge (Webster 2008). In the United States, Hurricane Katrina (2005) caused an estimated $81 billion in damage and 1833 deaths, mostly due to the flooding of New Orleans and coastal Mississippi (Knabb et al. 2006). In recent times, technology has improved enough to allow for relatively accurate forecasting of hurricane paths and intensities. Models such as ADCIRC (Luettich et al. 1992) and SLOSH (Jelesnianski et al. 1992) generate models of storm surge that have proven to be effective. Most studies, however, only focus on individual storms or theory, and do not give a broad, empirical overview of storm surge.

Furthermore, there are two paradigms in producing storm surge models. The first calls for as much accuracy as possible, and the second seeks to produce reasonably accurate metrics that can be calculated quickly with easy-to-measure parameters, and with as few variables as necessary. It is with the latter perspective in mind that I propose to investigate the amount of time before peak storm surge that gives the strongest correlation with bathymetry.

A secondary goal is to determine the strength of the correlation between the length of time spent over shallow water versus maximum storm tide, and to determine what ocean depth constitutes "shallow water." This will empirically confirm or deny the assertion that wind stress effects are dominant in water depths less than 40m (Signorini 1992). Along with this, it would be important to determine where these effects are occurring in relation to the storm center.

## Storm Surge Variables

There are several parameters that define a storm surge. Before attempting to find a temporal dependence on bathymetry, it is important to know the relative importance of the various mechanisms involved in creating the surge. Of course, this will depend on many factors and varies by the individual storm and local features, however, it is possible to get an idea of how much of the storm surge is caused by bathymetric effects. Most studies focus on the maximum storm surge height. However, it is important to recognize that storm surges vary significantly in spatial and temporal scopes, as well as peakedness in those domains.

Harris (1963) provides an early attempt at elucidating these variables, identifying five distinct processes: the pressure effect, the direct wind stress effect, the Coriolis effect, wave run-up, and the rainfall effect.

In a steady state, i.e., a situation where the pressure is not rapidly changing, lower pressures will cause the ocean surface to rise. This is known as the inverse barometer effect or the pressure set-up. Harris gives a theoretical relation of a 1cm rise in ocean level per 1mbar drop in atmospheric pressure. This effect operates under the condition that water is able to flow freely, which implies that there should be few obstructions to flow, such as shallow bathymetry or chokepoints (Harris 1963). The effect is most noticeable over the open ocean at depths greater than 40m, since water is able to flow more freely, and since the wind set-up has little effect at these depths (Signorini 1992). While this effect will

not cause a significant rise in sea level in bays, the pressure effect can cause a significant rise in estuaries (Harris 1963).

The direct wind effect, also known as the wind set-up, as conceived by Harris, includes both wind stress effects and bathymetric effects. Wind stress causes the largest rise in sea level at roughly the radius of maximum winds to the right of the storm's forward motion. The storm's angle of approach to the coast also has an influence (Signorini 1992; Weisberg 2006). However, angles within 20 degrees counterclockwise of shore-normal are known to be indistinguishable as far as influence on storm surge (Jelesnianski 1972 via Signorini 1992).

Jordan and Clayson (2008) used a version of the Princeton Ocean Model to determine that the relationship between storm surge ($\eta$) and wind speed ($v$) at the ocean surface is $\eta \propto v^{1.63}$, which they found was not appreciably different from using $\eta \propto v^2$. The power law $\eta \propto v^{1.63}$ was to found to correlate best when using the non-dimensionalized approximation $\eta \propto (v_{landfall}/v_0)^{1.63}$, where $v_0$ is arbitrarily defined as 33m/s, the threshold of hurricane-force winds (Kantha 2006). However, this approximation correlates best when using an average of wind speeds at 6, 12, 18, and 24 hours before landfall, or just using the wind speed at 12h instead of using $v_{landfall}$ (Jordan and Clayson 2008). This suggests that there is a lag between the intensity predictor and storm surge, i.e., an oceanic response time.

Stress at the ocean floor is also an important variable, and is often accounted for in two-dimensional models by a parameterization. This variable is usually included within the wind set-up. The mechanism proposed is that hurricane-induced current at the surface is balanced by a similar current in the opposite direction over deeper water (Rappaport and Fernandez-Partagas 1995). However, as it approaches the shore, shallow bathymetry and barriers (i.e., land) cause this mechanism to break down. The combined effects of friction at the bottom and shear stress from the top (Rappaport and Fernandez-Partagas 1995) cause the return current to slow down, stop, or reverse, resulting in a build-up of water. This is largely responsible for the oceanic response time mentioned above.

It is well known now that wind stress effects have the greatest influence on surges from hurricanes that traverse a gently sloping bathymetry. Walton and Dean (2009) demonstrated that for several transects of the Florida coastline, bathymetry can, in theory, cause the storm surge to vary over an order of magnitude for the same wind speed, depending on whether there is a steep or mild slope near shore. The distance a hurricane travels over the continental shelf was found to be correlated to storm surge height, as long as the water is shallow (Signorini 1992). For storms with large enough forward speeds, the timescale for translation is shorter than the timescale for the surge set up, and the storm surge will not reach its potential (Weisberg 2006). However, Rego and Li (2009) found a significant positive correlation between forward speed and maximum storm surge. Therefore, there is a forward speed that is ideal for surge generation. While increasing forward speeds generate increasing peak storm surges, it also has the effect of reducing the affected area (Rego and Li 2009). Additionally, fast-moving storms do not have time to build up water in bays or estuaries, so it will impact open coast more. Slower moving storms can inundate bays and estuaries, but lack the extra power from forward speed.

Chen (2008) suggests that the bathymetry around Hurricane Katrina's (2005) path was the primary mechanism responsible for the record 9m storm surge. When overlaying Katrina's intensity data with the path of Hurricane Frederick (1979), the hypothetical storm surge came out to be about 3.5m, comparable to Hurricane Ivan's (2004) surge of 3m (Chen 2008). Additionally, it was found that replacing the submerged deltaic lobes traversed by Katrina with a wide, sloping continental shelf caused the hypothetical storm surge to decrease to 5m.

According to Weaver and Slinn (2010), hurricanes themselves can alter bathymetry, which can cause small local variations. However, even local sea floor perturbations of ±20% alter the surge less

than ±5%, and mostly less than ±2%. Therefore, the effects of local sea floor variations from the currently known values are not likely to contribute a large error to calculations.

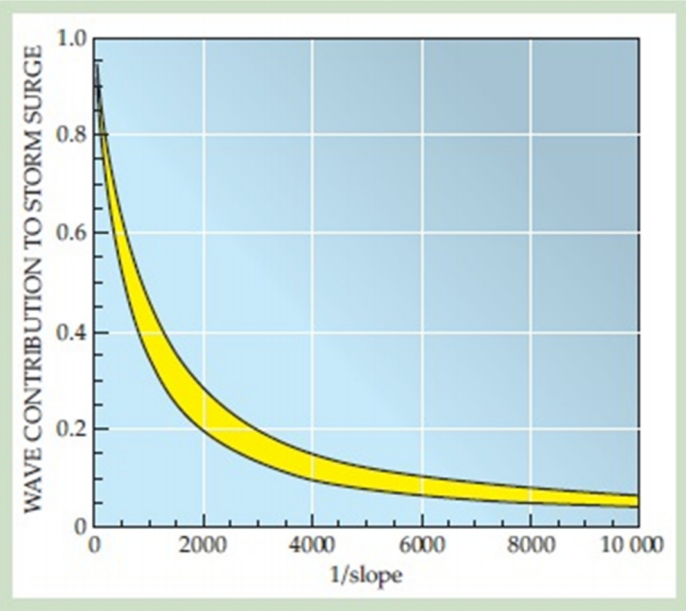


**Figure 1: The effect of wave shoaling on wave set up as a function of sea floor gradient (Resio and Westerink, 2008).**

Wave effects are an important part of storm surge, and can have a significant effect on the water level recorded (Granthem 1953). Wave shoaling causes a trade-off between wave heights and the wind stress component of storm surge. Steeper gradients near the shore result in larger waves and smaller storm surges, and milder gradients give the opposite effect (Resio and Westerink 2008). When one wave breaks on the shore, the water is often caught by another wave before it can return to sea, causing the water level to rise, and can easily account for 1m of surge, and possibly more under favorable conditions (Harris 1963). This is known as the wave set up. If the waves break at an angle, the wave set up will be smaller. The critical angle for the sea floor slope is about 30 degrees (Granthem 1953). This means that any other slope will produce smaller wave run-ups, and since sea shores are generally less inclined than 30 degrees, increased slope will generally increase the wave run-up and decrease the wind stress contribution.

Storm size is a recently recognized variable that is also included in the wind set up. It has significantly improved storm surge models since it was recognized as an important variable (Irish et al. 2008). Combined, the wind set up and wave set up account for 75-90% of storm surge on most mildly sloping portions of the US East and Gulf Coasts' continental shelves (Walton and Dean 2009). The Coriolis effect can have some influence over storm surge. In this situation, the wind stress causes an Ekman layer, which results in a bulk transport of water at a 90 degree angle to the right of the wind (in the northern hemisphere). This results in higher storm surges for coasts located to the right of the wind direction and lower surges for coasts to the left (Harris 1963). The last mechanism proposed by Harris is the rainfall effect. As sea level rises near the coast, the excess rain on land can pile up in the river bed as long as the flow gradient is onshore.

Though it is commonly cited from a US Army Corps of Engineers report that storm surge is attenuated 1m per 14.5km of marsh, there was significant variability in the study, with acceptable values ranging from 1m per 20km up to 1m per 7km (USACE 1963 via DiLiberto 2009). Later, it was reported that wetlands may actually have no influence at all in certain situations. The real effect is therefore complicated, but can be modeled with ADCIRC.

The mixing layer depth appears to have a significant effect on storm surge. Extending the layer from 10m to 50m results in a 13% decrease of maximum surface currents (Signorini 1992), which would reduce the ability of storm surges to form. Effectively, the momentum is being transferred downward instead of laterally.

## Numerical Models

**Table 1: Variables involved in storm surge and storm surge models**

| *Variable* | *Description* |
|---|---|
| $\eta$ | Average deviation of water level from mean |
| $\tau_s$ | Surface (wind) stress |
| $\tau_{bx}, \tau_{by}$ | Bottom stress; $\tau_{bx} = \bar{u}\tau_*$, $\tau_{by} = \bar{v}\tau_*$ |
| $\tau_*$ | $\tau_* = \frac{C_f(\bar{u}^2+\bar{v}^2)^{\frac{1}{2}}}{H}$ (Chezy's formula; Dawson et al., 2011) |
| $C_f$ | bottom drag coefficient |
| $h$ | Mean water depth (bathymetry) |
| $H$ | Actual water depth; $H = \eta + h$ |
| $W$ | Continental shelf width |
| $\vec{u}$ | Velocity vector |
| $\overleftrightarrow{T}$ | Stress tensor |
| $\vec{F}$ | Net external force |
| $\bar{u}, \bar{v}$ | Depth-averaged velocity |
| $f$ | Coriolis parameter ($f = 2\Omega \sin(\varphi)$) (where $\varphi$ is latitude) |
| $P_s$ | Sea surface pressure |
| $\rho_0$ | Reference density of water |
| $M_x, M_y$ | Horizontal momentum diffusion components |
| $E$ | Wave energy density |
| $N$ | Wave action density |
| $\sigma$ | Intrinsic angular frequency (relative frequency as observed in a frame of reference moving with the current velocity (Booij et al., 1999) |
| $\theta$ | Propagation direction of each wave component |
| $k$ | Wave number |
| $C_{gx}, C_{gy}, C_{g\sigma}, C_{g\theta}$ | Speeds of energy propagation in $x$, $y$, $\sigma$, or $\theta$ space, respectively |
| $H_m$ | Maximum wave height |
| $\gamma$ | Breaker parameter (can be constant or a function of the bottom slope, depending on model; Booij et al., 1999) |

The 2-dimensional shallow water equations are derived from the continuity and Navier-Stokes equations to model waves at depths less than about 100m (Harris 1963). They are given as

$$\frac{\partial \rho}{\partial t} + \nabla \cdot (\rho \vec{u}) = 0$$

$$\rho\left(\frac{\partial \vec{u}}{\partial t} + \vec{u} \cdot \nabla \vec{u}\right) = -\nabla P + \nabla \cdot \overleftrightarrow{T} + \vec{F}$$

respectively. The continuity equation describe the conservation of mass in fluids, while the Navier-Stokes equation describes the conservation of momentum

In shallow water, the continuity equation reduces to:

$$\frac{\partial H}{\partial t}+\frac{\partial(H\bar{u})}{\partial x}+\frac{\partial(H\bar{v})}{\partial y}=0$$

while the momentum equations reduce to the following two equations:

$$\frac{\partial(H\bar{u})}{\partial t}+\frac{\partial(H\bar{u}^2)}{\partial x}+\frac{\partial(H\bar{u}\bar{v})}{\partial y}=-gH\frac{\partial\eta}{\partial x}+\frac{\tau_{sx}-\tau_{bx}+F_x}{\rho}$$

$$\frac{\partial(H\bar{v})}{\partial t}+\frac{\partial(H\bar{u}\bar{v})}{\partial x}+\frac{\partial(H\bar{v}^2)}{\partial y}=-gH\frac{\partial\eta}{\partial y}+\frac{\tau_{sy}-\tau_{by}+F_y}{\rho}$$

For a region of ocean characterized by an onshore bathymetric profile with few changes in the cross-shore dimension, the $\partial/\partial y$ terms from the momentum equations will be small. Neglecting terms for momentum transport and pressure set up, the first momentum equation reduces to (Signorini 1992)

$$\frac{\partial\eta}{\partial x}=\frac{\tau_s+\tau_b}{\rho g h}$$

Since the $y$-dependence has already been neglected, $\partial\eta/\partial x$ can be approximated with the total derivative $d\eta/dx$. Although $h$ is highly dependent on $x$, treating it as a constant and assuming no bottom friction results in $\eta \propto (\tau_s/gh)W$ (Resio and Westerink 2008). Though this proportionality is oversimplified, it does illustrate the relationship between surge height, ocean depth, and continental shelf width.

The shallow water equations are employed in the ADCIRC model with some simplifications (Chen 2008):

$$\frac{\partial\eta}{\partial t}+\frac{\partial(H\bar{u})}{\partial x}+\frac{\partial(H\bar{v})}{\partial y}=0$$

$$\frac{\partial\bar{u}}{\partial t}+\bar{u}\frac{\partial\bar{u}}{\partial x}+\bar{v}\frac{\partial\bar{u}}{\partial y}-f\bar{v}=-\frac{\partial\left(\frac{P_s}{\rho_0}+g\eta\right)}{\partial x}+\frac{\tau_{sx}-\tau_{bx}}{\rho_0 H}+M_x$$

$$\frac{\partial\bar{v}}{\partial t}+\bar{u}\frac{\partial\bar{v}}{\partial x}+\bar{v}\frac{\partial\bar{v}}{\partial y}-f\bar{u}=-\frac{\partial\left(\frac{P_s}{\rho_0}+g\eta\right)}{\partial y}+\frac{\tau_{sy}-\tau_{by}}{\rho_0 H}+M_y$$

By the definition of $H$, the ADCIRC equations implicitly depend on bathymetry.

The SPLASH (Special Program to List the Amplitudes of Surges from Hurricanes) model is generally regarded as obsolete, and has effectively been replaced by the SLOSH model, which uses governing equations similar to the ones used in ADCIRC. The SPLASH model used a simple scheme for representing bathymetric parameters, the nomograph for bathymetry:

$$Storm\ Surge(US\ Gulf\ Coast)=S_pF_gF_m$$
$$Storm\ Surge(US\ East\ Coast)=S_pF_eF_m$$

where $S_p$ is the preliminary maximum surge height, $F_g$ and $F_e$ are shoaling parameters for the US Gulf and East Coasts, respectively, and $F_m$ is a factor representing direction of approach (Jelesnianski 1972 via Walton and Dean 2009). This metric accounts for about 72% of the variance in storm surges (Jelesnianski 1972).

The SWAN (Simulating Waves Nearshore) model is often coupled with ADCIRC to accurately model effects from wave generation, propagation, and dissipation (Chen 2008). This model is fairly complex, and contains dependencies on $h$ in numerous governing equations.

The spectral action balance equation is given by

$$\frac{\partial N}{\partial T}+\frac{\partial(c_x N)}{\partial x}+\frac{\partial\left(c_y N\right)}{\partial y}+\frac{\partial(c_\sigma N)}{\partial \sigma}+\frac{\partial(c_\theta N)}{\partial \theta}=\frac{S}{\sigma}$$

where the c constants are implicitly dependent on bathymetry. The wind input equation is the sole source of wave action.

$$S_{in}(\sigma,\theta)=A+BE(\sigma,\theta)$$

where A depends on wave frequency and direction, and B depends on wind speed and direction.

There are three ways energy is dissipated in the SWAN model: whitecapping, bottom friction, and depth induced wave breaking. The whitecapping equation is given as

$$S_{ds,w}(\sigma,\theta)=-\Gamma\bar{\sigma}\frac{k}{\bar{k}}E(\sigma,\theta)$$

where $\Gamma$ is a wave steepness dependent coefficient. Bottom friction is given as

$$S_{ds,b}(\sigma,\theta)=-C_{bottom}\frac{\sigma}{g^2\sinh^2(kh)}E(\sigma,\theta)$$

where $C_{bottom}$ is a bottom friction coefficient, which can be determined empirically or numerically. Since there is no basis to give preference to a certain field, the SWAN model uses simple models based on each. For the empirical part, $C_{bottom}=0.038\ \mathrm{m^2/s^3}$ for swell conditions and $C_{bottom}=0.067\ \mathrm{m^2/s^3}$ for wind-generated wave conditions (Booij et al. 1999). The numerical part uses equations from a drag law model ($C_{bottom}=C_f g u_{rms}$) and an eddy-viscosity model ($C_{bottom}=f_w g u_{rms}/\sqrt{2}$) where $C_f$ and $f_w$ are constants (Booij et al., 1999).

The depth induced wave breaking is much more convoluted, and the wave action term is given by

$$S_{ds,br}(\sigma,\theta)=-\frac{1}{4}\frac{E(\sigma,\theta)}{E_{tot}}Q_b\left(\frac{\sigma}{2\pi}\right)H_m^2$$

where $H_m=\gamma d$ and $Q_b$ is determined by the transcendental equation

$$\frac{1-Q_b}{lnQ_b}=-8\frac{E_{tot}}{H_m^2}$$

In addition to wave energy balance equations, SWAN also models non-linear wave-wave interactions. Quadruplet wave-wave interactions are predominant in domains with deep water, while triad wave-wave interactions predominate in shallow water. Quadruplet wave-wave interactions shift wave energy away from the spectral peak. Since white capping dissipates energy, this effectively shifts

the spectral peak downward. Triad wave-wave interaction transfer energy from lower frequencies to higher frequencies, and in the parameterization used in SWAN, it has complex, nested dependencies on $h$.

# METHOD

The information from SURGEDAT offers an aggregated set of information on storm tide heights and locations (Needham, *personal communication*, 2012). Though there is information present for many parts of the globe, relatively complete coverage is limited to the Gulf of Mexico, and therefore has the least selection bias. To correlate these storm tide data with bathymetry, though, a bathymetric map is necessary.

A variety of different bathymetry data sets exist, as well as a number of applications to process them. Therefore, it is important to understand the pros and cons of the available data products. The foremost concerns should be the region the grid covers, its resolution, and spacing. The region of study is between approximately 32°N and 19.5°N, and 99°W and 76°W. There are numerous maps available, and enough gridded data that it is only important to mention the best candidates for use with the proposed analyses.

The standard grids for global coverage include ETOPO1 (Amante and Eakins 2009), GEBCO, SRTM30_PLUS (Becker et al. 2009), and GMRT (Ryan et al. 2009). The first three have equal grid spacing of 1 arcminute, 1 arcminute or 30 arcseconds, and 30 arcseconds respectively. GMRT by its nature has variable grid spacing, but for coastal areas, it can be accurate to within 100km in certain areas. The output is a list of equally spaced coordinate pairs and ocean depths, arranged primarily in order of decreasing latitude, and secondarily in order of decreasing west longitude.

For the Gulf Coast of the US, the US Coastal Relief Model Grids provide resolution down to 3 arcseconds, and can be easily generated using the NOAA's GEODAS Grid Translator. However, this map only covers the region of interest down to 24N, so it would make sense to split the region between two maps. This complicates computing unnecessarily, so I opted to use the SRTM30_PLUS for most of the graphs, since it offers good resolution, and the maps can be made easily at http://topex.ucsd.edu/cgi-bin/get_srtm30.cgi. To ensure that there were no serious anomalies due to map issues, I used ETOPO1, GMRT, and SRTM30 and attained similar statistics for each. The SRTM30 graphs appear to have less scatter, which should be expected with higher resolution.

Data for storm tides and storm tracks were derived from SURGEDAT and HURDAT (Needham, *personal communication*, 2012; Jarvinen et al. 1984). Since the data includes storm tide rather than storm surge, a large error is introduced, depending on the relative heights of the tide and the storm surge. Storm tracks are estimated by determining the coordinates of the hurricane center at the time when the peak surge occurred (called "landfall" for the purposes of this study), and for each three hour interval before then, up to 36h before landfall. These coordinate pairs can be used to find an ocean depth in the bathymetry file.

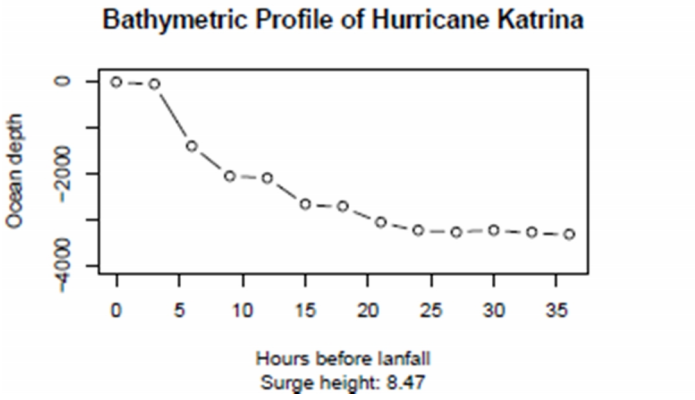


**Figure 2: Bathymetric profile of Hurricane Katrina (2008), the largest recorded surge in the data set**

Not all storms are over the Gulf of Mexico for the entire 36h window, so missing values are used for the program. This may be due to a storm entering the Gulf of Mexico from another area, or forming within 36h of landfall. Additionally, the maximum storm surge is commonly cited as 40-50km from the center (Hsu 1998; Kerr 2000; Schwerdt 1979)

I compiled a list of the coordinates from the bathymetry file closest to where the storm's coordinates were given in Hal's data by using a binary search algorithm on the unique values for latitudes and longitudes to find the closest coordinates to the actual storm center. The resulting coordinate pair can be used to find the ocean depth in the bathymetry file. Since the resolution of the bathymetry map is under a kilometer at most, this approximation does not introduce much error.

A simple correction was applied by shifting them 98km due east, which was derived a posteriori. found to give the optimal correlation between time over water less than 40m deep and surge height. I used roughly this approximation at first by mistake, since the literature cites radii of 40-50km, however, the results of a grid search in terms of radius justified the correction mentioned above, rather than the one commonly cited. The bathymetry at those points is then decided to be the ocean depth for a given storm at a given time before landfall. The resulting bathymetry table can be applied in several different ways.

The Pearson correlation coefficient ($r$) was employed for all the statistical analyses, and is defined as

$$r = \frac{1}{n-1}\sum_{i=1}^{n}\left(\frac{X_i - \bar{X}}{s_x}\right)\left(\frac{Y_i - \bar{Y}}{s_y}\right)$$

where $X_i$ is a given value from a set, $\bar{X}$ is the sample mean, $s_x$ is the standard deviation, and similarly for the $Y$ variables. An algorithm for this can be found in the R "stats" package. The variance ($r^2$) is usually understood as the percentage of the total variation that can be explained by the correlation. These correlations are designated "significant" if the probability of obtaining the correlation from random data (the p-value) falls below a certain threshold, usually given as $p < 0.05$ or $p < 0.01$. For the purposes of this study, $p < 0.05$ is designated significant, and many of the graphs have red lines to demarcate this value. It is important to note that smaller sample sizes increase the threshold for the correlation to be significant, as demonstrated in Figure 2.

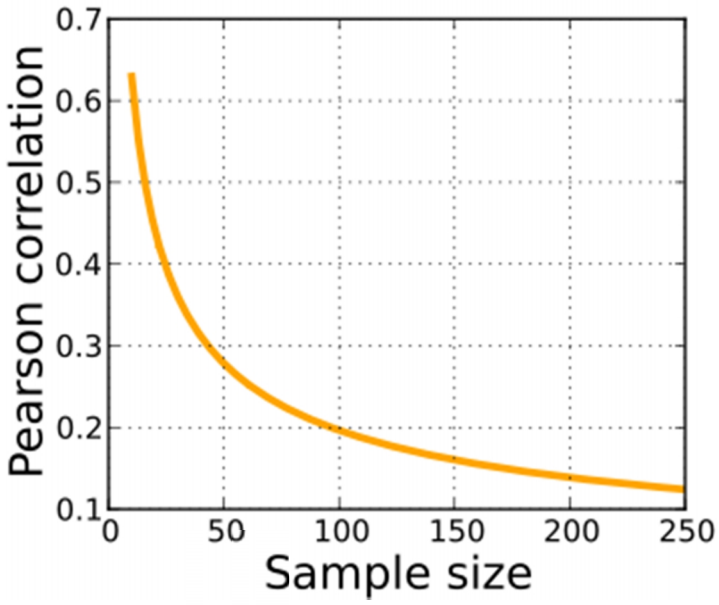


**Figure 3: Graph of $p = 0.05$. Adapted from: Skbkekas. *File:Correlation Significance.svg*. Digital image. *Wikipedia*. 15 Feb. 2010. Web. 8 May 2012. <http://en.wikipedia.org/wiki/File:Correlation_significance.svg>.**

The ocean depths for the various surge events were correlated with the maximum storm tide heights. To gain a better understanding of which storms contribute to the correlations the most, I implemented low- and high-pass filters to sequentially remove high and low surge events from analysis, respectively. Sample sizes are not necessarily the same for each time interval, and in general, the sample size decreases with increasing time interval, as should be expected.

The amount of time the storm tide spent over various ocean depths was estimated. I iteratively defined cutoff depths of 1m to 100m spaced at 1m intervals. This domain was chosen because 100m depths mark the boundary between shallow and deep water (Harris 1963). The time was found by

interpolating each storm's bathymetry data to find the first time it rose above the cutoff depth. For each cutoff depth, I found the Pearson correlation coefficient and p-values for time spent over shallow water versus the maximum storm tide.

# RESULTS

## Optimal time interval

The filtered data can be viewed in two different ways: by holding the storm count at landfall constant for varying time intervals, or by holding the time interval constant while varying the storm count. These approaches reveal two different patterns, and it is therefore important to consider both aspects.

For the high-pass filter for constant storm count, the strongest correlations generally occurred when the 89 highest surge events were analyzed. Statistically significant ($p < .05$) correlations between bathymetry and storm tide were found for all time intervals from 3h to 18h before landfall at the 95% confidence level. The strongest significant correlation occurred at 9h with 46 surge events included ($r = -0.3906, p = 0.0004$). Holding the time interval constant reveals that the P-values at 9h remain consistently significant for more selective filters than other intervals, for all filters using 46 or more surge events, although the 6h P-values are nearly as consistent.

Using a low-pass filter reveals that the strong 6h, 9h, and 12h correlations seen in the high-pass filter are only present in the least filtered analyses. However, there are statistically significant correlations at 18h and 21h for more selective filters than at other intervals. The 21h correlations are not consistent, so these may need further investigation. This effect is not as strong as the high-pass filter for 9h, and is present for most filters using 91 or more storms.

## Optimal cutoff depth

For the shelf, although the correlations for depths shallower than 15m (except for 7m) are not statistically significant, there is a noticeable trend of strengthening correlations from that cutoff depth to approximately 40m. The decreased statistical significance for shallower depths is caused by the lower sample sizes available to each analysis.

Though I mistakenly used an initial radius of 90km when doing this calculation when the literature usually claims a maximum wind radius of 40-50km, the data suggests that this value is not far from where it should be. After discovering this discrepancy, I created graphs to determine what the optimal radius and angle should be. Since hurricanes rotate counterclockwise in the northern

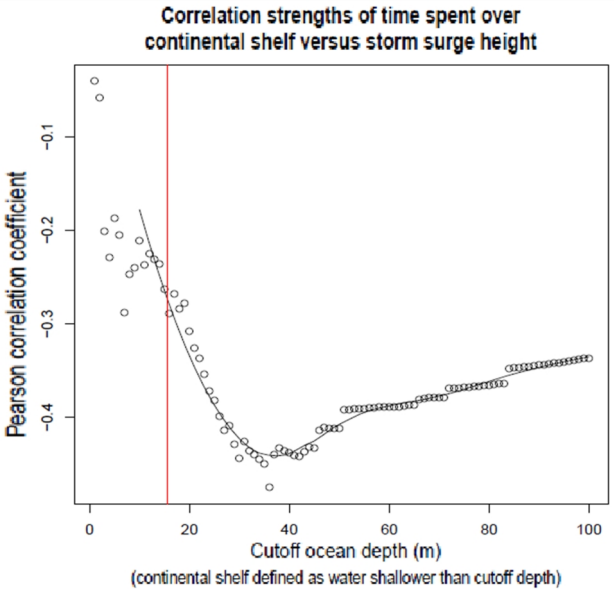


**Figure 4: Optimal cutoff depth at 98km due east of the average storm center**

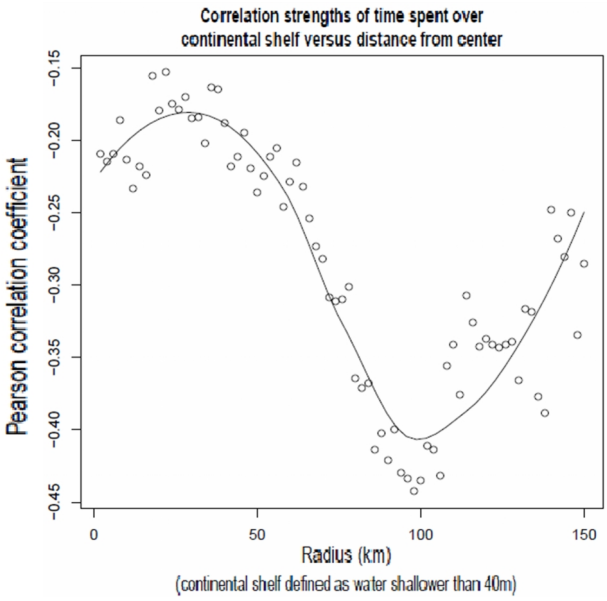


**Figure 5: Optimal radius for 40m cutoff depth and due east**

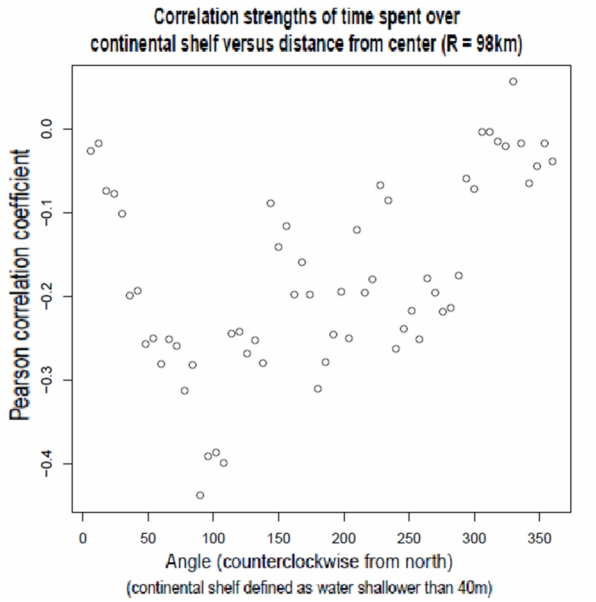


**Figure 6: Optimal angle for 40m cutoff depth at 98km from storm center**

hemisphere, there is an additive interference between forward speed and the hurricane's winds directly to the right of the direction of forward motion. Since hurricanes in the region of interest generally have a northern trajectory due to hurricane recurve, the optimal angle should be due east (90°). Radii were incremented in 2km intervals, and angles in 6° intervals clockwise from north. The cutoff depth was set at 40m, and the correlation between time spent over the continental shelf and maximum storm tide height were graphed by radius and angle. The optimal position for a cutoff depth of 40m appears to be at 98km and 90°, so there appears to be no angular discrepancy. Due to computing constraints, a grid search of radius and angle would be impractical at the moment, but dithering in the region reveals that this feature is locally stable, showing up in a more or less diminished form between about 80-130km and 80°-100°.

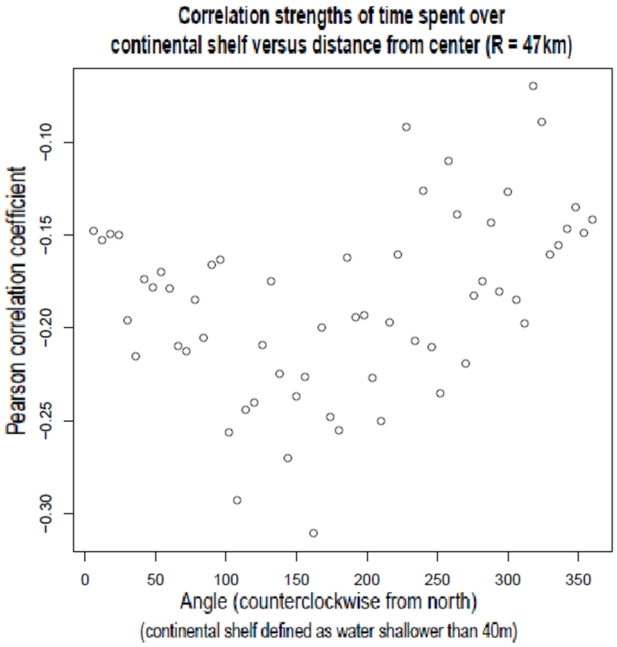


**Figure 7: Optimal angle for 40m cutoff depth at 47km from storm center**

Using grids with 30 arcsecond spacing proved to reduce scatter in the cutoff depth plot relative to grids with 1 arcminute spacing, while grids with 1 arcminute spacing appear to have a similar amount of scatter by inspection. Regardless of the map however, the peak at roughly R=98km remains.

# CONCLUSIONS

Using the storm surges rather than storm tides would result in stronger correlations than the ones presented herein, since tides introduce a large amount of noise.

The strongest correlation for cutoff depth ($r = -0.474683$, $p = .000008$) occurred at the 36m level, along with the lowest p-value. Using greater depths result in weaker correlations and higher p-values, implying that the storm tide's correlation with ocean depth is fully accounted for at approximately 40m. This corroborates Signorini's (1992) assertion that the pressure set up is most noticeable at depths of 40m or greater. Therefore, ocean depths less than about 40m contribute to the storm tide while ocean depths greater than 40m do not.

Using a radius of 98km yields the strongest correlations for bathymetric effects on storm tide. It is commonly stated (e.g., Masters 2012) that the maximum storm surge generally coincides with the radius of maximum wind, which is generally understood to be 40-50km on average.

Although the data set includes storms of various intensities, and the intensities themselves vary over time, this should still be cause for concern. It is well known that the hurricane's barometric pressure is lowest in the eye, therefore, the pressure set up is highest at the center of the storm. It may be that the bathymetric effect is counterweighted to some extent by the pressure set up. Additionally, there may be a sampling bias, since storms in the area of interest are often mature, possibly becoming extratropical, and may have larger eyes than a random sample.

Alternatively, the radius of maximum bathymetric effects may simply not coincide with the radius of maximum surge. The only conceivable explanation is that there is a net radial transport of water towards the center of the storm—which is heavily influenced by bathymetry—and this is more important than the bathymetry at the radius of maximum surge. This result warrants further investigation.

# SOURCES


AMS 1973: Policy statement on hurricanes by the American Meteorological Society. *Bull. Amer. Meteor. Soc.*, 54: 46-47.

Booij, N., R.C. Ris, and L.H. Holthuijsen. (1999). A third-generation wave model for coastal regions. Part 1, model description and validation. *Journal Geophysical Research* 104C4: 7649–7666.

Chen, Q., L. Wang, R. Tawes, (2008): Hydrodynamic response of northeastern Gulf of Mexico to hurricanes. *Estuaries and Coasts*, 31, 1098-1116.

Corps of Engineers, US Army Engineer District, New Orleans, Interim Survey Report, Morgan City, Louisiana and Vicinity, serial no. 63, US Army Engineer District, New Orleans, LA (November 1963).

Dawson, Clint, et al., (2011): Discontinuous Galerkin methods for modeling Hurricane storm surge. *Advances in Water Resources*, 34(9): pp. 1165-1176

DiLiberto, Tom. "Verification of a Storm Surge Modeling System for the New York City – Long Island Region." Thesis. Stony Brook University, 2009. Web. 8 Mar. 2012.

Dube, S.K., A.D. Rao, P.C. Sinha, T.S. Murty, N. Bahulayan, (1997): Storm surge in the Bay of Bengal and Arabian Sea: The problem and its prediction. *Mausam*, 48, 283-304.

Harris, L.D., (1963): Characteristics of the Hurricane Storm Surge. U.S. Weather Bureau, *Technical Paper No. 48.*

Hsu, S.A. and Z. Yan, (1998): A Note on the Radius of Maximum Wind for Hurricanes. *Journal of Coastal Research,* 14(2), 667-668

Irish, J.L., D.T. Resio, J.J. Ratcliff (2008): The influence of storm size on hurricane surge, *JOURNAL OF PHYSICAL OCEANOGRAPHY* Volume: 38 Issue: 9 Pages: 2003-2013

Jarvinen, B. R., C. J. Neumann, and M. A. S. Davis, (1984): A tropical cyclone data tape for the North Atlantic Basin, 1886-1983: Contents, limitations, and uses. NOAA Technical Memorandum NWS NHC 22, Coral Gables, Florida, 21 pp.

Jelesnianski, C. P. (1972): SPLASH (Special Program to List Amplitudes of Surges From Hurricanes) I. Landfall Storms. U.S. Department of Commerce, *NOAA Technical Memorandum NWS TDL-46*, Rockville, MD.

Jelesnianski, C. P., J. Chen, and W. A. Shaffer, (1992): SLOSH: Sea, lake, and overland surges from hurricanes. NOAA Technical Report NWS 48, National Oceanic and Atmospheric Administration, U. S. Department of Commerce, 71 pp.

Jordan II, M.R., and C.A. Clayson, (2008): A new approach to using wind speed for prediction of tropical cyclone generated storm surge. *Geophysical Research Letters*, 35, article number: L13802.

Kantha, L. H. (2006), Time to replace the Saffir-Simpson hurricane scale?, Eos Trans. AGU, 87, 3–6.

Kerr, A.M. (2000): Discussion of: Hsu, S.A. and Yan, Z. 1998. A Note on the Radius of Maximum Wind for Hurricanes. *Journal of Coastal Research*, 14(2), 667-668: *Journal of Coastal Research,* 16(2), 494-495

Knabb, R.D., J.R. Rhome, D.P. Brown, 2006: National Hurricane Center Tropical Cyclone Report on Hurricane Katrina. Published on the Web at: http://www.nhc.noaa.gov/pdf/TCR-AL122005_Katrina.pdf

Liaw, Andy. "[R] Pearson Corelation and P-value for Matrix." Letter to John Fox. 18 Apr. 2005. Web. 8 May 2012. <https://stat.ethz.ch/pipermail/r-help/2005-April/069743.html>.

Luettich, R.A., J.J. Westerink, and N.W. Scheffner (1992): ADCIRC: an advanced three-dimensional circulation model for shelves, coasts and estuaries. Report 1: Theory and Methodology of ADCIRC-2DDI & ADCIRC-3DL. Technical Rep., DRP-92-6, U.S. Army Corps of Engineers.

Masters, Jeffrey. "Characteristics of Storm Surges." *Storm Surge Characteristics*. Web. 09 May 2012. <http://www.wunderground.com/hurricane/surge_characteristics.asp>.

Needham, Hal, and Barry D. Keim (2011). Storm Surge: Physical Processes and an Impact Scale, Recent Hurricane Research - Climate, Dynamics, and Societal Impacts, Prof. Anthony Lupo (Ed.), ISBN: 978-953-307-238-8, InTech, Available from: http://www.intechopen.com/books/recent-hurricane-research-climate-dynamics-and-societal-impacts/storm-surge-physical-processes-and-an-impact-scale

Needham, Hal. *SURGEDAT*. Southern Climate Impacts Planning Program. Web. 08 May 2012. <http://surge.srcc.lsu.edu/>.

R Development Core Team (2012). R: A language and environment for statistical computing. R Foundation for Statistical Computing, Vienna, Austria. ISBN 3-900051-07-0, URL http://www.R-project.org/

Rappaport, E.N, and J.J. Fernandez-Partagas, (1995): The deadliest Atlantic tropical cyclones, 1492-1994. *NOAA Technical Memorandum NWS NHC-47*, National Hurricane Center, 41 pp.

Rego, J. L., and C. Li (2009): On theimportance of the forward speed of hurricanes in storm surge forecasting: A numerical study. *Geophys. Res. Lett.*, 36

Resio, D. T., and J. J. Westerink, (2008): Hurricanes and the Physics of Surges. *Physics Today*, **61**, 33-38.

Ryan, W. B. F., et al. (2009), Global Multi-Resolution Topography synthesis, Geochem. Geophys. Geosyst., 10, Q03014, doi:10.1029/2008GC002332.

Schwerdt, R.W., F.P. Ho, and R.R. Watkins, (1979): Meteorological criteria for standard project hurricane and probable maximum hurricane windfields, Gulf and east coasts of the United States. *NOAA Technical Report NWS 23*, pp1-315.

Signorini, J. S., J. S. Wei, and C. D. Miller, Feb. (1992): Hurricane-Induced Surge and Currents on the Texas-Louisiana Shelf. *J. Geophys. Res.*, **97**, 2229-2242.

Walton, Todd L. Jr., and Robert G. Dean (2009): Influence of Florida Bathymetry on Wind Stress Component of Storm Surge. *Coastal Engineering Journal*, 51(4), 297-308.

Weaver, R.J., and D.N. Slinn (2010): Influence of bathymetric fluctuations on coastal storm surge, *Coastal Engineering*, 57(1), 62-70

Webster, P. J., 2008: Myanmar's deadly daffodil. *Nat. Geosci.*, 1, 488–490.

Weisberg, Robert H., and Lianyuan Zheng: (2006) Hurricane storm surge simulations for Tampa Bay. *Estuaries and Coasts*, 29(6A), 899–913

## Data References

Amante, C. and B. W. Eakins, ETOPO1 1 Arc-Minute Global Relief Model: Procedures, Data Sources and Analysis. NOAA Technical Memorandum NESDIS NGDC-24, 19 pp, March 2009

The GEBCO_08 Grid, http://www.gebco.net/

Becker, J. J., D. T. Sandwell, W. H. F. Smith, J. Braud, B. Binder, J. Depner, D. Fabre, J. Factor, S. Ingalls, S-H. Kim, R. Ladner, K. Marks, S. Nelson, A. Pharaoh, R. Trimmer, J. Von Rosenberg, G. Wallace, P. Weatherall., Global Bathymetry and Elevation Data at 30 Arc Seconds Resolution: SRTM30_PLUS, Marine Geodesy, 32:4, 355-371, 2009

NOAA National Geophysical Data Center, U.S. Coastal Relief Model, http://www.ngdc.noaa.gov/mgg/coastal/crm.html

Ryan, W.B.F., S.M. Carbotte, J.O. Coplan, S. O'Hara, A. Melkonian, R. Arko, R.A. Weissel, V. Ferrini, A. Goodwillie, F. Nitsche, J. Bonczkowski, and R. Zemsky (2009), Global Multi-Resolution Topography synthesis, Geochem. Geophys. Geosyst., 10, Q03014, doi:10.1029/2008GC002332

# GRAPHS

- Bathymetric profiles of all storms in data set, except Hurricane Katrina(see *Figure 2*)
- High-pass statistics by number of storms in sample
- High-pass statistics by time interval
- Low-pass statistics by time interval
- Optimal cutoff depth graph at 98km and 90$^{o}$, with statistics (same as *Figure 4*)
- Cutoff depth graphs at 95km and 90$^{o}$, using different maps (ETOPO1, GMRT, and SRMT30, respectively)

# BATHYMETRY PROFILES

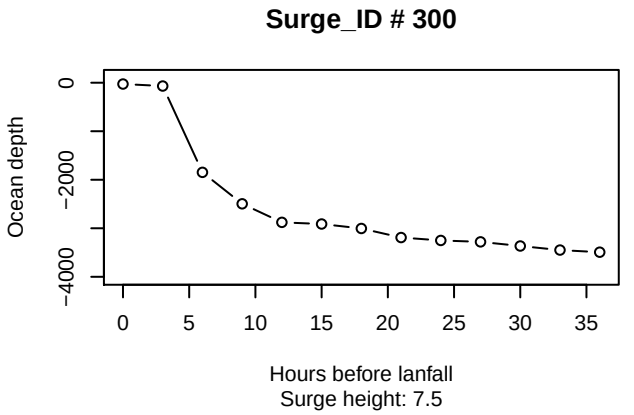
Surge_ID # 300
Ocean depth
0
−2000
−4000
0
5
10
15
20
25
30
35
Hours before lanfall
Surge height: 7.5

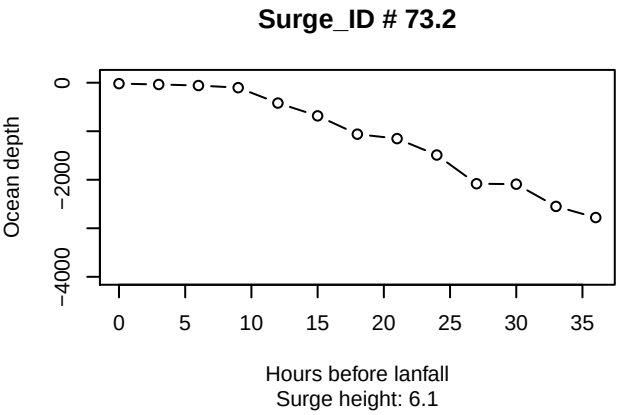
Surge_ID # 73.2
Ocean depth
0
−2000
−4000
0
5
10
15
20
25
30
35
Hours before lanfall
Surge height: 6.1

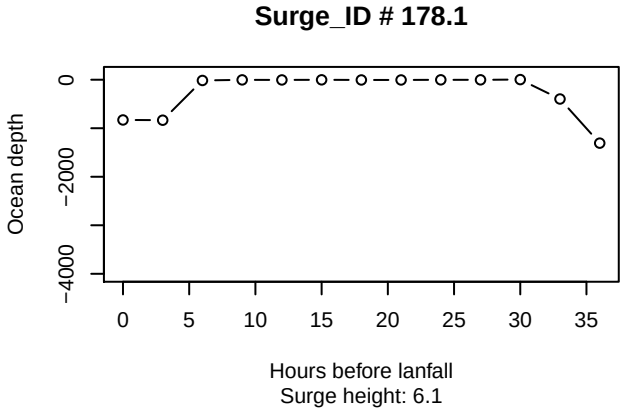
Surge_ID # 178.1
Ocean depth
0
−2000
−4000
0
5
10
15
20
25
30
35
Hours before lanfall
Surge height: 6.1

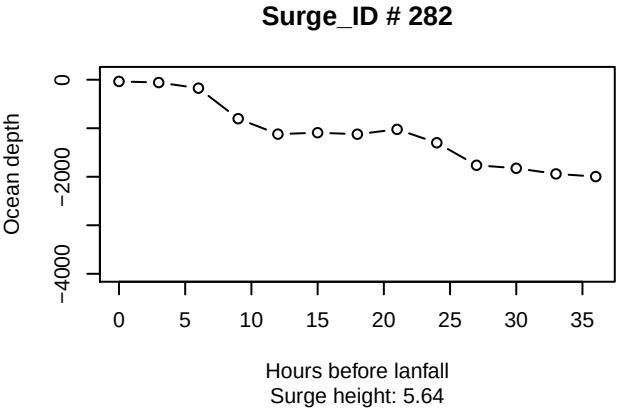
Surge_ID # 282
Ocean depth
0
−2000
−4000
0
5
10
15
20
25
30
35
Hours before lanfall
Surge height: 5.64

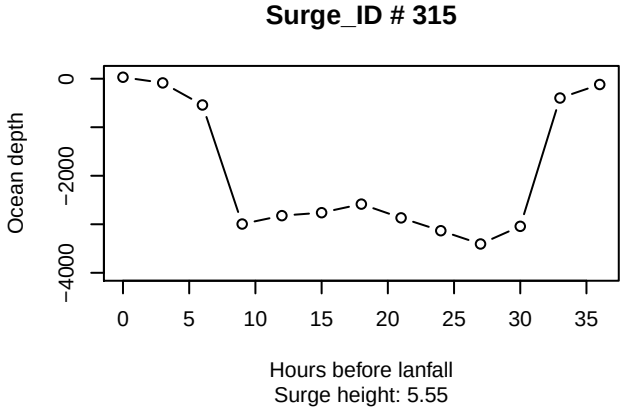
Surge_ID # 315
Ocean depth
0
−2000
−4000
0
5
10
15
20
25
30
35
Hours before lanfall
Surge height: 5.55

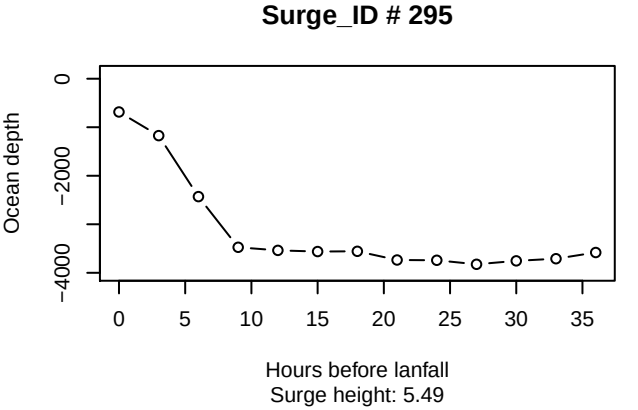
Surge_ID # 295
Ocean depth
0
−2000
−4000
0
5
10
15
20
25
30
35
Hours before lanfall
Surge height: 5.49

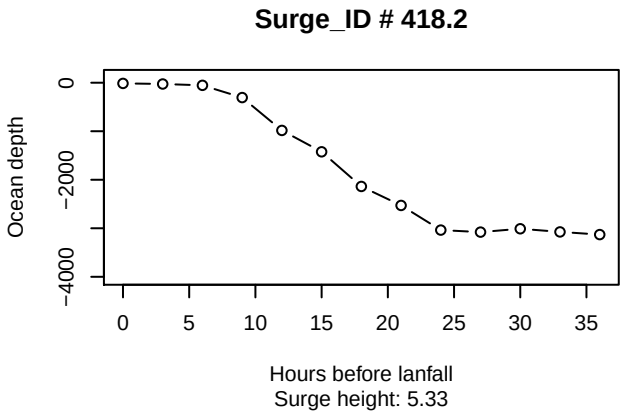
Surge_ID # 418.2
Ocean depth
0
−2000
−4000
0 5 10 15 20 25 30 35
Hours before lanfall
Surge height: 5.33

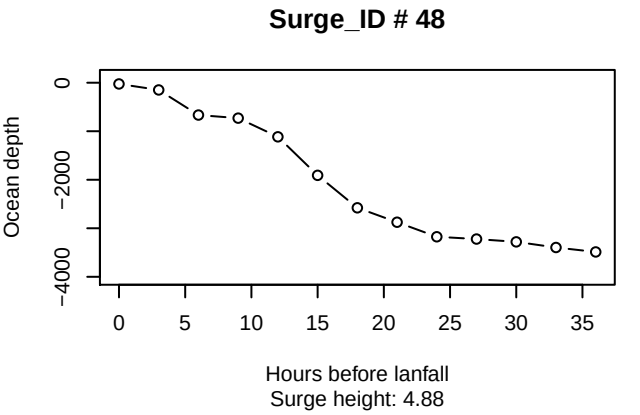
Surge_ID # 48
Ocean depth
0
−2000
−4000
0 5 10 15 20 25 30 35
Hours before lanfall
Surge height: 4.88

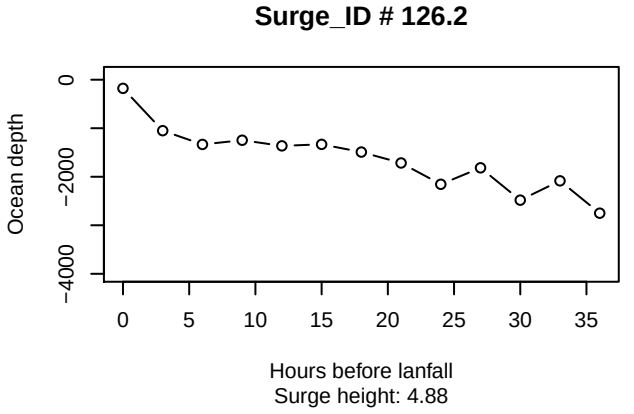
Surge_ID # 126.2
Ocean depth
0
−2000
−4000
0 5 10 15 20 25 30 35
Hours before lanfall
Surge height: 4.88

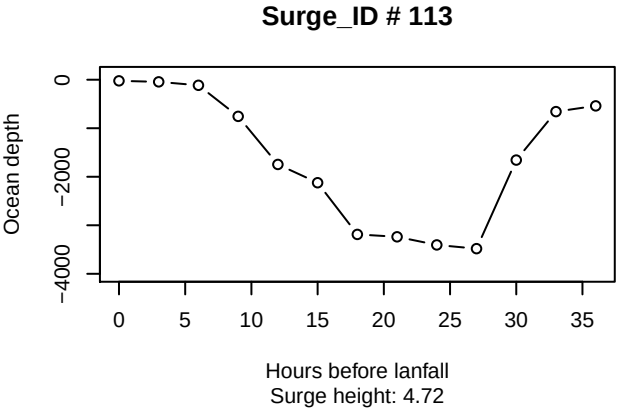
Surge_ID # 113
Ocean depth
0
−2000
−4000
0 5 10 15 20 25 30 35
Hours before lanfall
Surge height: 4.72

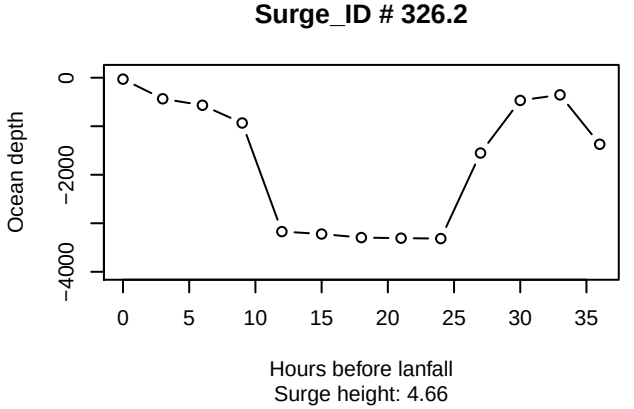
Surge_ID # 326.2
Ocean depth
0
−2000
−4000
0 5 10 15 20 25 30 35
Hours before lanfall
Surge height: 4.66

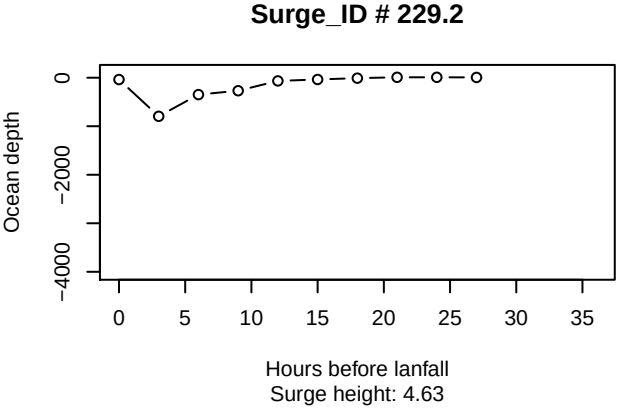
Surge_ID # 229.2
Ocean depth
0
−2000
−4000
0 5 10 15 20 25 30 35
Hours before lanfall
Surge height: 4.63

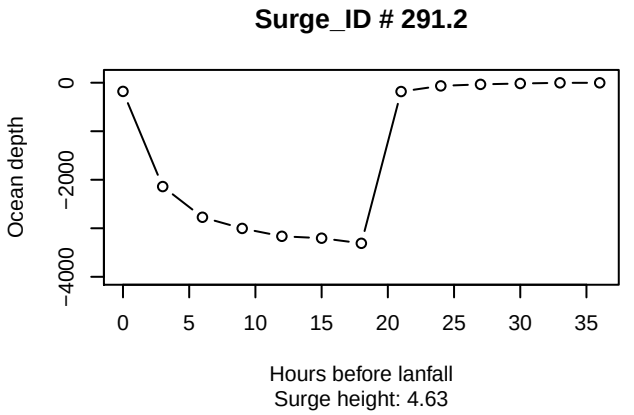
Surge_ID # 291.2
Ocean depth
0
−2000
−4000
0 5 10 15 20 25 30 35
Hours before lanfall
Surge height: 4.63

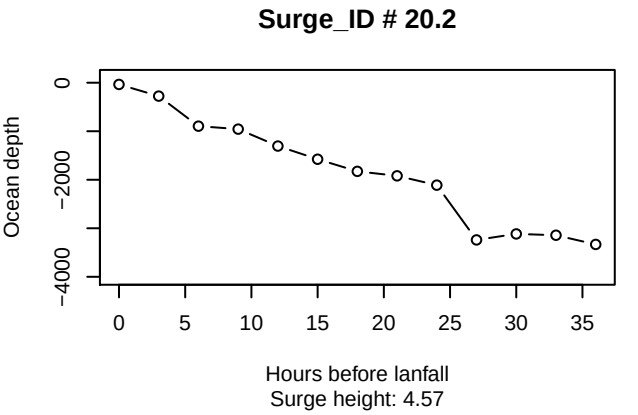
Surge_ID # 20.2
Ocean depth
0
−2000
−4000
0 5 10 15 20 25 30 35
Hours before lanfall
Surge height: 4.57

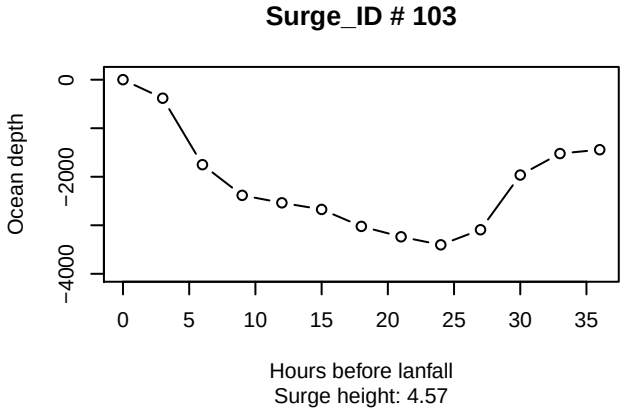
Surge_ID # 103
Ocean depth
0
−2000
−4000
0 5 10 15 20 25 30 35
Hours before lanfall
Surge height: 4.57

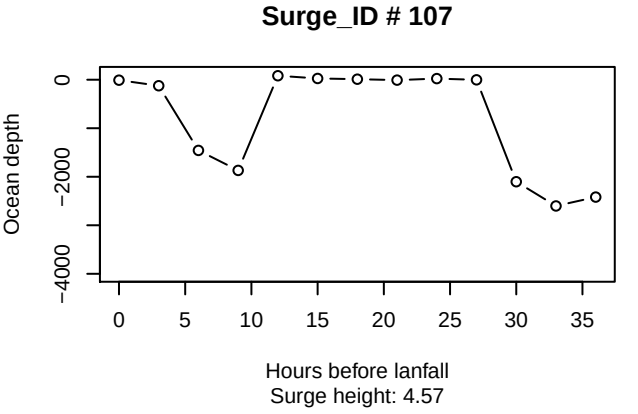
Surge_ID # 107
Ocean depth
0
−2000
−4000
0 5 10 15 20 25 30 35
Hours before lanfall
Surge height: 4.57

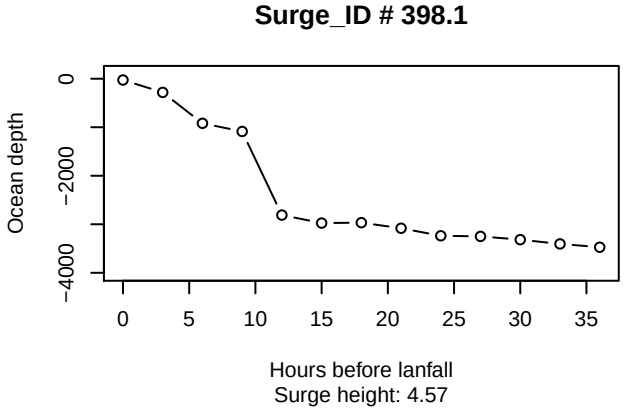
Surge_ID # 398.1
Ocean depth
0
−2000
−4000
0 5 10 15 20 25 30 35
Hours before lanfall
Surge height: 4.57

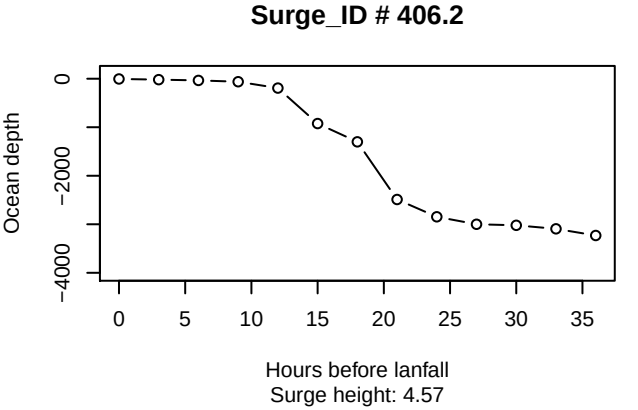
Surge_ID # 406.2
Ocean depth
0
−2000
−4000
0 5 10 15 20 25 30 35
Hours before lanfall
Surge height: 4.57

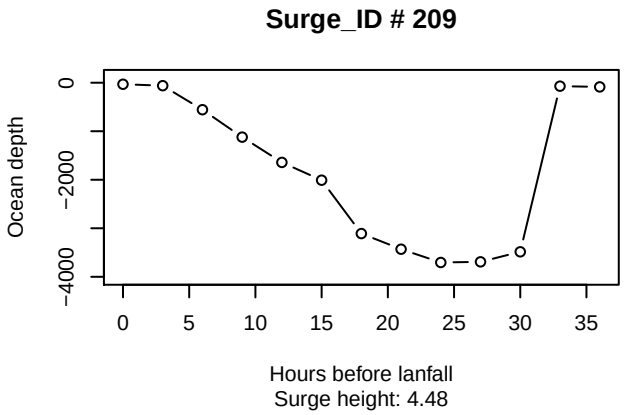
Surge_ID # 209
Ocean depth
0
−2000
−4000
0
5
10
15
20
25
30
35
Hours before lanfall
Surge height: 4.48

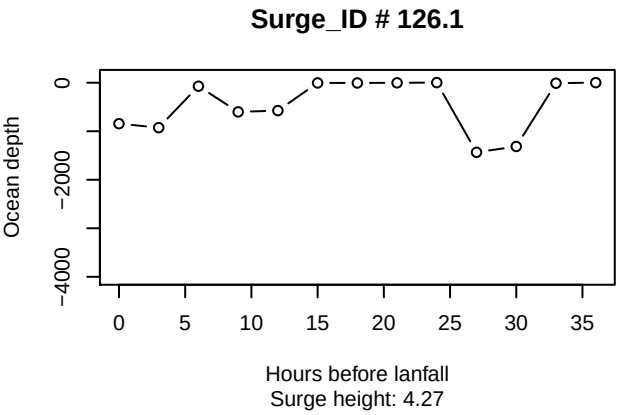
Surge_ID # 126.1
Ocean depth
0
−2000
−4000
0
5
10
15
20
25
30
35
Hours before lanfall
Surge height: 4.27

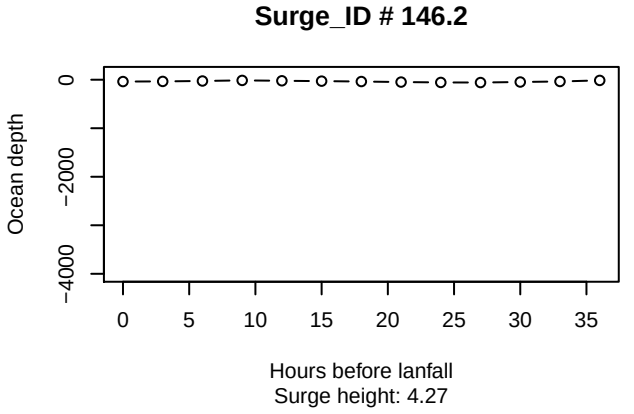
Surge_ID # 146.2
Ocean depth
0
−2000
−4000
0
5
10
15
20
25
30
35
Hours before lanfall
Surge height: 4.27

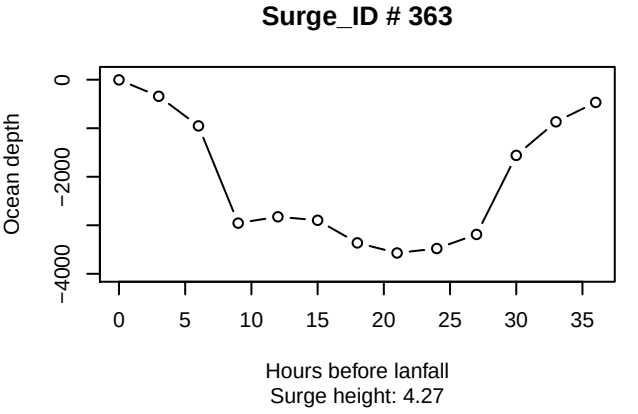
Surge_ID # 363
Ocean depth
0
−2000
−4000
0
5
10
15
20
25
30
35
Hours before lanfall
Surge height: 4.27

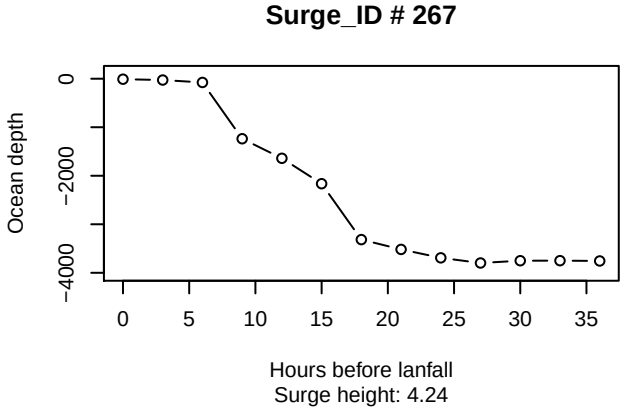
Surge_ID # 267
Ocean depth
0
−2000
−4000
0
5
10
15
20
25
30
35
Hours before lanfall
Surge height: 4.24

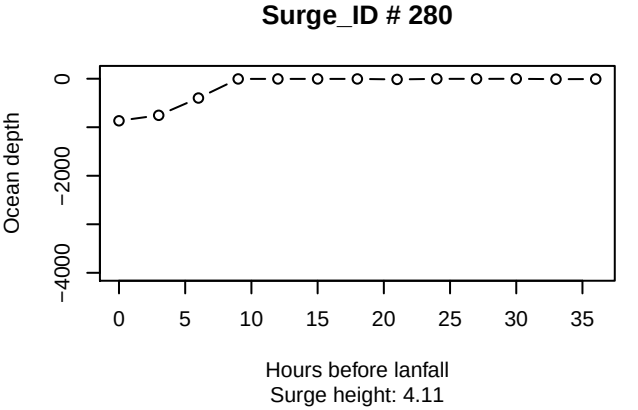
Surge_ID # 280
Ocean depth
0
−2000
−4000
0
5
10
15
20
25
30
35
Hours before lanfall
Surge height: 4.11

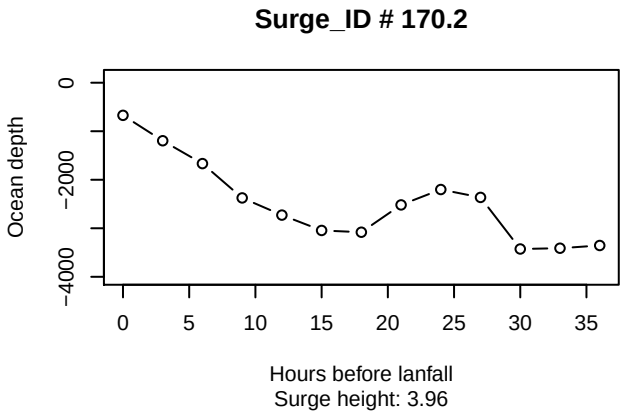
Surge_ID # 170.2
Ocean depth
0
−2000
−4000
0 5 10 15 20 25 30 35
Hours before lanfall
Surge height: 3.96

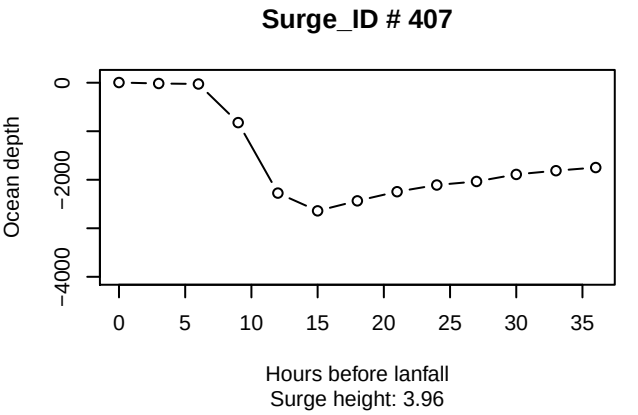
Surge_ID # 407
Ocean depth
0
−2000
−4000
0 5 10 15 20 25 30 35
Hours before lanfall
Surge height: 3.96

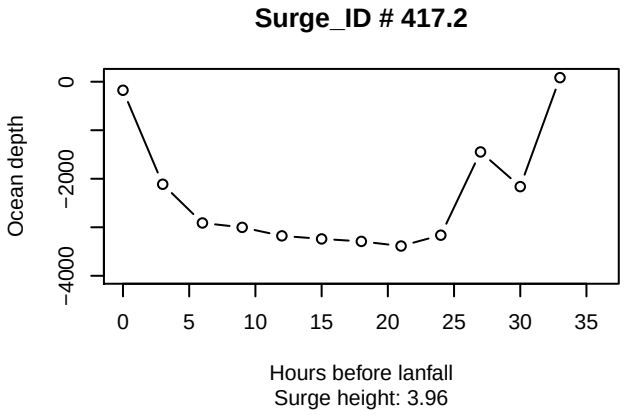
Surge_ID # 417.2
Ocean depth
0
−2000
−4000
0 5 10 15 20 25 30 35
Hours before lanfall
Surge height: 3.96

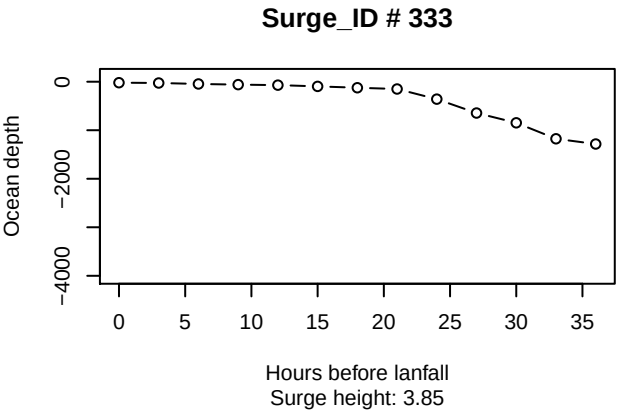
Surge_ID # 333
Ocean depth
0
−2000
−4000
0 5 10 15 20 25 30 35
Hours before lanfall
Surge height: 3.85

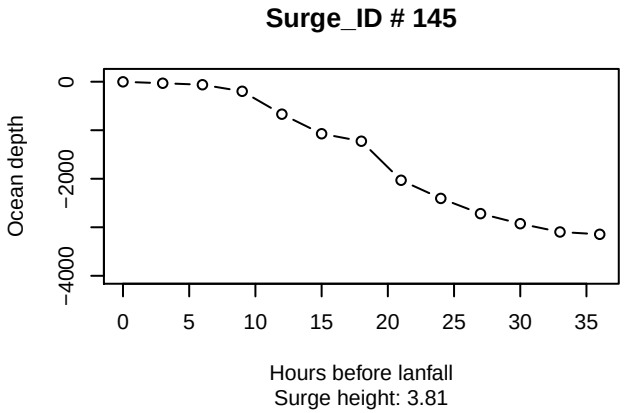
Surge_ID # 145
Ocean depth
0
−2000
−4000
0 5 10 15 20 25 30 35
Hours before lanfall
Surge height: 3.81

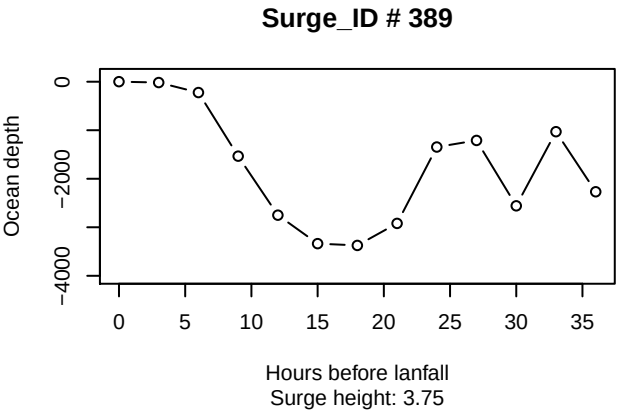
Surge_ID # 389
Ocean depth
0
−2000
−4000
0 5 10 15 20 25 30 35
Hours before lanfall
Surge height: 3.75

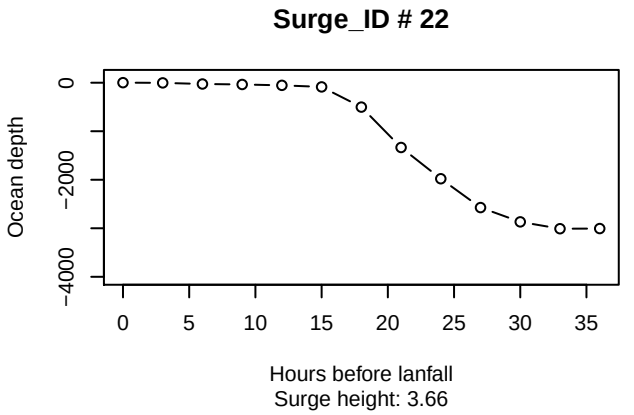
Surge_ID # 22
Ocean depth
0
−2000
−4000
0 5 10 15 20 25 30 35
Hours before lanfall
Surge height: 3.66

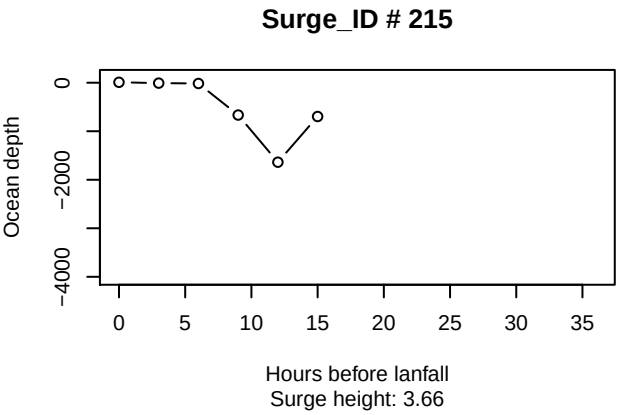
Surge_ID # 215
Ocean depth
0
−2000
−4000
0 5 10 15 20 25 30 35
Hours before lanfall
Surge height: 3.66

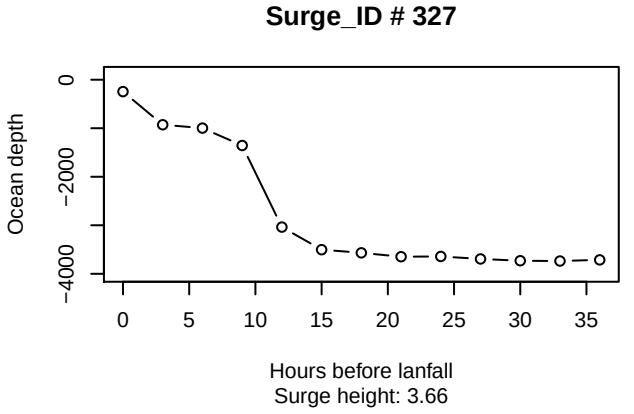
Surge_ID # 327
Ocean depth
0
−2000
−4000
0 5 10 15 20 25 30 35
Hours before lanfall
Surge height: 3.66

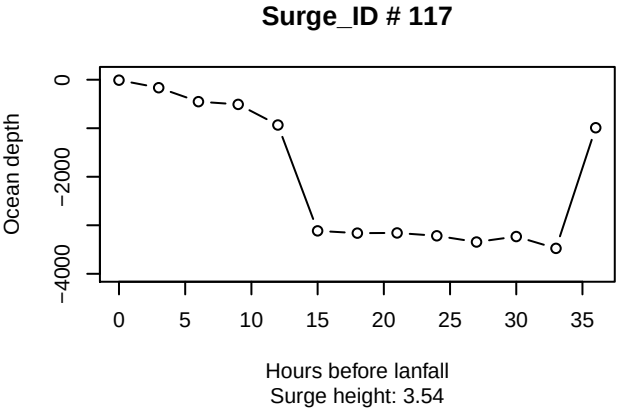
Surge_ID # 117
Ocean depth
0
−2000
−4000
0 5 10 15 20 25 30 35
Hours before lanfall
Surge height: 3.54

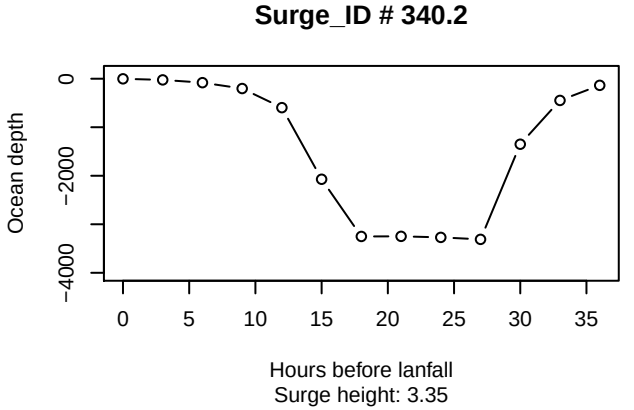
Surge_ID # 340.2
Ocean depth
0
−2000
−4000
0 5 10 15 20 25 30 35
Hours before lanfall
Surge height: 3.35

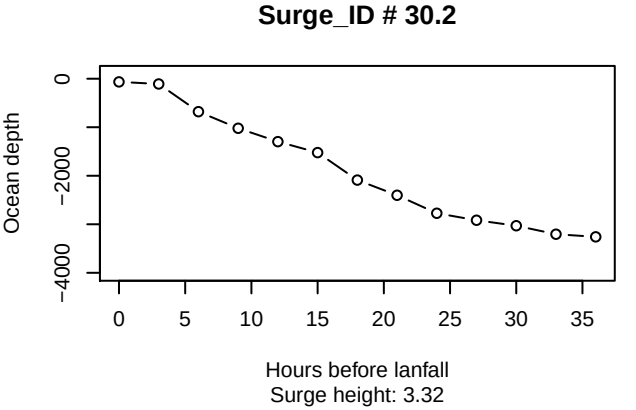
Surge_ID # 30.2
Ocean depth
0
−2000
−4000
0 5 10 15 20 25 30 35
Hours before lanfall
Surge height: 3.32

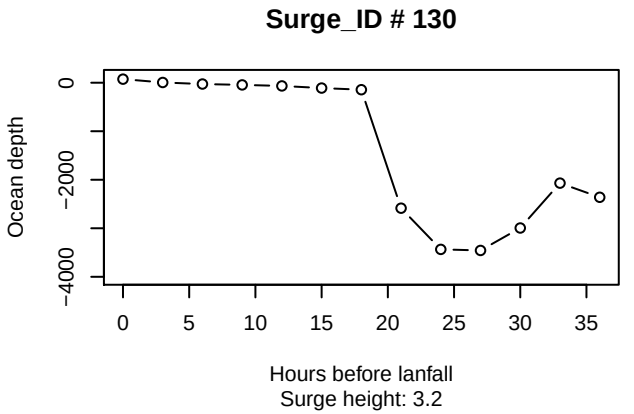
Surge_ID # 130
Ocean depth
0
−2000
−4000
0 5 10 15 20 25 30 35
Hours before lanfall
Surge height: 3.2

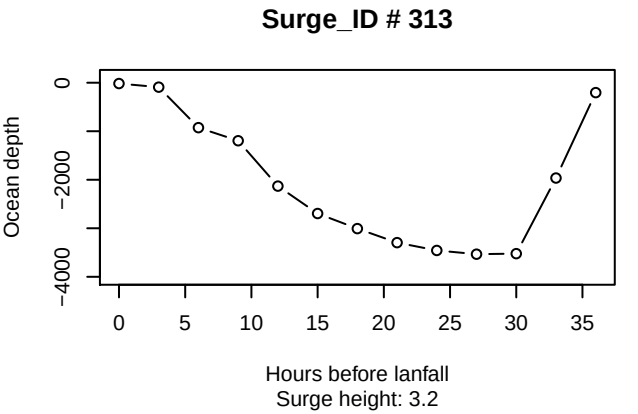
Surge_ID # 313
Ocean depth
0
−2000
−4000
0 5 10 15 20 25 30 35
Hours before lanfall
Surge height: 3.2

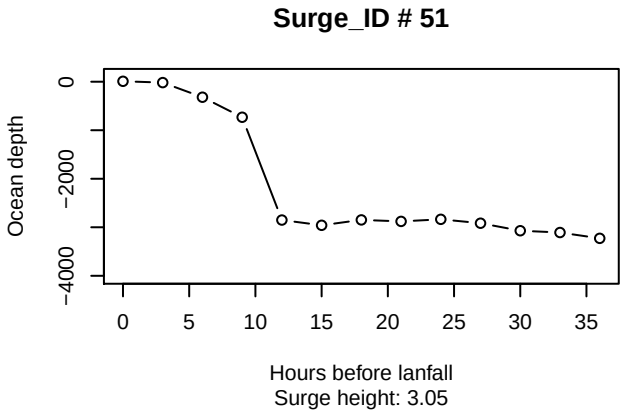
Surge_ID # 51
Ocean depth
0
−2000
−4000
0 5 10 15 20 25 30 35
Hours before lanfall
Surge height: 3.05

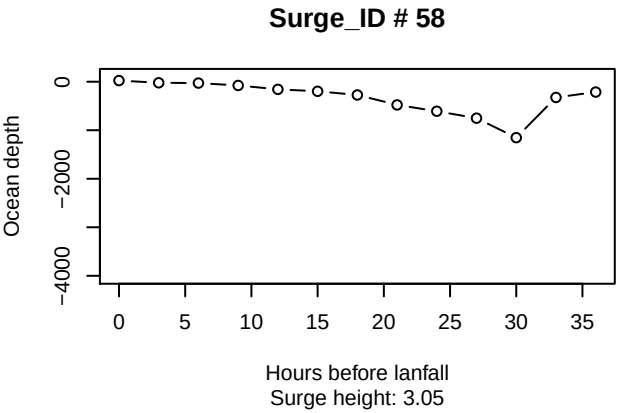
Surge_ID # 58
Ocean depth
0
−2000
−4000
0 5 10 15 20 25 30 35
Hours before lanfall
Surge height: 3.05

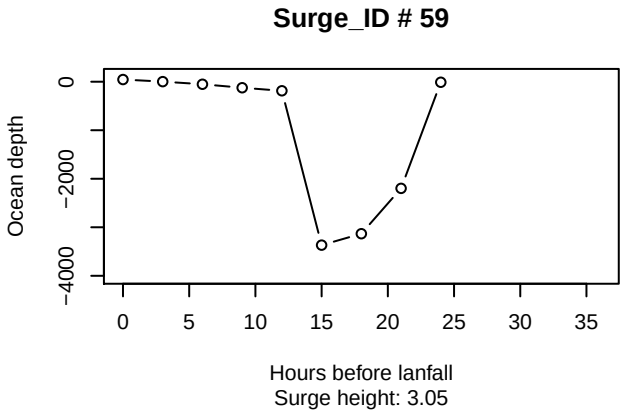
Surge_ID # 59
Ocean depth
0
−2000
−4000
0 5 10 15 20 25 30 35
Hours before lanfall
Surge height: 3.05

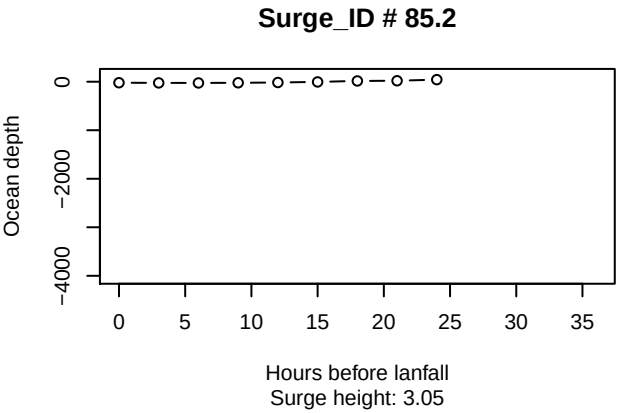
Surge_ID # 85.2
Ocean depth
0
−2000
−4000
0 5 10 15 20 25 30 35
Hours before lanfall
Surge height: 3.05

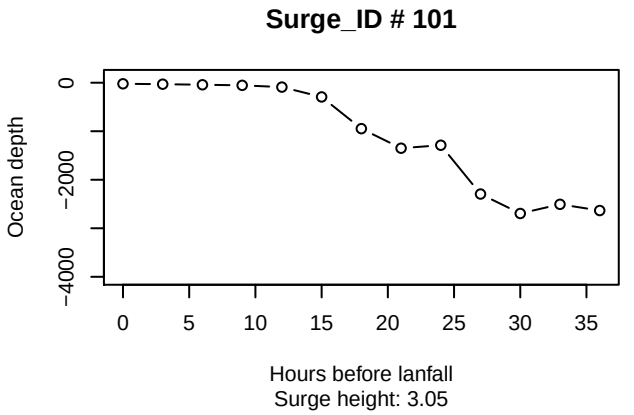
Surge_ID # 101
Ocean depth
0
−2000
−4000
0 5 10 15 20 25 30 35
Hours before lanfall
Surge height: 3.05

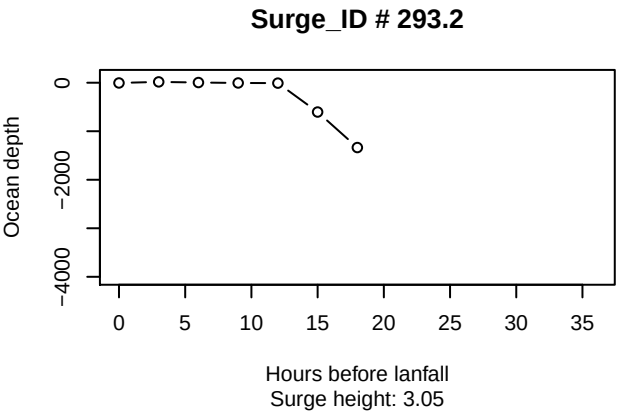
Surge_ID # 293.2
Ocean depth
0
−2000
−4000
0 5 10 15 20 25 30 35
Hours before lanfall
Surge height: 3.05

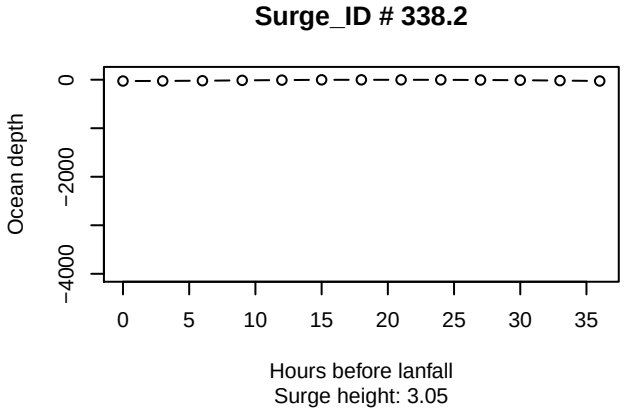
Surge_ID # 338.2
Ocean depth
0
−2000
−4000
0 5 10 15 20 25 30 35
Hours before lanfall
Surge height: 3.05

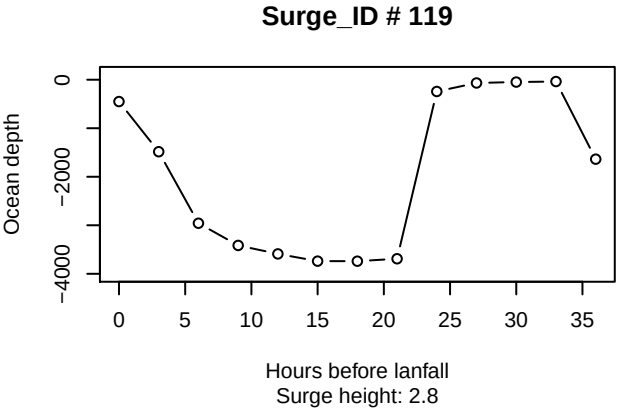
Surge_ID # 119
Ocean depth
0
−2000
−4000
0 5 10 15 20 25 30 35
Hours before lanfall
Surge height: 2.8

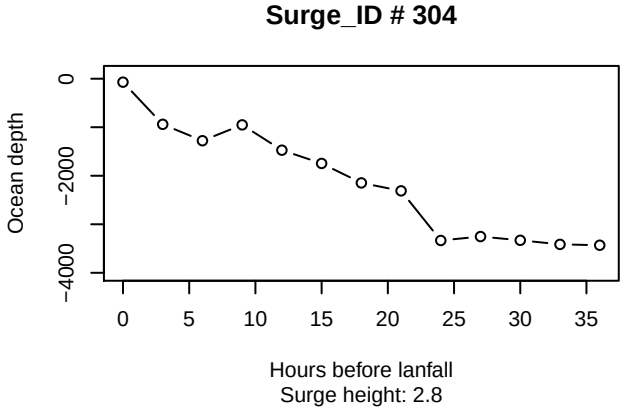
Surge_ID # 304
Ocean depth
0
−2000
−4000
0 5 10 15 20 25 30 35
Hours before lanfall
Surge height: 2.8

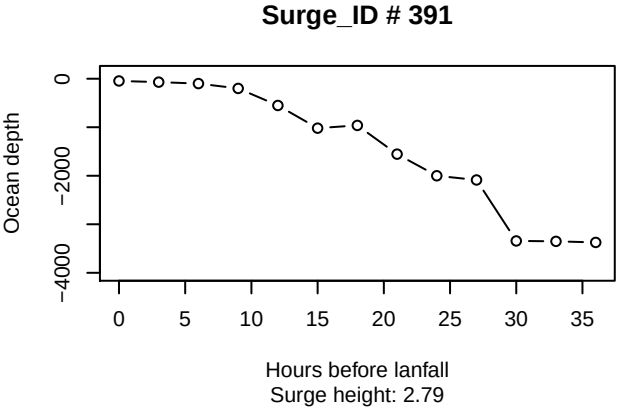
Surge_ID # 391
Ocean depth
0
−2000
−4000
0 5 10 15 20 25 30 35
Hours before lanfall
Surge height: 2.79

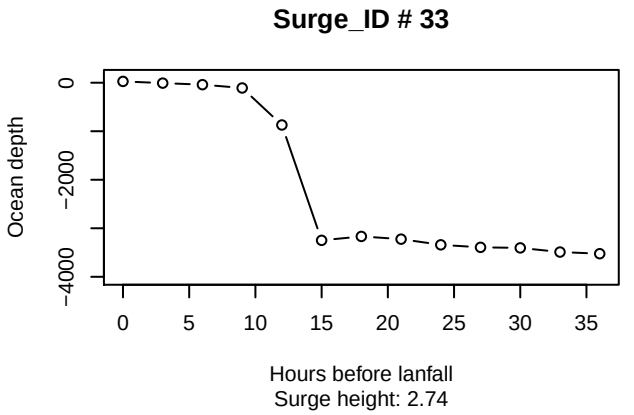
Surge_ID # 33
Ocean depth
0
−2000
−4000
0 5 10 15 20 25 30 35
Hours before lanfall
Surge height: 2.74

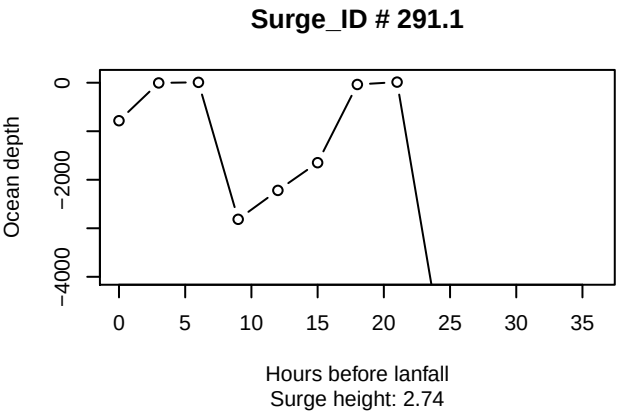
Surge_ID # 291.1
Ocean depth
0
−2000
−4000
0 5 10 15 20 25 30 35
Hours before lanfall
Surge height: 2.74

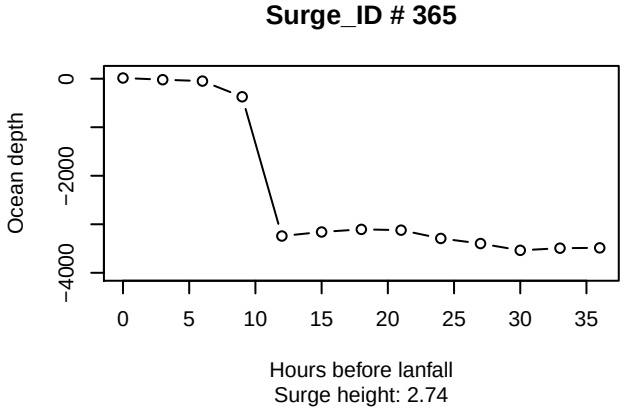
Surge_ID # 365
Ocean depth
0
−2000
−4000
0 5 10 15 20 25 30 35
Hours before lanfall
Surge height: 2.74

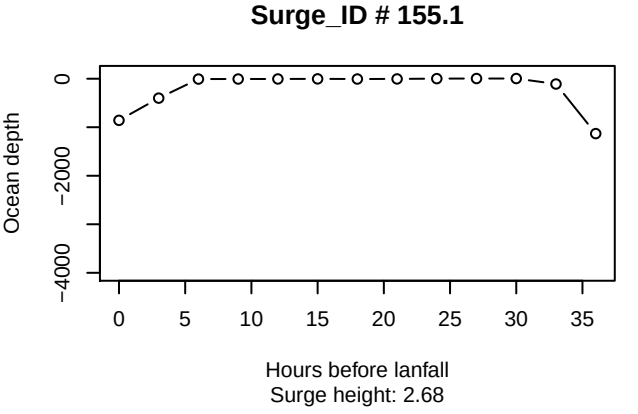
Surge_ID # 155.1
Ocean depth
0
−2000
−4000
0 5 10 15 20 25 30 35
Hours before lanfall
Surge height: 2.68

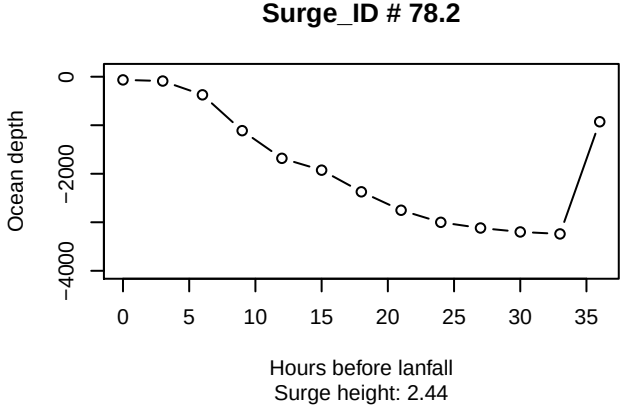
Surge_ID # 78.2
Ocean depth
0
−2000
−4000
0 5 10 15 20 25 30 35
Hours before lanfall
Surge height: 2.44

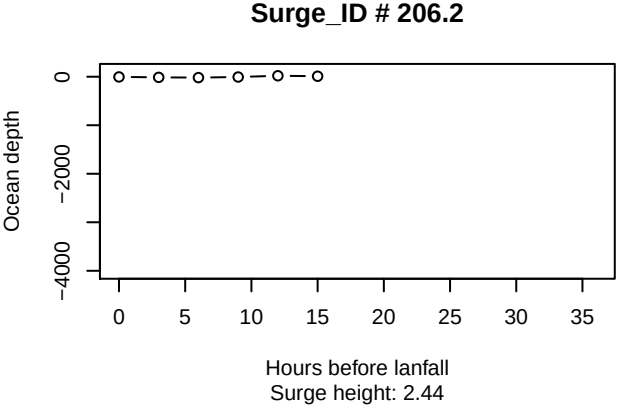
Surge_ID # 206.2
Ocean depth
0
−2000
−4000
0 5 10 15 20 25 30 35
Hours before lanfall
Surge height: 2.44

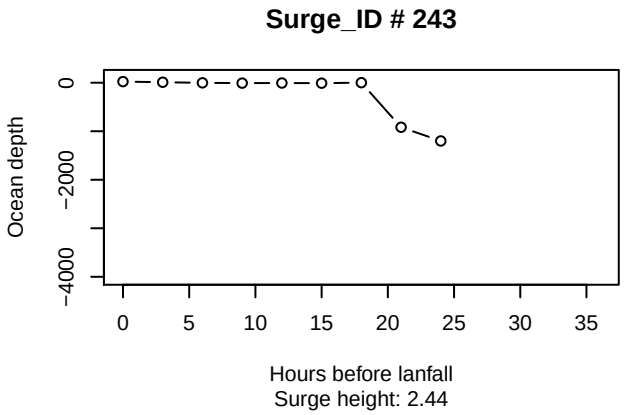
Surge_ID # 243
Ocean depth
0
−2000
−4000
0 5 10 15 20 25 30 35
Hours before lanfall
Surge height: 2.44

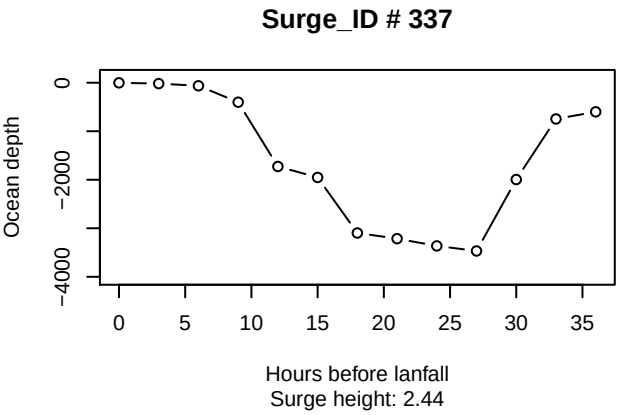
Surge_ID # 337
Ocean depth
0
−2000
−4000
0 5 10 15 20 25 30 35
Hours before lanfall
Surge height: 2.44

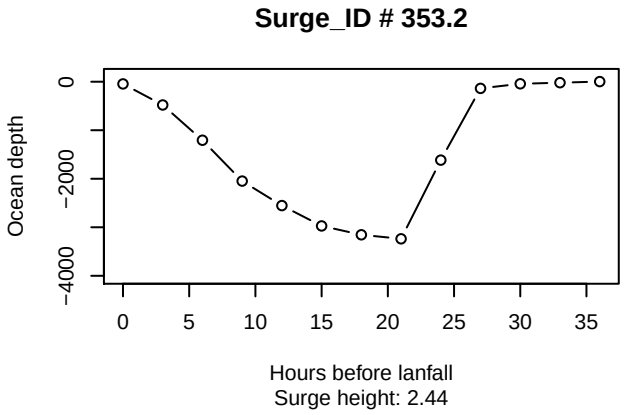
Surge_ID # 353.2
Ocean depth
0
−2000
−4000
0 5 10 15 20 25 30 35
Hours before lanfall
Surge height: 2.44

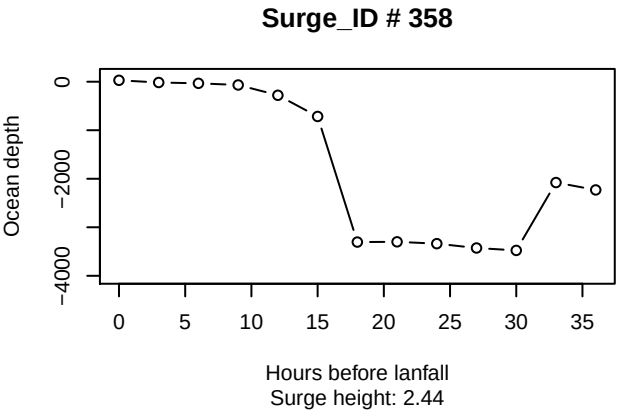
Surge_ID # 358
Ocean depth
0
−2000
−4000
0 5 10 15 20 25 30 35
Hours before lanfall
Surge height: 2.44

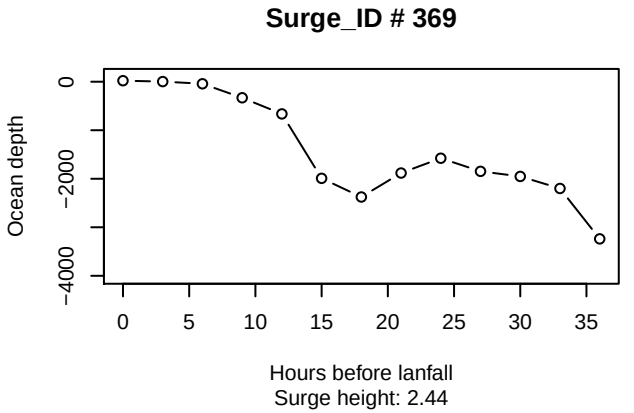
Surge_ID # 369
Ocean depth
0
−2000
−4000
0 5 10 15 20 25 30 35
Hours before lanfall
Surge height: 2.44

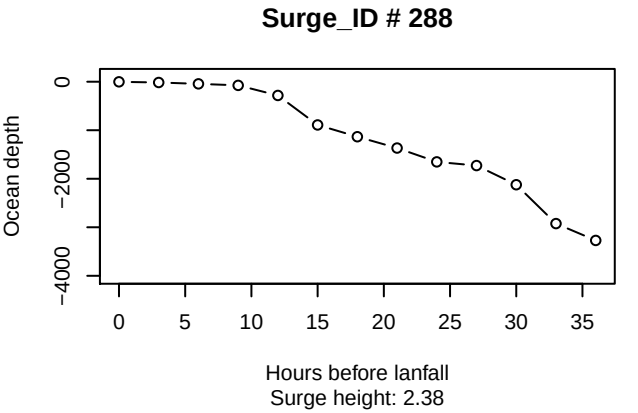
Surge_ID # 288
Ocean depth
0
−2000
−4000
0 5 10 15 20 25 30 35
Hours before lanfall
Surge height: 2.38

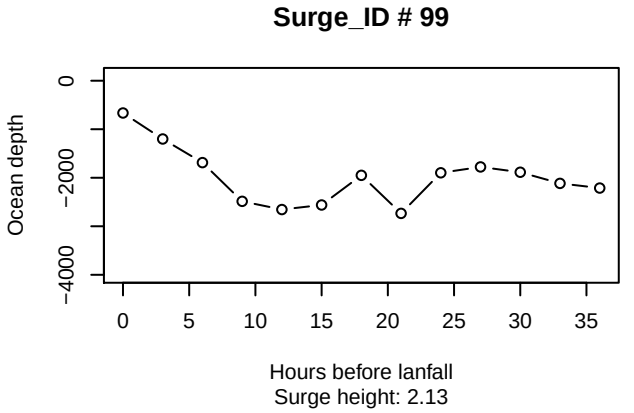
Surge_ID # 99
Ocean depth
0
−2000
−4000
0
5
10
15
20
25
30
35
Hours before lanfall
Surge height: 2.13

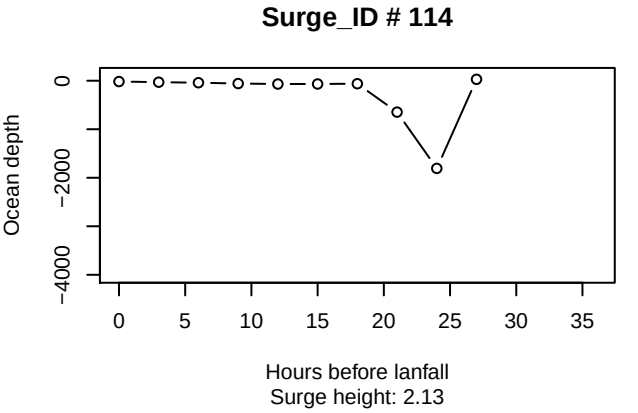
Surge_ID # 114
Ocean depth
0
−2000
−4000
0
5
10
15
20
25
30
35
Hours before lanfall
Surge height: 2.13

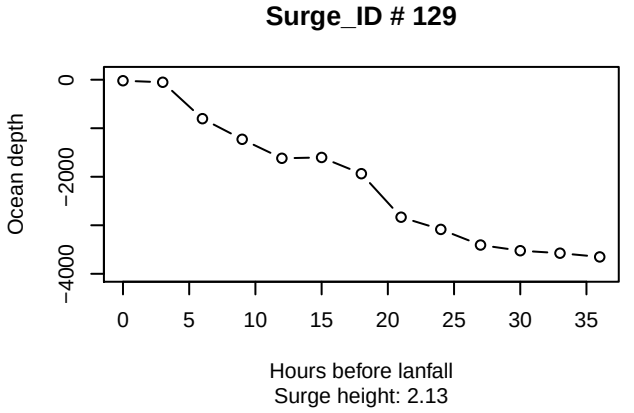
Surge_ID # 129
Ocean depth
0
−2000
−4000
0
5
10
15
20
25
30
35
Hours before lanfall
Surge height: 2.13

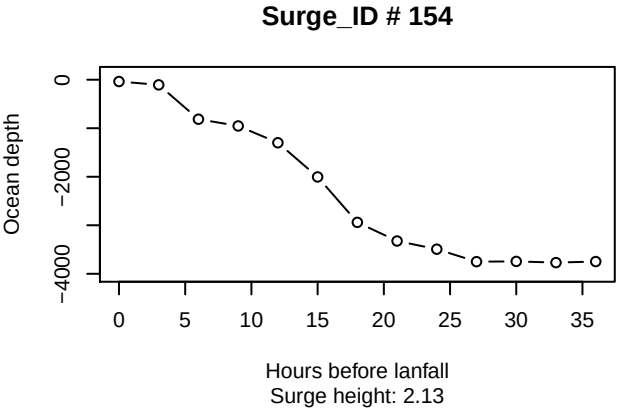
Surge_ID # 154
Ocean depth
0
−2000
−4000
0
5
10
15
20
25
30
35
Hours before lanfall
Surge height: 2.13

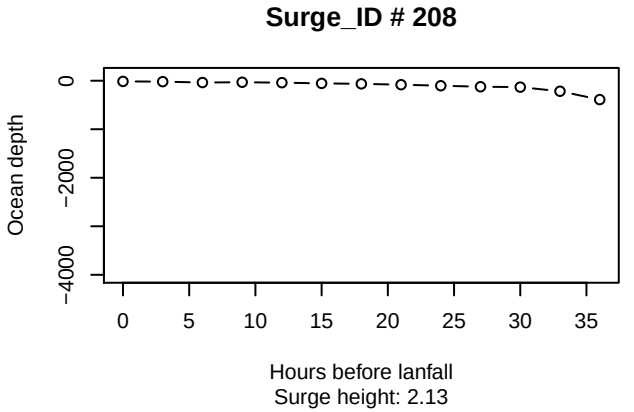
Surge_ID # 208
Ocean depth
0
−2000
−4000
0
5
10
15
20
25
30
35
Hours before lanfall
Surge height: 2.13

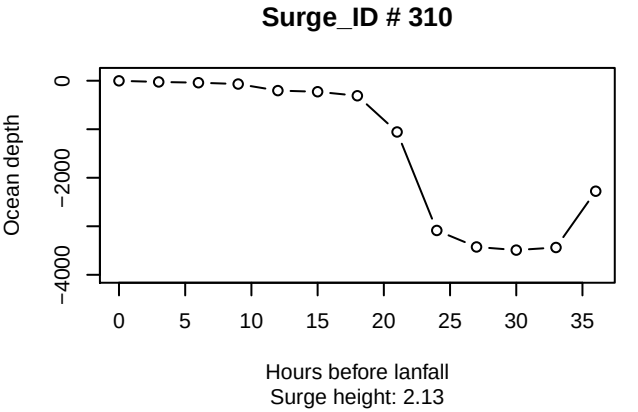
Surge_ID # 310
Ocean depth
0
−2000
−4000
0
5
10
15
20
25
30
35
Hours before lanfall
Surge height: 2.13

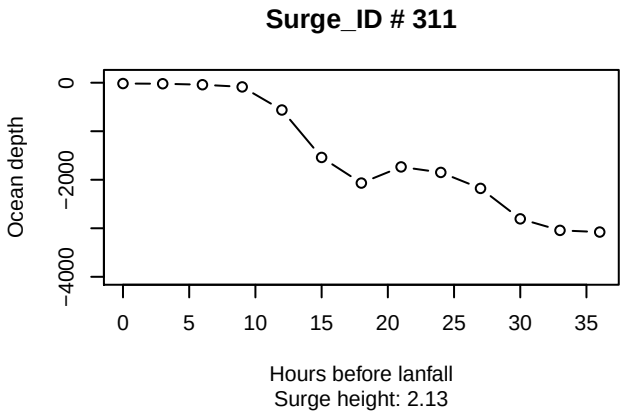
Surge_ID # 311
Ocean depth
0
−2000
−4000
0 5 10 15 20 25 30 35
Hours before lanfall
Surge height: 2.13

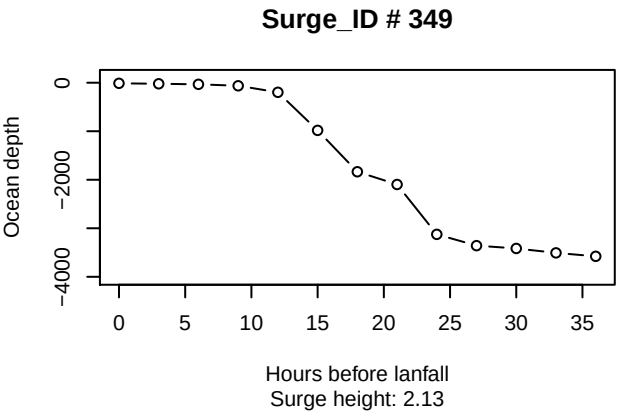
Surge_ID # 349
Ocean depth
0
−2000
−4000
0 5 10 15 20 25 30 35
Hours before lanfall
Surge height: 2.13

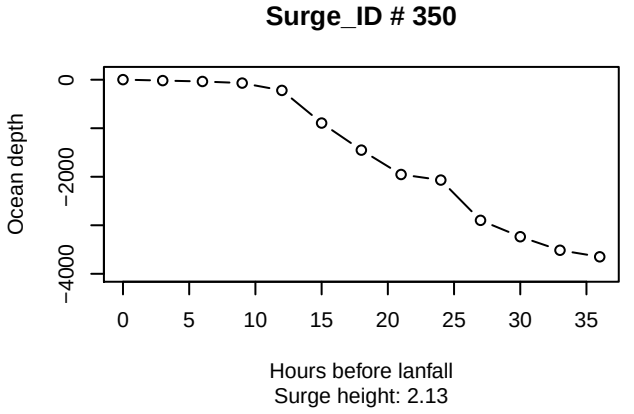
Surge_ID # 350
Ocean depth
0
−2000
−4000
0 5 10 15 20 25 30 35
Hours before lanfall
Surge height: 2.13

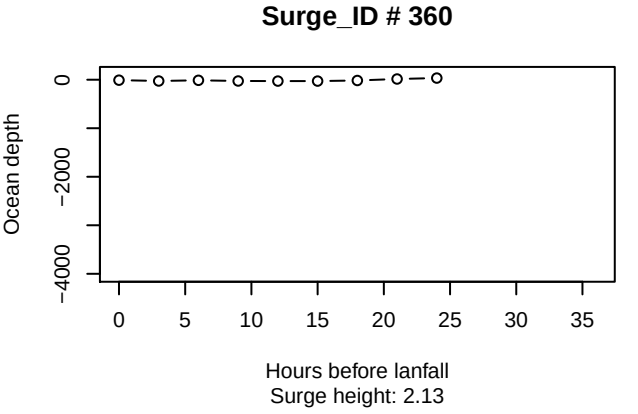
Surge_ID # 360
Ocean depth
0
−2000
−4000
0 5 10 15 20 25 30 35
Hours before lanfall
Surge height: 2.13

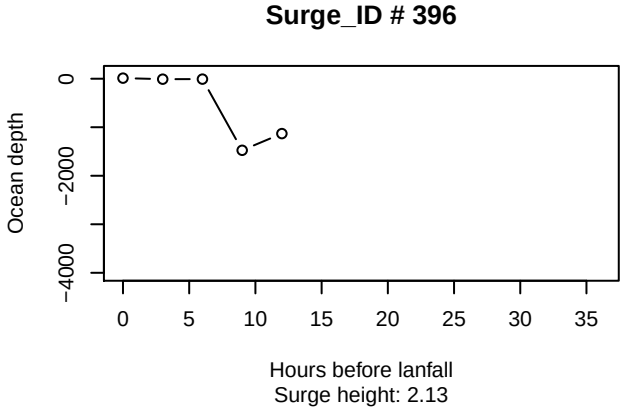
Surge_ID # 396
Ocean depth
0
−2000
−4000
0 5 10 15 20 25 30 35
Hours before lanfall
Surge height: 2.13

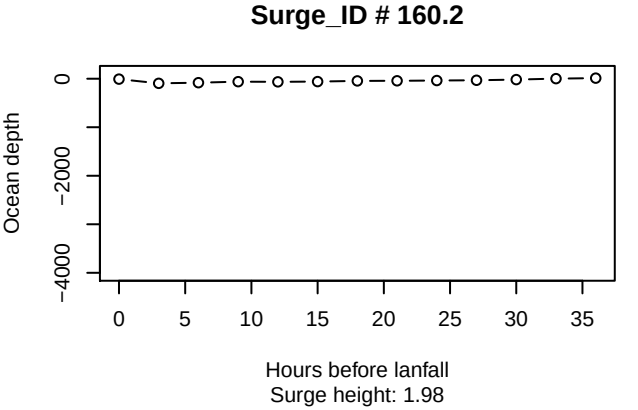
Surge_ID # 160.2
Ocean depth
0
−2000
−4000
0 5 10 15 20 25 30 35
Hours before lanfall
Surge height: 1.98

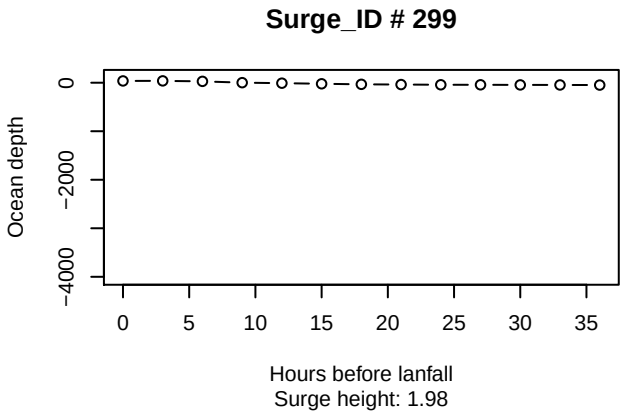
Surge_ID # 299
Ocean depth
0
−2000
−4000
0 5 10 15 20 25 30 35
Hours before lanfall
Surge height: 1.98

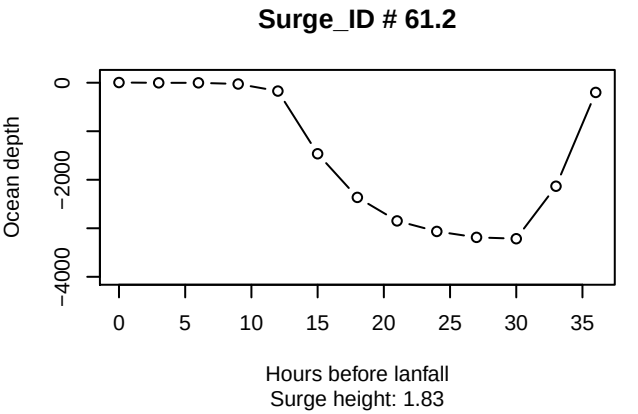
Surge_ID # 61.2
Ocean depth
0
−2000
−4000
0 5 10 15 20 25 30 35
Hours before lanfall
Surge height: 1.83

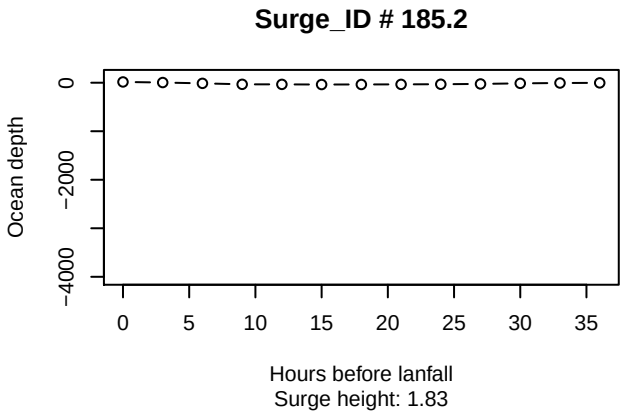
Surge_ID # 185.2
Ocean depth
0
−2000
−4000
0 5 10 15 20 25 30 35
Hours before lanfall
Surge height: 1.83

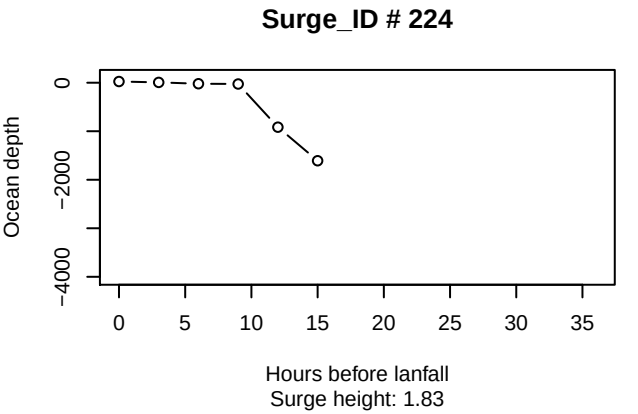
Surge_ID # 224
Ocean depth
0
−2000
−4000
0 5 10 15 20 25 30 35
Hours before lanfall
Surge height: 1.83

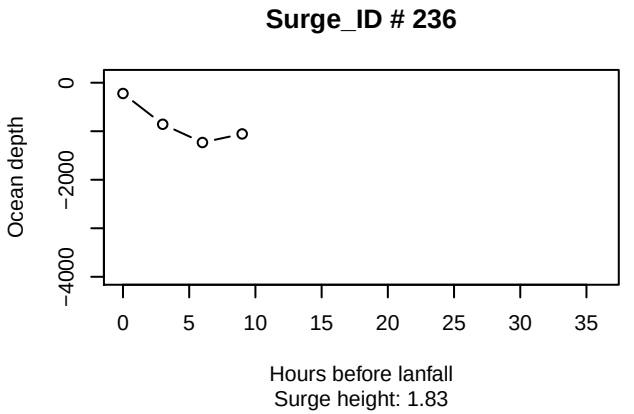
Surge_ID # 236
Ocean depth
0
−2000
−4000
0 5 10 15 20 25 30 35
Hours before lanfall
Surge height: 1.83

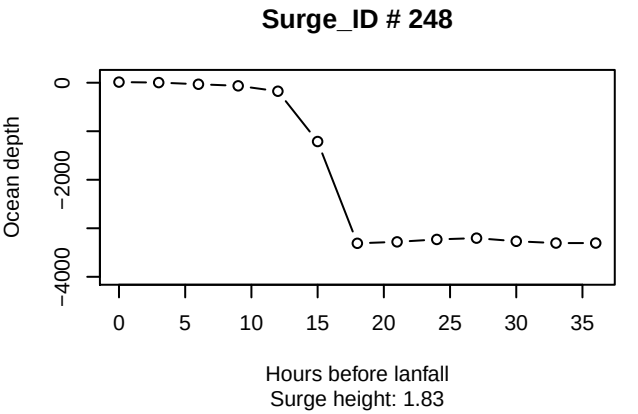
Surge_ID # 248
Ocean depth
0
−2000
−4000
0 5 10 15 20 25 30 35
Hours before lanfall
Surge height: 1.83

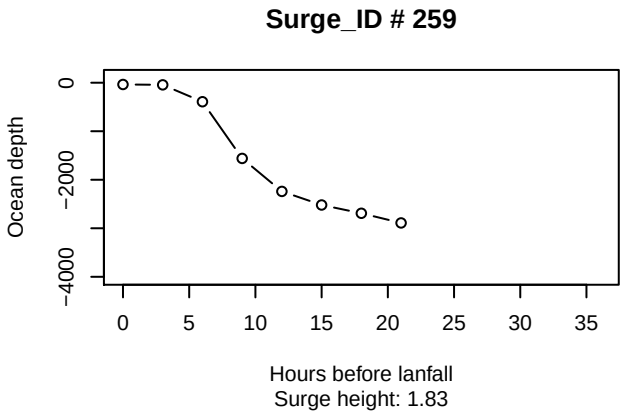
Surge_ID # 259
Ocean depth
0
−2000
−4000
0 5 10 15 20 25 30 35
Hours before lanfall
Surge height: 1.83

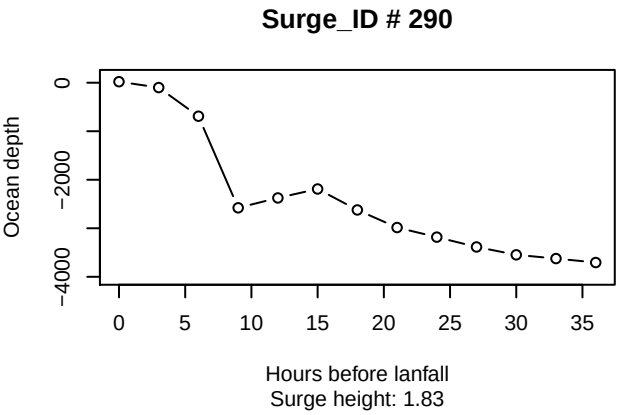
Surge_ID # 290
Ocean depth
0
−2000
−4000
0 5 10 15 20 25 30 35
Hours before lanfall
Surge height: 1.83

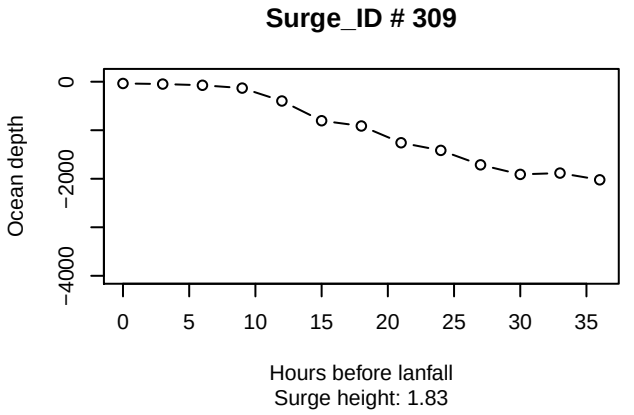
Surge_ID # 309
Ocean depth
0
−2000
−4000
0 5 10 15 20 25 30 35
Hours before lanfall
Surge height: 1.83

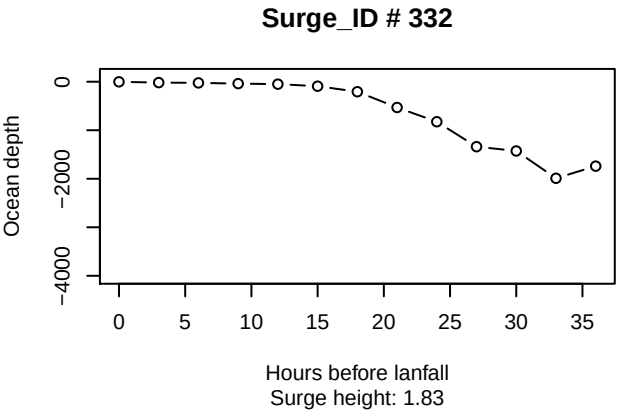
Surge_ID # 332
Ocean depth
0
−2000
−4000
0 5 10 15 20 25 30 35
Hours before lanfall
Surge height: 1.83

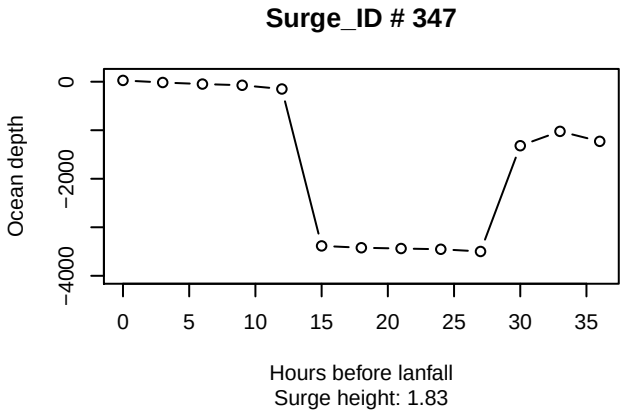
Surge_ID # 347
Ocean depth
0
−2000
−4000
0 5 10 15 20 25 30 35
Hours before lanfall
Surge height: 1.83

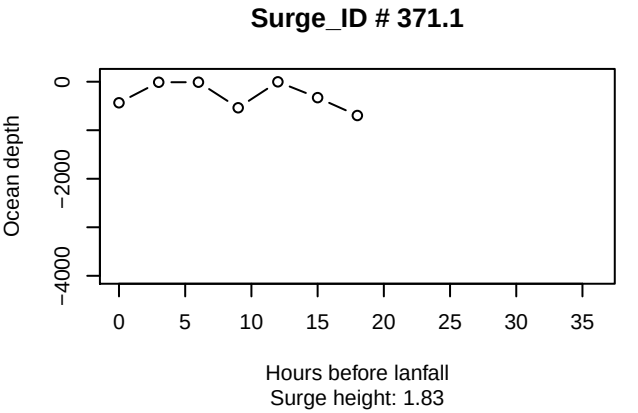
Surge_ID # 371.1
Ocean depth
0
−2000
−4000
0 5 10 15 20 25 30 35
Hours before lanfall
Surge height: 1.83

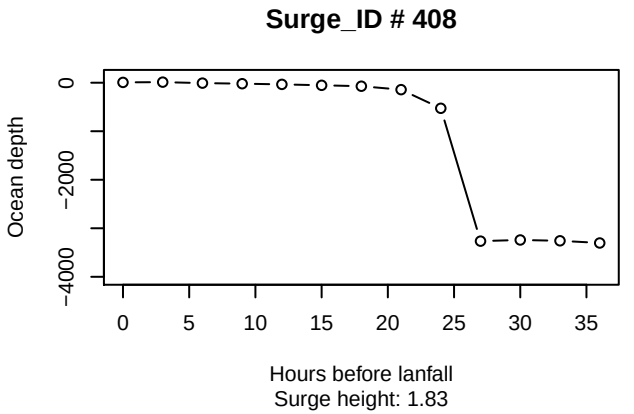
Surge_ID # 408
Ocean depth
0
−2000
−4000
0 5 10 15 20 25 30 35
Hours before lanfall
Surge height: 1.83

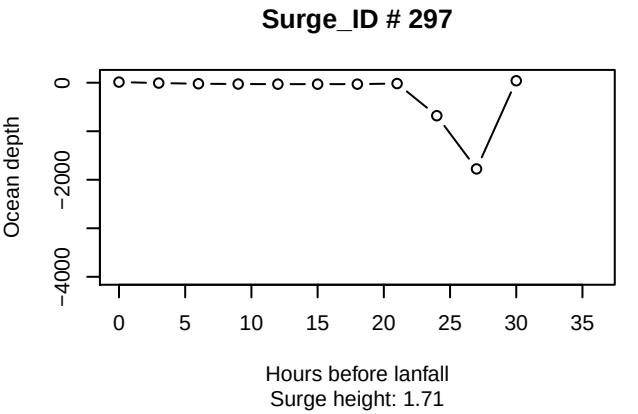
Surge_ID # 297
Ocean depth
0
−2000
−4000
0 5 10 15 20 25 30 35
Hours before lanfall
Surge height: 1.71

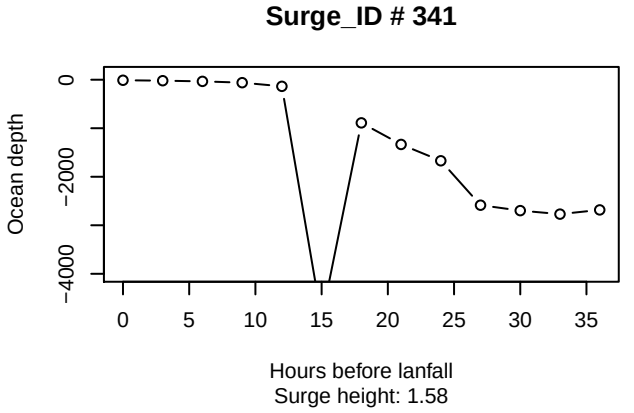
Surge_ID # 341
Ocean depth
0
−2000
−4000
0 5 10 15 20 25 30 35
Hours before lanfall
Surge height: 1.58

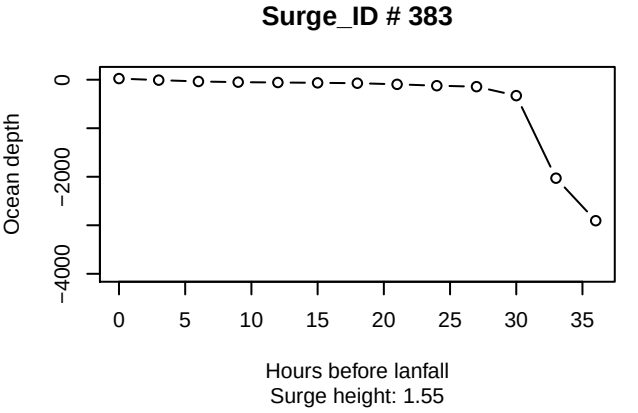
Surge_ID # 383
Ocean depth
0
−2000
−4000
0 5 10 15 20 25 30 35
Hours before lanfall
Surge height: 1.55

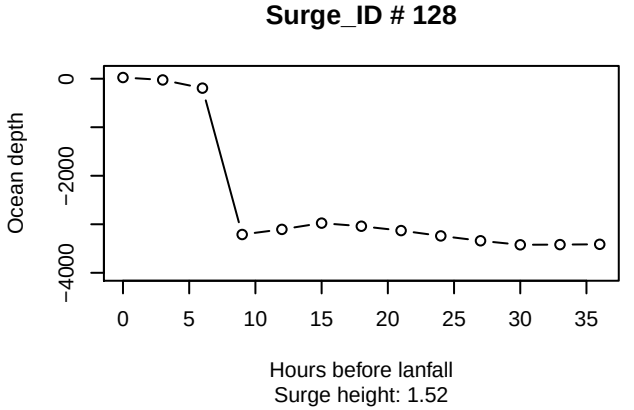
Surge_ID # 128
Ocean depth
0
−2000
−4000
0 5 10 15 20 25 30 35
Hours before lanfall
Surge height: 1.52

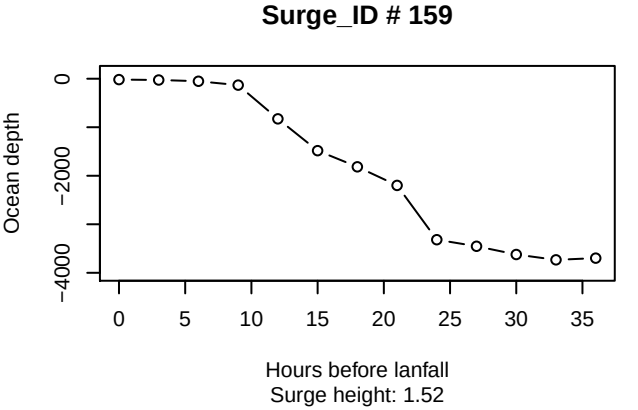
Surge_ID # 159
Ocean depth
0
−2000
−4000
0 5 10 15 20 25 30 35
Hours before lanfall
Surge height: 1.52

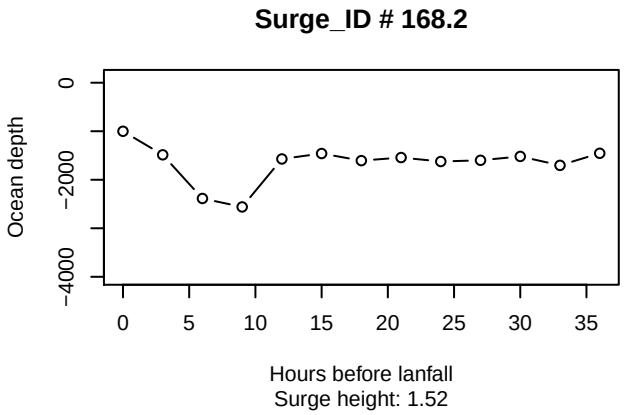
Surge_ID # 168.2
Ocean depth
0
−2000
−4000
0 5 10 15 20 25 30 35
Hours before lanfall
Surge height: 1.52

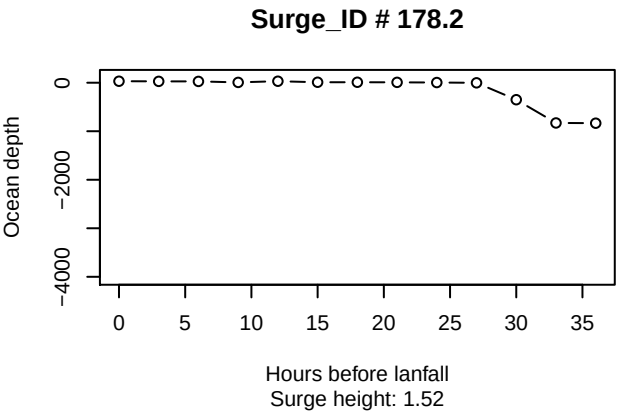
Surge_ID # 178.2
Ocean depth
0
−2000
−4000
0 5 10 15 20 25 30 35
Hours before lanfall
Surge height: 1.52

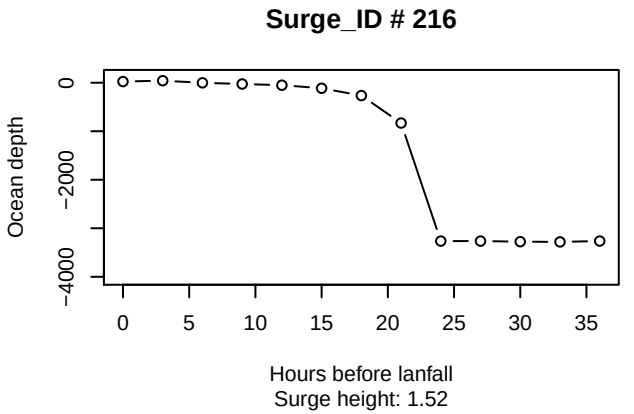
Surge_ID # 216
Ocean depth
0
−2000
−4000
0 5 10 15 20 25 30 35
Hours before lanfall
Surge height: 1.52

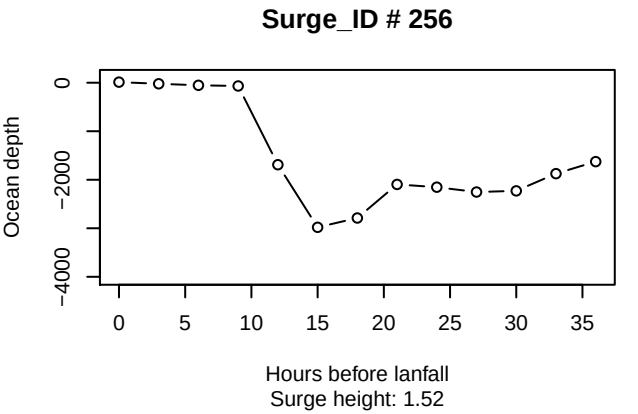
Surge_ID # 256
Ocean depth
0
−2000
−4000
0 5 10 15 20 25 30 35
Hours before lanfall
Surge height: 1.52

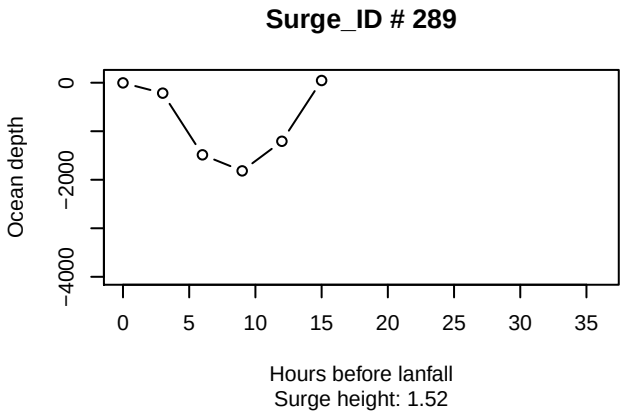
Surge_ID # 289
Ocean depth
0
−2000
−4000
0 5 10 15 20 25 30 35
Hours before lanfall
Surge height: 1.52

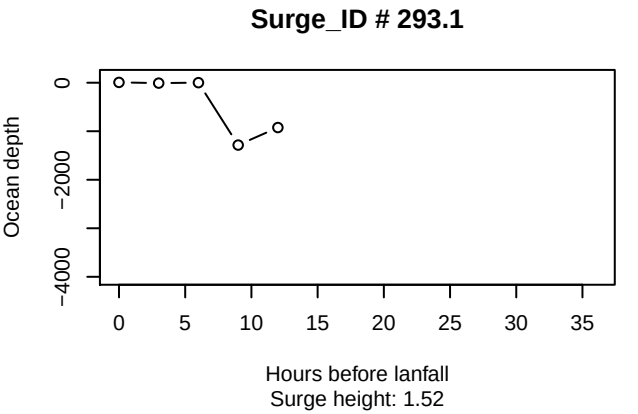
Surge_ID # 293.1
Ocean depth
0
−2000
−4000
0 5 10 15 20 25 30 35
Hours before lanfall
Surge height: 1.52

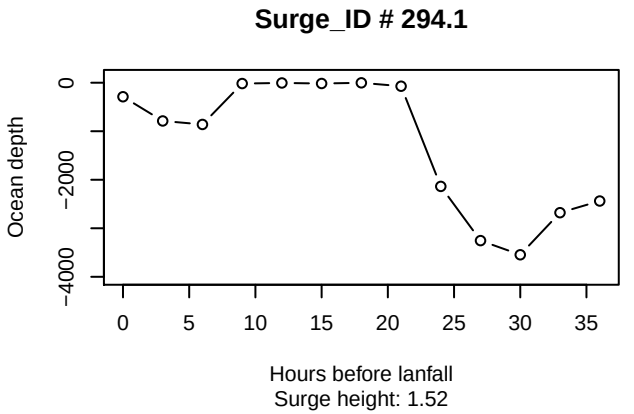
Surge_ID # 294.1
Ocean depth
0
−2000
−4000
0
5
10
15
20
25
30
35
Hours before lanfall
Surge height: 1.52

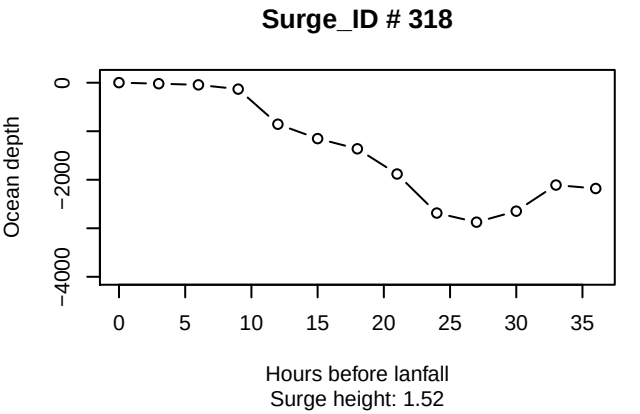
Surge_ID # 318
Ocean depth
0
−2000
−4000
0
5
10
15
20
25
30
35
Hours before lanfall
Surge height: 1.52

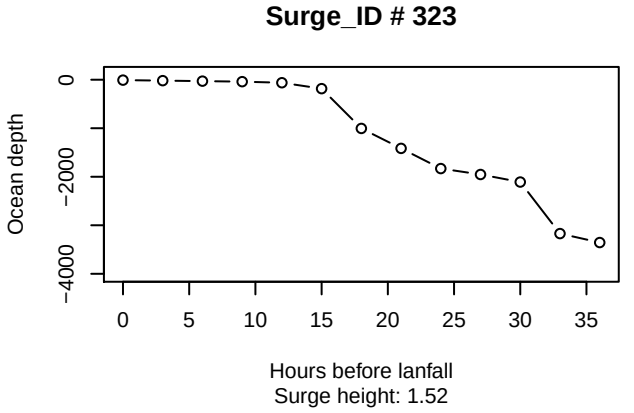
Surge_ID # 323
Ocean depth
0
−2000
−4000
0
5
10
15
20
25
30
35
Hours before lanfall
Surge height: 1.52

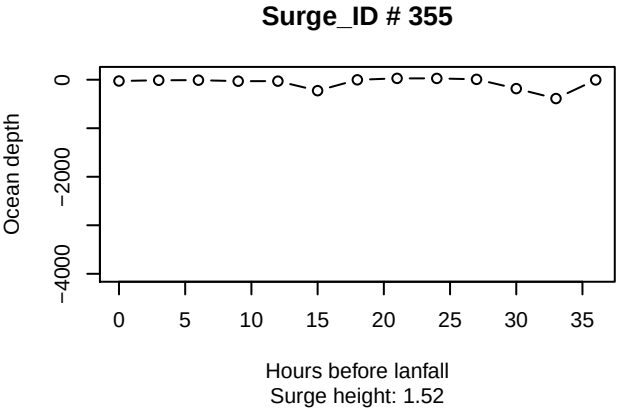
Surge_ID # 355
Ocean depth
0
−2000
−4000
0
5
10
15
20
25
30
35
Hours before lanfall
Surge height: 1.52

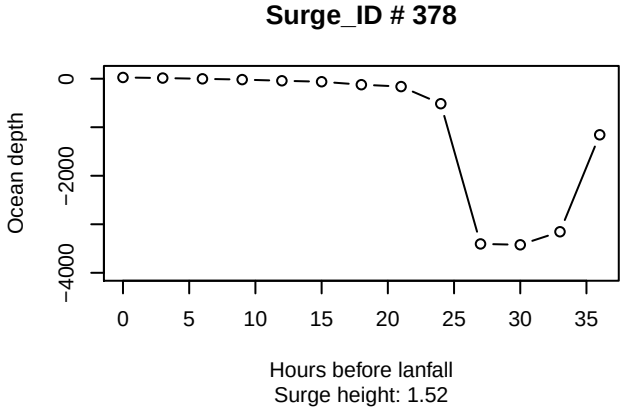
Surge_ID # 378
Ocean depth
0
−2000
−4000
0
5
10
15
20
25
30
35
Hours before lanfall
Surge height: 1.52

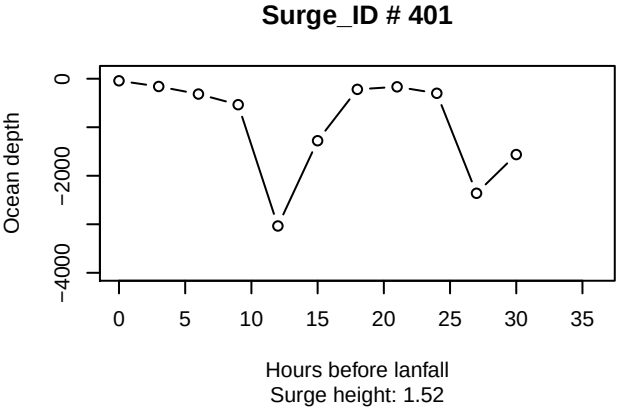
Surge_ID # 401
Ocean depth
0
−2000
−4000
0
5
10
15
20
25
30
35
Hours before lanfall
Surge height: 1.52

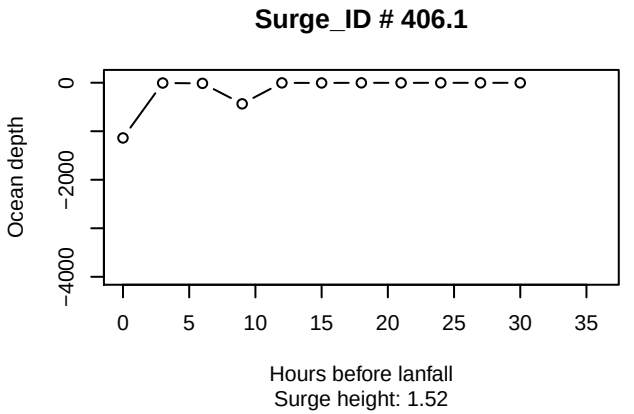
Surge_ID # 406.1
Ocean depth
0
−2000
−4000
0 5 10 15 20 25 30 35
Hours before lanfall
Surge height: 1.52

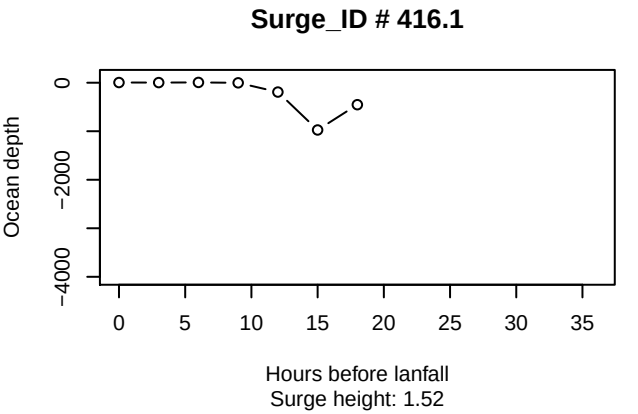
Surge_ID # 416.1
Ocean depth
0
−2000
−4000
0 5 10 15 20 25 30 35
Hours before lanfall
Surge height: 1.52

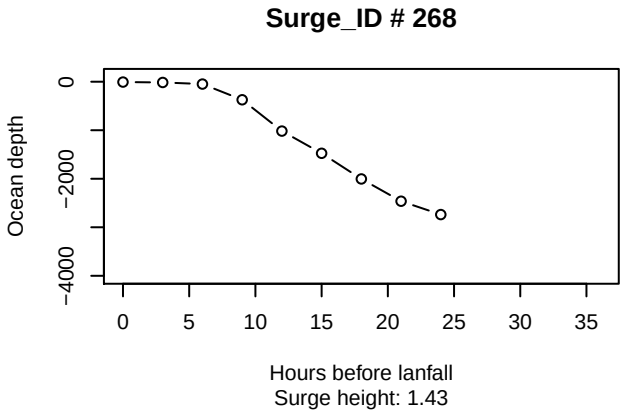
Surge_ID # 268
Ocean depth
0
−2000
−4000
0 5 10 15 20 25 30 35
Hours before lanfall
Surge height: 1.43

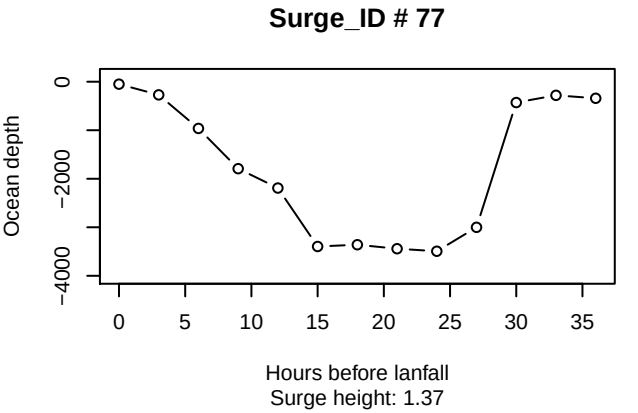
Surge_ID # 77
Ocean depth
0
−2000
−4000
0 5 10 15 20 25 30 35
Hours before lanfall
Surge height: 1.37

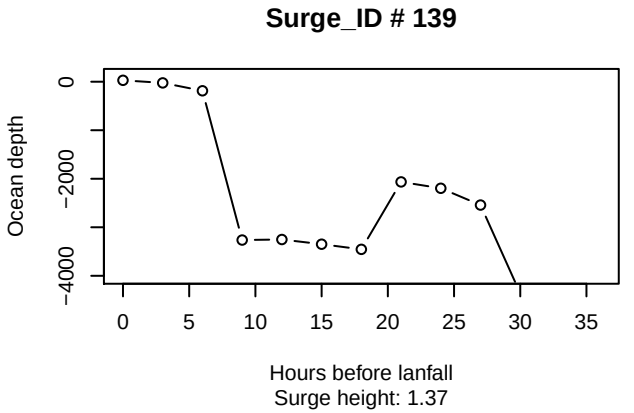
Surge_ID # 139
Ocean depth
0
−2000
−4000
0 5 10 15 20 25 30 35
Hours before lanfall
Surge height: 1.37

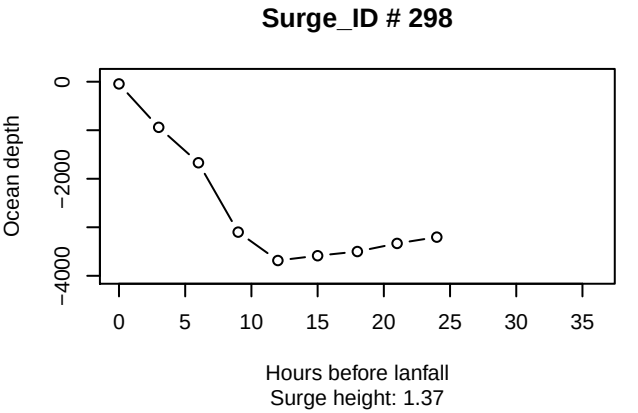
Surge_ID # 298
Ocean depth
0
−2000
−4000
0 5 10 15 20 25 30 35
Hours before lanfall
Surge height: 1.37

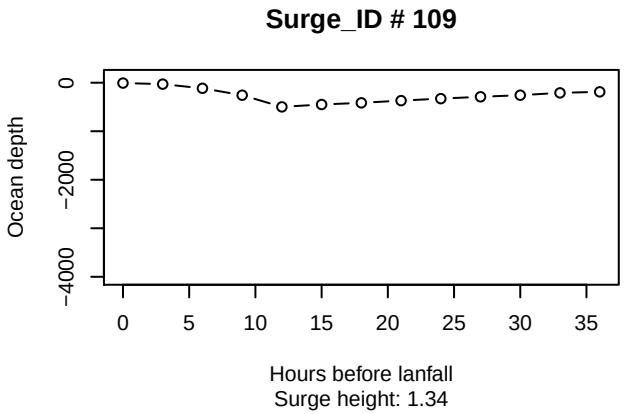
Surge_ID # 109
Ocean depth
0
−2000
−4000
0 5 10 15 20 25 30 35
Hours before lanfall
Surge height: 1.34

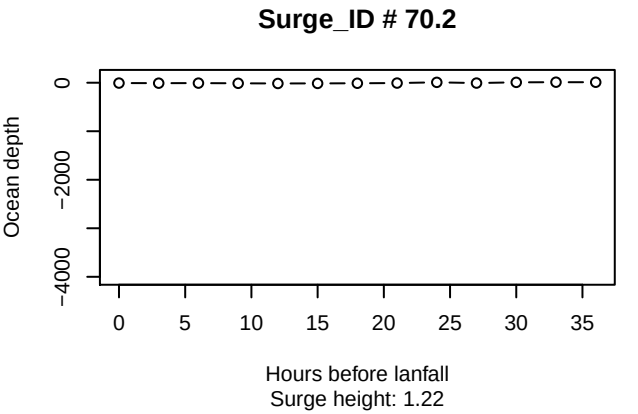
Surge_ID # 70.2
Ocean depth
0
−2000
−4000
0 5 10 15 20 25 30 35
Hours before lanfall
Surge height: 1.22

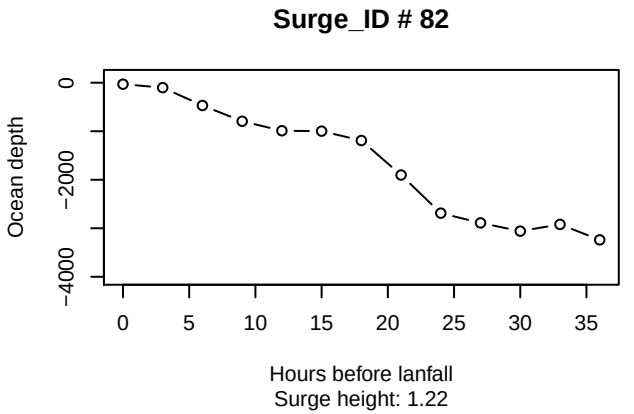
Surge_ID # 82
Ocean depth
0
−2000
−4000
0 5 10 15 20 25 30 35
Hours before lanfall
Surge height: 1.22

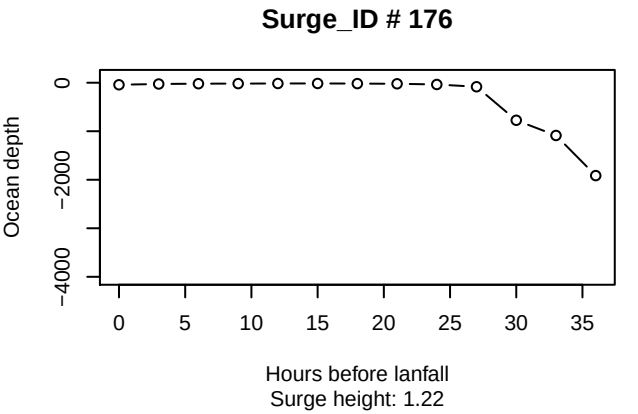
Surge_ID # 176
Ocean depth
0
−2000
−4000
0 5 10 15 20 25 30 35
Hours before lanfall
Surge height: 1.22

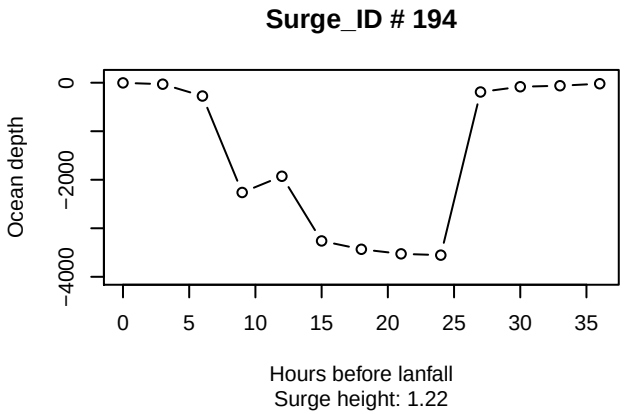
Surge_ID # 194
Ocean depth
0
−2000
−4000
0 5 10 15 20 25 30 35
Hours before lanfall
Surge height: 1.22

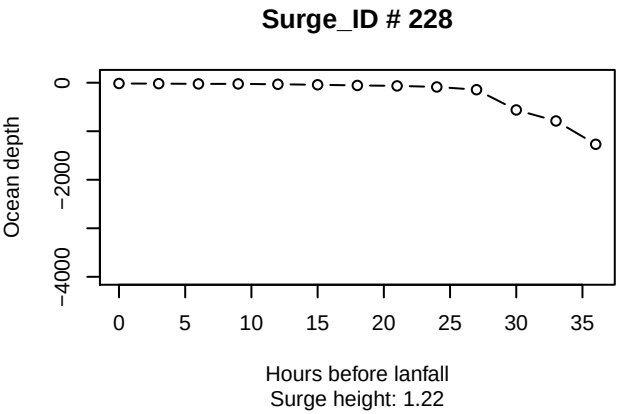
Surge_ID # 228
Ocean depth
0
−2000
−4000
0 5 10 15 20 25 30 35
Hours before lanfall
Surge height: 1.22

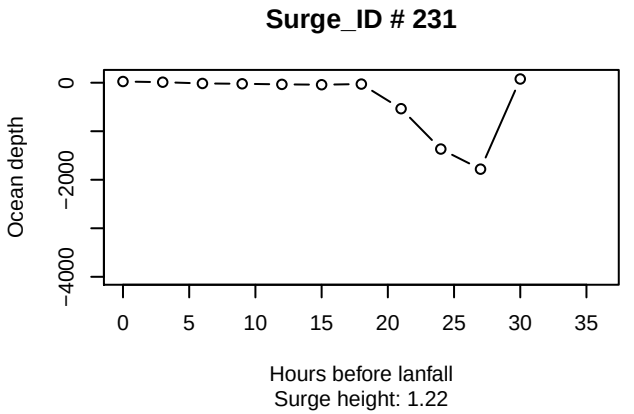
Surge_ID # 231
Ocean depth
0
−2000
−4000
0 5 10 15 20 25 30 35
Hours before lanfall
Surge height: 1.22

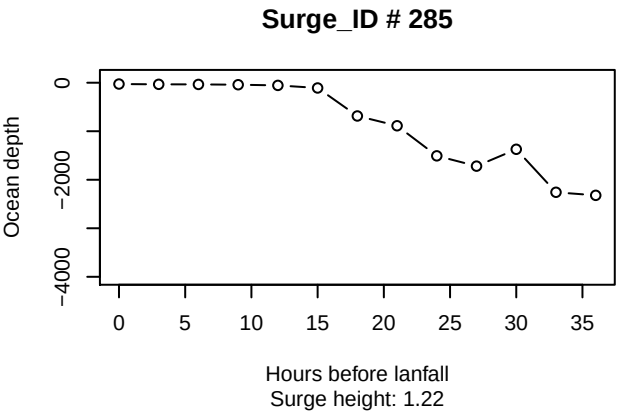
Surge_ID # 285
Ocean depth
0
−2000
−4000
0 5 10 15 20 25 30 35
Hours before lanfall
Surge height: 1.22

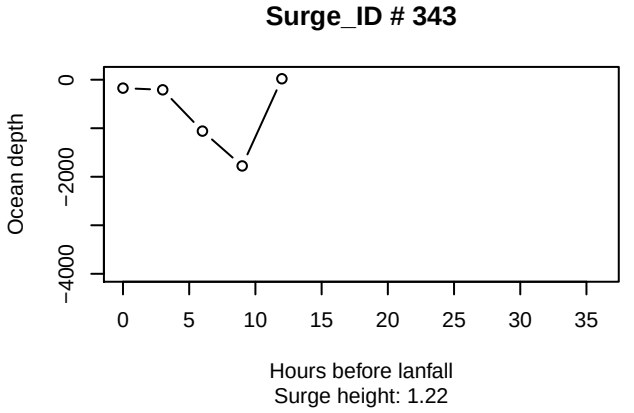
Surge_ID # 343
Ocean depth
0
−2000
−4000
0 5 10 15 20 25 30 35
Hours before lanfall
Surge height: 1.22

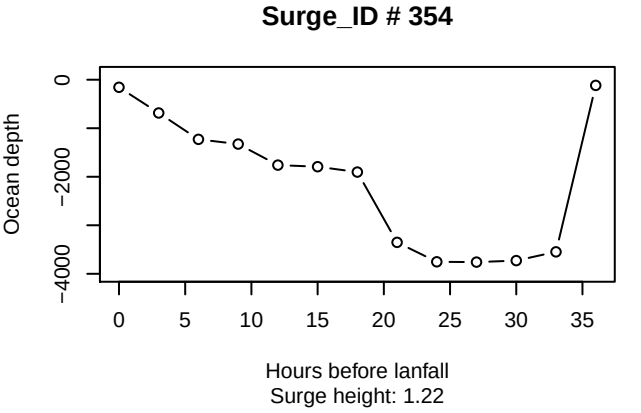
Surge_ID # 354
Ocean depth
0
−2000
−4000
0 5 10 15 20 25 30 35
Hours before lanfall
Surge height: 1.22

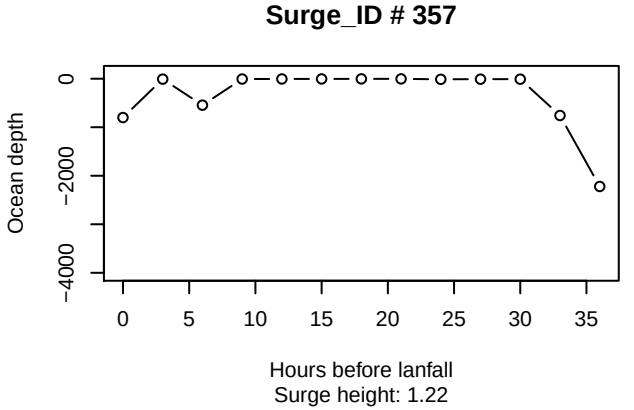
Surge_ID # 357
Ocean depth
0
−2000
−4000
0 5 10 15 20 25 30 35
Hours before lanfall
Surge height: 1.22

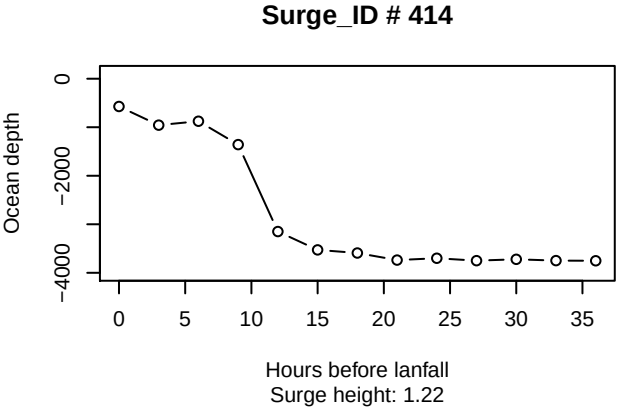
Surge_ID # 414
Ocean depth
0
−2000
−4000
0 5 10 15 20 25 30 35
Hours before lanfall
Surge height: 1.22

# HIGH-PASS STATISTICS BY SAMPLE SIZE

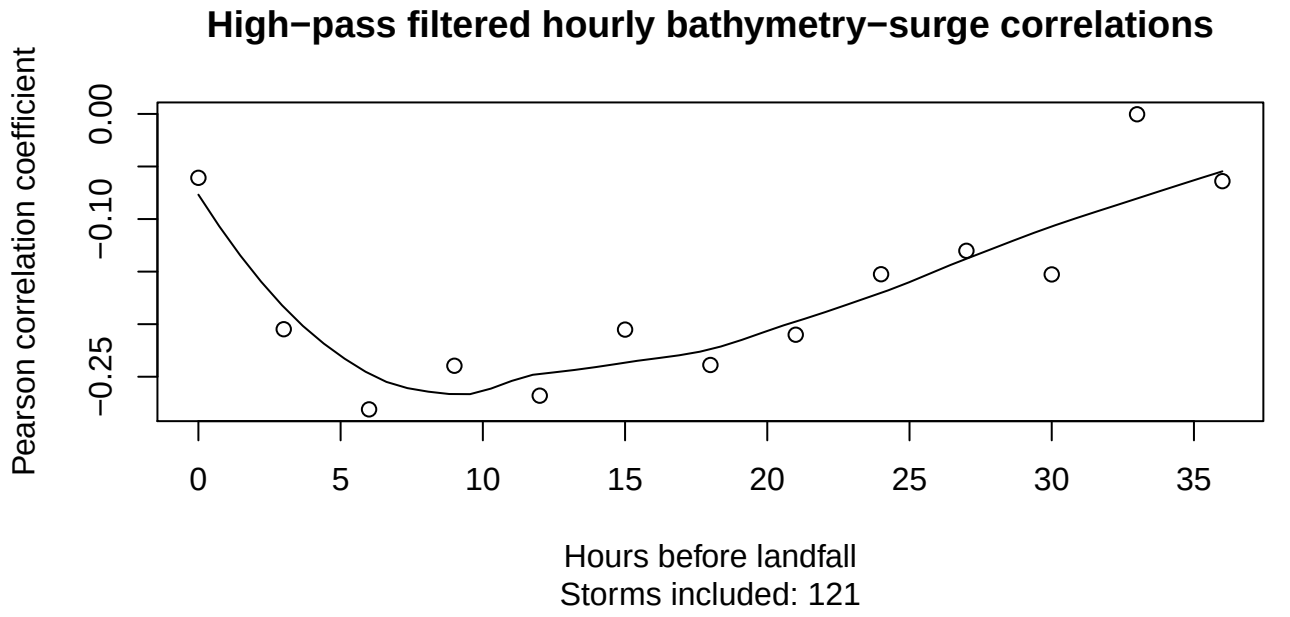
High−pass filtered hourly bathymetry−surge correlations
Pearson correlation coefficient
0.00
−0.10
−0.25
0
5
10
15
20
25
30
35
Hours before landfall
Storms included: 121

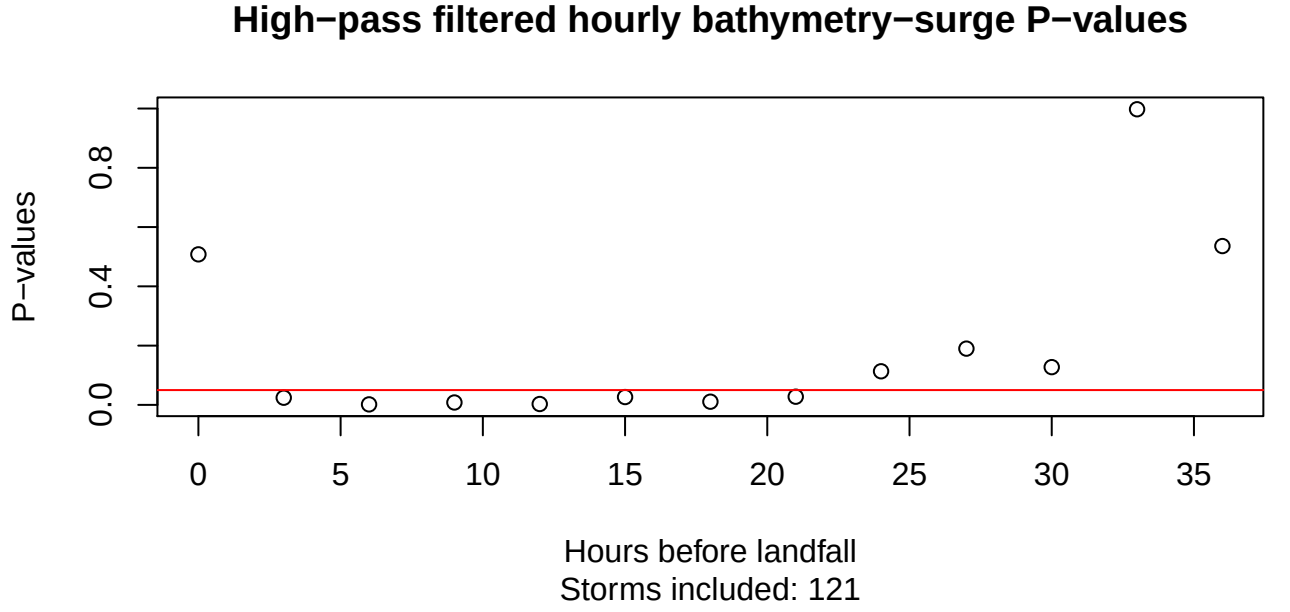
High−pass filtered hourly bathymetry−surge P−values
P−values
0.0
0.4
0.8
0
5
10
15
20
25
30
35
Hours before landfall
Storms included: 121

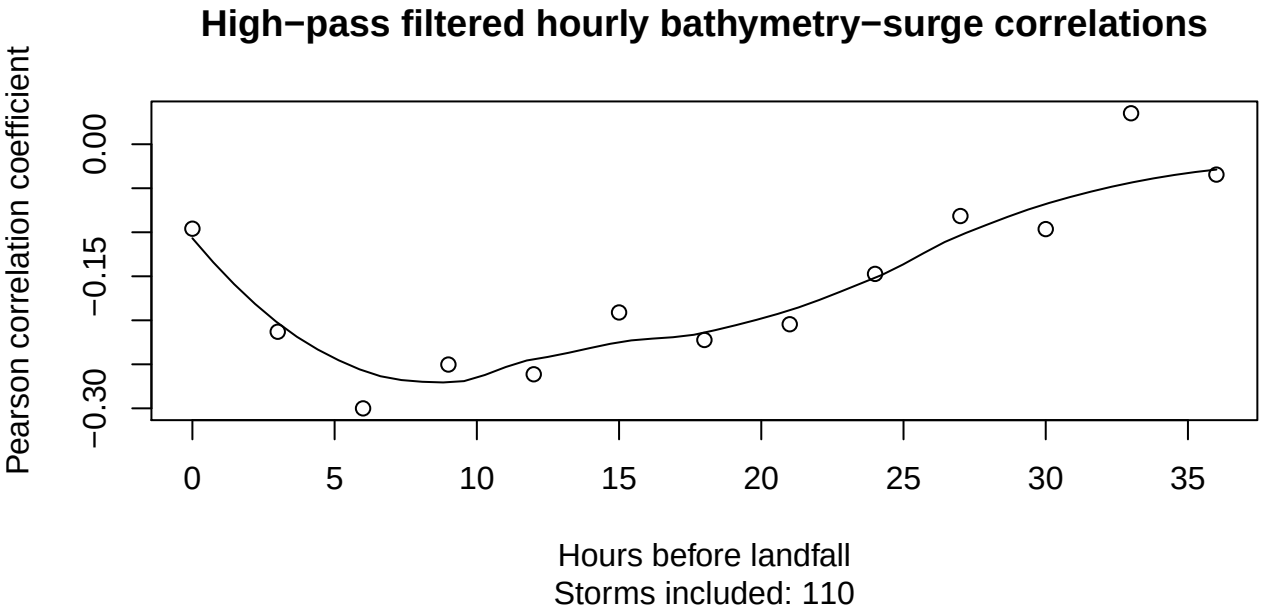
High−pass filtered hourly bathymetry−surge correlations
Pearson correlation coefficient
0.00
−0.15
−0.30
0
5
10
15
20
25
30
35
Hours before landfall
Storms included: 110

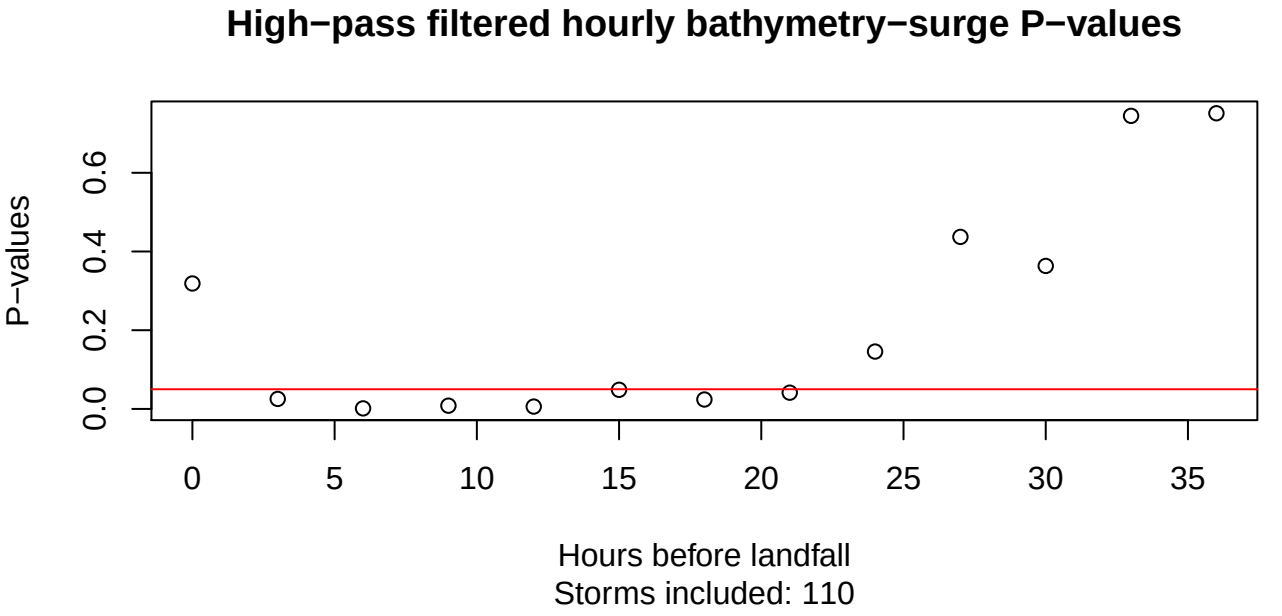
High−pass filtered hourly bathymetry−surge P−values
P−values
0.0
0.2
0.4
0.6
0
5
10
15
20
25
30
35
Hours before landfall
Storms included: 110

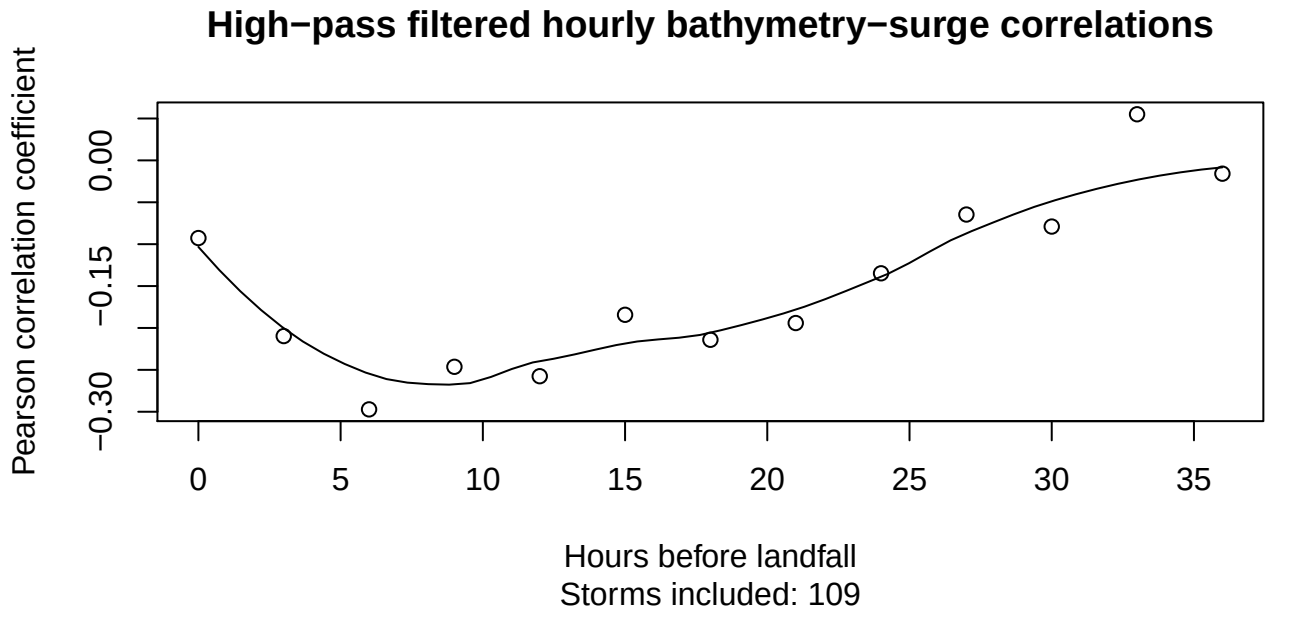
High−pass filtered hourly bathymetry−surge correlations
Pearson correlation coefficient
−0.30
−0.15
0.00
0
5
10
15
20
25
30
35
Hours before landfall
Storms included: 109

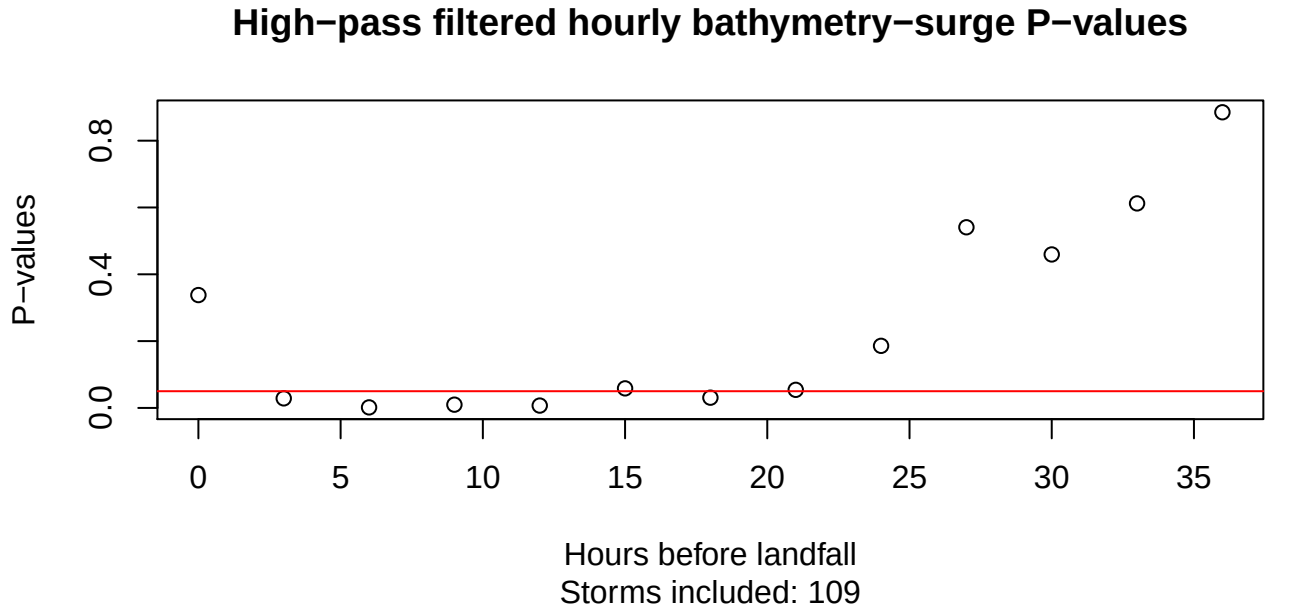
High−pass filtered hourly bathymetry−surge P−values
P−values
0.0
0.4
0.8
0
5
10
15
20
25
30
35
Hours before landfall
Storms included: 109

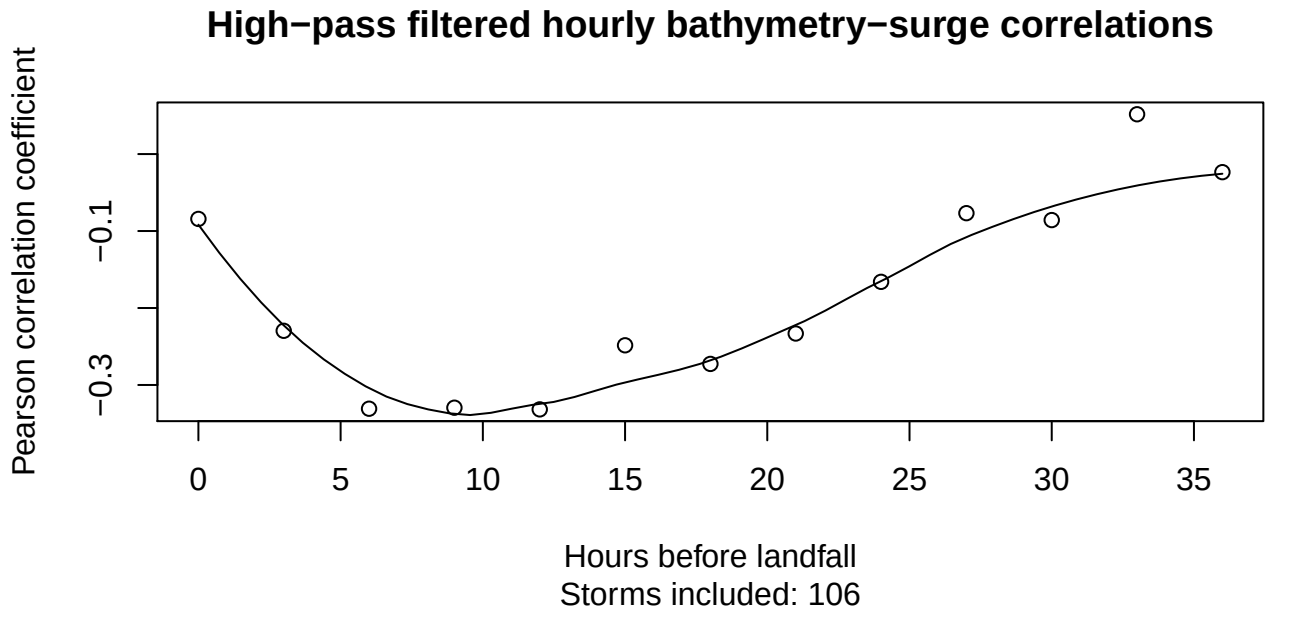
High−pass filtered hourly bathymetry−surge correlations
Pearson correlation coefficient
−0.3
−0.1
0
5
10
15
20
25
30
35
Hours before landfall
Storms included: 106

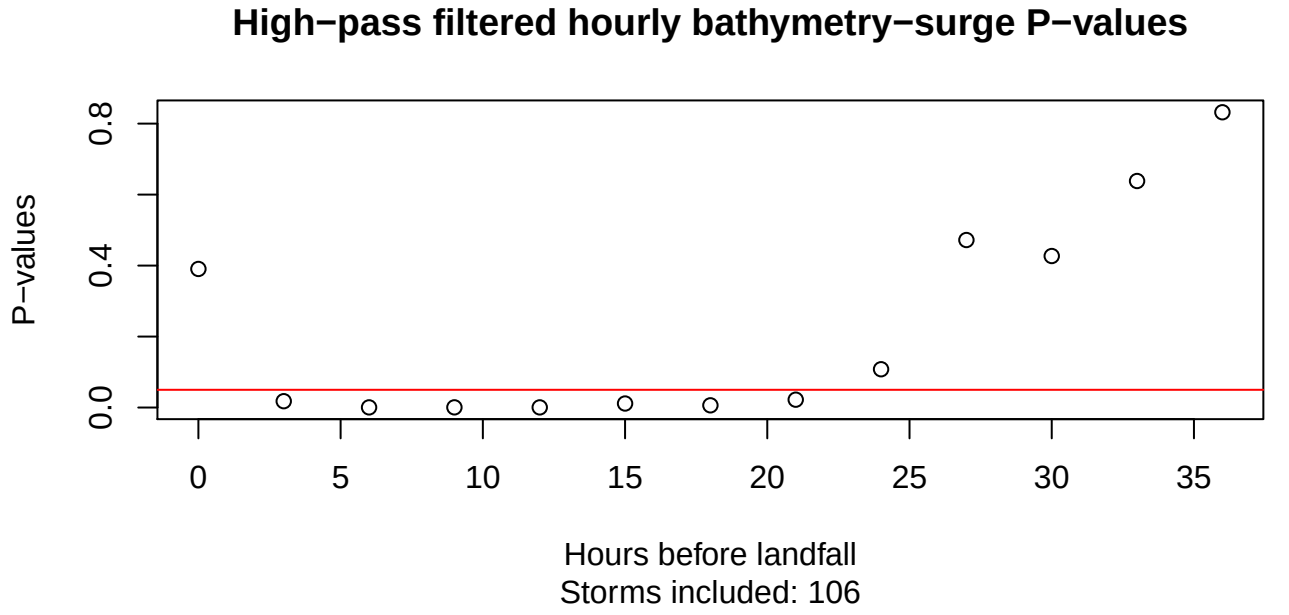
High−pass filtered hourly bathymetry−surge P−values
P−values
0.0
0.4
0.8
0
5
10
15
20
25
30
35
Hours before landfall
Storms included: 106

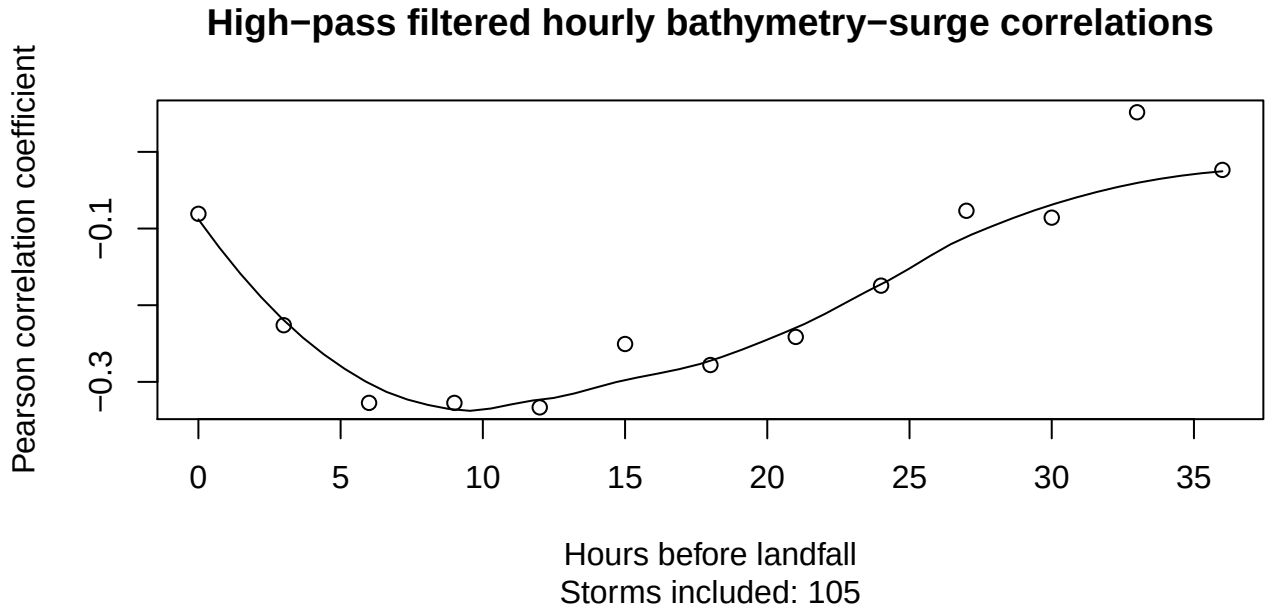
High−pass filtered hourly bathymetry−surge correlations
Pearson correlation coefficient
−0.3
−0.1
0
5
10
15
20
25
30
35
Hours before landfall
Storms included: 105

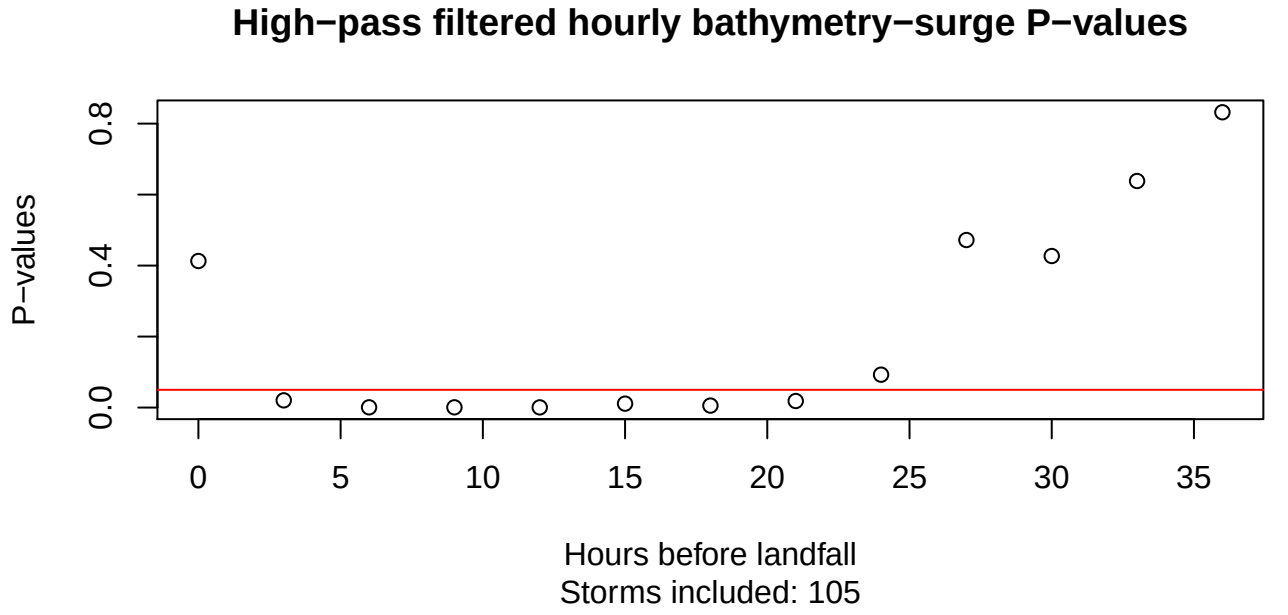
High−pass filtered hourly bathymetry−surge P−values
P−values
0.0
0.4
0.8
0
5
10
15
20
25
30
35
Hours before landfall
Storms included: 105

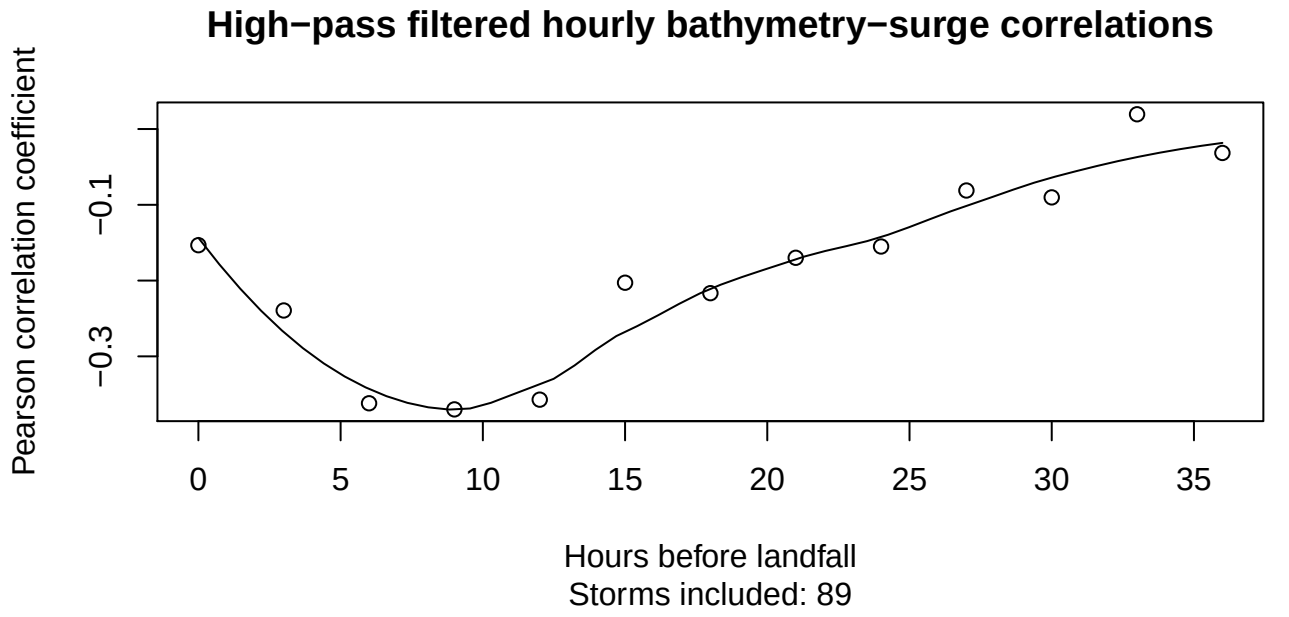
High−pass filtered hourly bathymetry−surge correlations
Pearson correlation coefficient
−0.3
−0.1
0
5
10
15
20
25
30
35
Hours before landfall
Storms included: 89

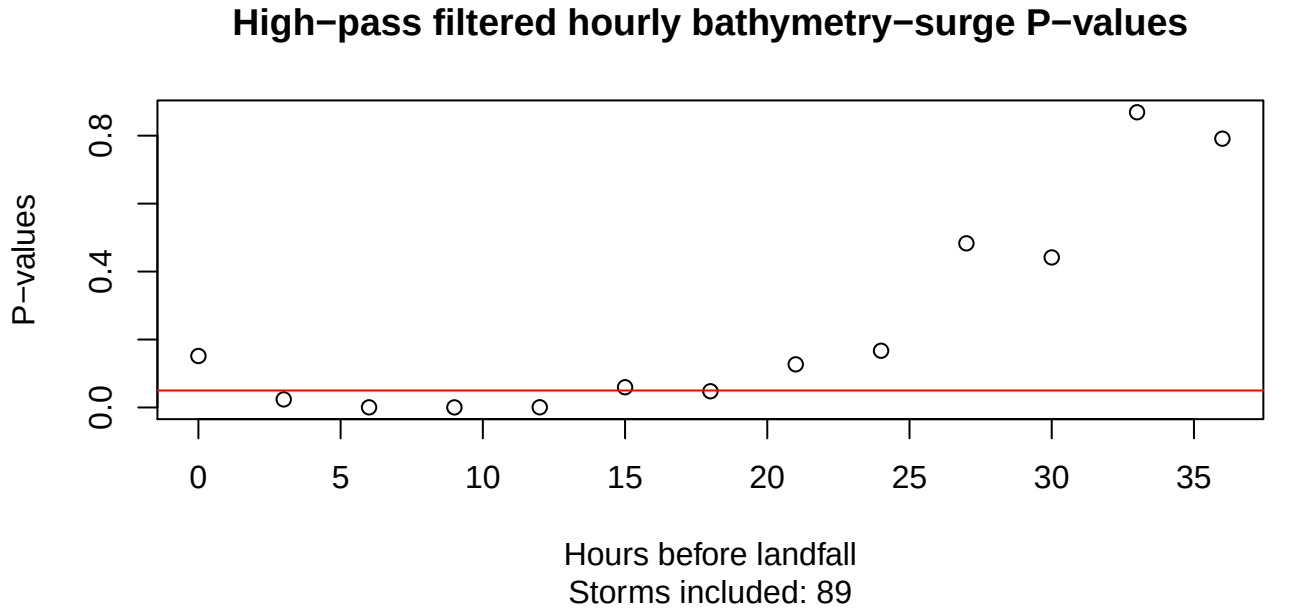
High−pass filtered hourly bathymetry−surge P−values
P−values
0.0
0.4
0.8
0
5
10
15
20
25
30
35
Hours before landfall
Storms included: 89

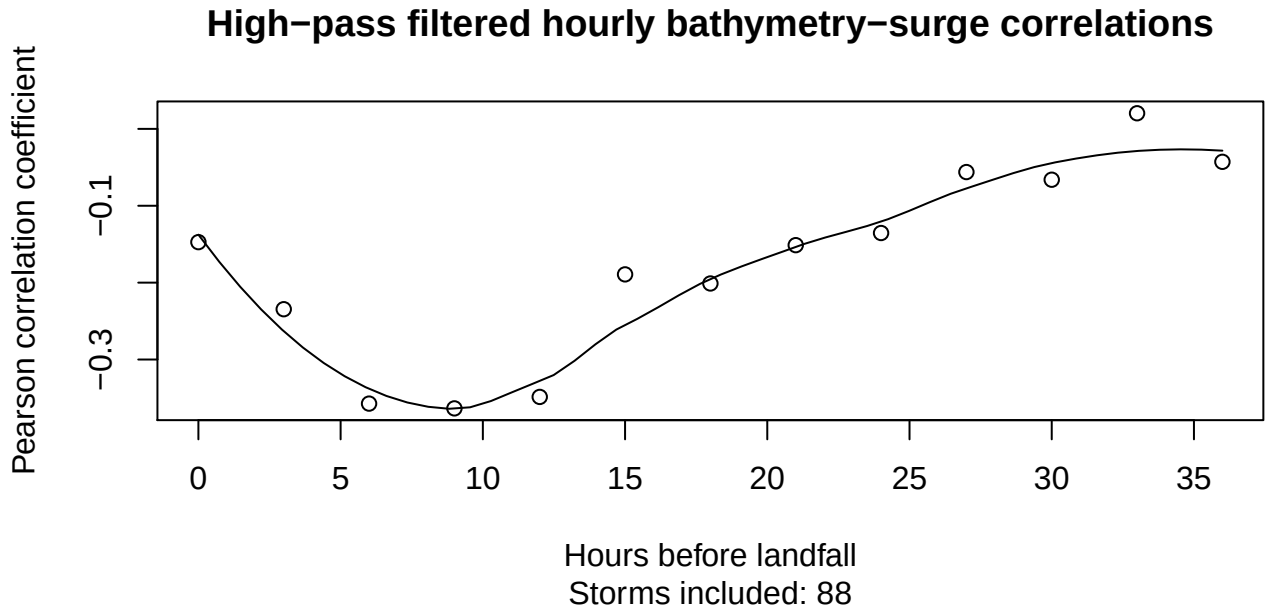
High−pass filtered hourly bathymetry−surge correlations
Pearson correlation coefficient
−0.3
−0.1
0
5
10
15
20
25
30
35
Hours before landfall
Storms included: 88

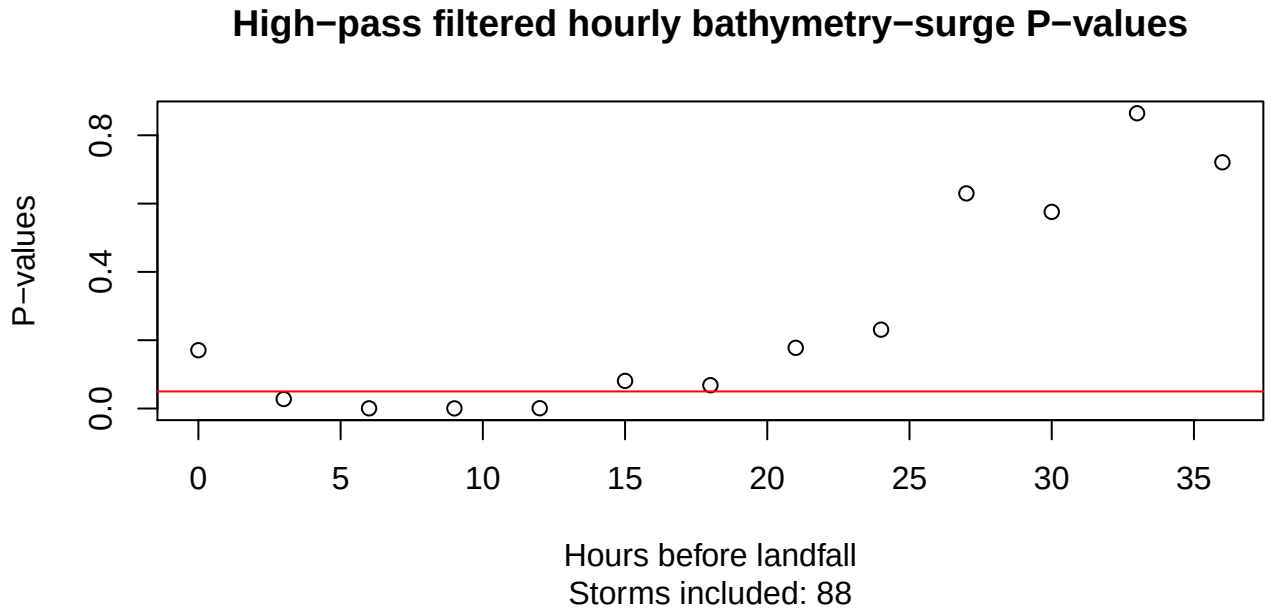
High−pass filtered hourly bathymetry−surge P−values
P−values
0.0
0.4
0.8
0
5
10
15
20
25
30
35
Hours before landfall
Storms included: 88

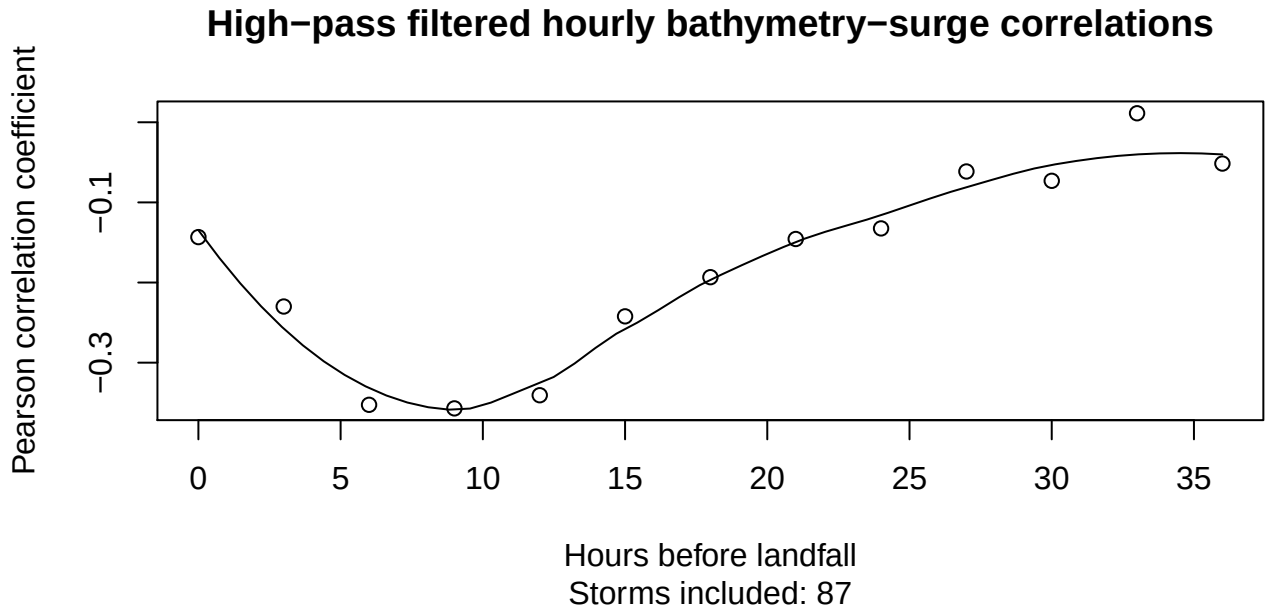
High−pass filtered hourly bathymetry−surge correlations
Pearson correlation coefficient
−0.3
−0.1
0
5
10
15
20
25
30
35
Hours before landfall
Storms included: 87

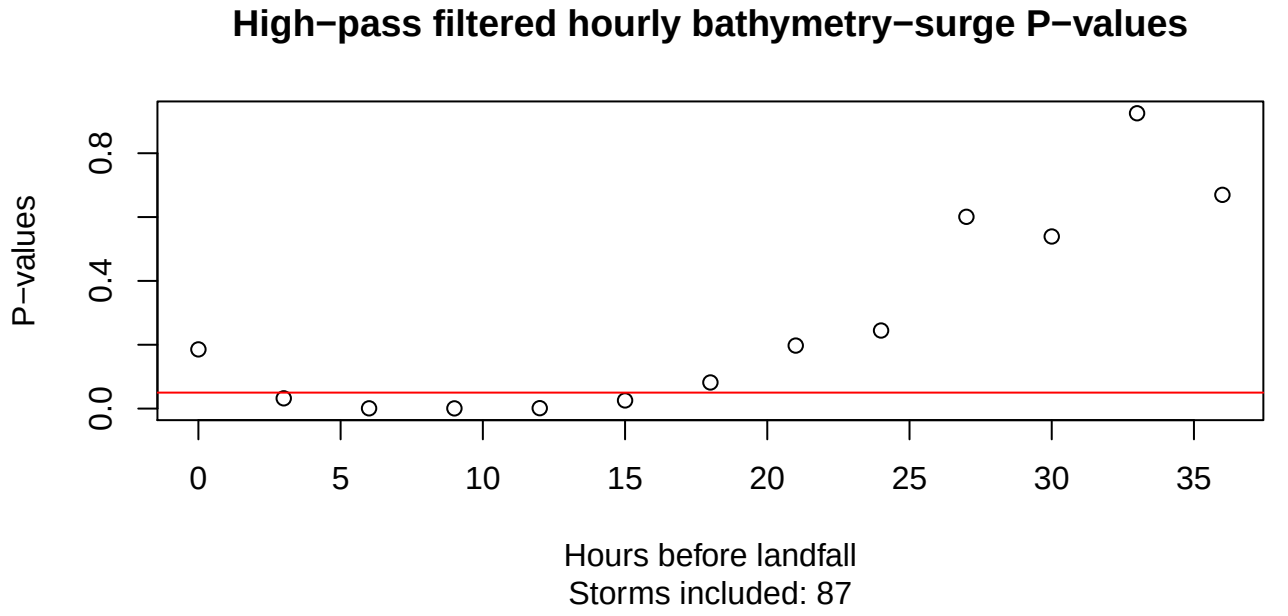
High−pass filtered hourly bathymetry−surge P−values
P−values
0.0
0.4
0.8
0
5
10
15
20
25
30
35
Hours before landfall
Storms included: 87

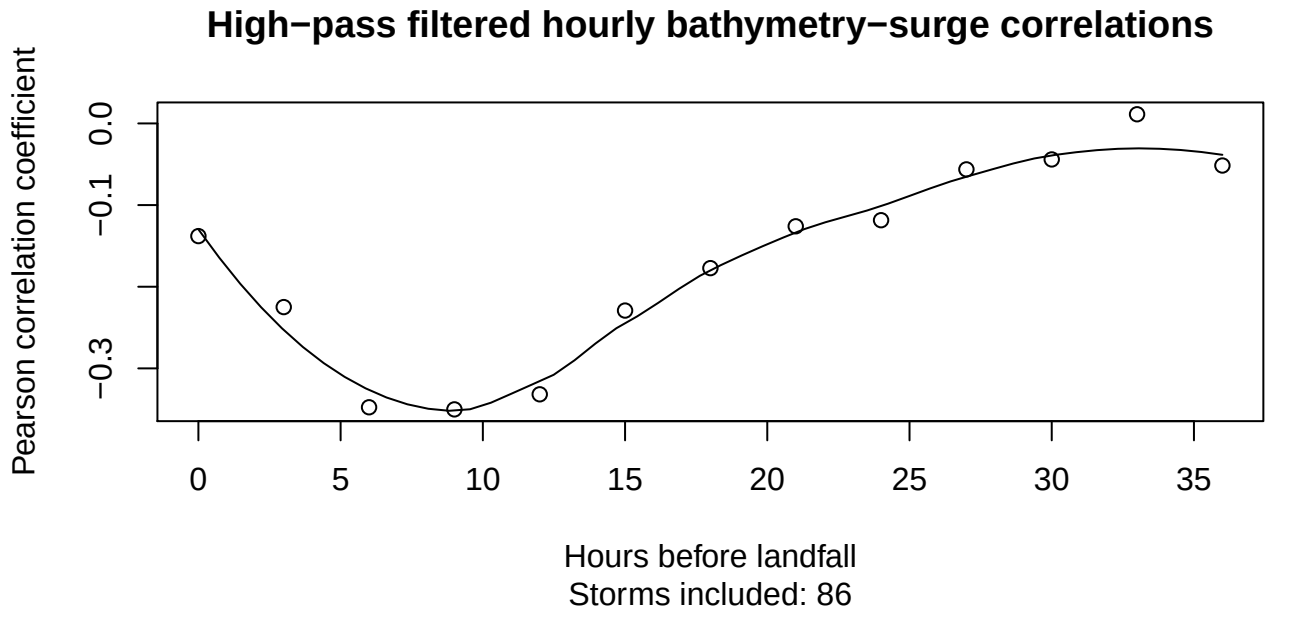
High−pass filtered hourly bathymetry−surge correlations
Pearson correlation coefficient
0.0
−0.1
−0.3
0
5
10
15
20
25
30
35
Hours before landfall
Storms included: 86

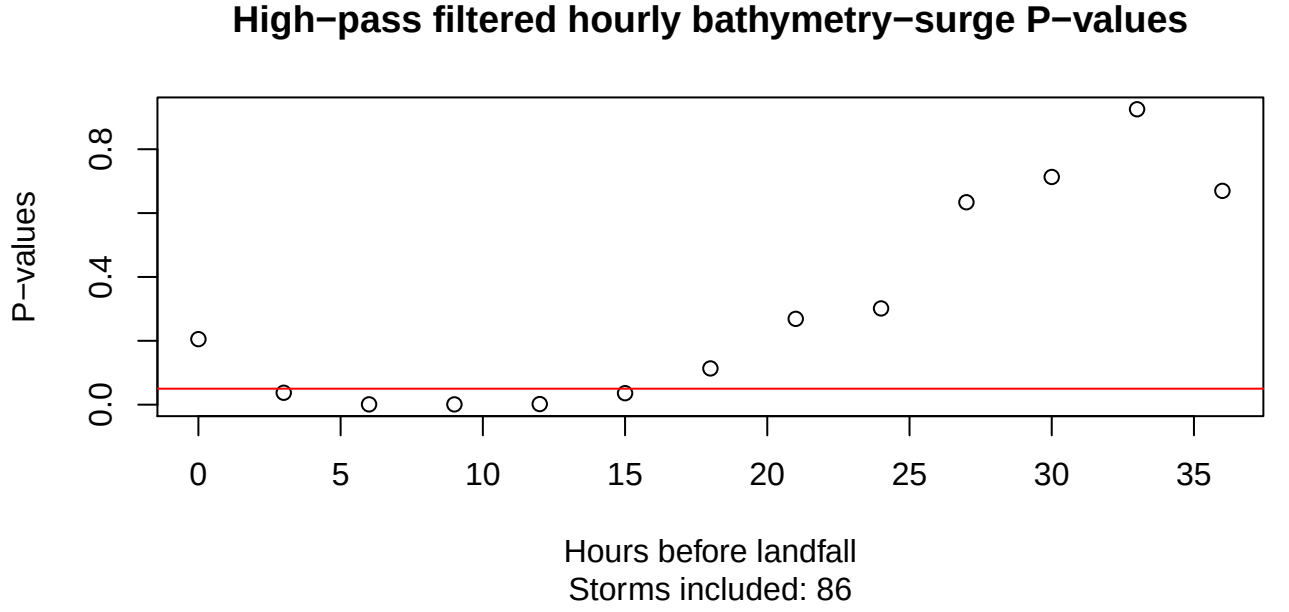
High−pass filtered hourly bathymetry−surge P−values
P−values
0.0
0.4
0.8
0
5
10
15
20
25
30
35
Hours before landfall
Storms included: 86

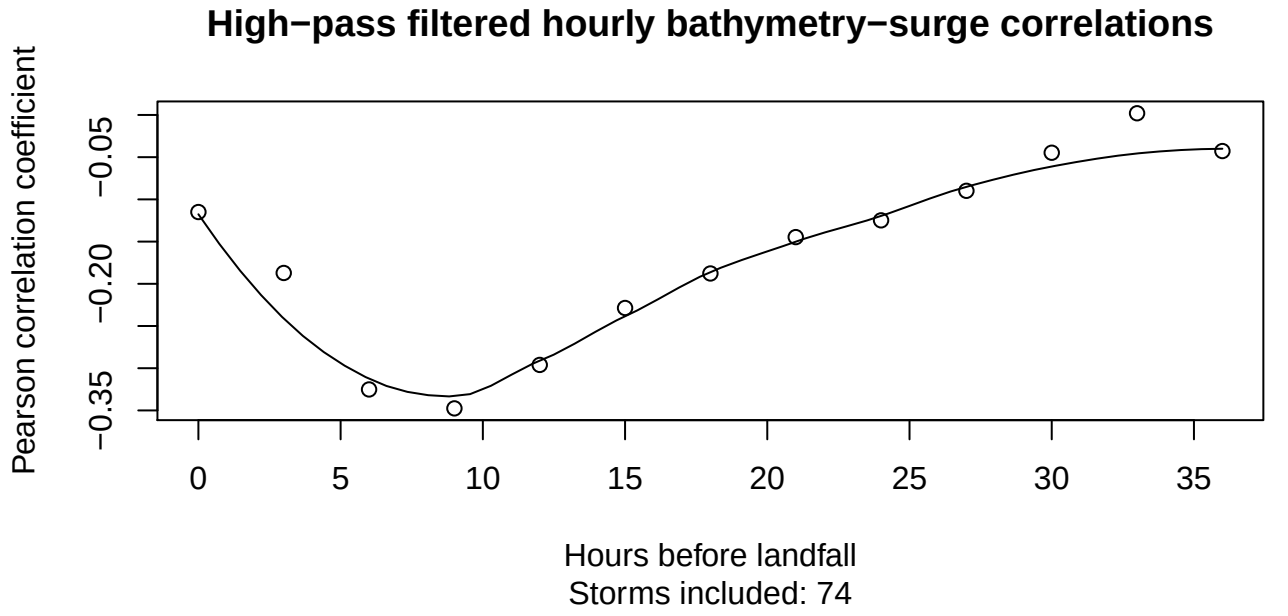
High−pass filtered hourly bathymetry−surge correlations
Pearson correlation coefficient
−0.35
−0.20
−0.05
0
5
10
15
20
25
30
35
Hours before landfall
Storms included: 74

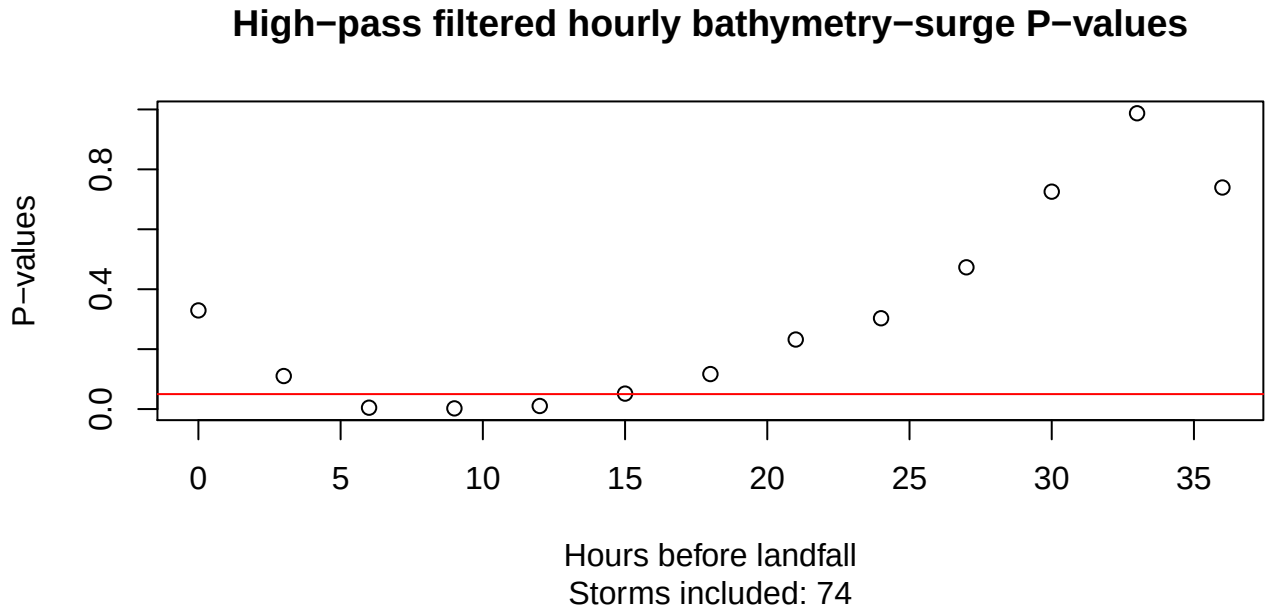
High−pass filtered hourly bathymetry−surge P−values
P−values
0.0
0.4
0.8
0
5
10
15
20
25
30
35
Hours before landfall
Storms included: 74

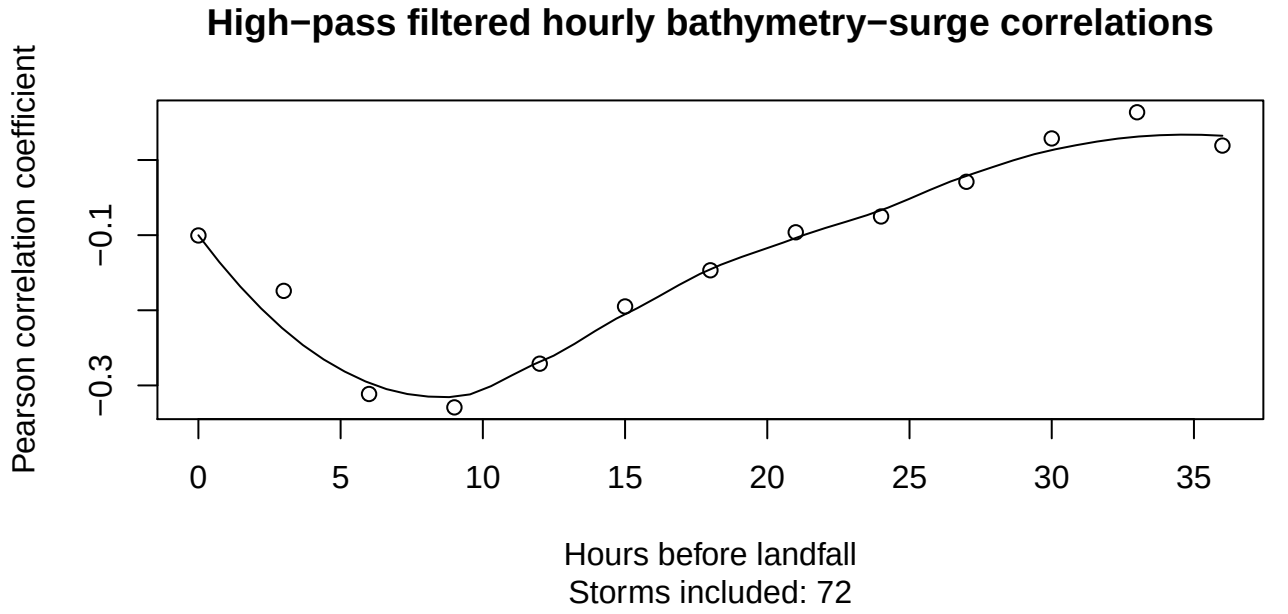
High−pass filtered hourly bathymetry−surge correlations
Pearson correlation coefficient
−0.3
−0.1
0
5
10
15
20
25
30
35
Hours before landfall
Storms included: 72

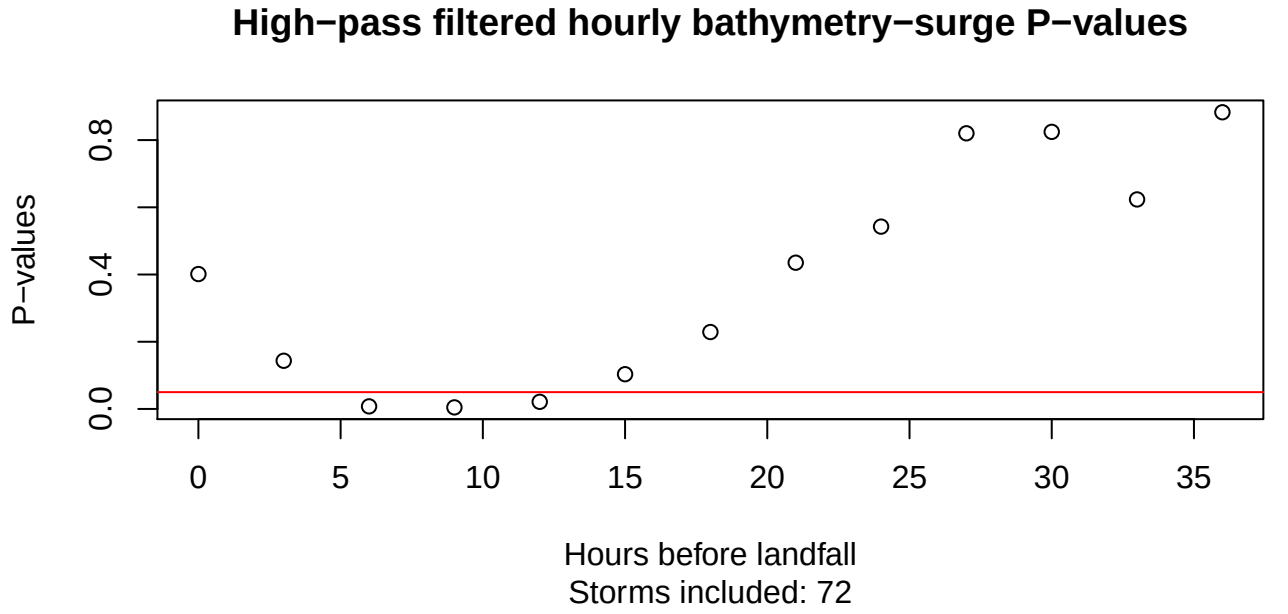
High−pass filtered hourly bathymetry−surge P−values
P−values
0.0
0.4
0.8
0
5
10
15
20
25
30
35
Hours before landfall
Storms included: 72

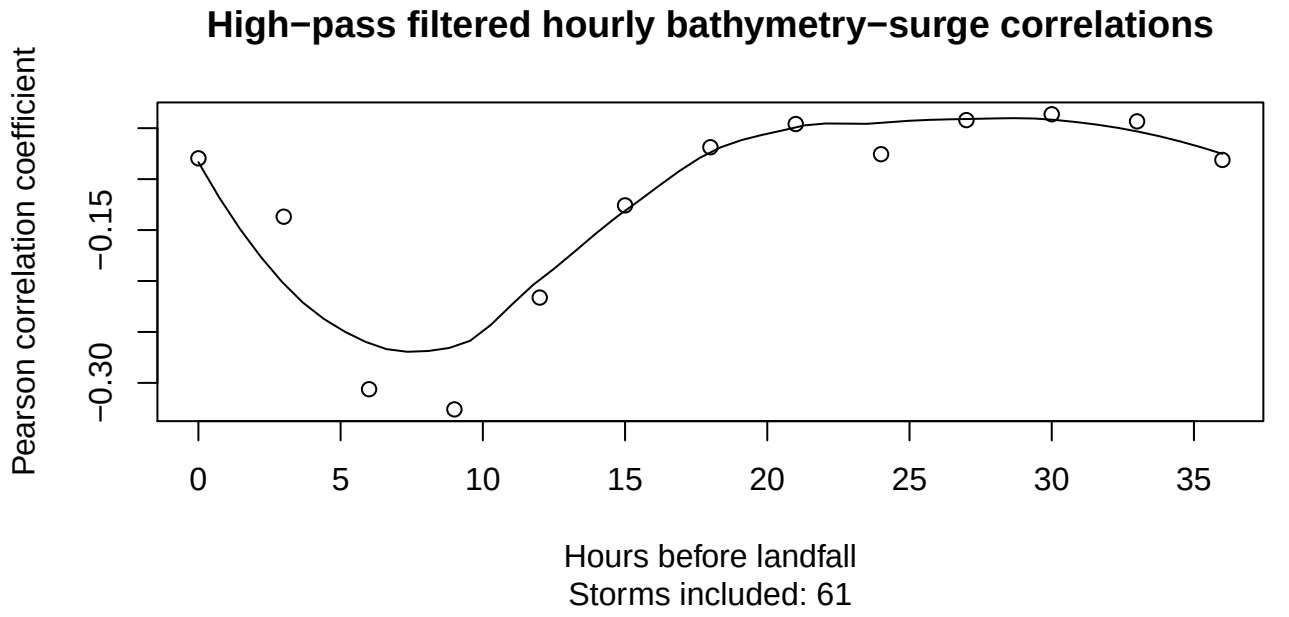
High−pass filtered hourly bathymetry−surge correlations
Pearson correlation coefficient
−0.30
−0.15
0
5
10
15
20
25
30
35
Hours before landfall
Storms included: 61

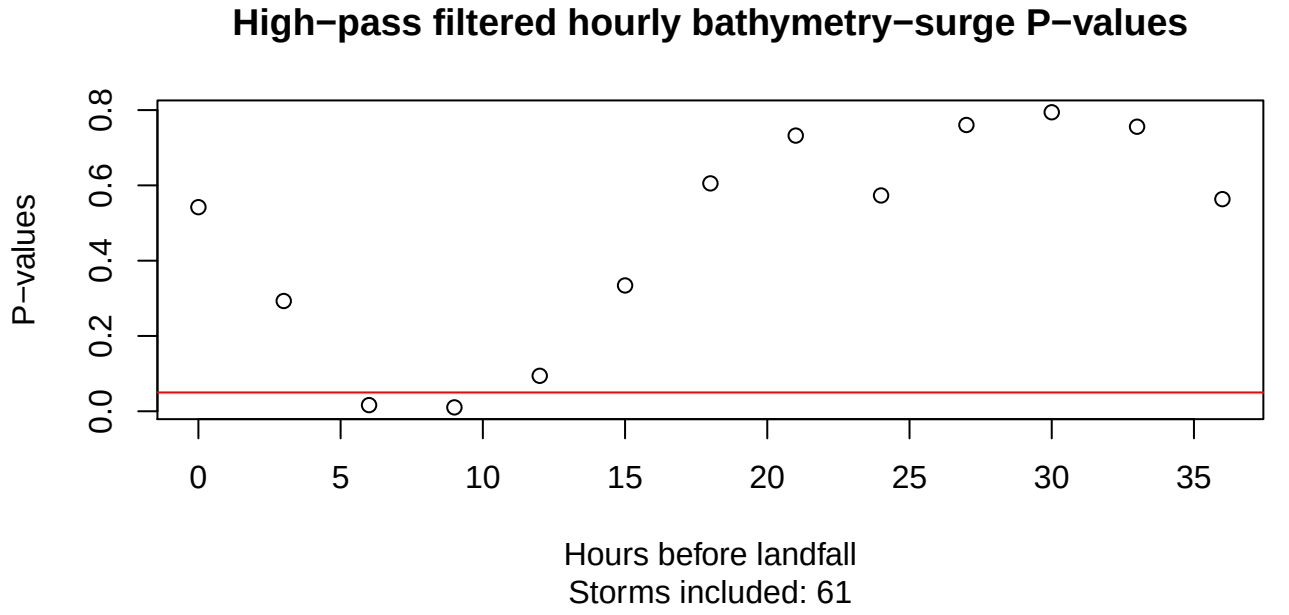
High−pass filtered hourly bathymetry−surge P−values
P−values
0.0
0.2
0.4
0.6
0.8
0
5
10
15
20
25
30
35
Hours before landfall
Storms included: 61

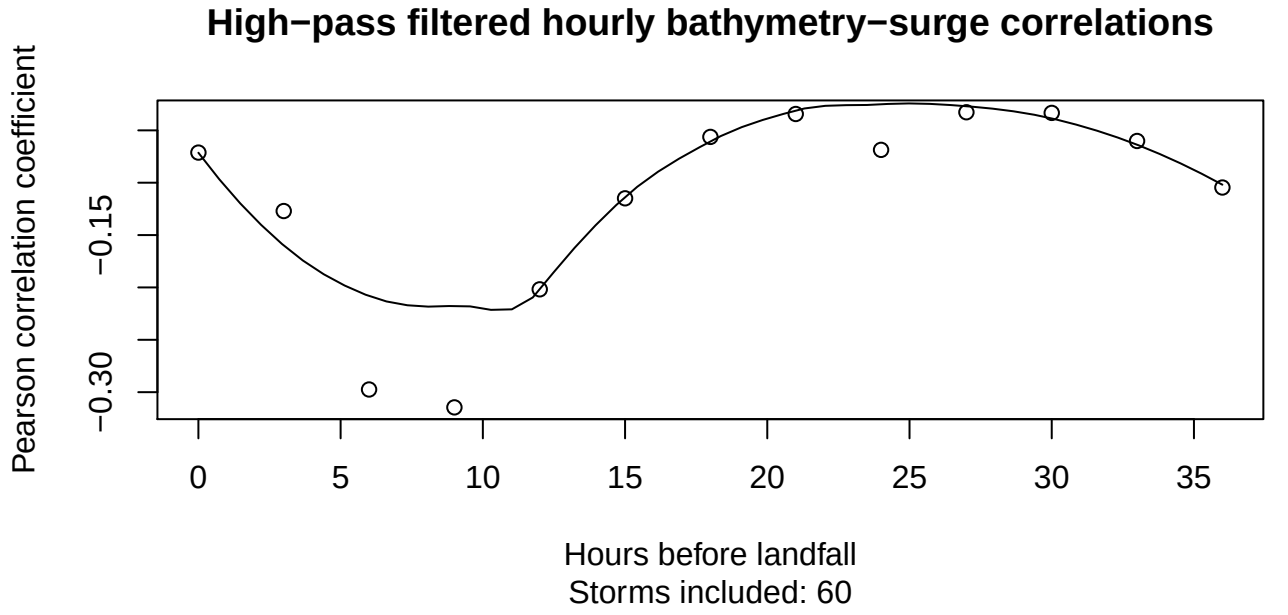
High−pass filtered hourly bathymetry−surge correlations
Pearson correlation coefficient
−0.30
−0.15
0
5
10
15
20
25
30
35
Hours before landfall
Storms included: 60

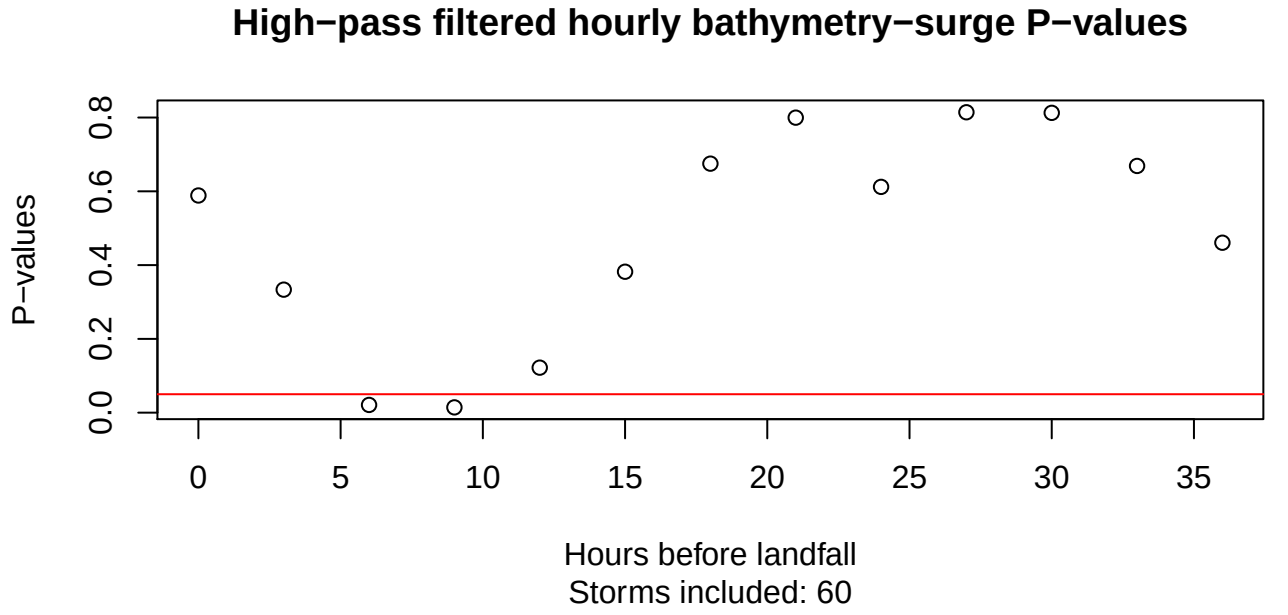
High−pass filtered hourly bathymetry−surge P−values
P−values
0.0
0.2
0.4
0.6
0.8
0
5
10
15
20
25
30
35
Hours before landfall
Storms included: 60

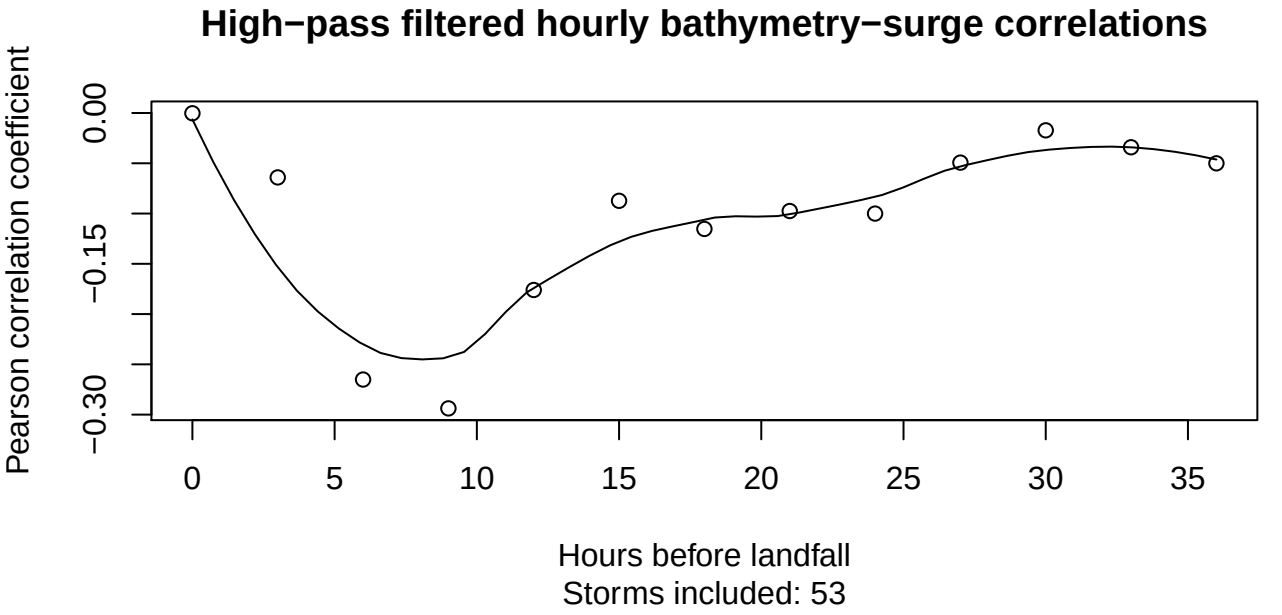
High−pass filtered hourly bathymetry−surge correlations
Pearson correlation coefficient
0.00
−0.15
−0.30
0
5
10
15
20
25
30
35
Hours before landfall
Storms included: 53

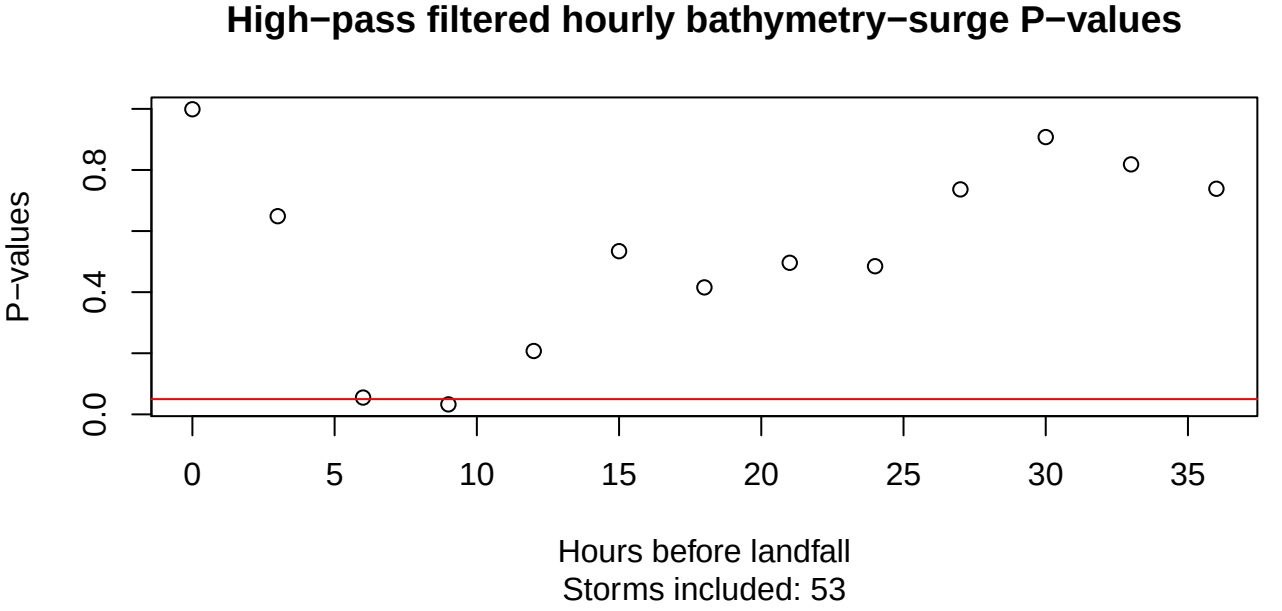
High−pass filtered hourly bathymetry−surge P−values
P−values
0.0
0.4
0.8
0
5
10
15
20
25
30
35
Hours before landfall
Storms included: 53

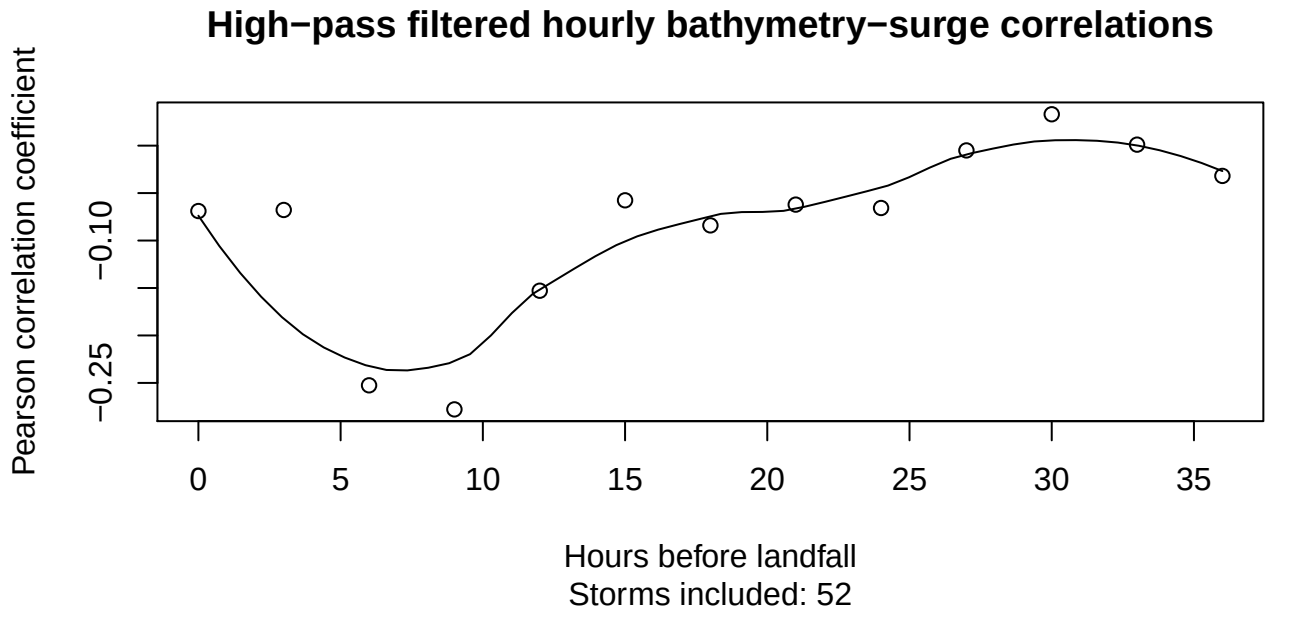
High−pass filtered hourly bathymetry−surge correlations
Pearson correlation coefficient
−0.25
−0.10
0
5
10
15
20
25
30
35
Hours before landfall
Storms included: 52

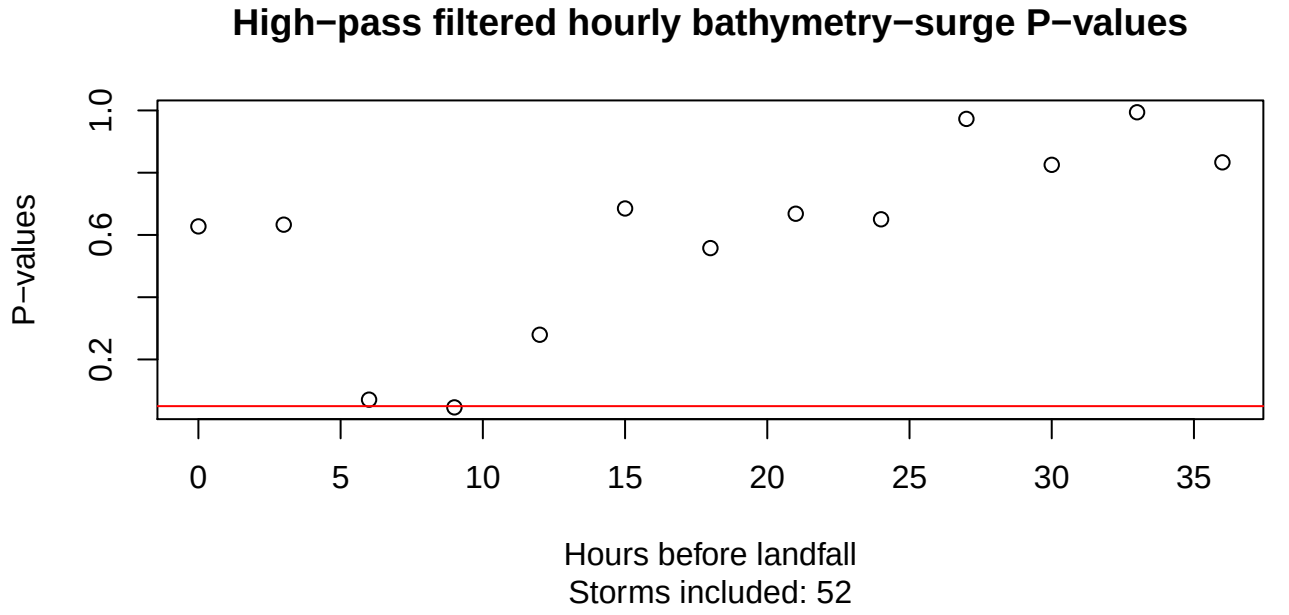
High−pass filtered hourly bathymetry−surge P−values
P−values
0.2
0.6
1.0
0
5
10
15
20
25
30
35
Hours before landfall
Storms included: 52

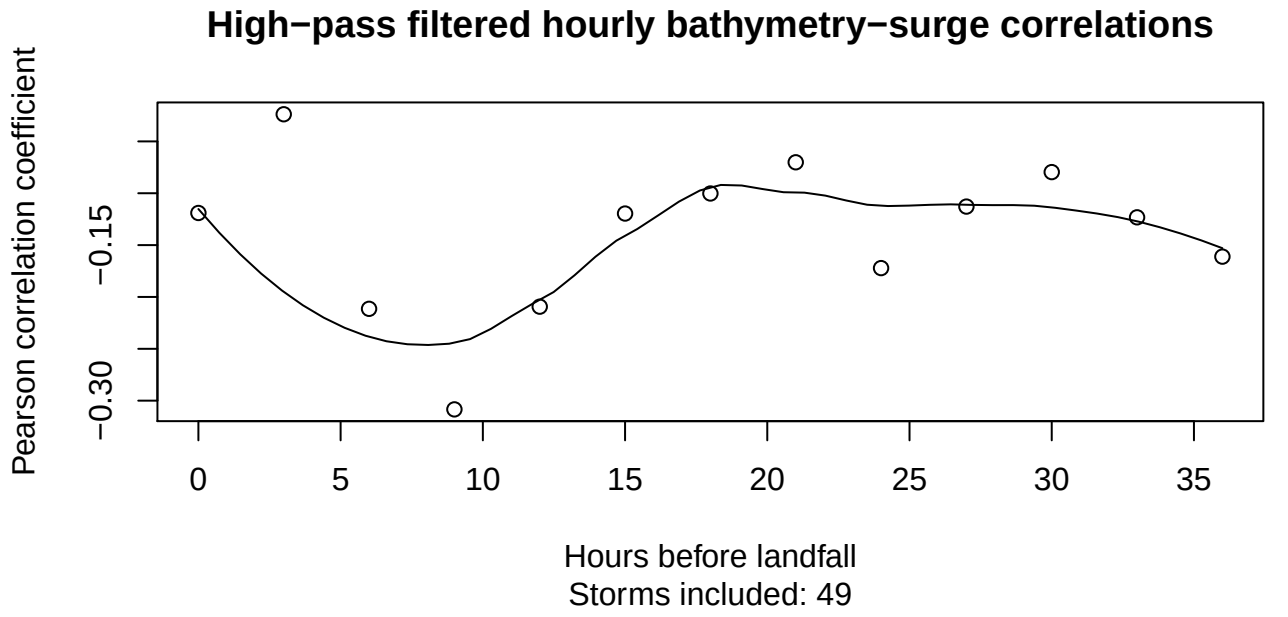
High−pass filtered hourly bathymetry−surge correlations
Pearson correlation coefficient
−0.30
−0.15
0
5
10
15
20
25
30
35
Hours before landfall
Storms included: 49

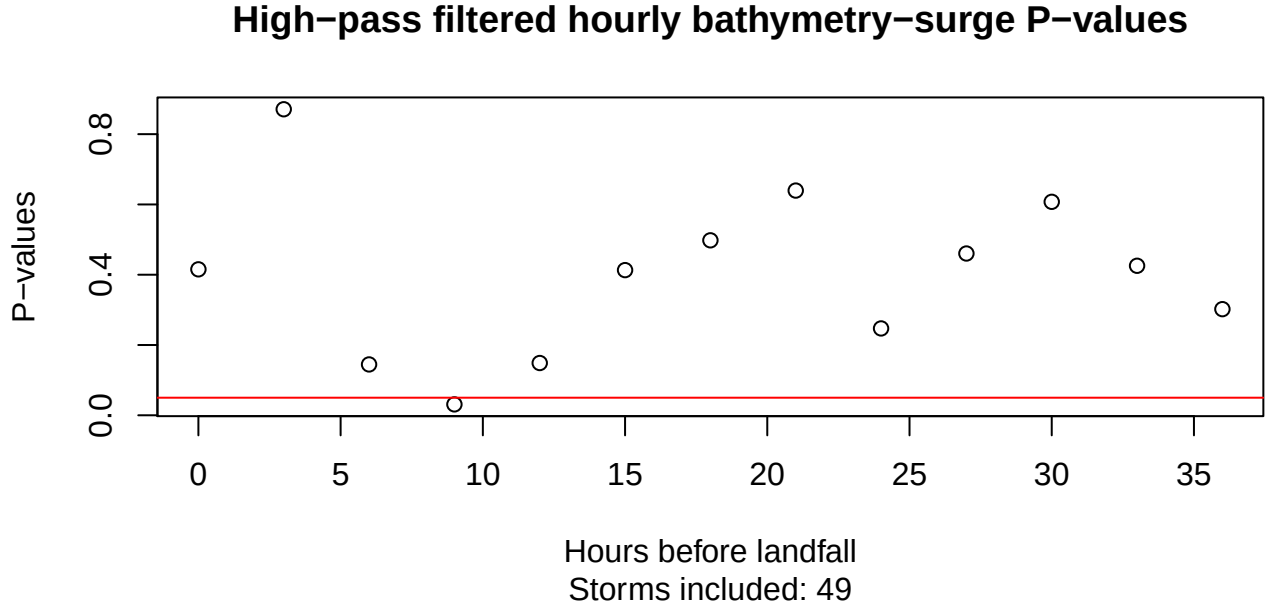
High−pass filtered hourly bathymetry−surge P−values
P−values
0.0
0.4
0.8
0
5
10
15
20
25
30
35
Hours before landfall
Storms included: 49

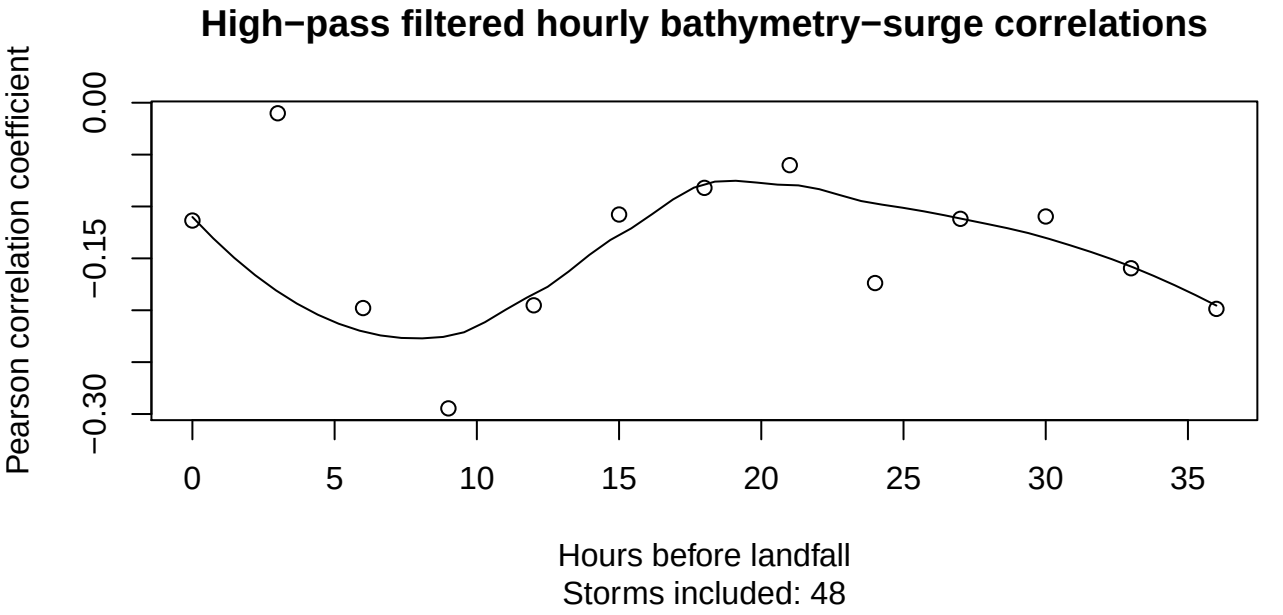
High−pass filtered hourly bathymetry−surge correlations
Pearson correlation coefficient
0.00
−0.15
−0.30
0
5
10
15
20
25
30
35
Hours before landfall
Storms included: 48

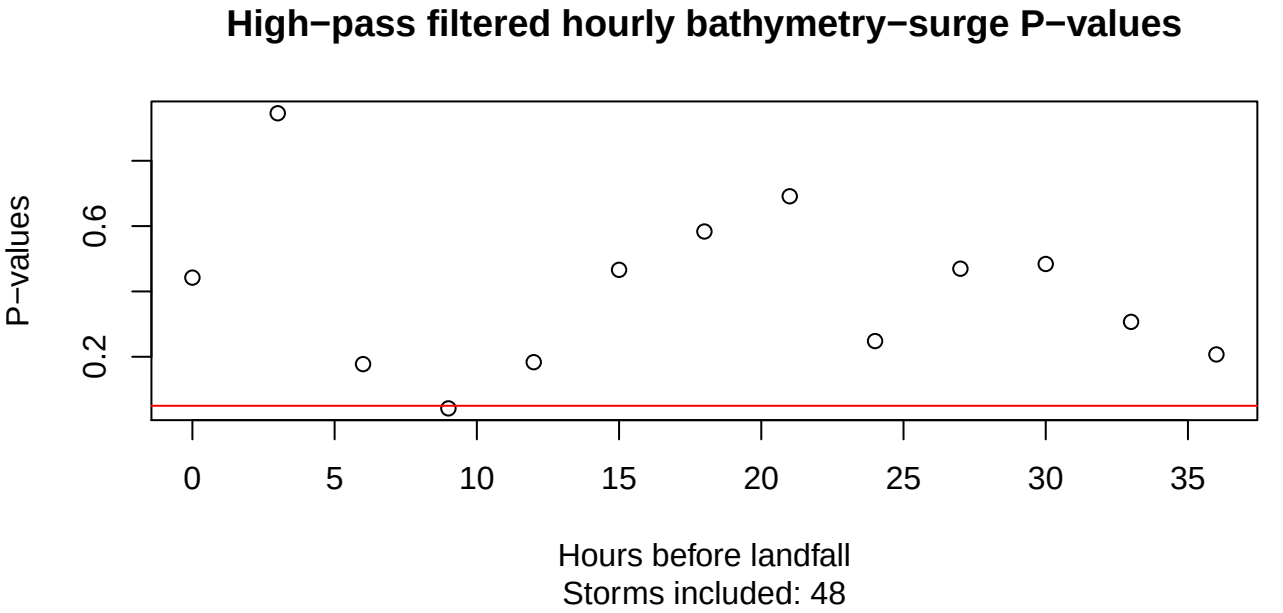
High−pass filtered hourly bathymetry−surge P−values
P−values
0.6
0.2
0
5
10
15
20
25
30
35
Hours before landfall
Storms included: 48

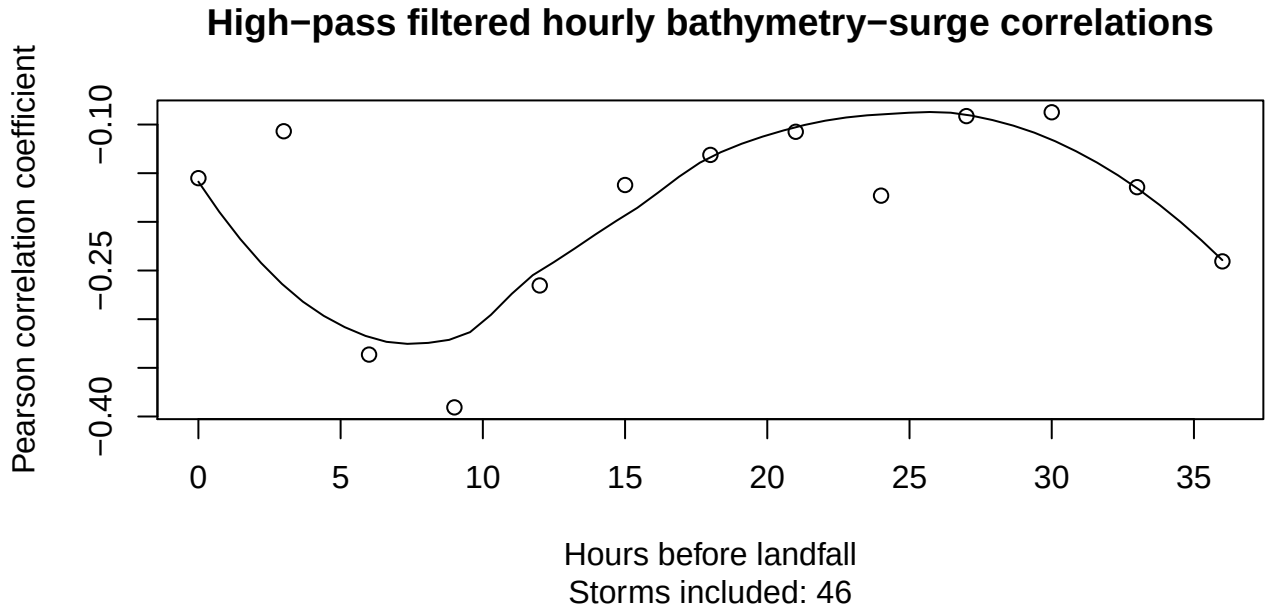
High−pass filtered hourly bathymetry−surge correlations
Pearson correlation coefficient
−0.10
−0.25
−0.40
0
5
10
15
20
25
30
35
Hours before landfall
Storms included: 46

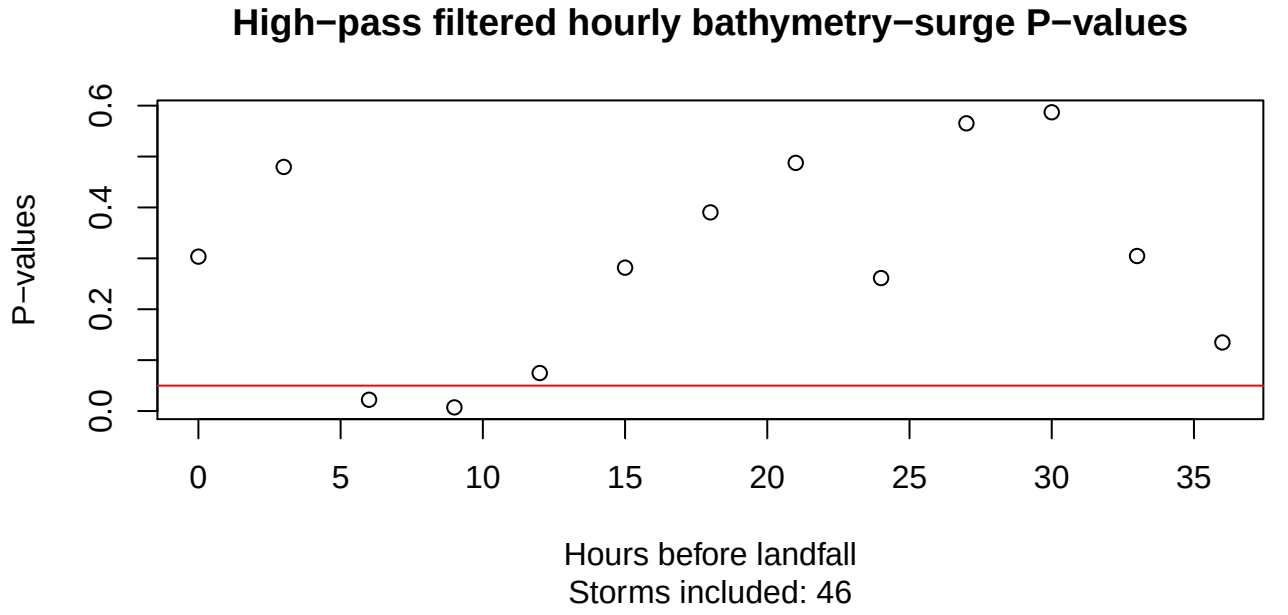
High−pass filtered hourly bathymetry−surge P−values
P−values
0.0
0.2
0.4
0.6
0
5
10
15
20
25
30
35
Hours before landfall
Storms included: 46

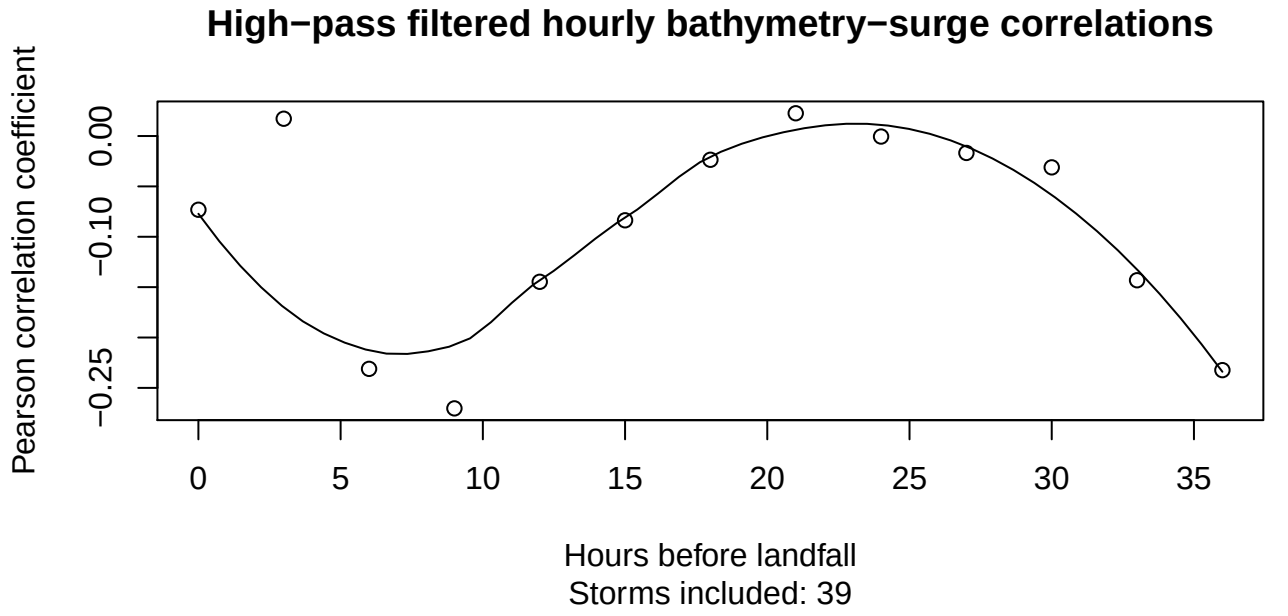
High−pass filtered hourly bathymetry−surge correlations
Pearson correlation coefficient
0.00
−0.10
−0.25
0
5
10
15
20
25
30
35
Hours before landfall
Storms included: 39

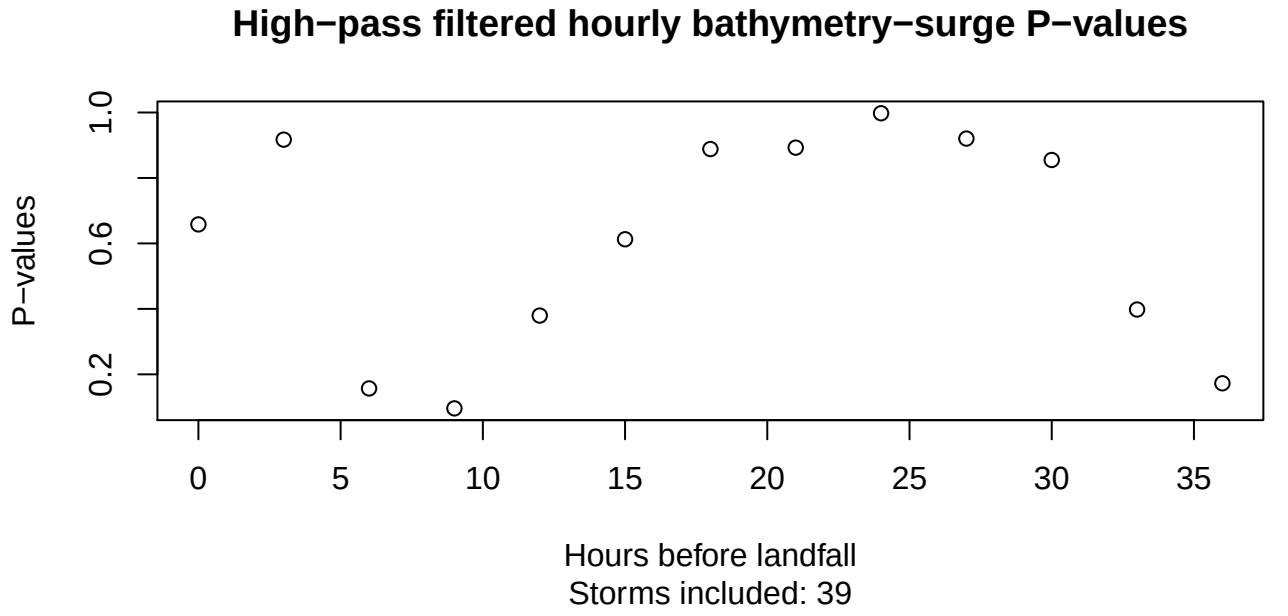
High−pass filtered hourly bathymetry−surge P−values
P−values
1.0
0.6
0.2
0
5
10
15
20
25
30
35
Hours before landfall
Storms included: 39

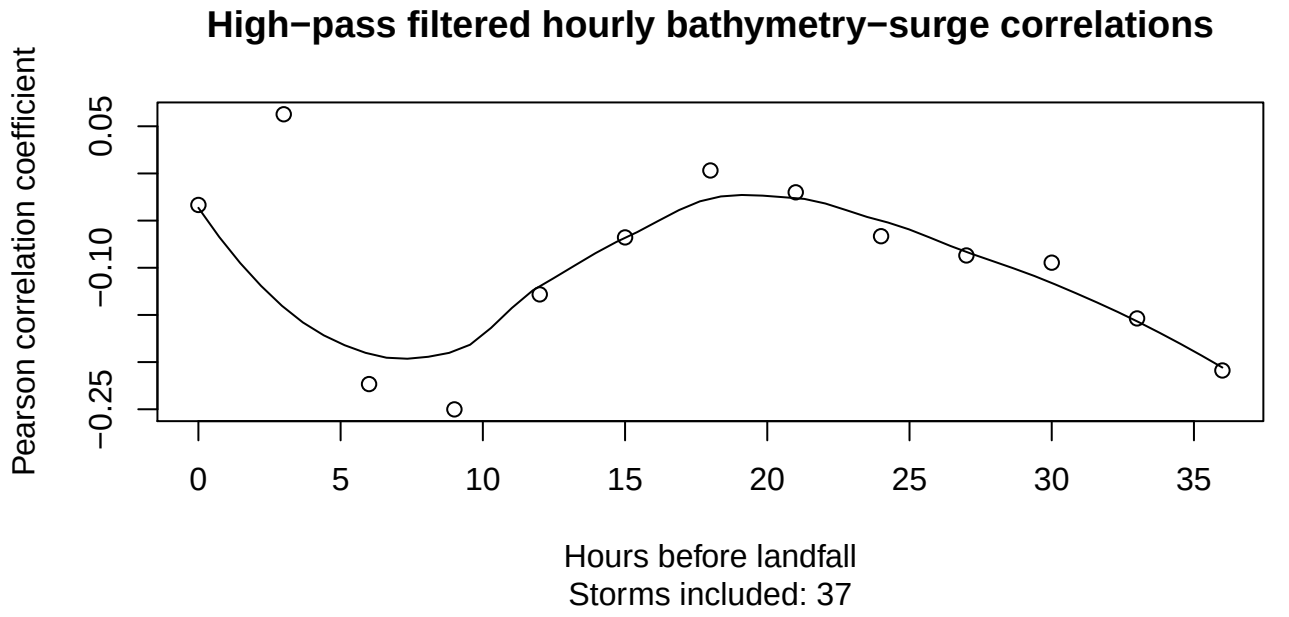
High−pass filtered hourly bathymetry−surge correlations
Pearson correlation coefficient
0.05
−0.10
−0.25
0
5
10
15
20
25
30
35
Hours before landfall
Storms included: 37

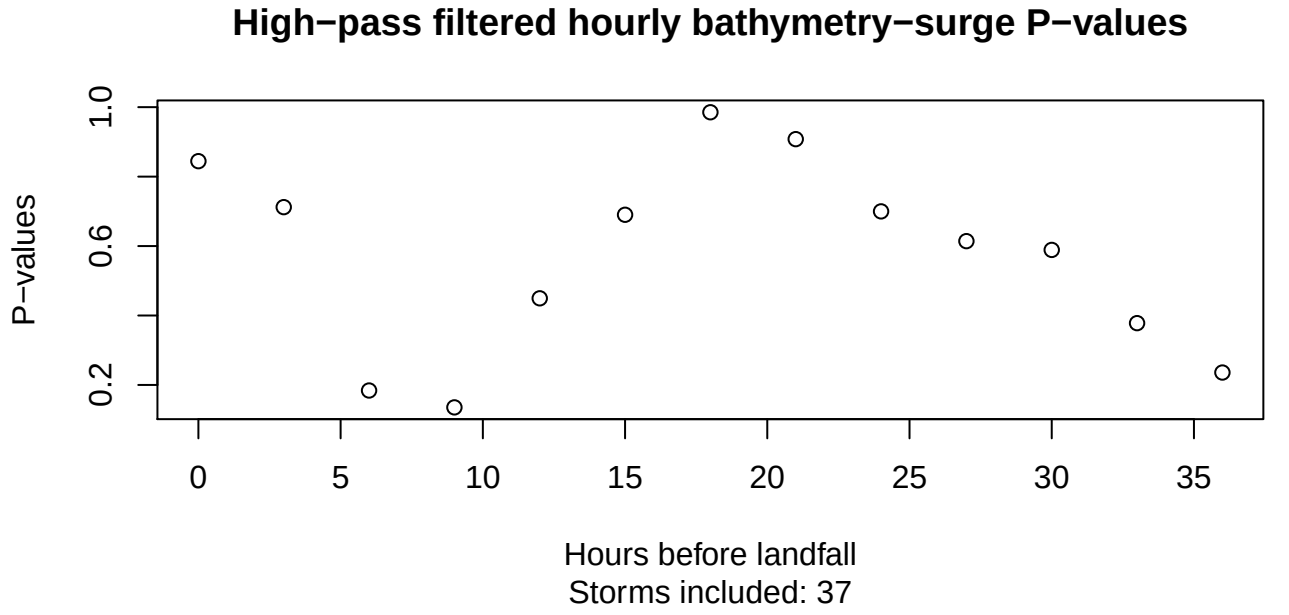
High−pass filtered hourly bathymetry−surge P−values
P−values
1.0
0.6
0.2
0
5
10
15
20
25
30
35
Hours before landfall
Storms included: 37

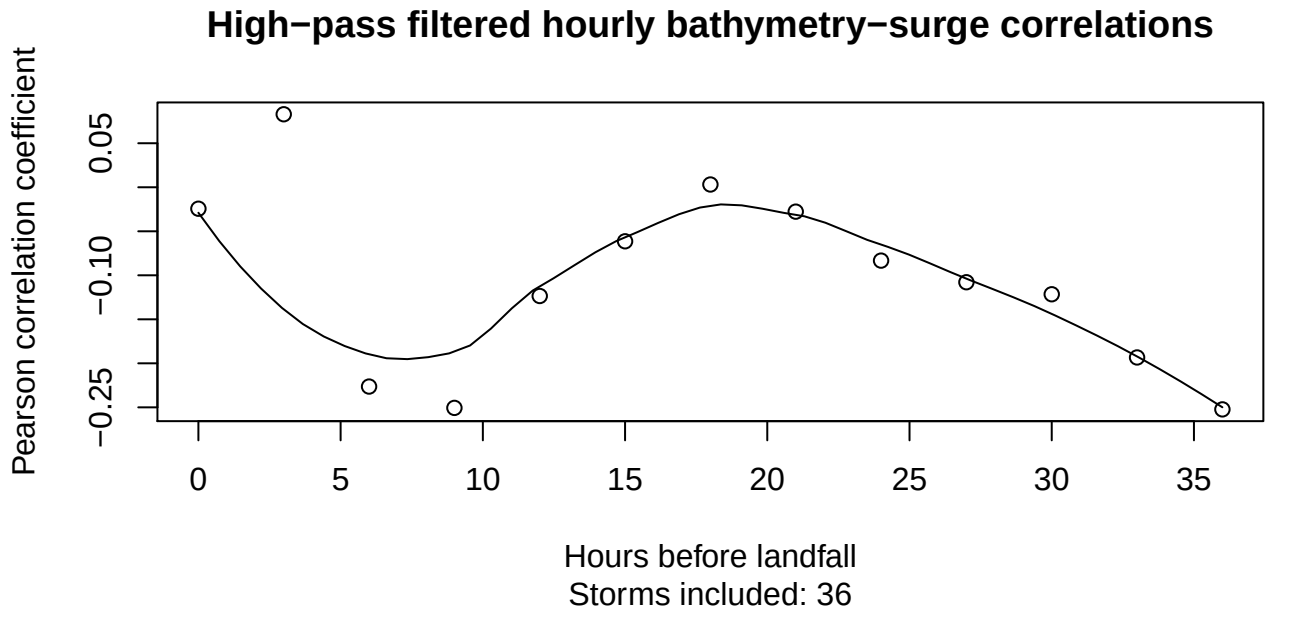
High−pass filtered hourly bathymetry−surge correlations
Pearson correlation coefficient
0.05
−0.10
−0.25
0
5
10
15
20
25
30
35
Hours before landfall
Storms included: 36

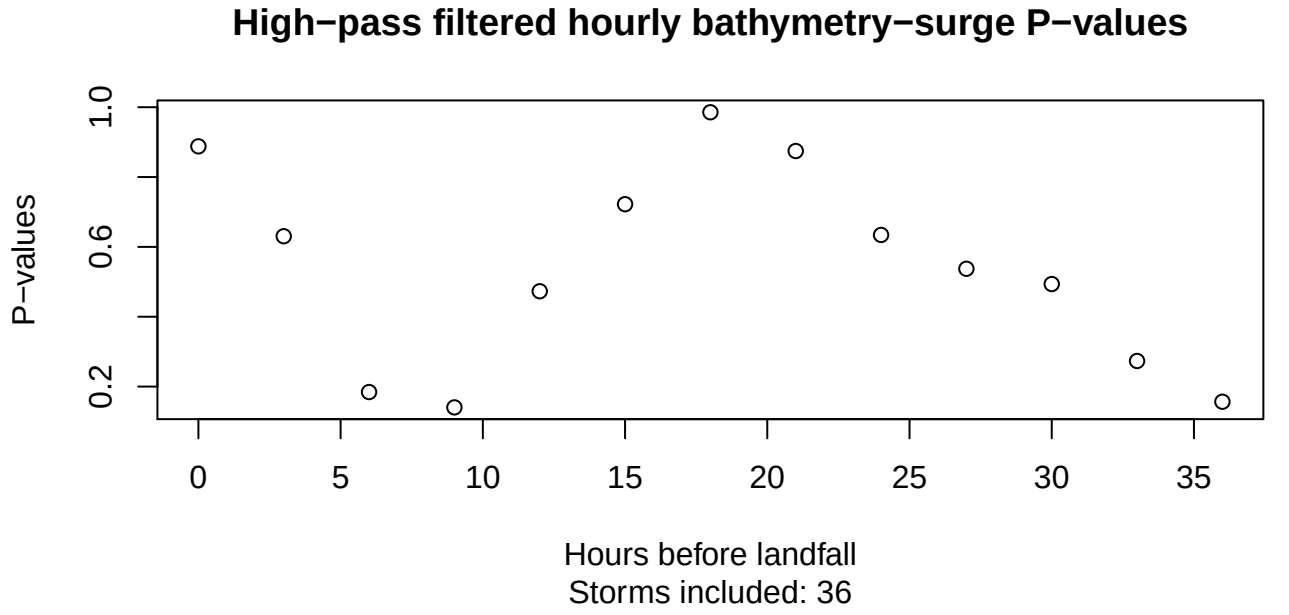
High−pass filtered hourly bathymetry−surge P−values
P−values
1.0
0.6
0.2
0
5
10
15
20
25
30
35
Hours before landfall
Storms included: 36

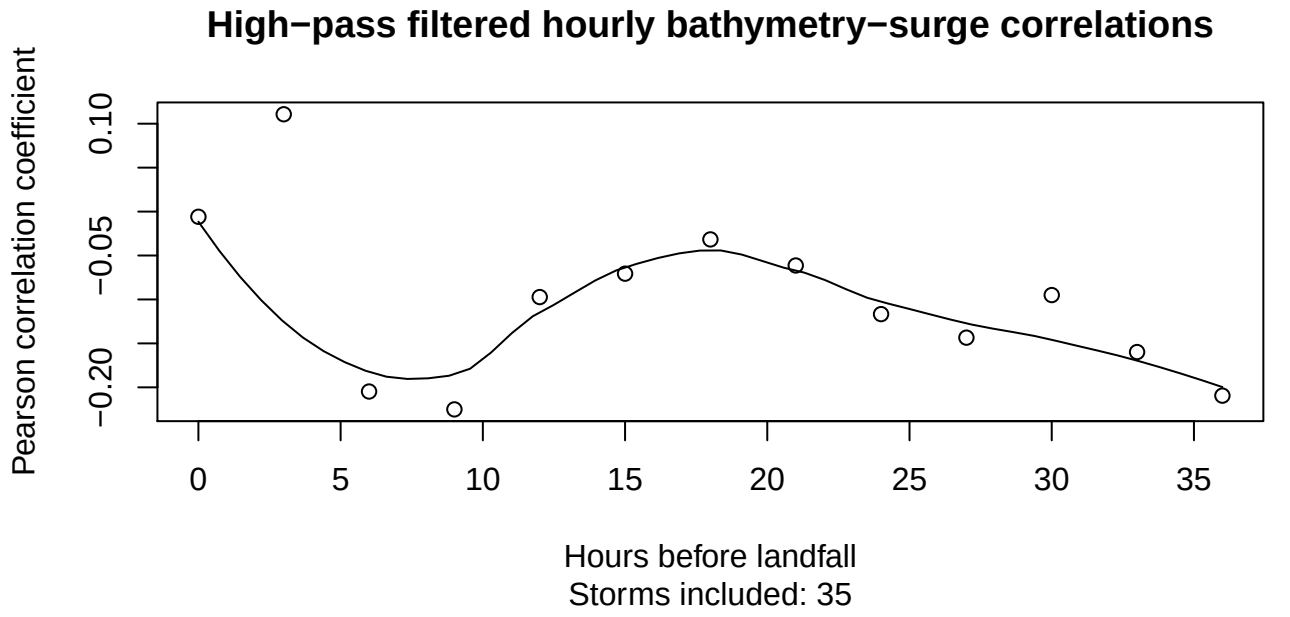
High−pass filtered hourly bathymetry−surge correlations
Pearson correlation coefficient
0.10
−0.05
−0.20
0
5
10
15
20
25
30
35
Hours before landfall
Storms included: 35

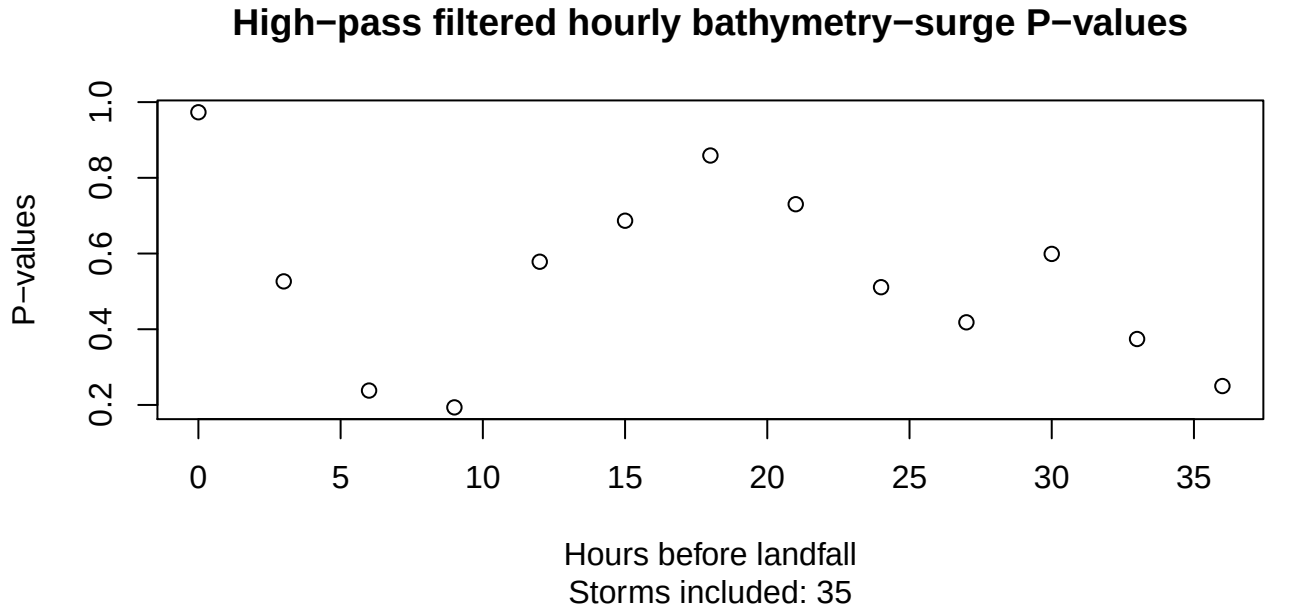
High−pass filtered hourly bathymetry−surge P−values
P−values
1.0
0.8
0.6
0.4
0.2
0
5
10
15
20
25
30
35
Hours before landfall
Storms included: 35

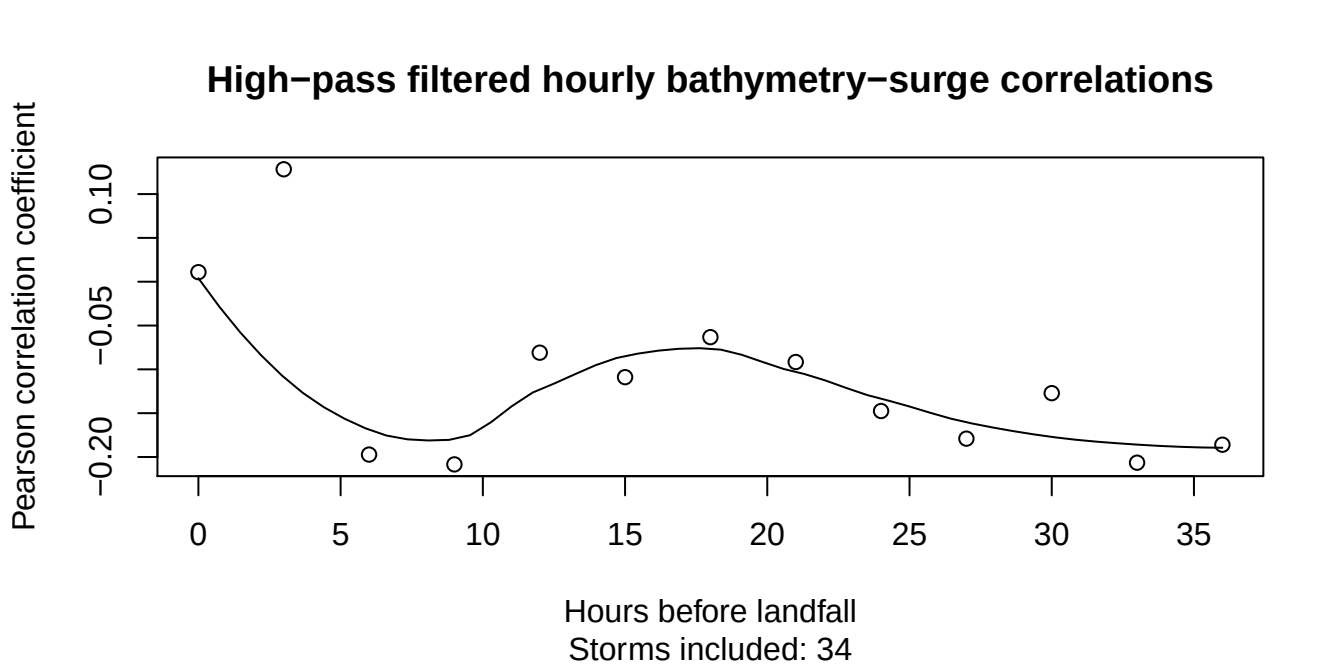
High−pass filtered hourly bathymetry−surge correlations
Pearson correlation coefficient
0.10
−0.05
−0.20
0
5
10
15
20
25
30
35
Hours before landfall
Storms included: 34

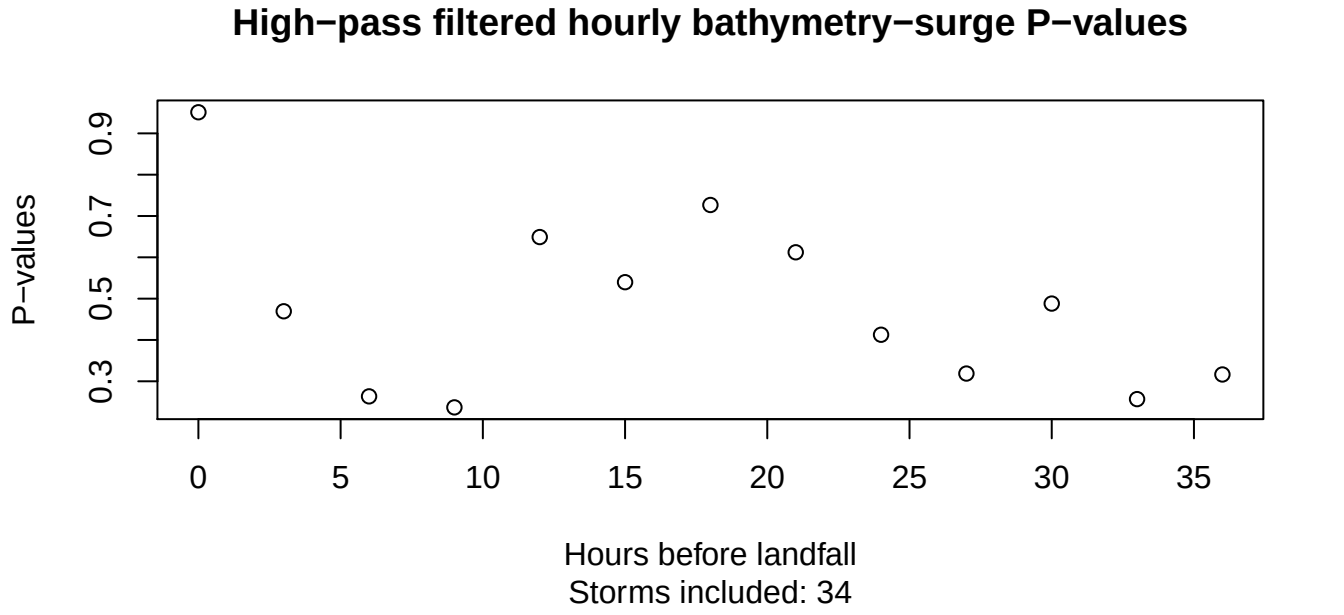
High−pass filtered hourly bathymetry−surge P−values
P−values
0.9
0.7
0.5
0.3
0
5
10
15
20
25
30
35
Hours before landfall
Storms included: 34

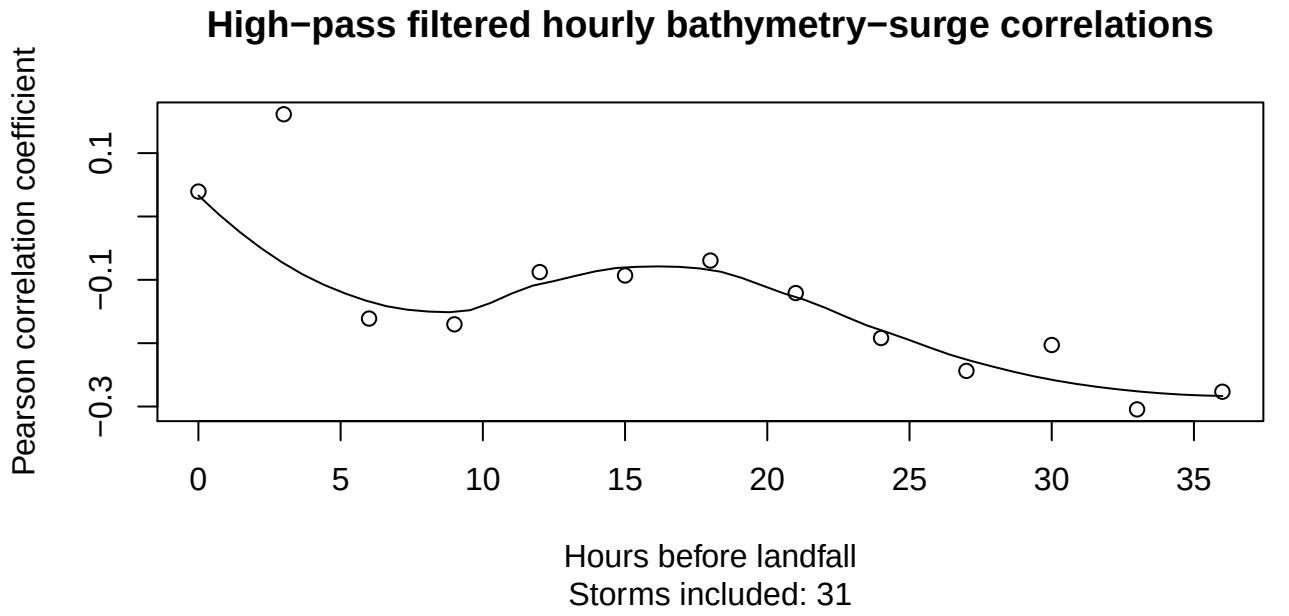
High−pass filtered hourly bathymetry−surge correlations
Pearson correlation coefficient
−0.3
−0.1
0.1
0
5
10
15
20
25
30
35
Hours before landfall
Storms included: 31

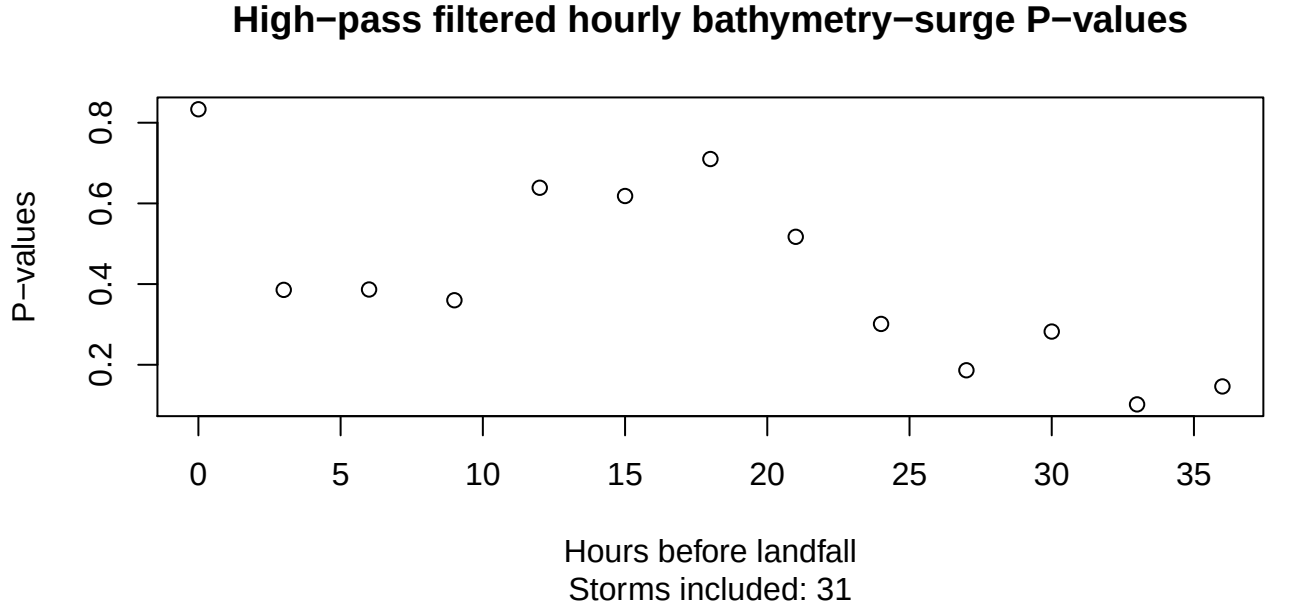
High−pass filtered hourly bathymetry−surge P−values
P−values
0.2
0.4
0.6
0.8
0
5
10
15
20
25
30
35
Hours before landfall
Storms included: 31

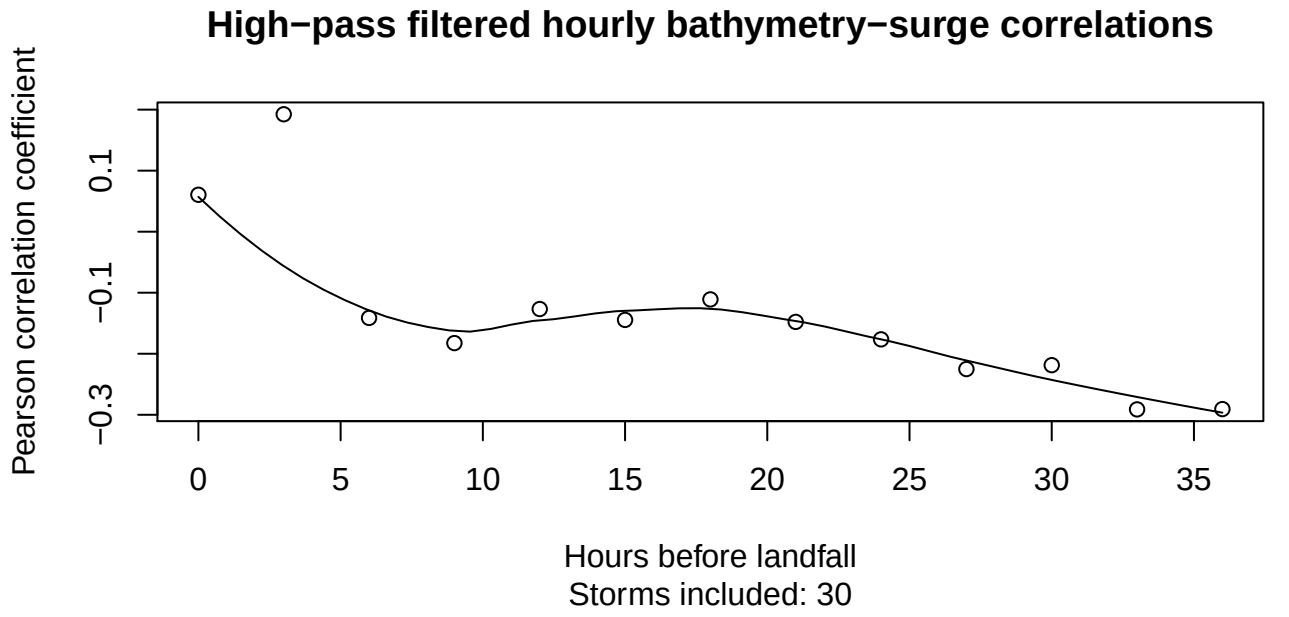
High−pass filtered hourly bathymetry−surge correlations
Pearson correlation coefficient
0.1
−0.1
−0.3
0
5
10
15
20
25
30
35
Hours before landfall
Storms included: 30

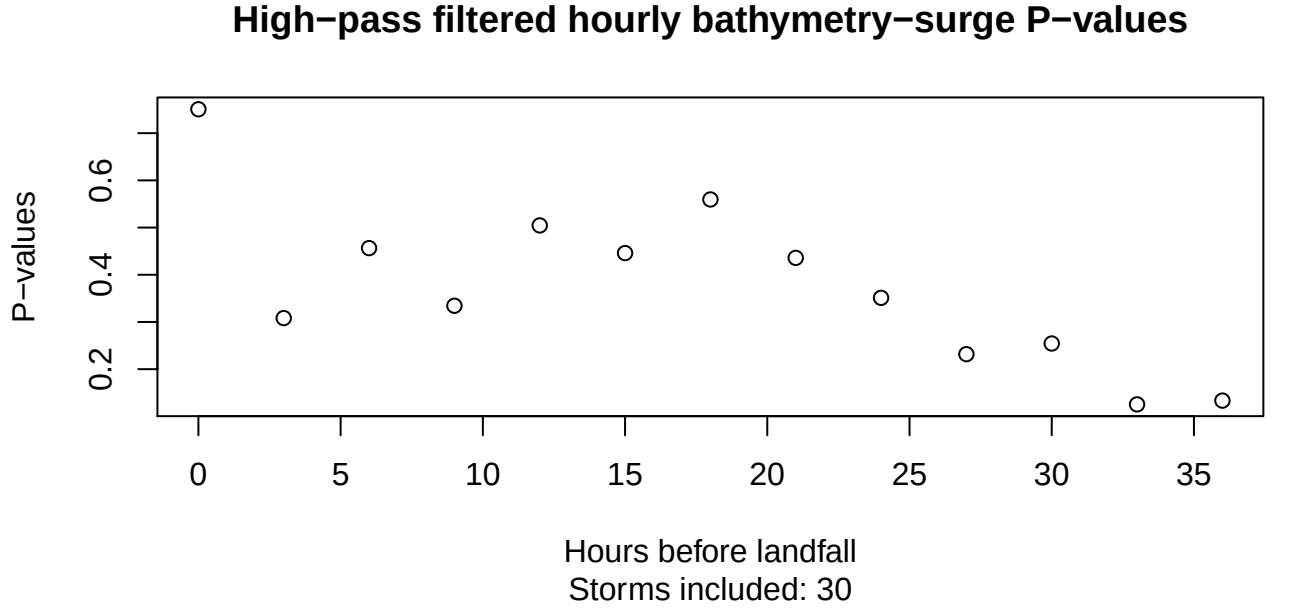
High−pass filtered hourly bathymetry−surge P−values
P−values
0.2
0.4
0.6
0
5
10
15
20
25
30
35
Hours before landfall
Storms included: 30

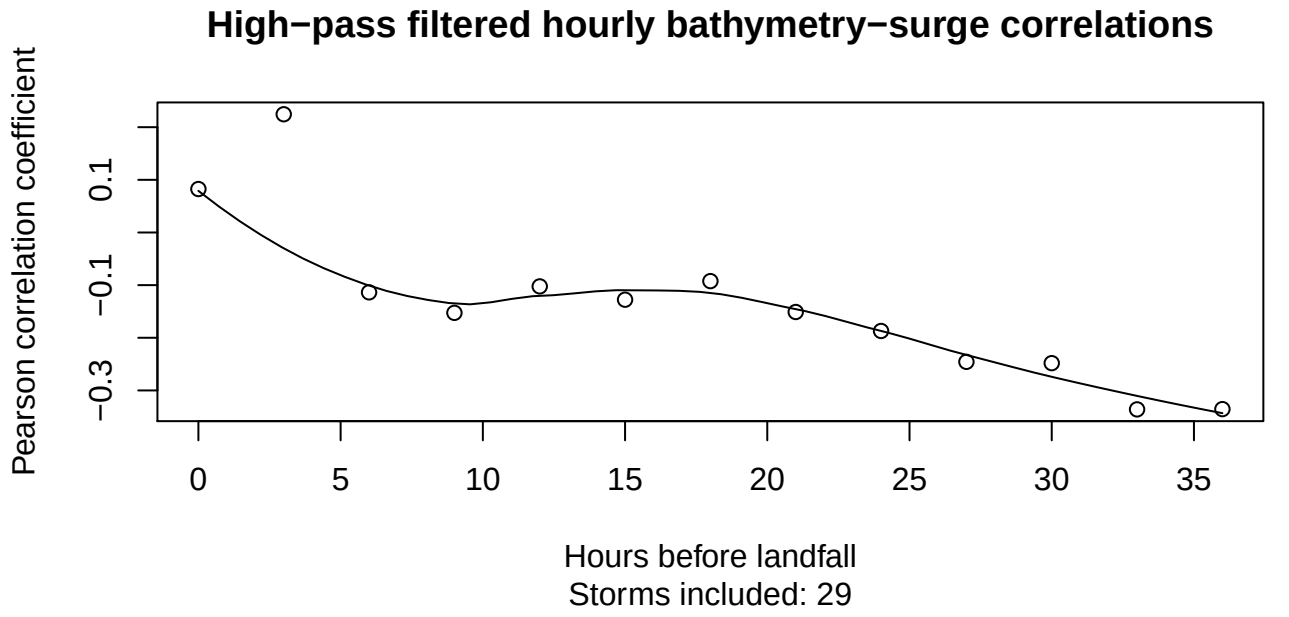
High−pass filtered hourly bathymetry−surge correlations
Pearson correlation coefficient
0.1
−0.1
−0.3
0
5
10
15
20
25
30
35
Hours before landfall
Storms included: 29

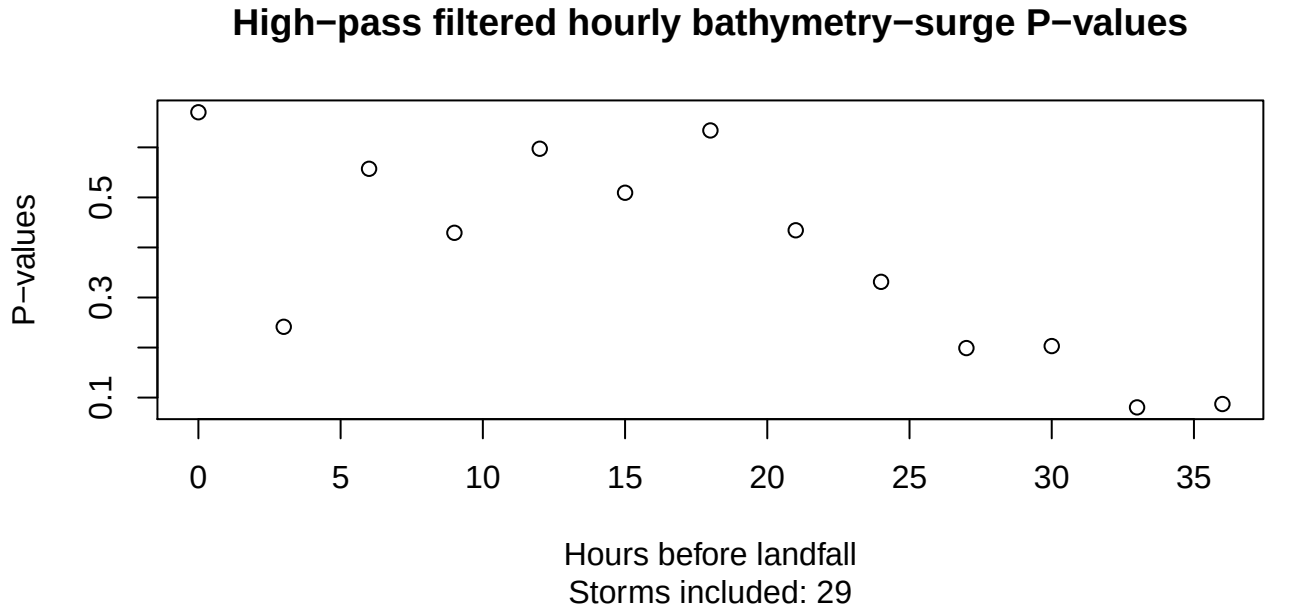
High−pass filtered hourly bathymetry−surge P−values
P−values
0.5
0.3
0.1
0
5
10
15
20
25
30
35
Hours before landfall
Storms included: 29

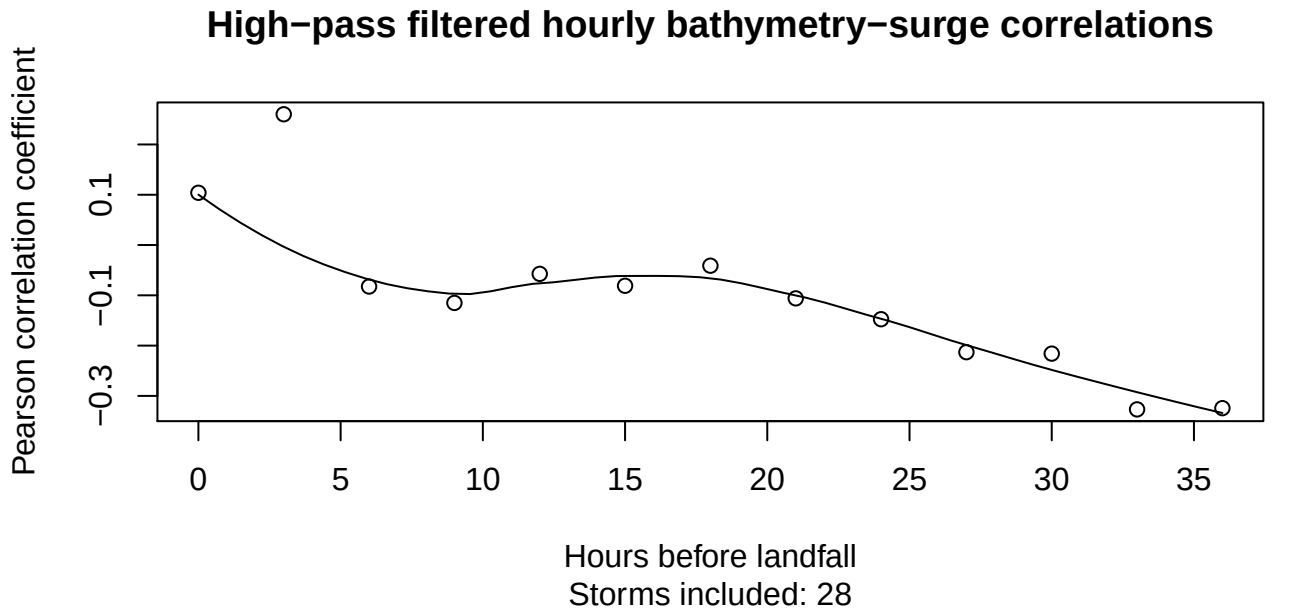
High−pass filtered hourly bathymetry−surge correlations
Pearson correlation coefficient
−0.3
−0.1
0.1
0
5
10
15
20
25
30
35
Hours before landfall
Storms included: 28

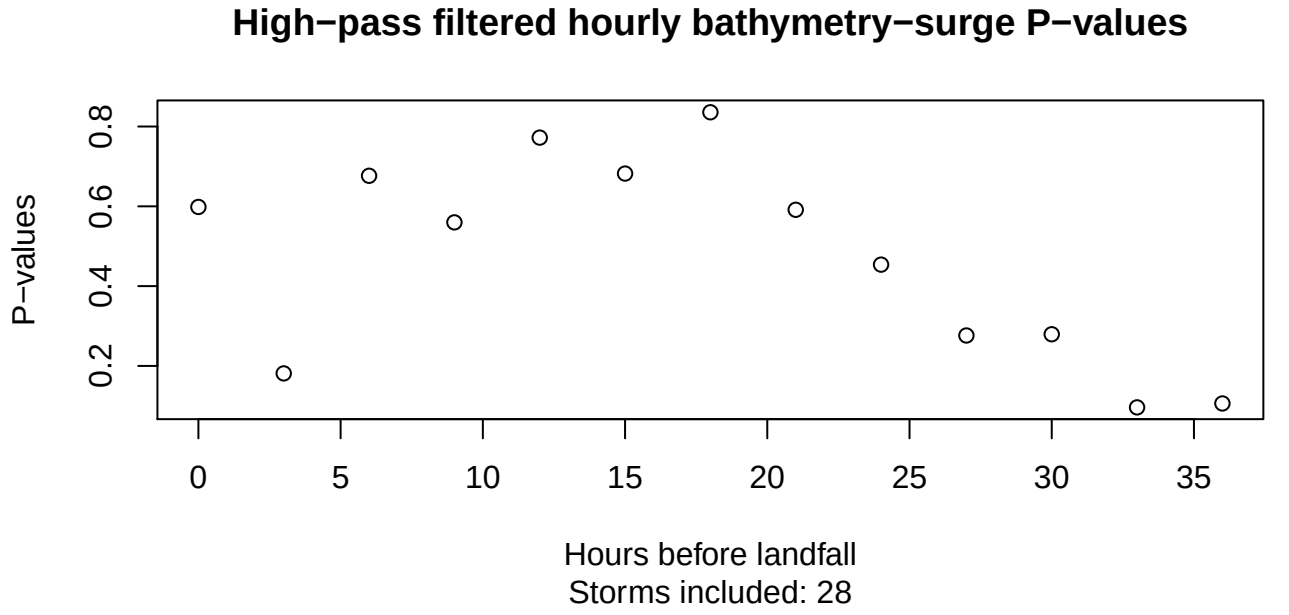
High−pass filtered hourly bathymetry−surge P−values
P−values
0.2
0.4
0.6
0.8
0
5
10
15
20
25
30
35
Hours before landfall
Storms included: 28

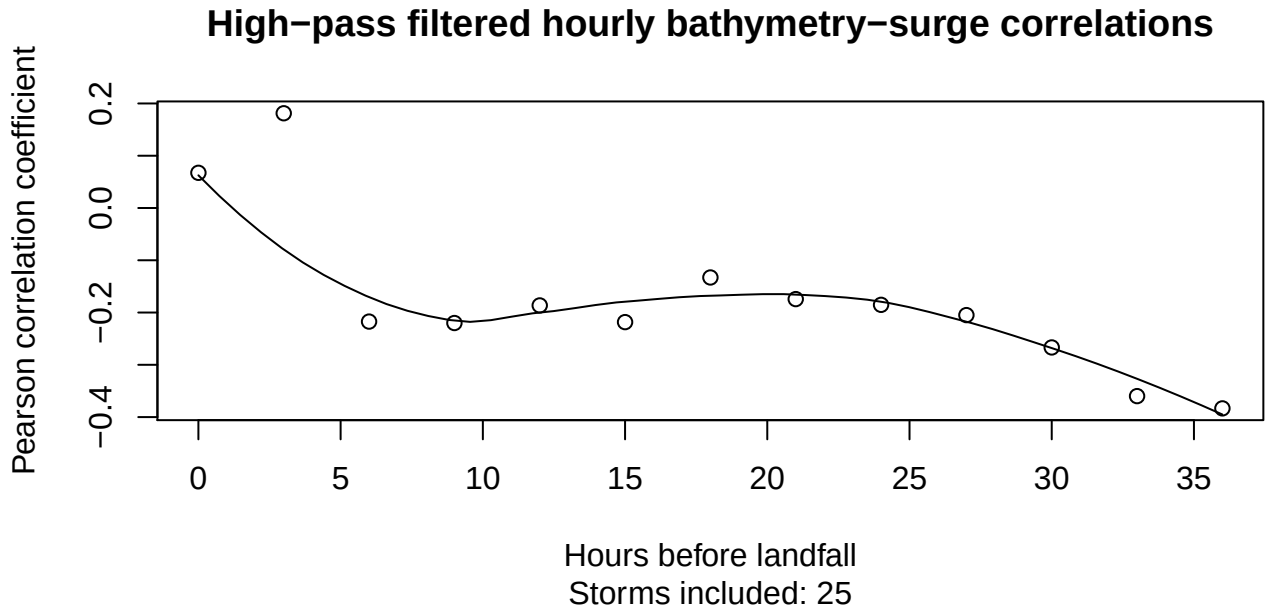
High−pass filtered hourly bathymetry−surge correlations
Pearson correlation coefficient
0.2
0.0
−0.2
−0.4
0
5
10
15
20
25
30
35
Hours before landfall
Storms included: 25

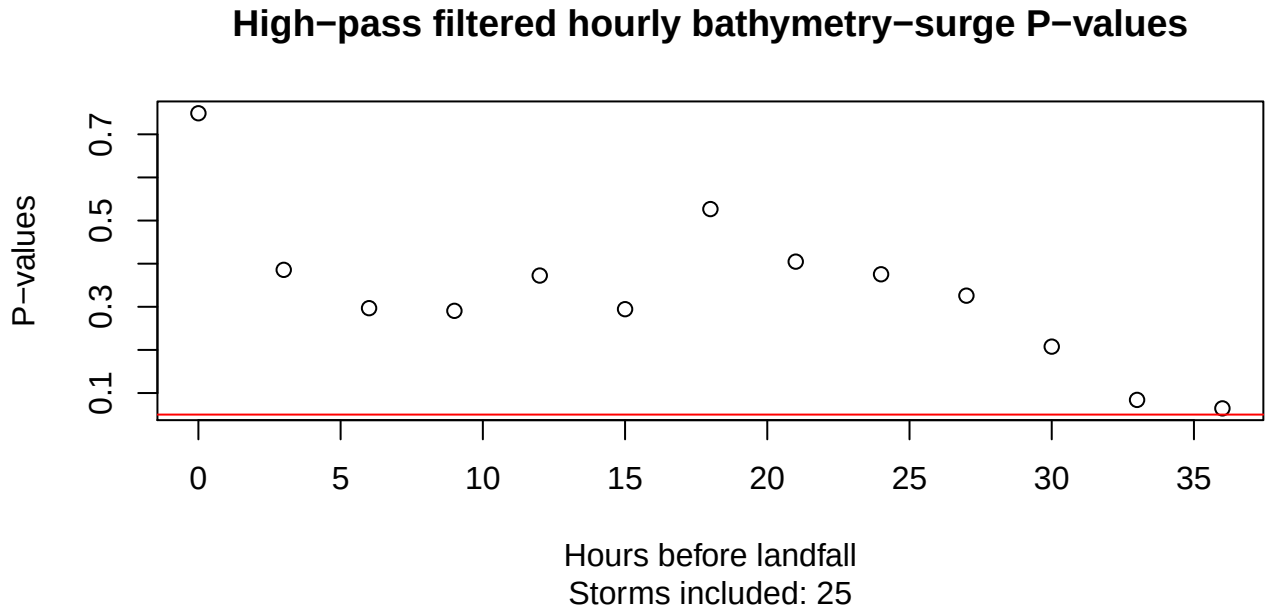
High−pass filtered hourly bathymetry−surge P−values
P−values
0.7
0.5
0.3
0.1
0
5
10
15
20
25
30
35
Hours before landfall
Storms included: 25

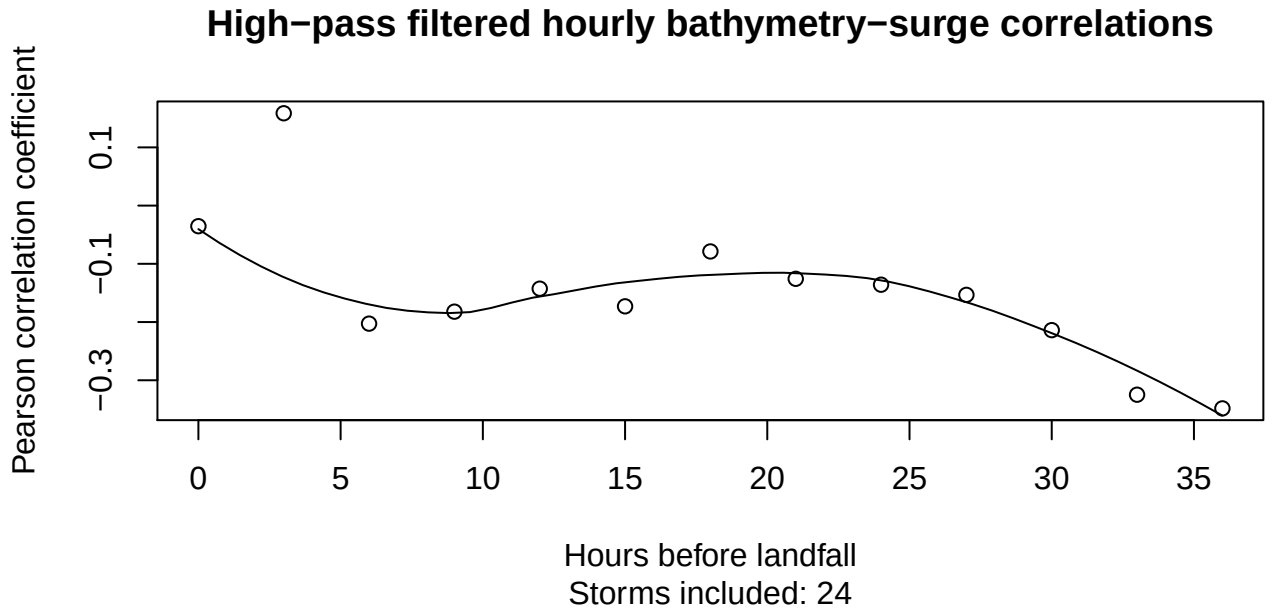
High−pass filtered hourly bathymetry−surge correlations
Pearson correlation coefficient
0.1
−0.1
−0.3
0
5
10
15
20
25
30
35
Hours before landfall
Storms included: 24

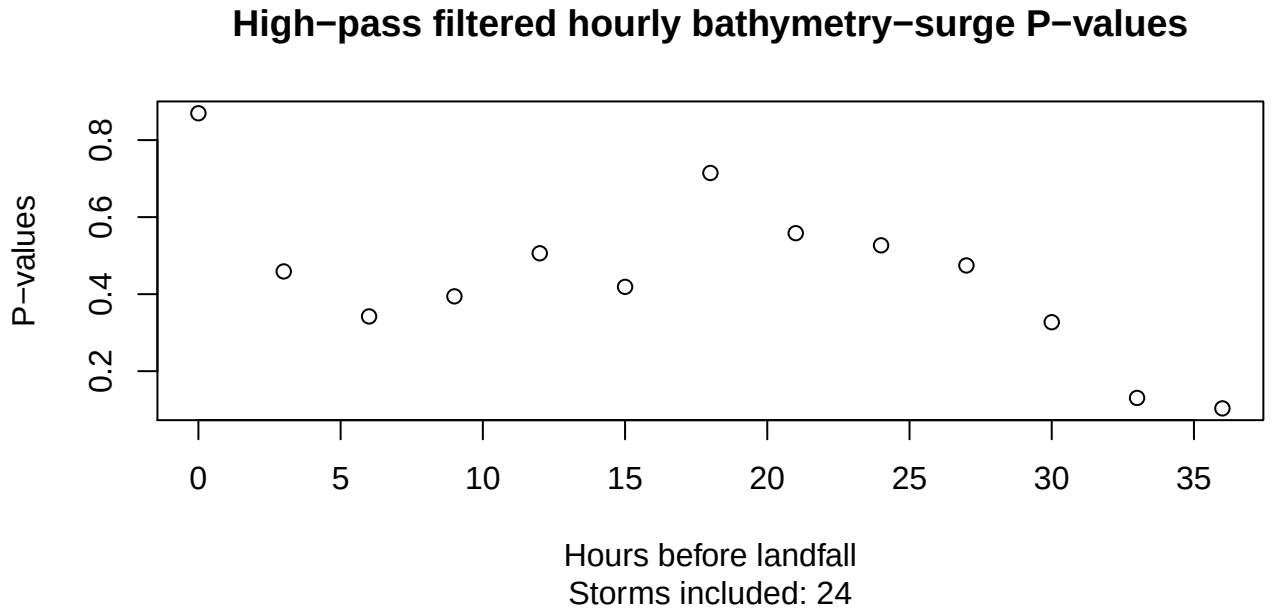
High−pass filtered hourly bathymetry−surge P−values
P−values
0.8
0.6
0.4
0.2
0
5
10
15
20
25
30
35
Hours before landfall
Storms included: 24

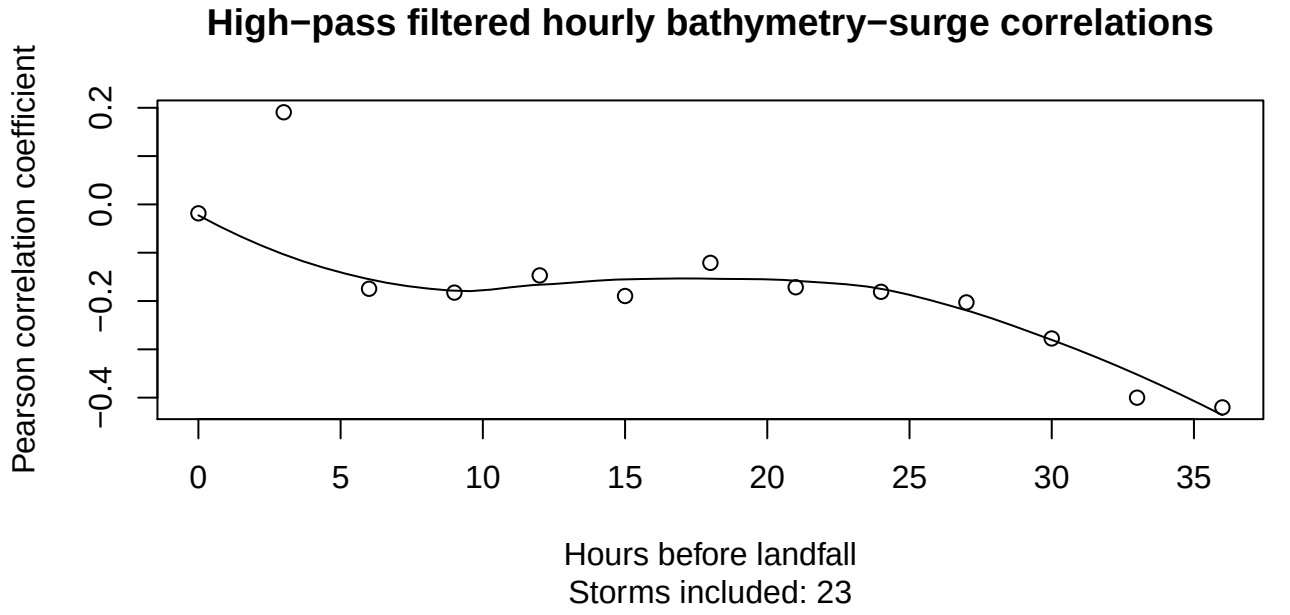
High−pass filtered hourly bathymetry−surge correlations
Pearson correlation coefficient
0.2
0.0
−0.2
−0.4
0
5
10
15
20
25
30
35
Hours before landfall
Storms included: 23

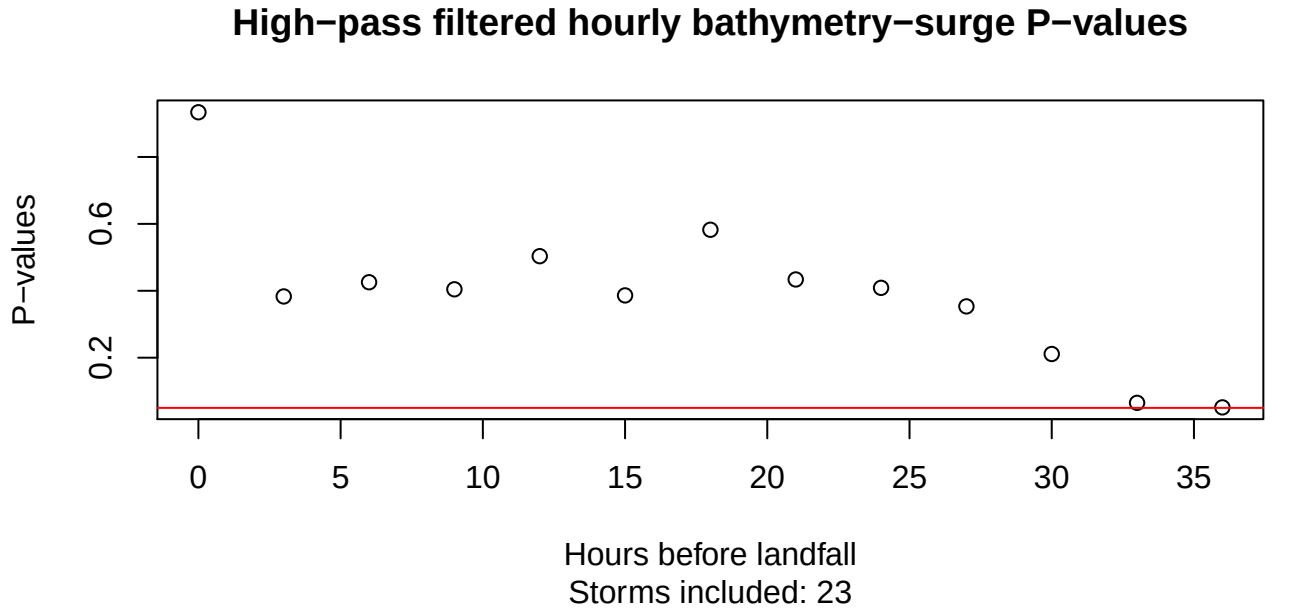
High−pass filtered hourly bathymetry−surge P−values
P−values
0.6
0.2
0
5
10
15
20
25
30
35
Hours before landfall
Storms included: 23

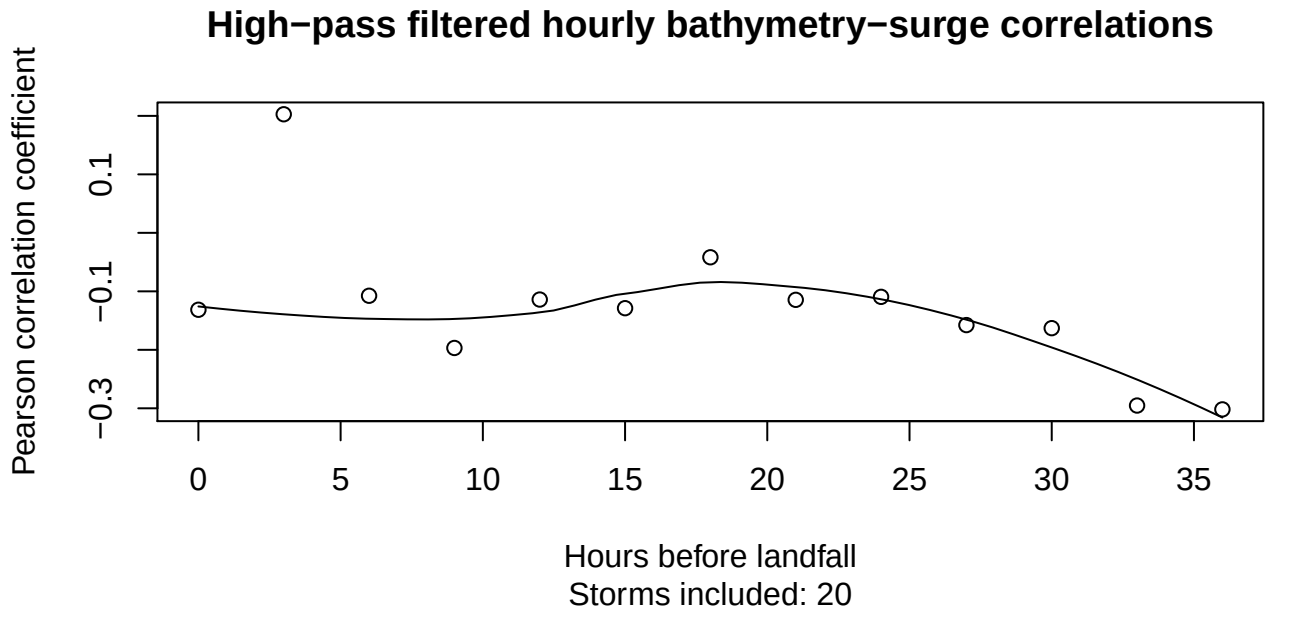
High−pass filtered hourly bathymetry−surge correlations
Pearson correlation coefficient
0.1
−0.1
−0.3
0
5
10
15
20
25
30
35
Hours before landfall
Storms included: 20

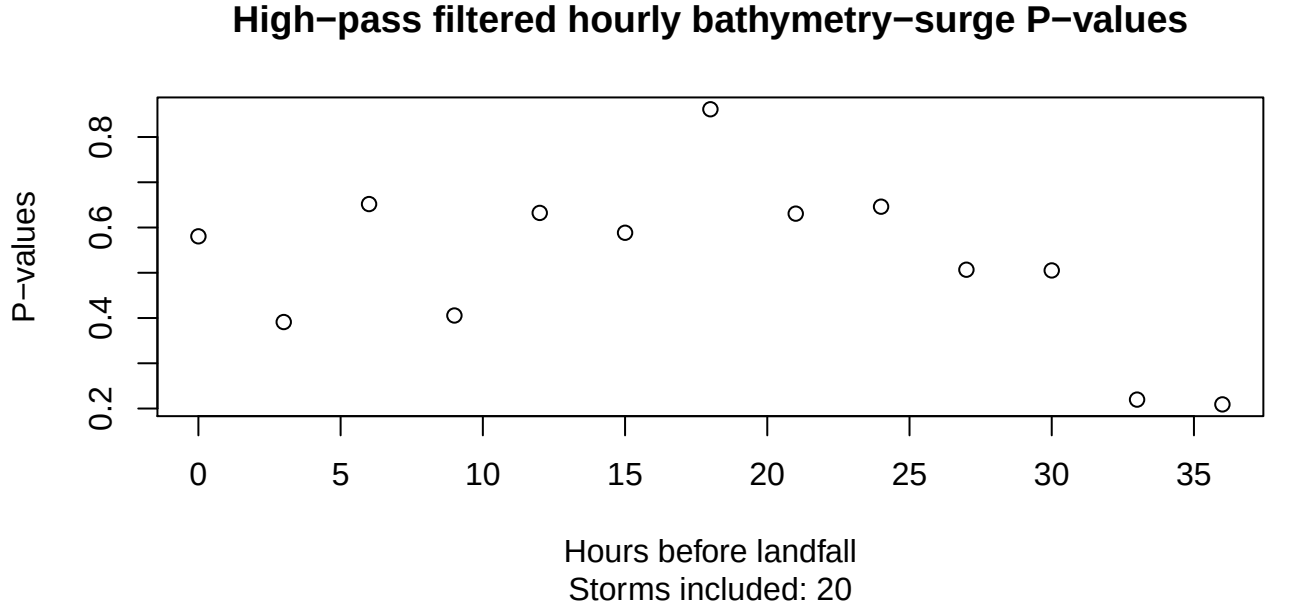
High−pass filtered hourly bathymetry−surge P−values
P−values
0.8
0.6
0.4
0.2
0
5
10
15
20
25
30
35
Hours before landfall
Storms included: 20

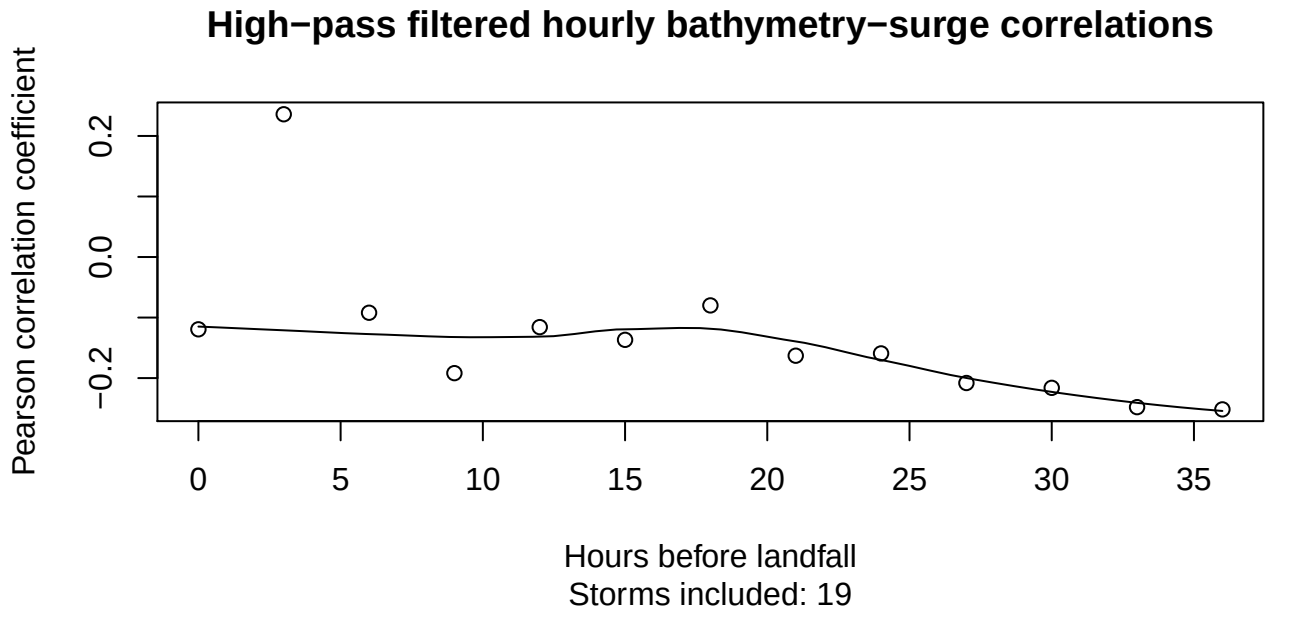
High−pass filtered hourly bathymetry−surge correlations
Pearson correlation coefficient
0.2
0.0
−0.2
0
5
10
15
20
25
30
35
Hours before landfall
Storms included: 19

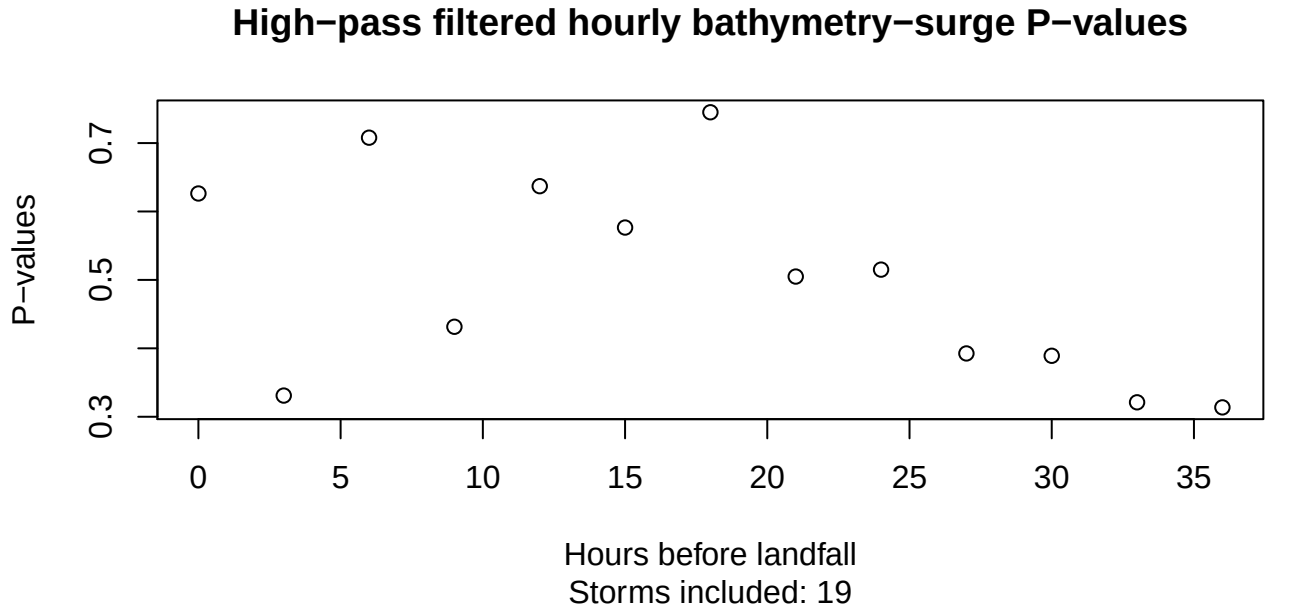
High−pass filtered hourly bathymetry−surge P−values
P−values
0.7
0.5
0.3
0
5
10
15
20
25
30
35
Hours before landfall
Storms included: 19

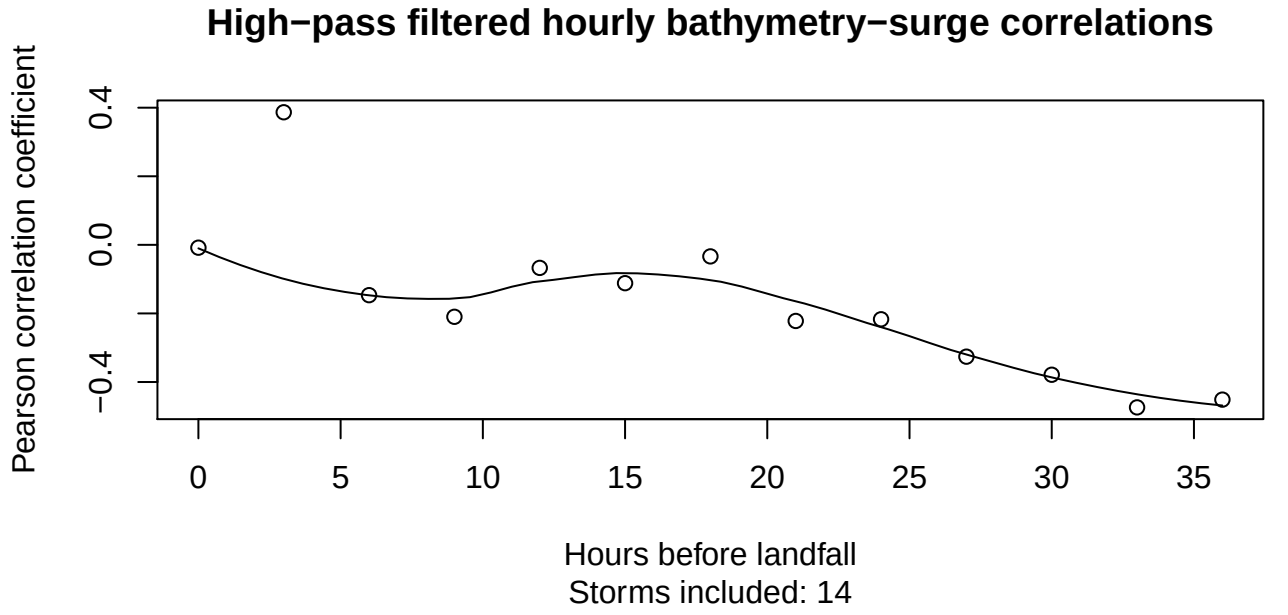
High−pass filtered hourly bathymetry−surge correlations
Pearson correlation coefficient
0.4
0.0
−0.4
0
5
10
15
20
25
30
35
Hours before landfall
Storms included: 14

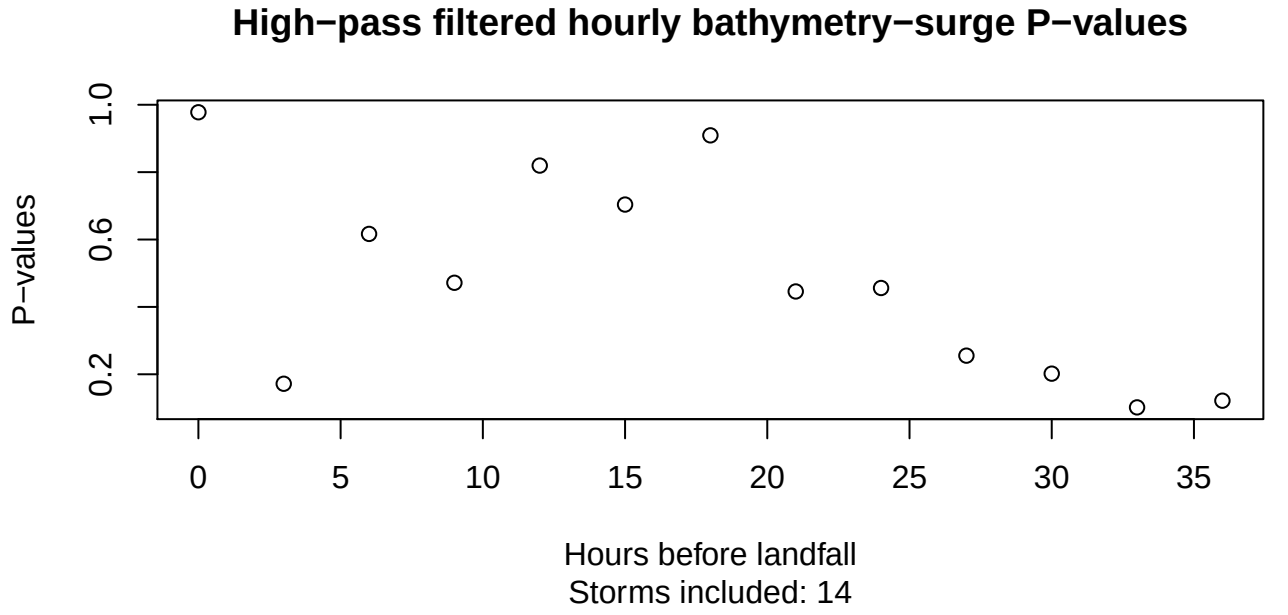
High−pass filtered hourly bathymetry−surge P−values
P−values
1.0
0.6
0.2
0
5
10
15
20
25
30
35
Hours before landfall
Storms included: 14

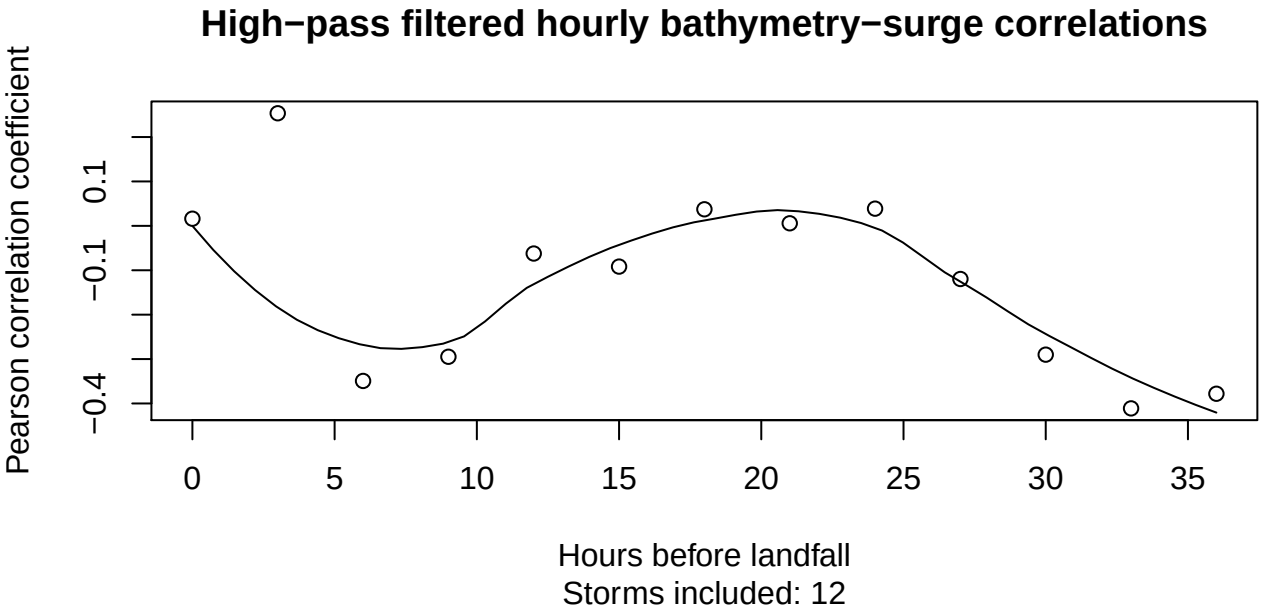
High−pass filtered hourly bathymetry−surge correlations
Pearson correlation coefficient
−0.4
−0.1
0.1
0
5
10
15
20
25
30
35
Hours before landfall
Storms included: 12

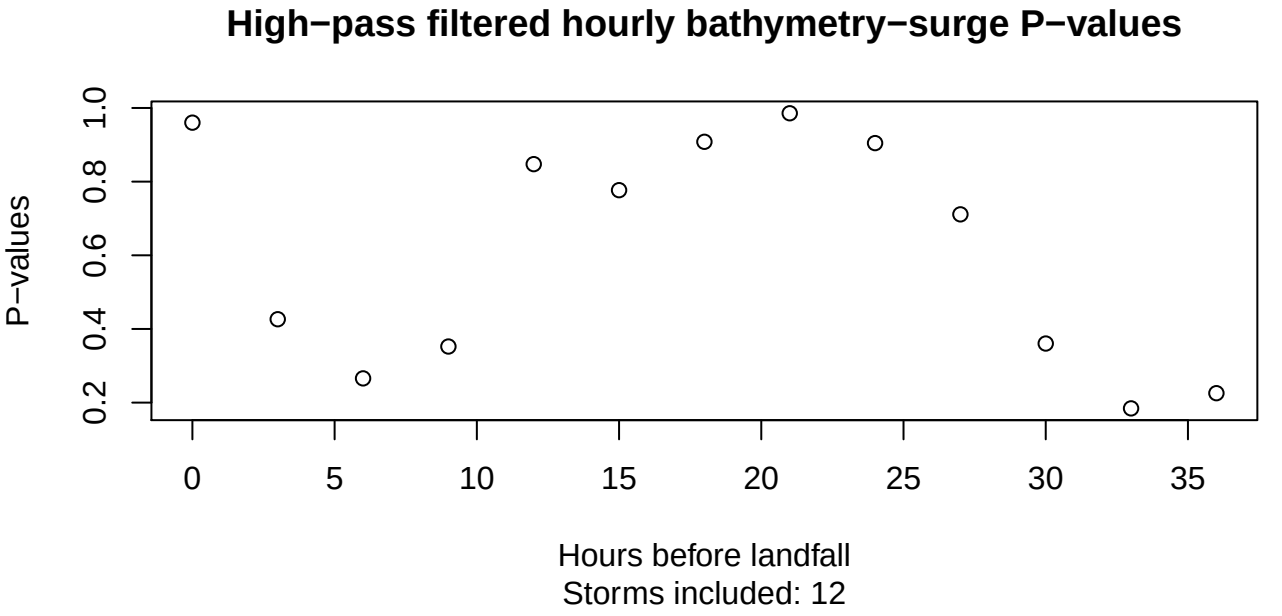
High−pass filtered hourly bathymetry−surge P−values
P−values
0.2
0.4
0.6
0.8
1.0
0
5
10
15
20
25
30
35
Hours before landfall
Storms included: 12

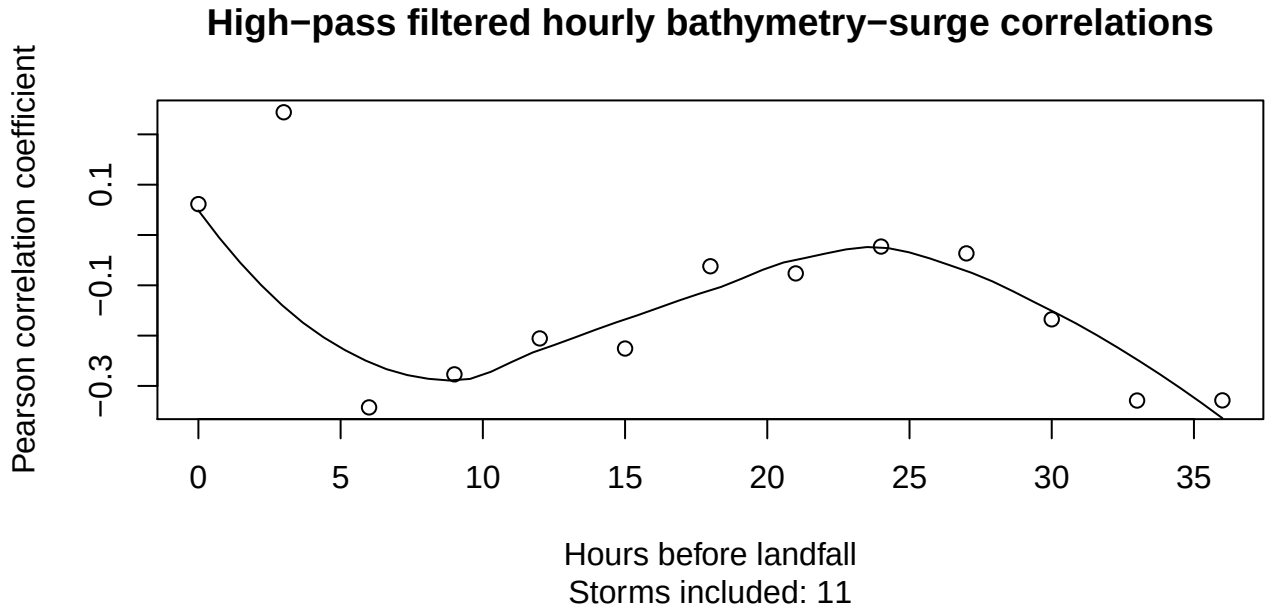
High−pass filtered hourly bathymetry−surge correlations
Pearson correlation coefficient
−0.3
−0.1
0.1
0
5
10
15
20
25
30
35
Hours before landfall
Storms included: 11

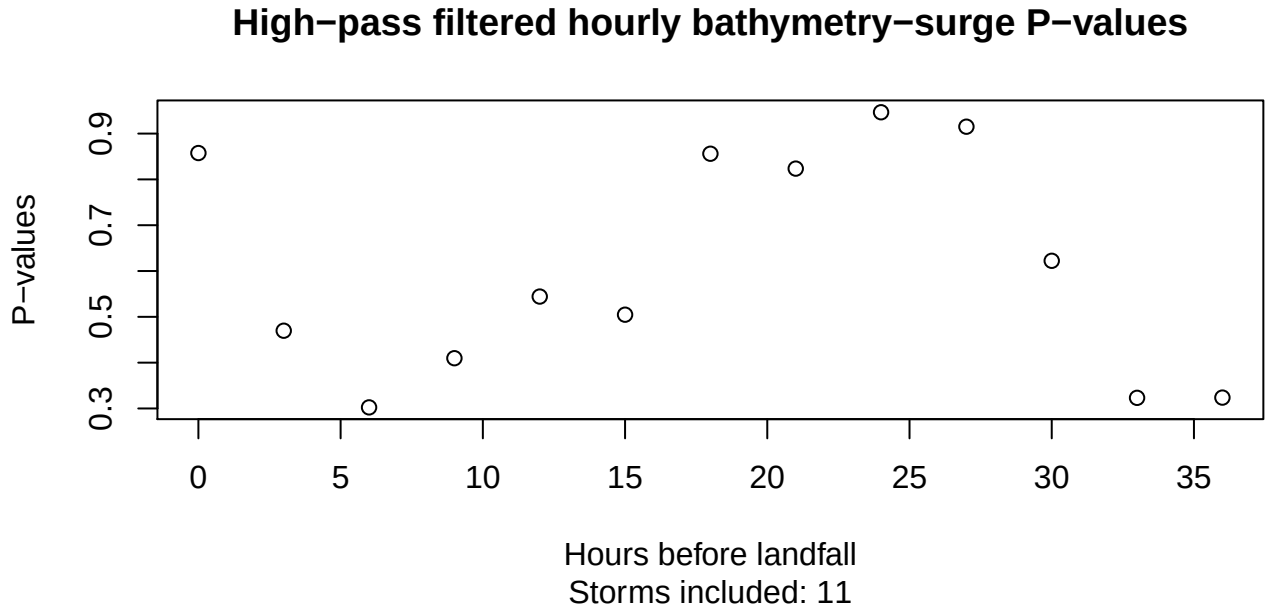
High−pass filtered hourly bathymetry−surge P−values
P−values
0.3
0.5
0.7
0.9
0
5
10
15
20
25
30
35
Hours before landfall
Storms included: 11

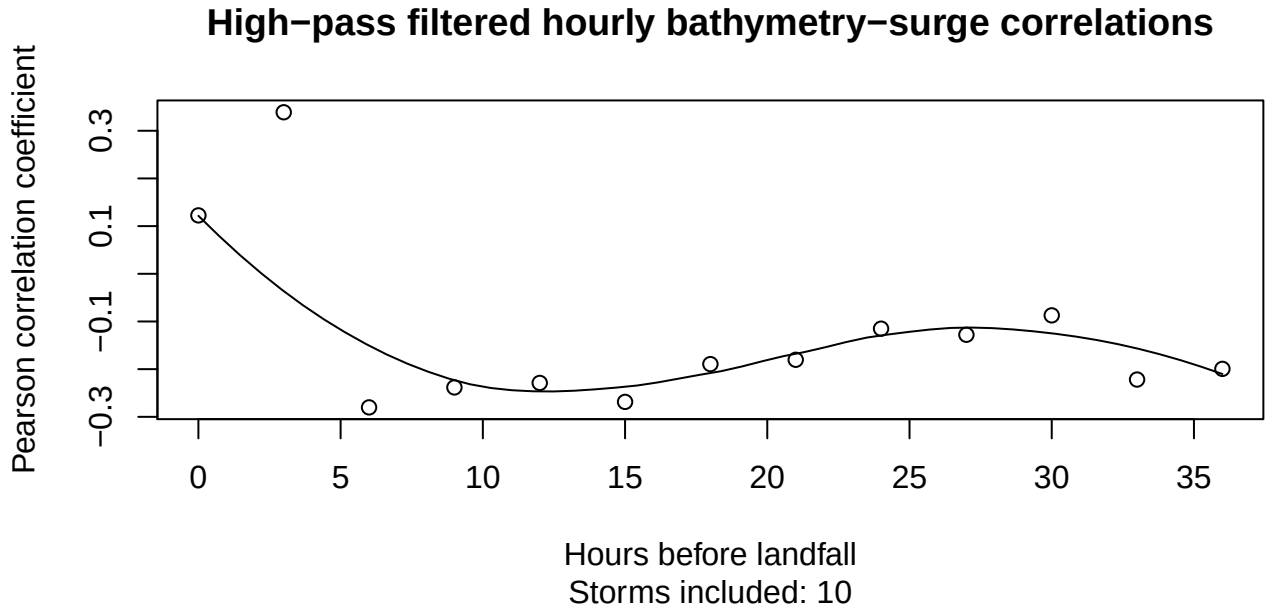
High−pass filtered hourly bathymetry−surge correlations
Pearson correlation coefficient
−0.3
−0.1
0.1
0.3
0
5
10
15
20
25
30
35
Hours before landfall
Storms included: 10

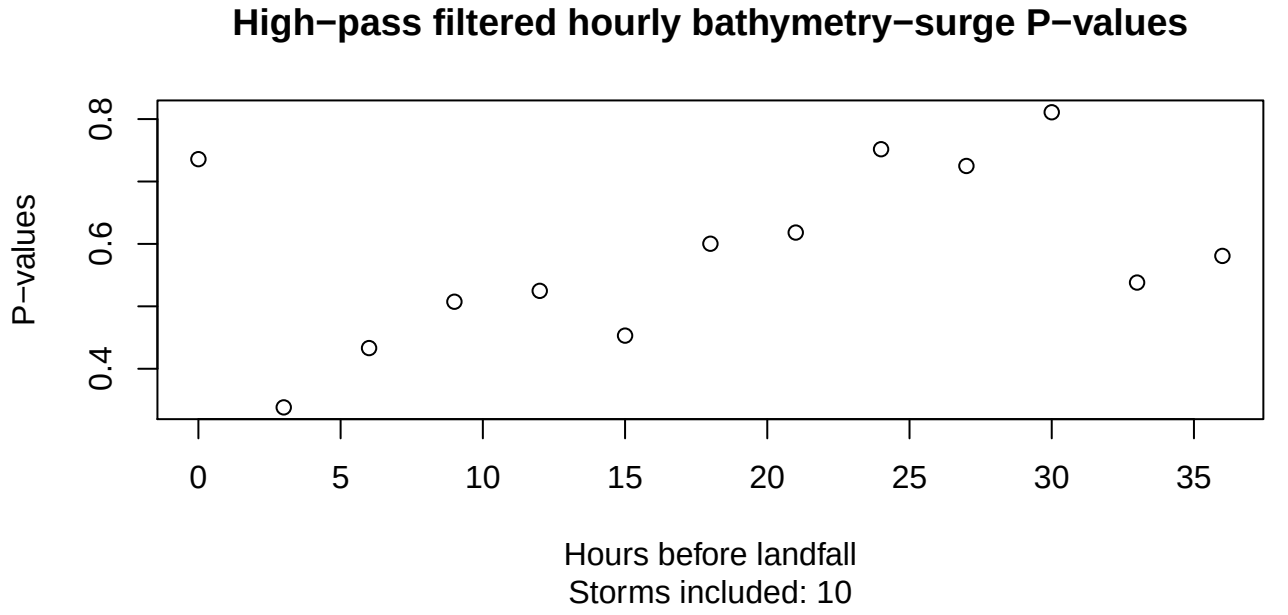
High−pass filtered hourly bathymetry−surge P−values
P−values
0.4
0.6
0.8
0
5
10
15
20
25
30
35
Hours before landfall
Storms included: 10

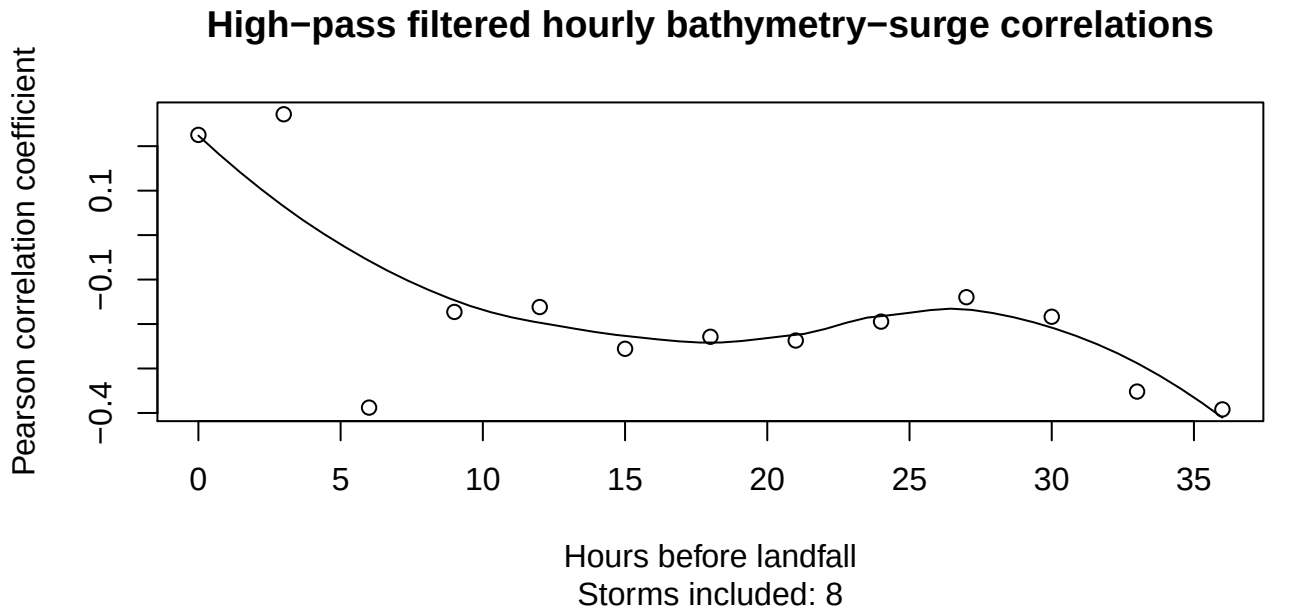
High−pass filtered hourly bathymetry−surge correlations
Pearson correlation coefficient
−0.4
−0.1
0.1
0
5
10
15
20
25
30
35
Hours before landfall
Storms included: 8

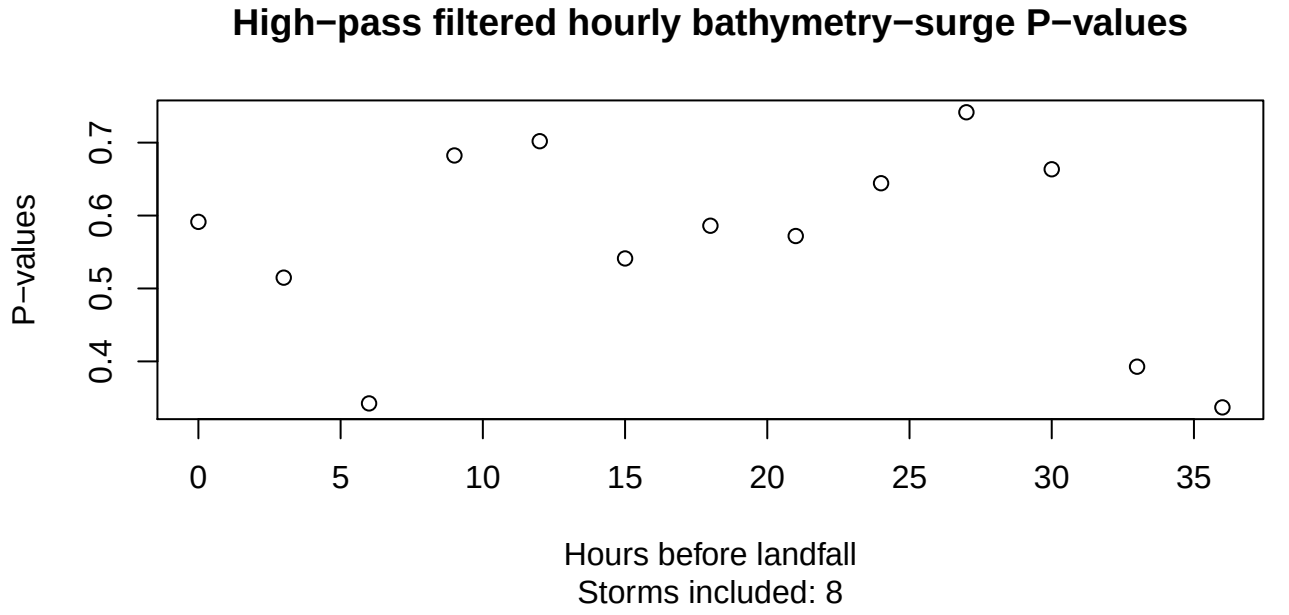
High−pass filtered hourly bathymetry−surge P−values
P−values
0.4
0.5
0.6
0.7
0
5
10
15
20
25
30
35
Hours before landfall
Storms included: 8

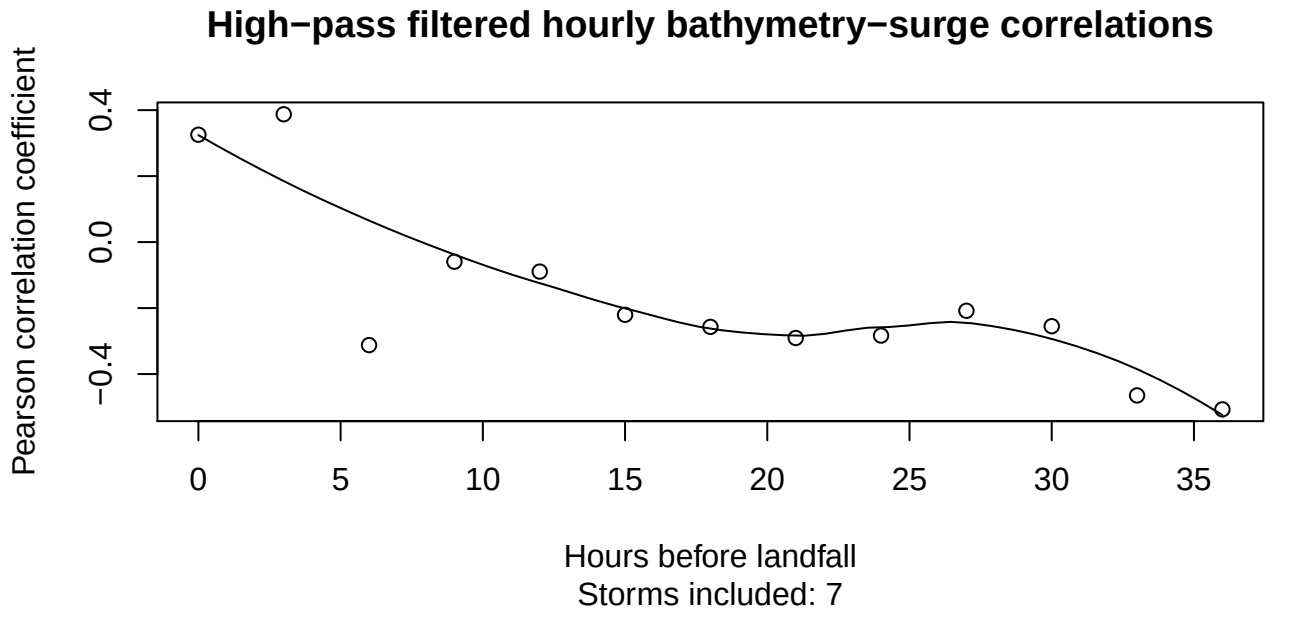
High−pass filtered hourly bathymetry−surge correlations
Pearson correlation coefficient
0.4
0.0
−0.4
0
5
10
15
20
25
30
35
Hours before landfall
Storms included: 7

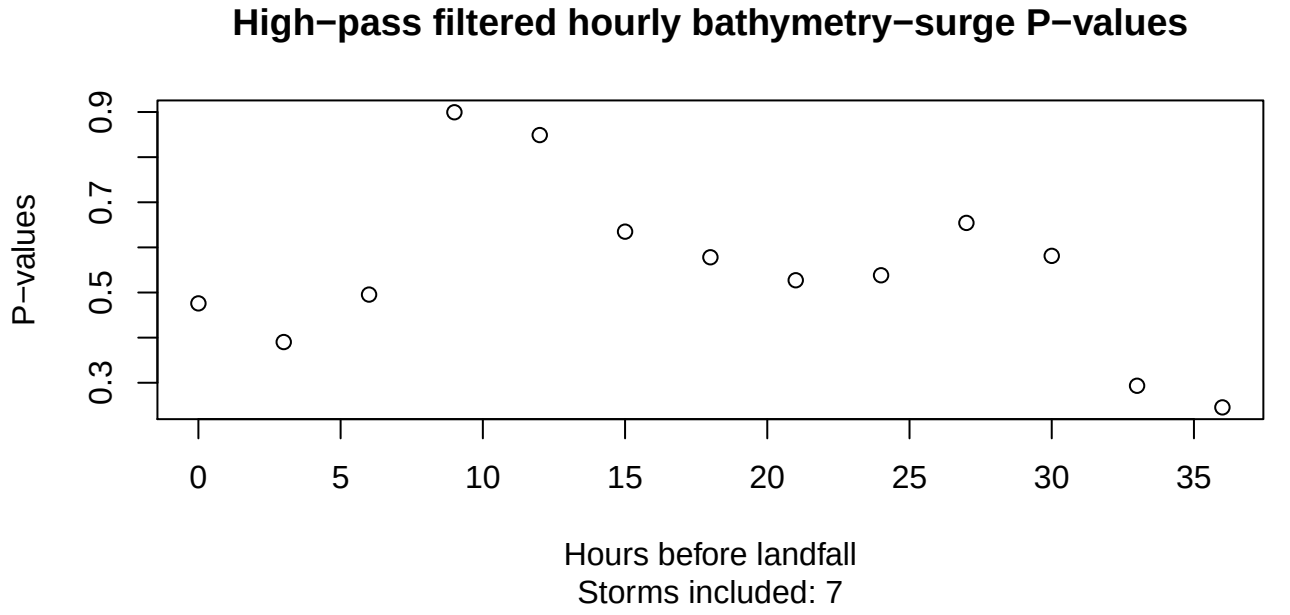
High−pass filtered hourly bathymetry−surge P−values
P−values
0.9
0.7
0.5
0.3
0
5
10
15
20
25
30
35
Hours before landfall
Storms included: 7

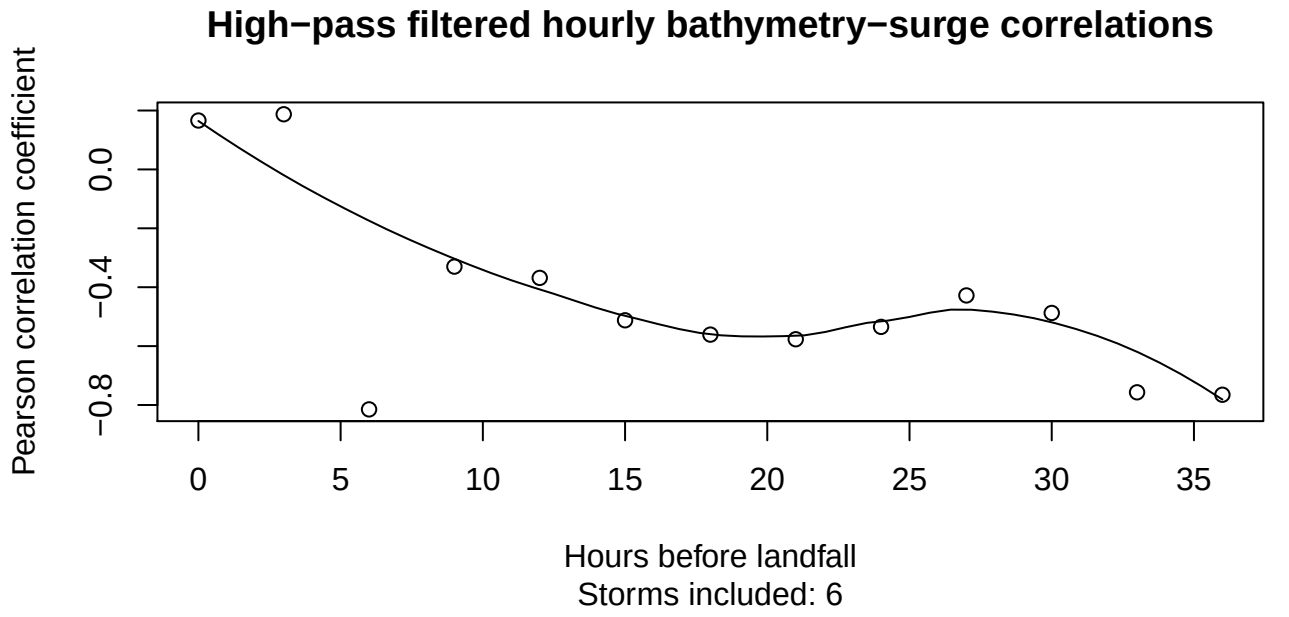
High−pass filtered hourly bathymetry−surge correlations
Pearson correlation coefficient
0.0
−0.4
−0.8
0
5
10
15
20
25
30
35
Hours before landfall
Storms included: 6

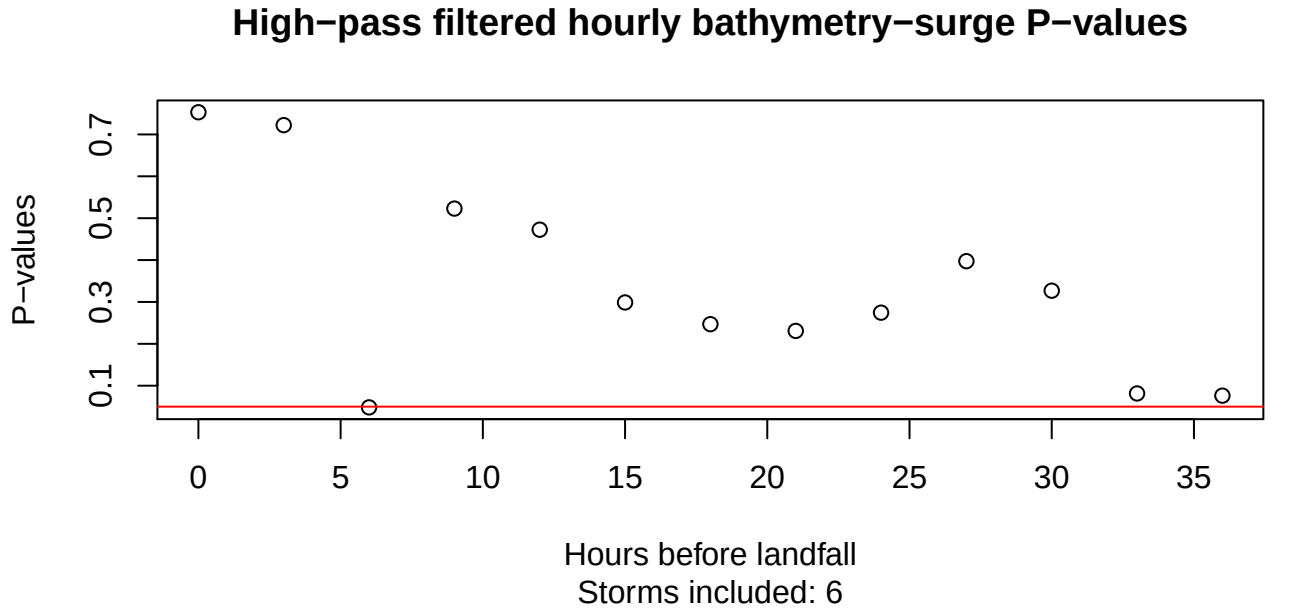
High−pass filtered hourly bathymetry−surge P−values
P−values
0.7
0.5
0.3
0.1
0
5
10
15
20
25
30
35
Hours before landfall
Storms included: 6

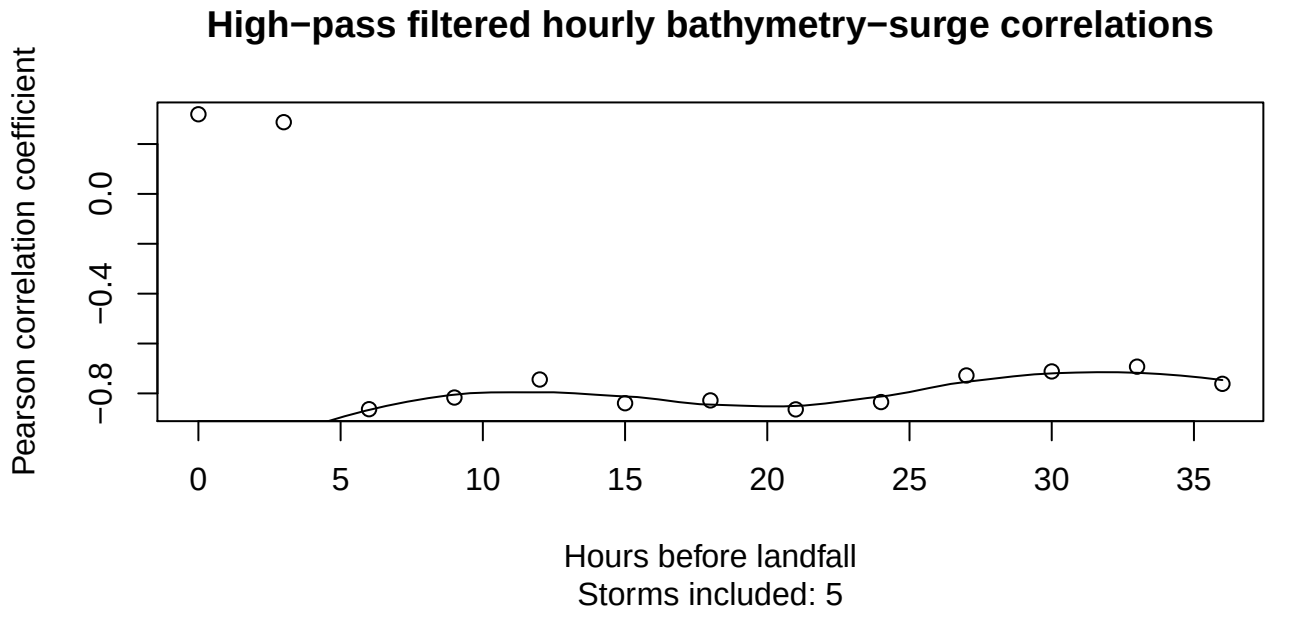
High−pass filtered hourly bathymetry−surge correlations
Pearson correlation coefficient
−0.8
−0.4
0.0
0
5
10
15
20
25
30
35
Hours before landfall
Storms included: 5

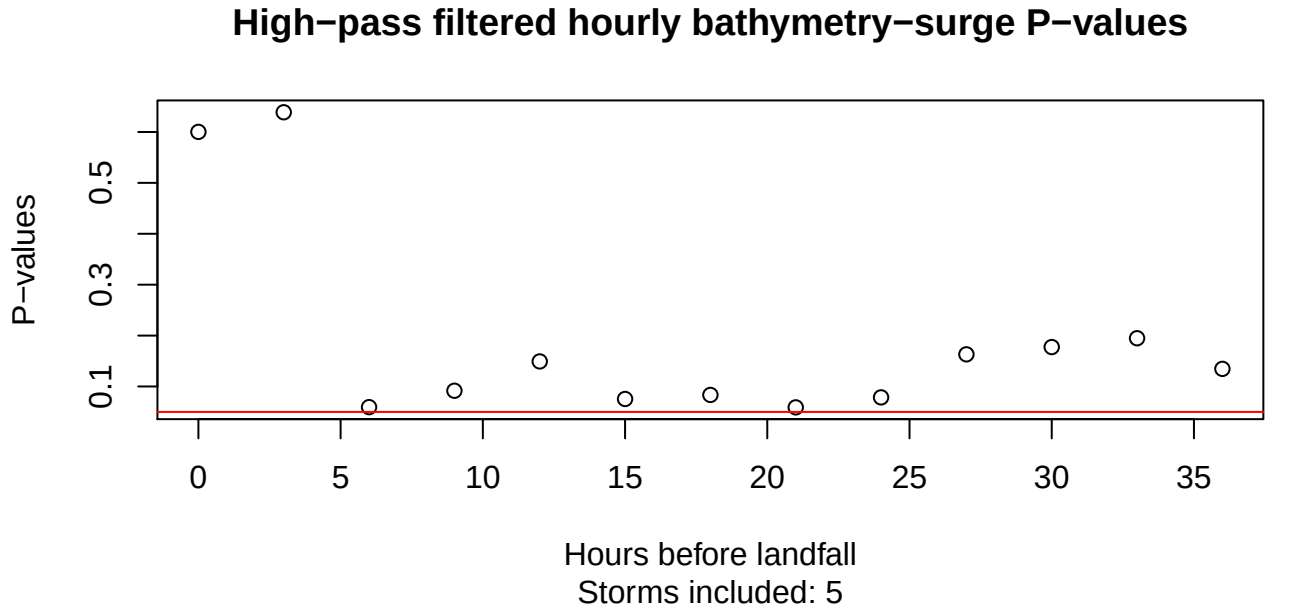
High−pass filtered hourly bathymetry−surge P−values
P−values
0.1
0.3
0.5
0
5
10
15
20
25
30
35
Hours before landfall
Storms included: 5

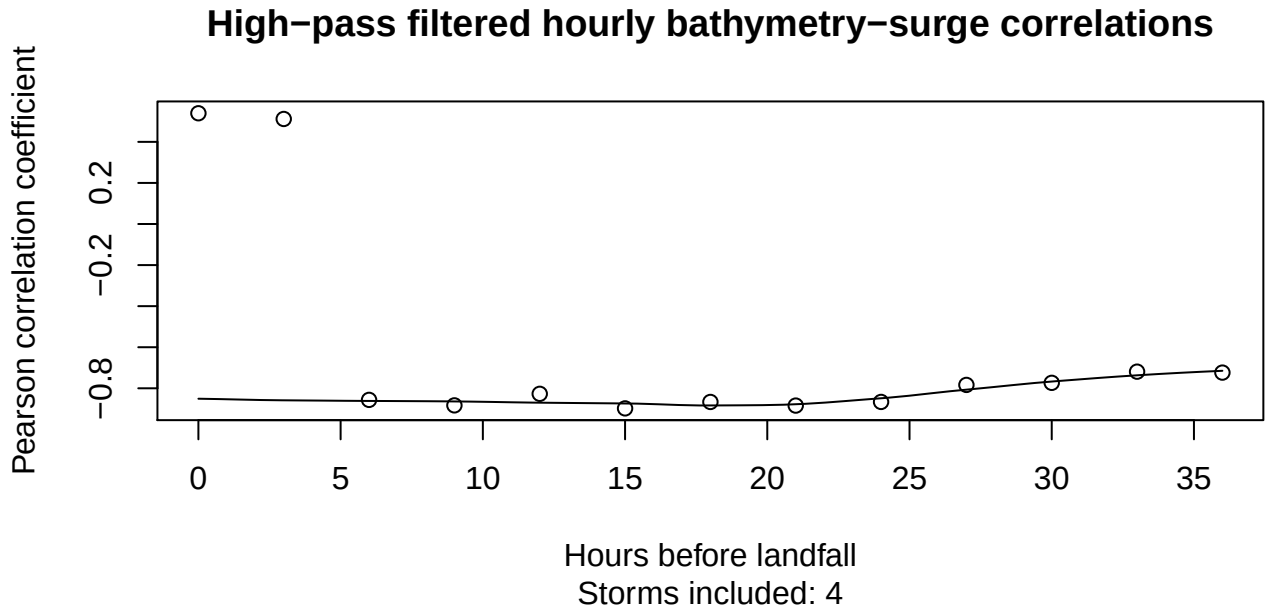
High−pass filtered hourly bathymetry−surge correlations
Pearson correlation coefficient
−0.8
−0.2
0.2
0
5
10
15
20
25
30
35
Hours before landfall
Storms included: 4

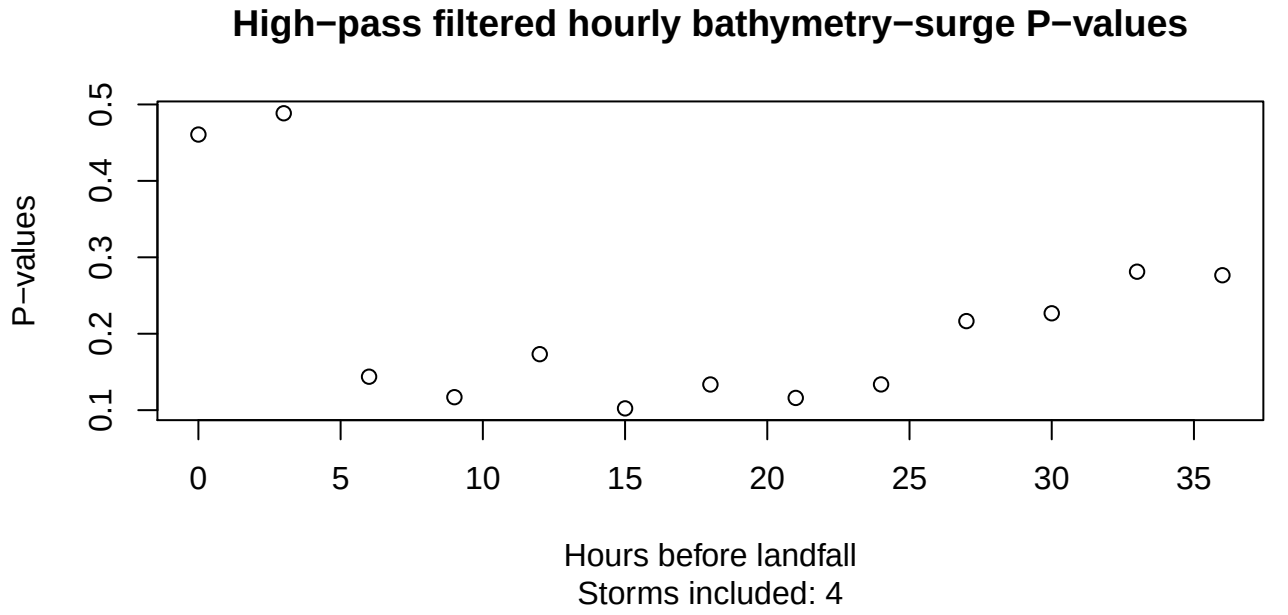
High−pass filtered hourly bathymetry−surge P−values
P−values
0.1
0.2
0.3
0.4
0.5
0
5
10
15
20
25
30
35
Hours before landfall
Storms included: 4

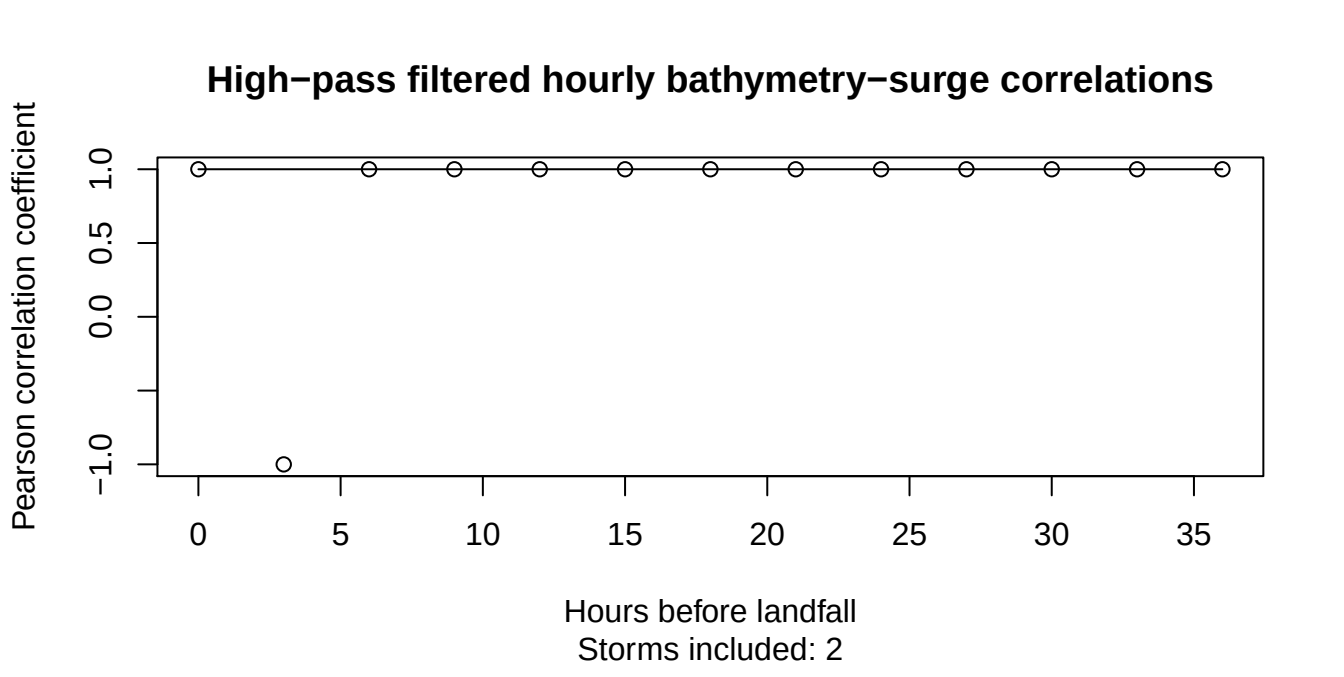
High−pass filtered hourly bathymetry−surge correlations
Pearson correlation coefficient
−1.0
0.0
0.5
1.0
0
5
10
15
20
25
30
35
Hours before landfall
Storms included: 2

# HIGH-PASS STATISTICS BY TIME INTERVAL

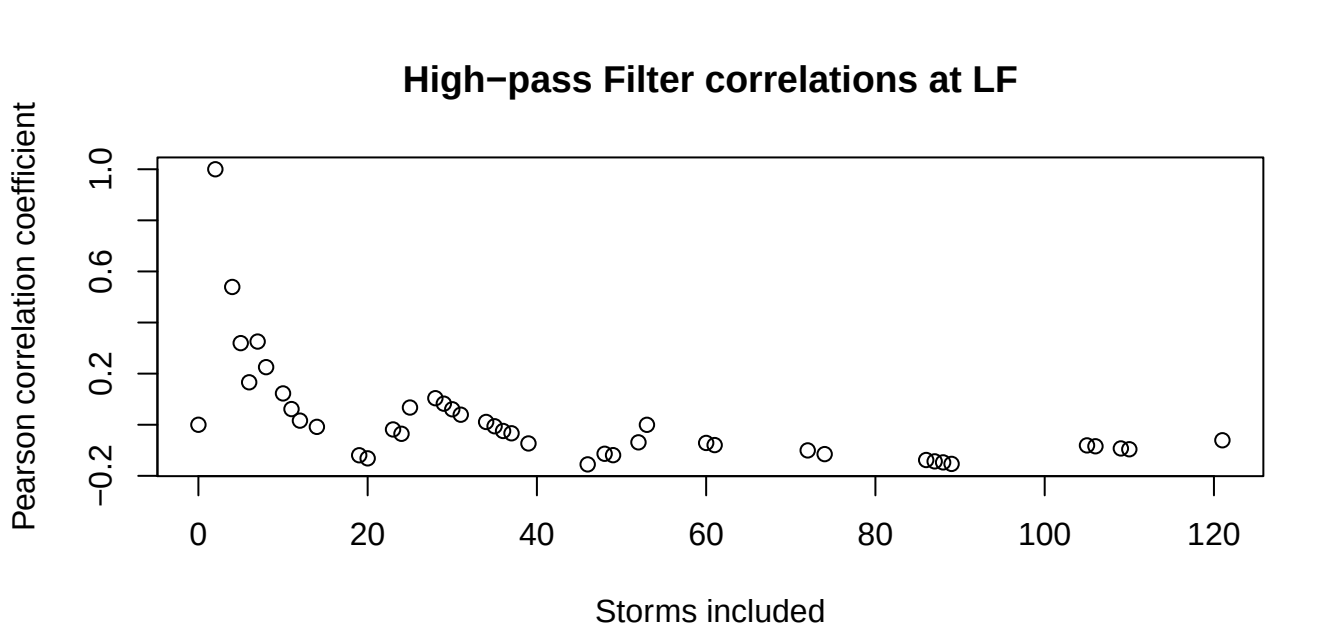
High−pass Filter correlations at LF
Pearson correlation coefficient
−0.2
0.2
0.6
1.0
0
20
40
60
80
100
120
Storms included

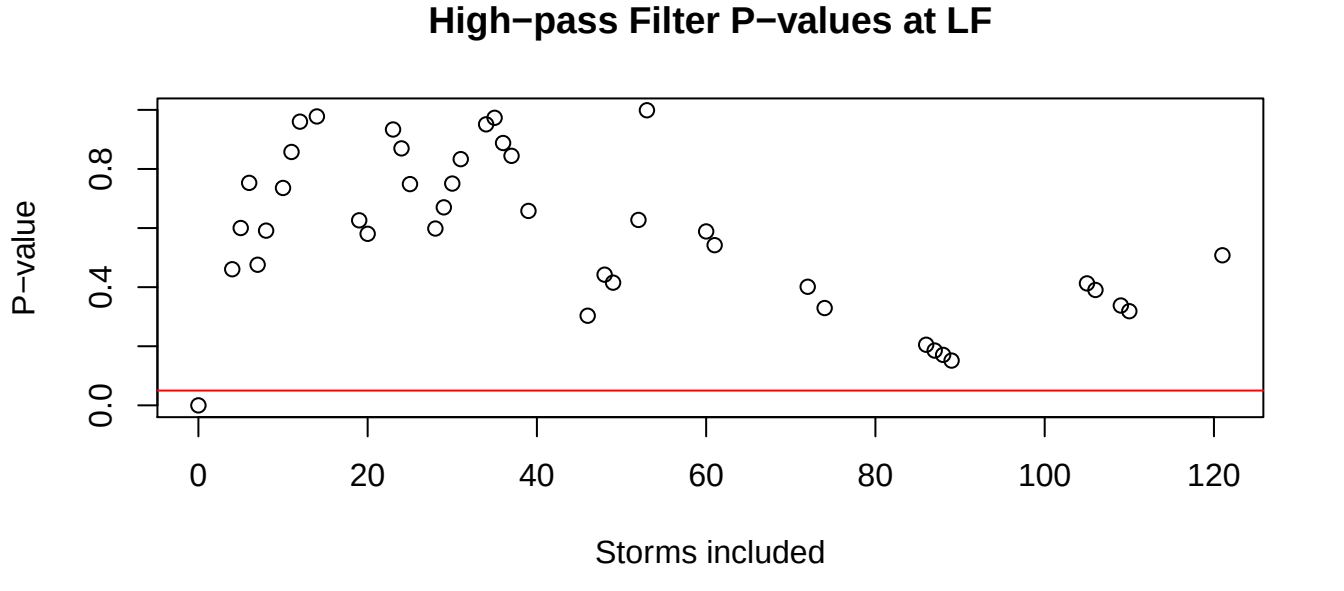
High−pass Filter P−values at LF
P−value
0.0
0.4
0.8
0
20
40
60
80
100
120
Storms included

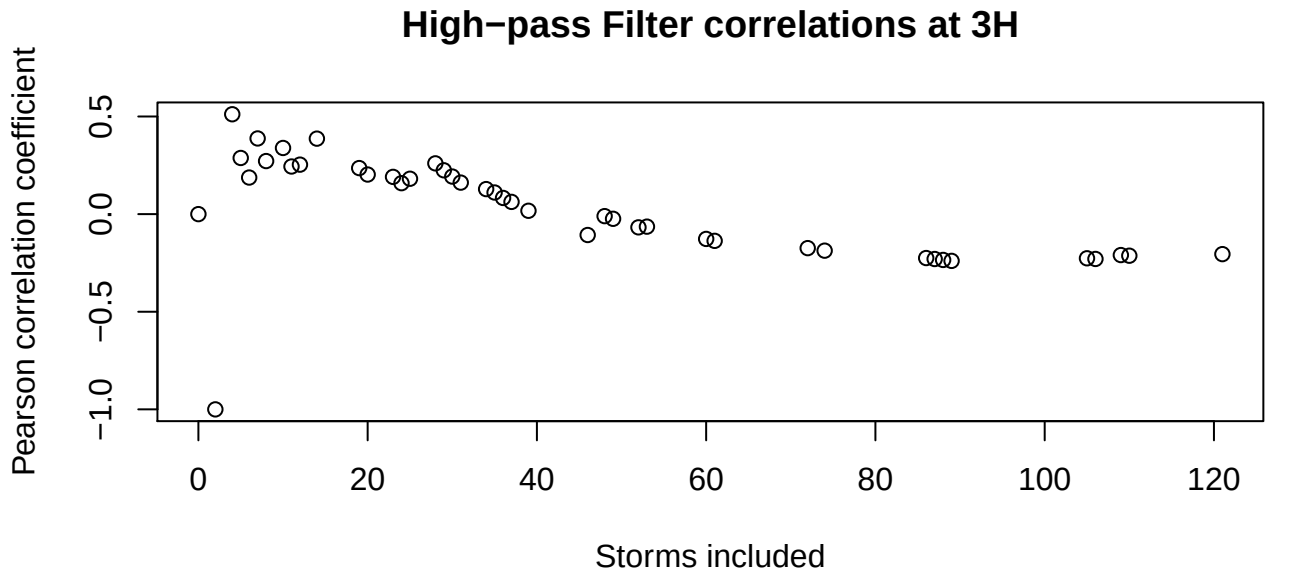
High−pass Filter correlations at 3H
Pearson correlation coefficient
−1.0
−0.5
0.0
0.5
0
20
40
60
80
100
120
Storms included

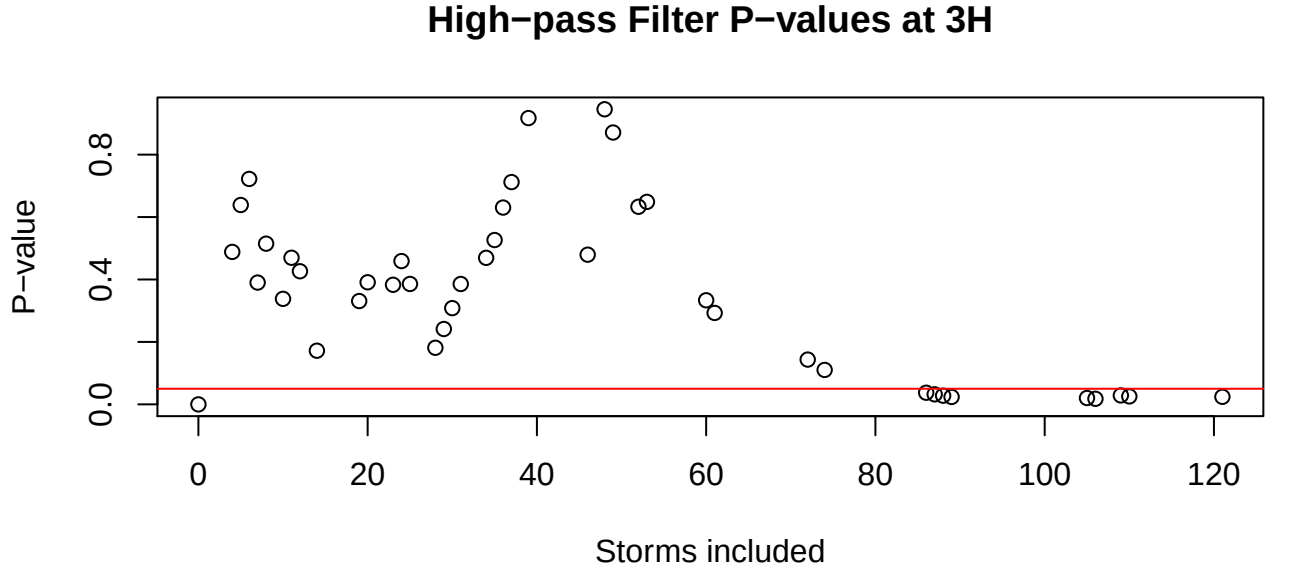
High−pass Filter P−values at 3H
P−value
0.0
0.4
0.8
0
20
40
60
80
100
120
Storms included

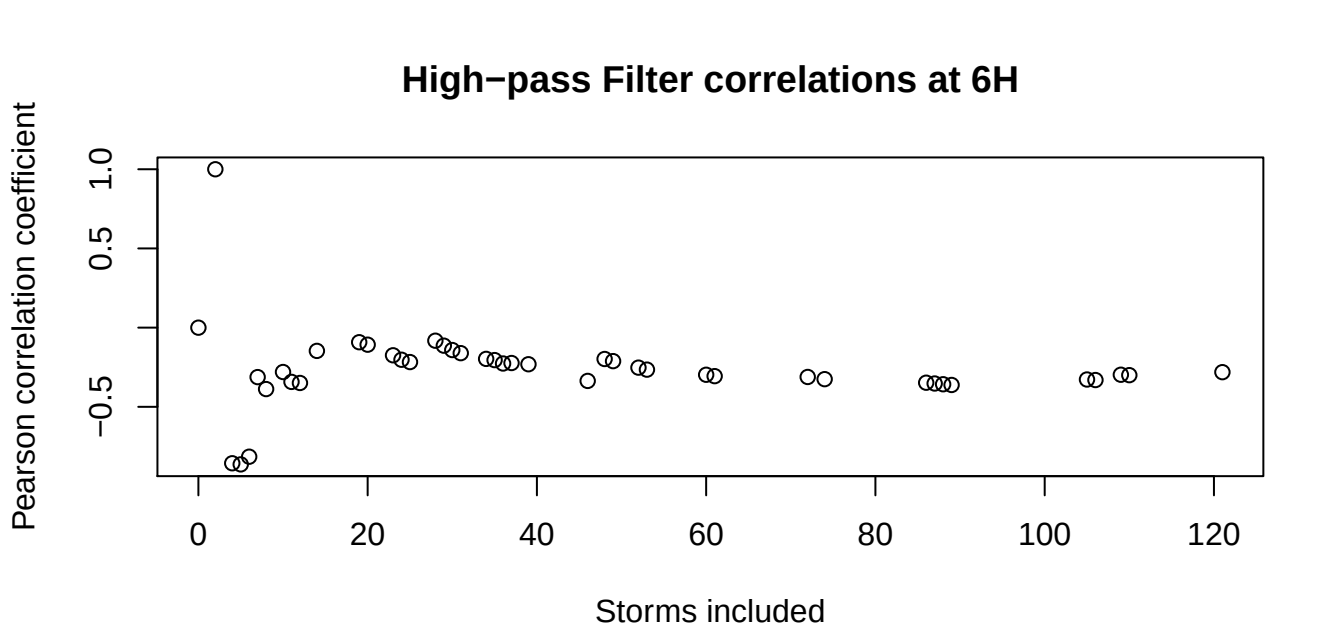
High−pass Filter correlations at 6H
Pearson correlation coefficient
1.0
0.5
−0.5
0
20
40
60
80
100
120
Storms included

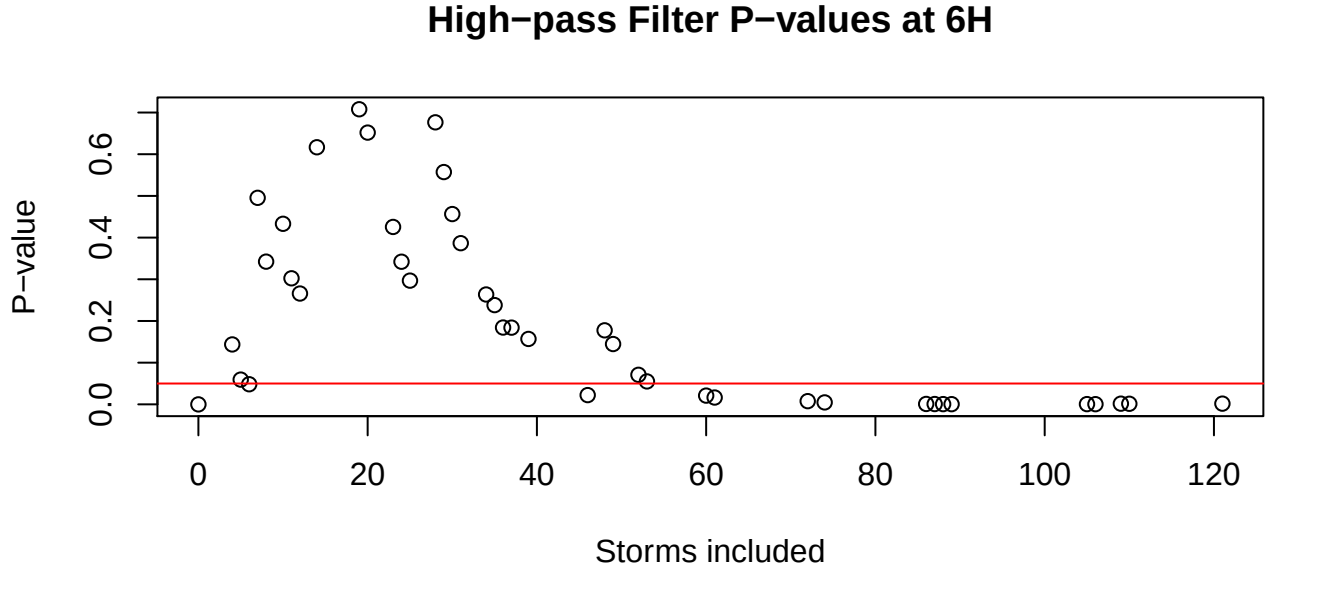
High−pass Filter P−values at 6H
P−value
0.0
0.2
0.4
0.6
0
20
40
60
80
100
120
Storms included

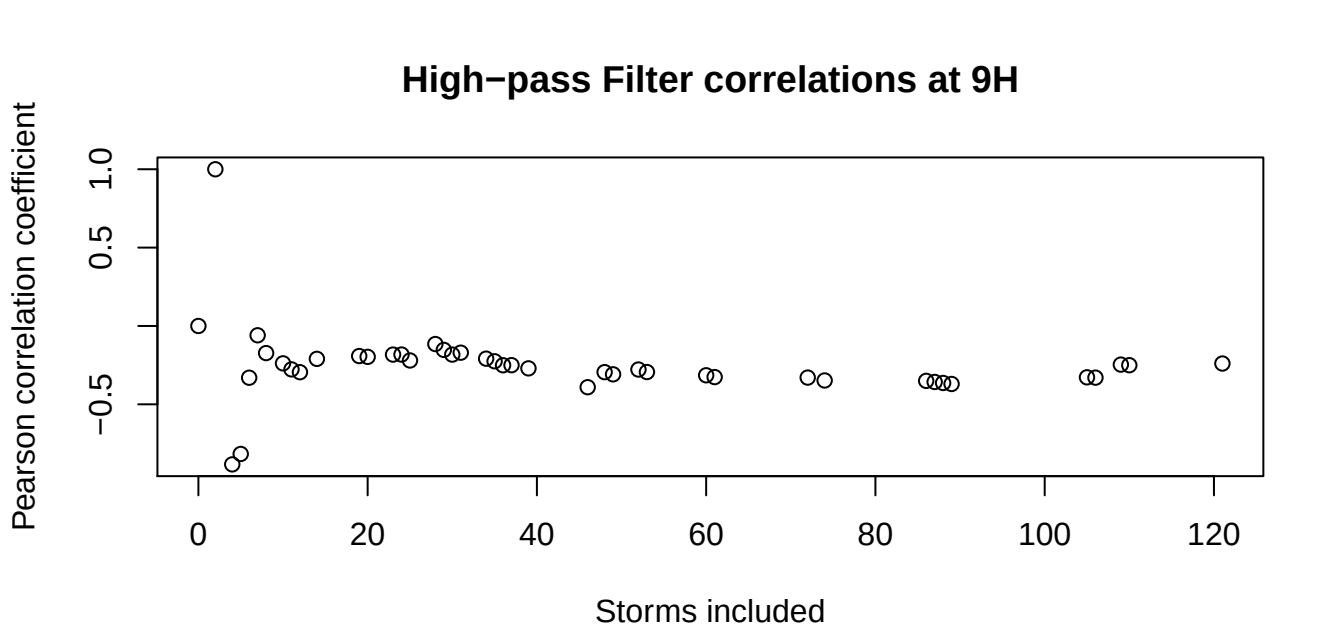
High−pass Filter correlations at 9H
Pearson correlation coefficient
1.0
0.5
−0.5
0
20
40
60
80
100
120
Storms included

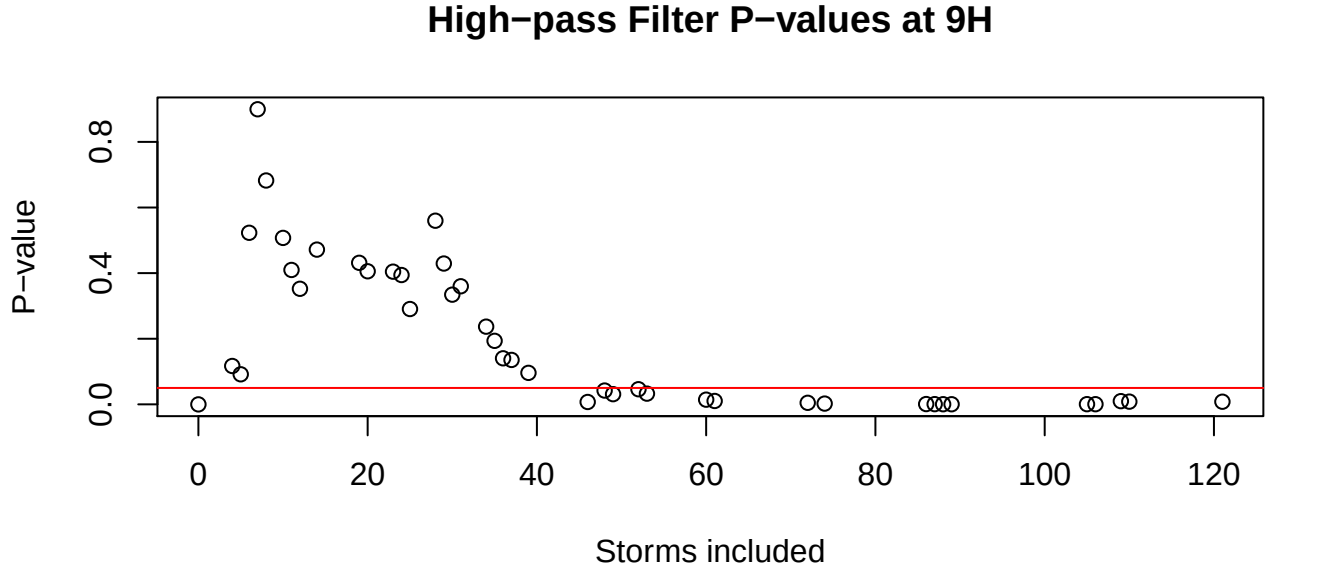
High−pass Filter P−values at 9H
P−value
0.8
0.4
0.0
0
20
40
60
80
100
120
Storms included

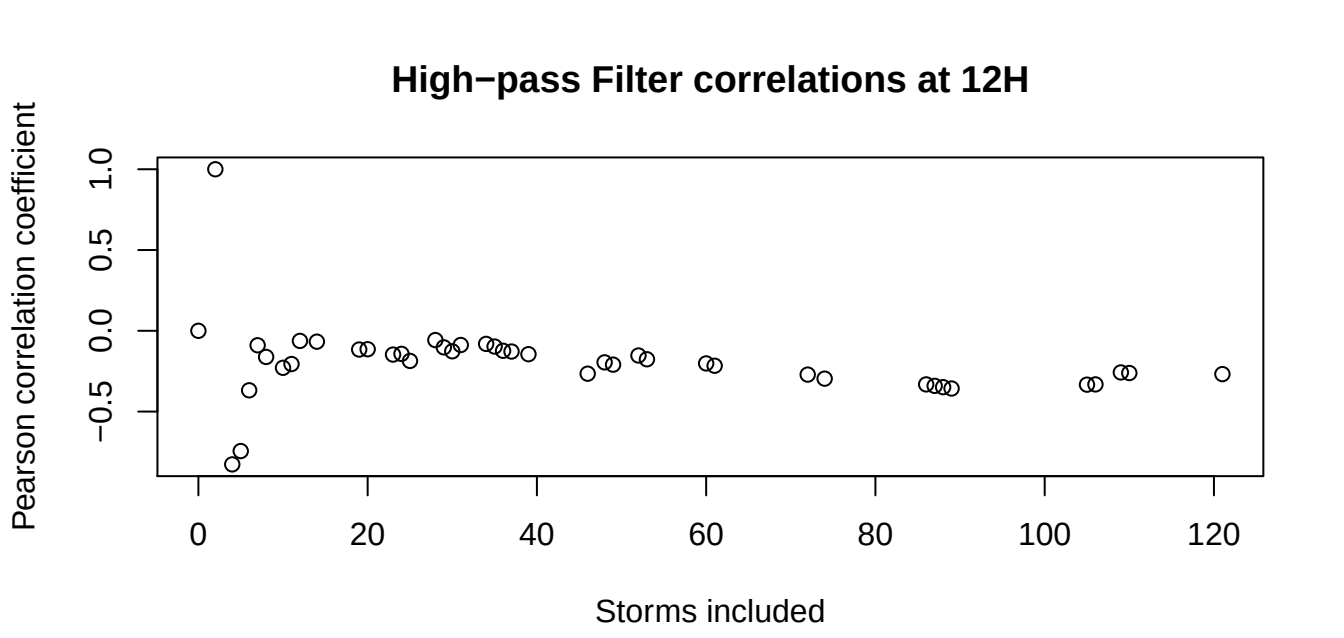
High−pass Filter correlations at 12H
Pearson correlation coefficient
−0.5
0.0
0.5
1.0
0
20
40
60
80
100
120
Storms included

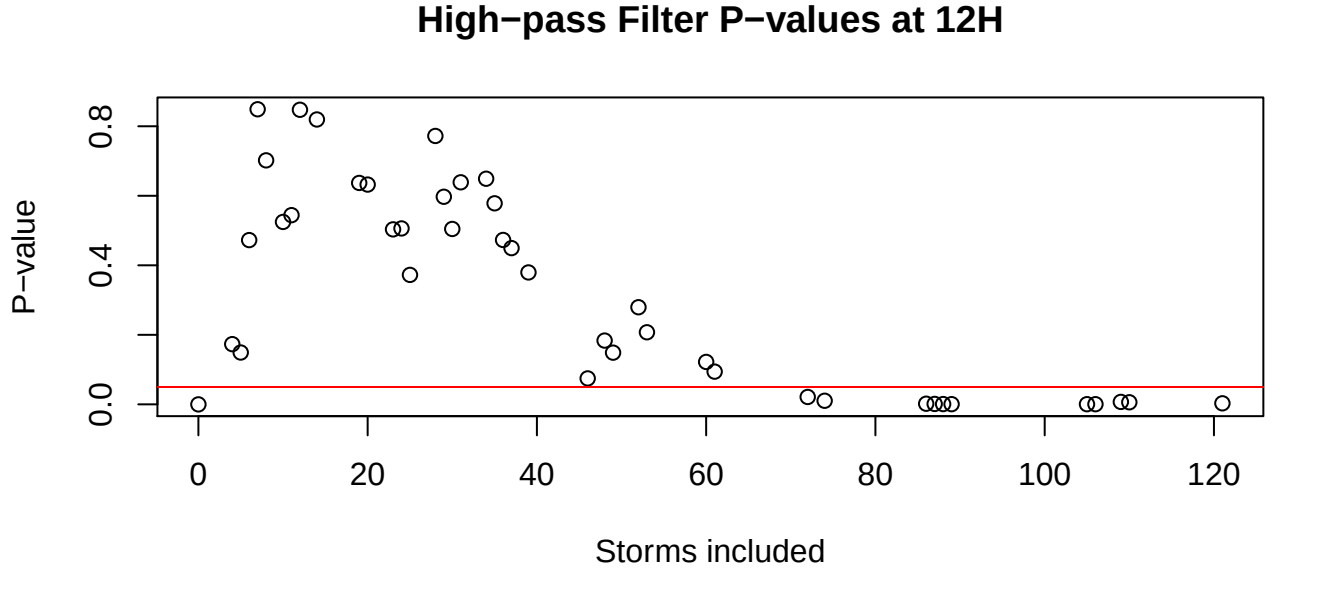
High−pass Filter P−values at 12H
P−value
0.0
0.4
0.8
0
20
40
60
80
100
120
Storms included

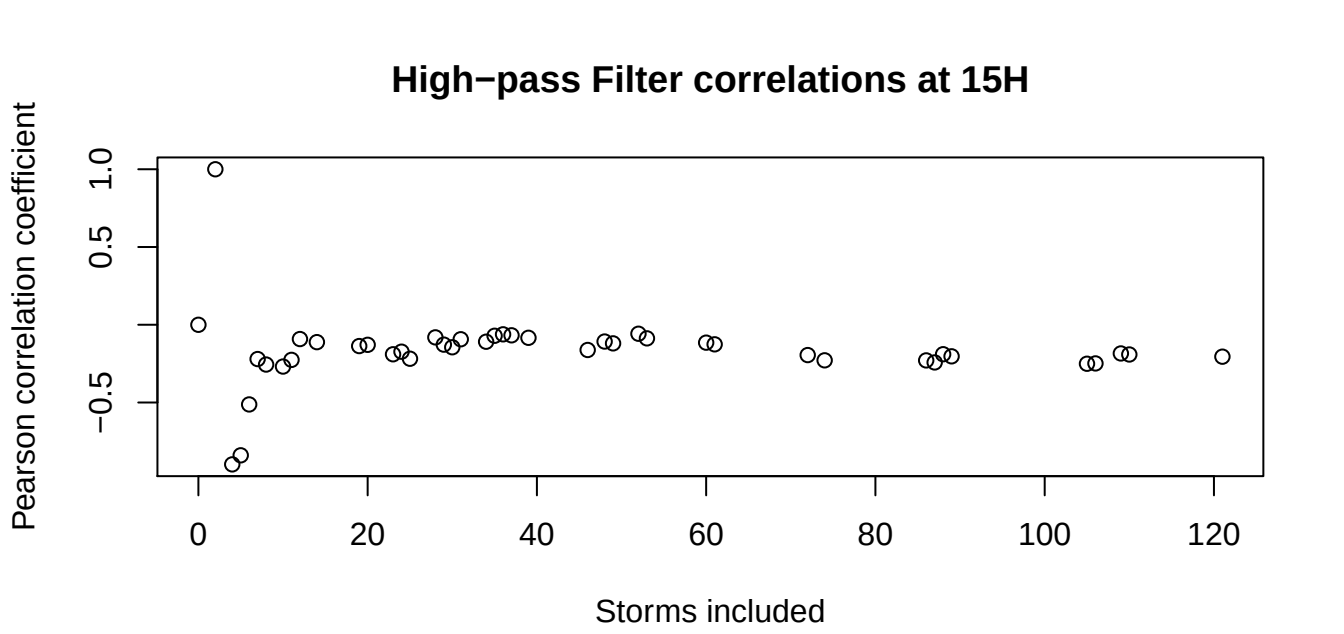
High−pass Filter correlations at 15H
Pearson correlation coefficient
1.0
0.5
−0.5
0
20
40
60
80
100
120
Storms included

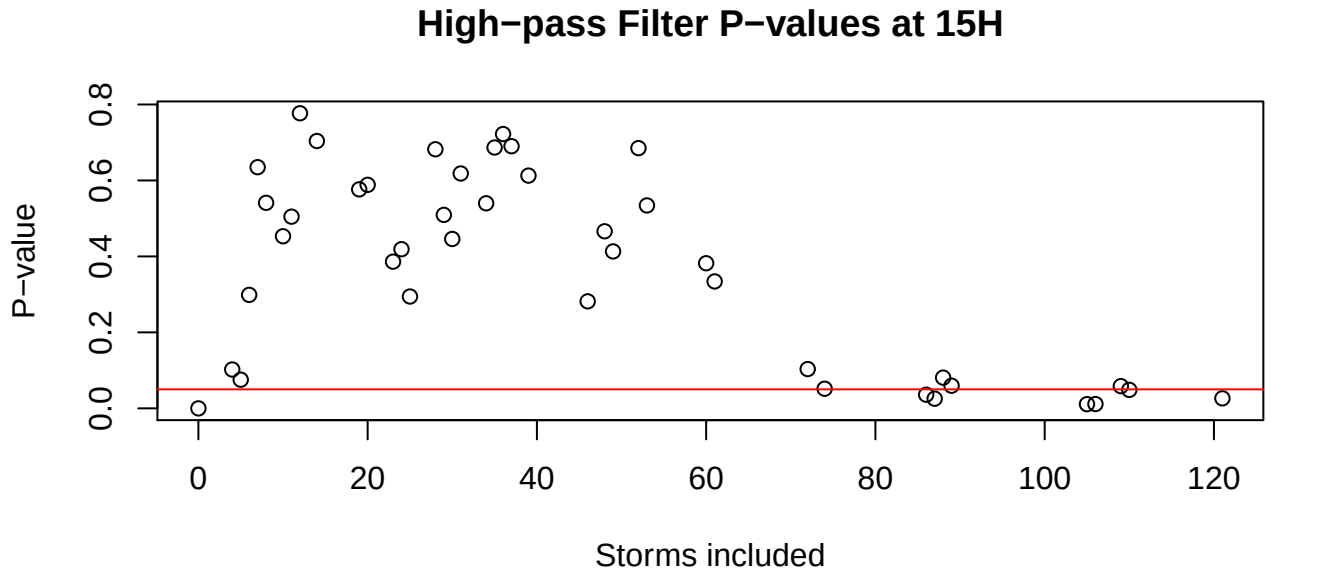
High−pass Filter P−values at 15H
P−value
0.8
0.6
0.4
0.2
0.0
0
20
40
60
80
100
120
Storms included

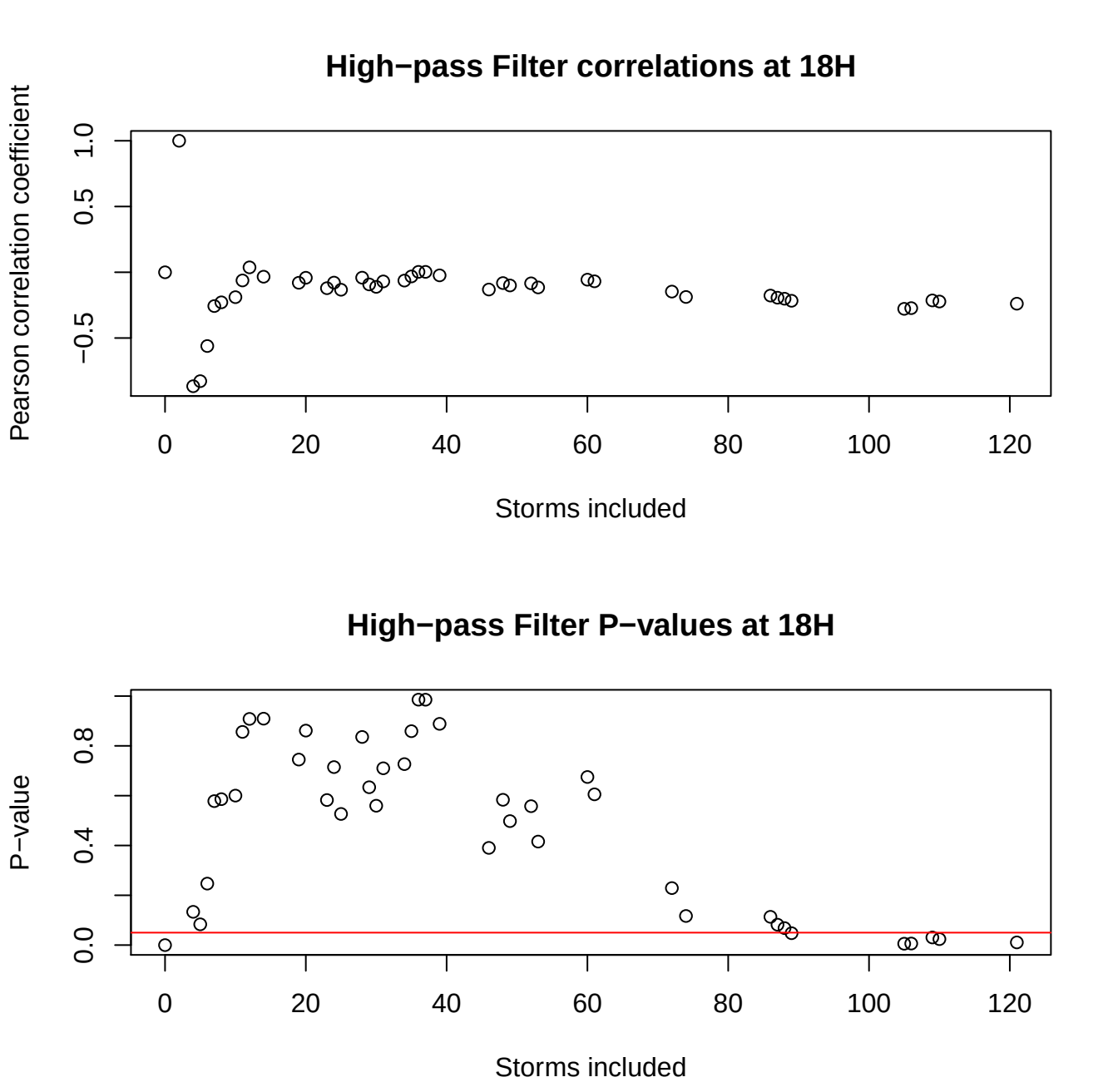
High−pass Filter correlations at 18H
Pearson correlation coefficient
1.0
0.5
−0.5
0
20
40
60
80
100
120
Storms included
High−pass Filter P−values at 18H
P−value
0.8
0.4
0.0
0
20
40
60
80
100
120
Storms included

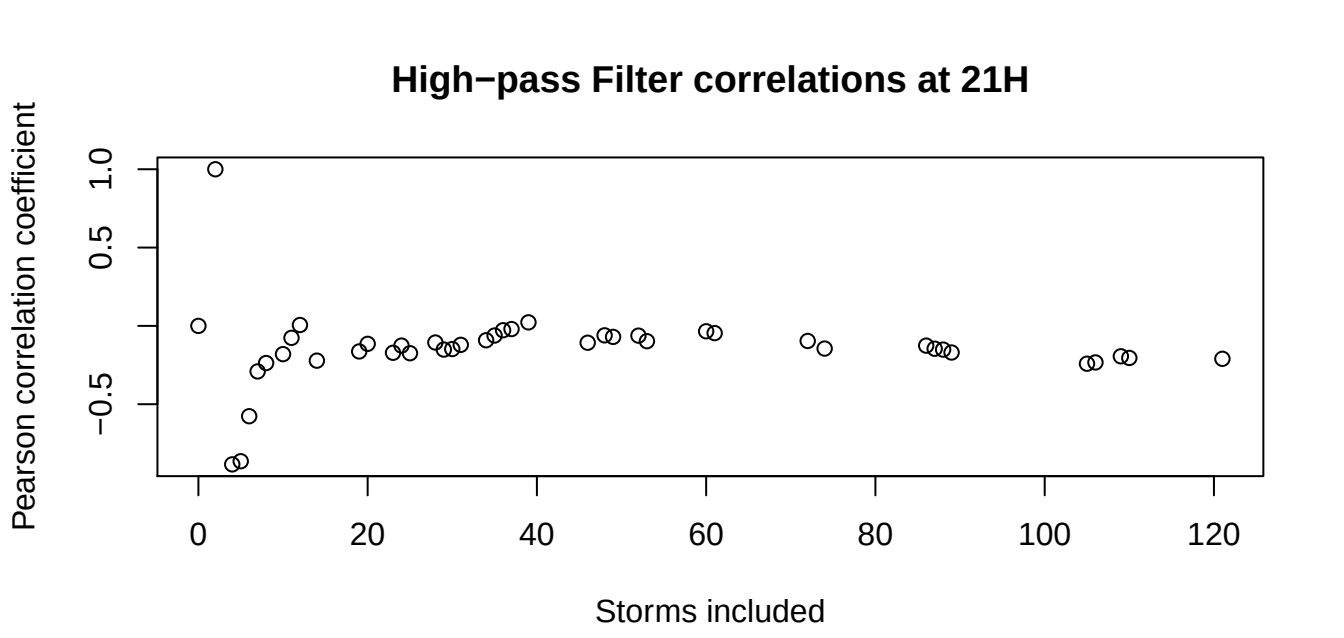
High−pass Filter correlations at 21H
Pearson correlation coefficient
1.0
0.5
−0.5
0
20
40
60
80
100
120
Storms included

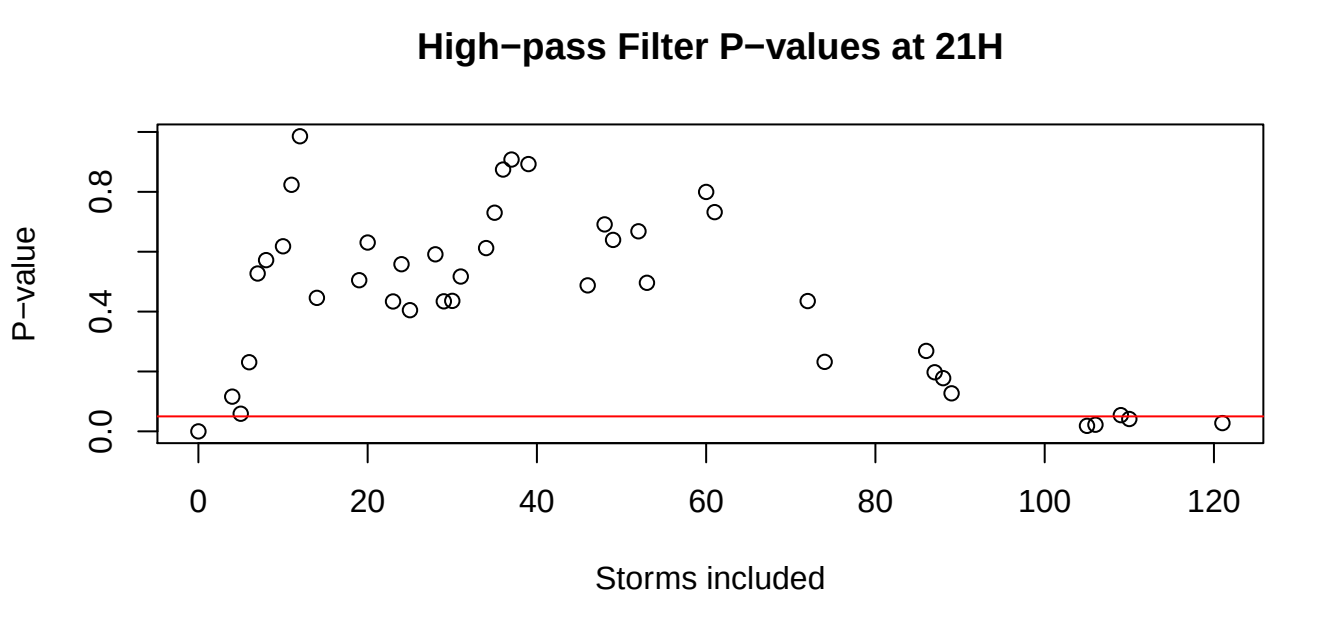
High−pass Filter P−values at 21H
P−value
0.8
0.4
0.0
0
20
40
60
80
100
120
Storms included

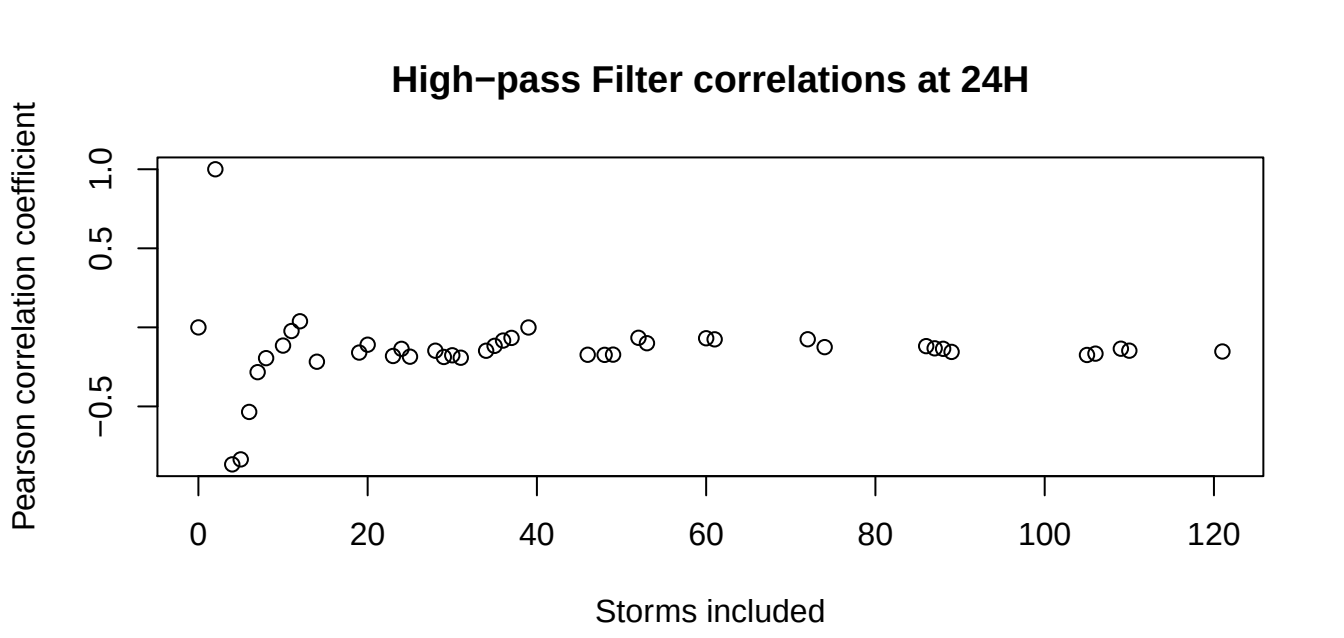
High−pass Filter correlations at 24H
Pearson correlation coefficient
1.0
0.5
−0.5
0
20
40
60
80
100
120
Storms included

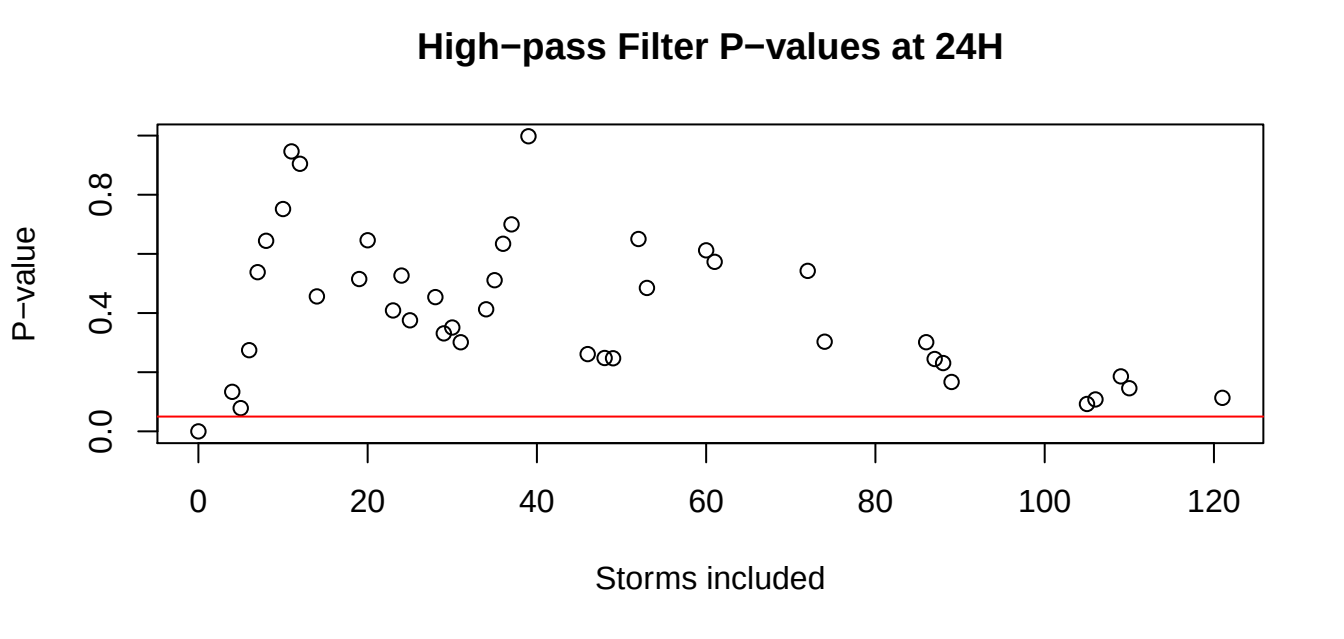
High−pass Filter P−values at 24H
P−value
0.8
0.4
0.0
0
20
40
60
80
100
120
Storms included

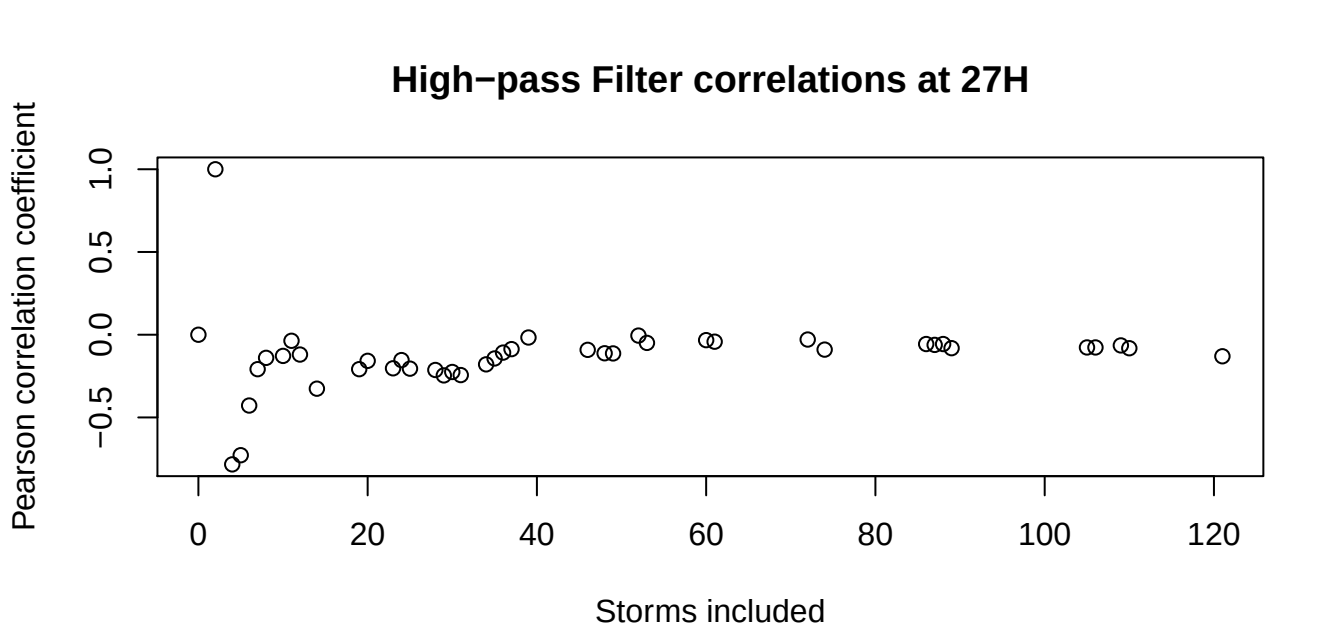
High−pass Filter correlations at 27H
Pearson correlation coefficient
1.0
0.5
0.0
−0.5
0
20
40
60
80
100
120
Storms included

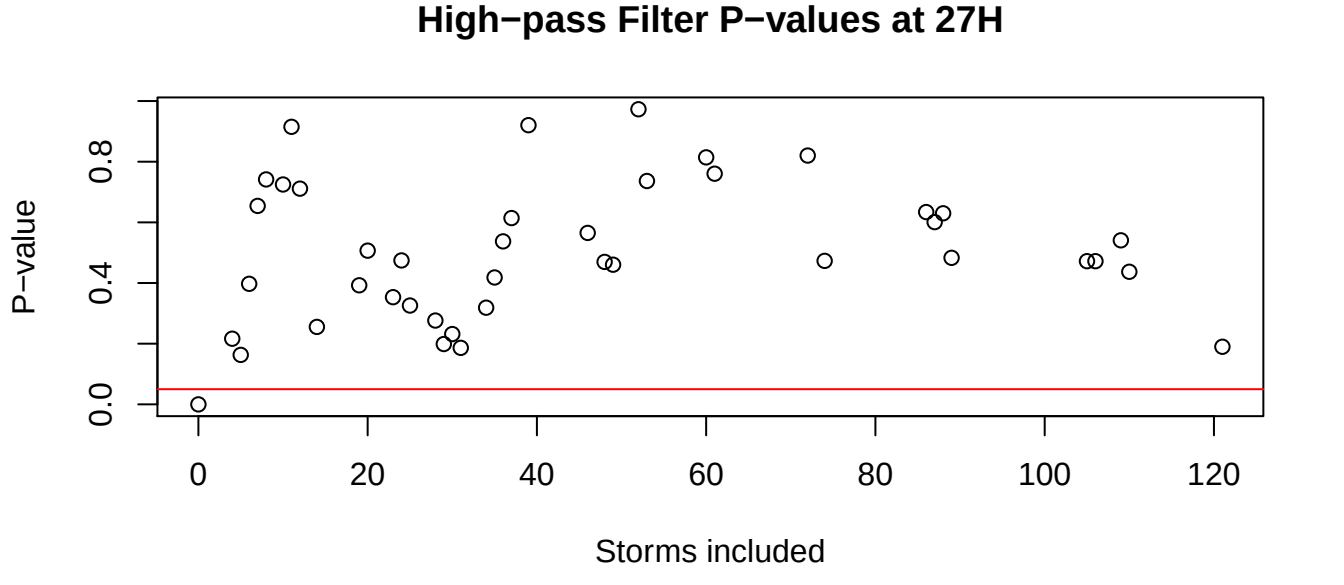
High−pass Filter P−values at 27H
P−value
0.8
0.4
0.0
0
20
40
60
80
100
120
Storms included

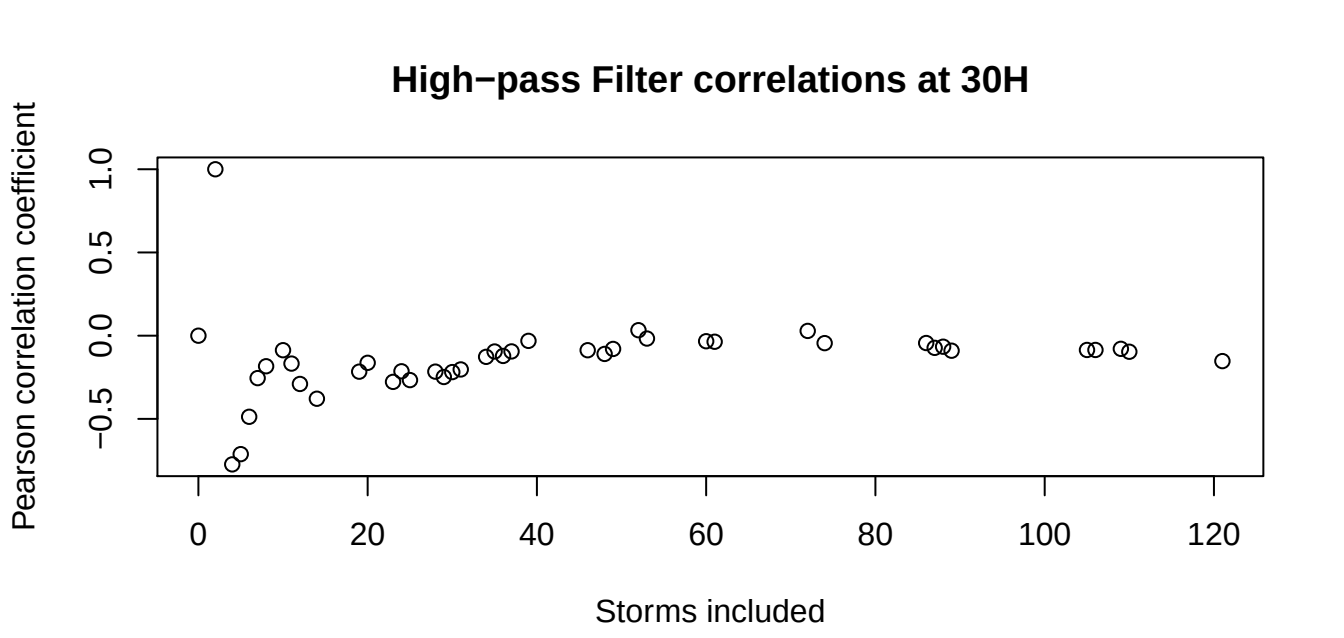
High−pass Filter correlations at 30H
Pearson correlation coefficient
1.0
0.5
0.0
−0.5
0
20
40
60
80
100
120
Storms included

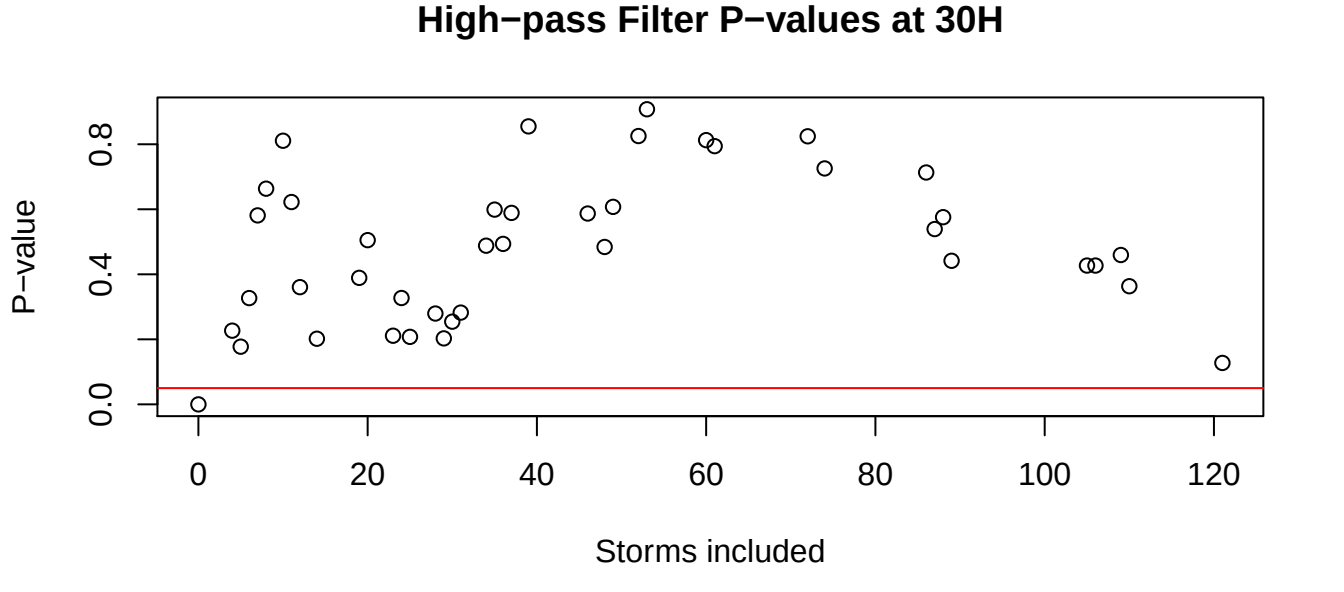
High−pass Filter P−values at 30H
P−value
0.8
0.4
0.0
0
20
40
60
80
100
120
Storms included

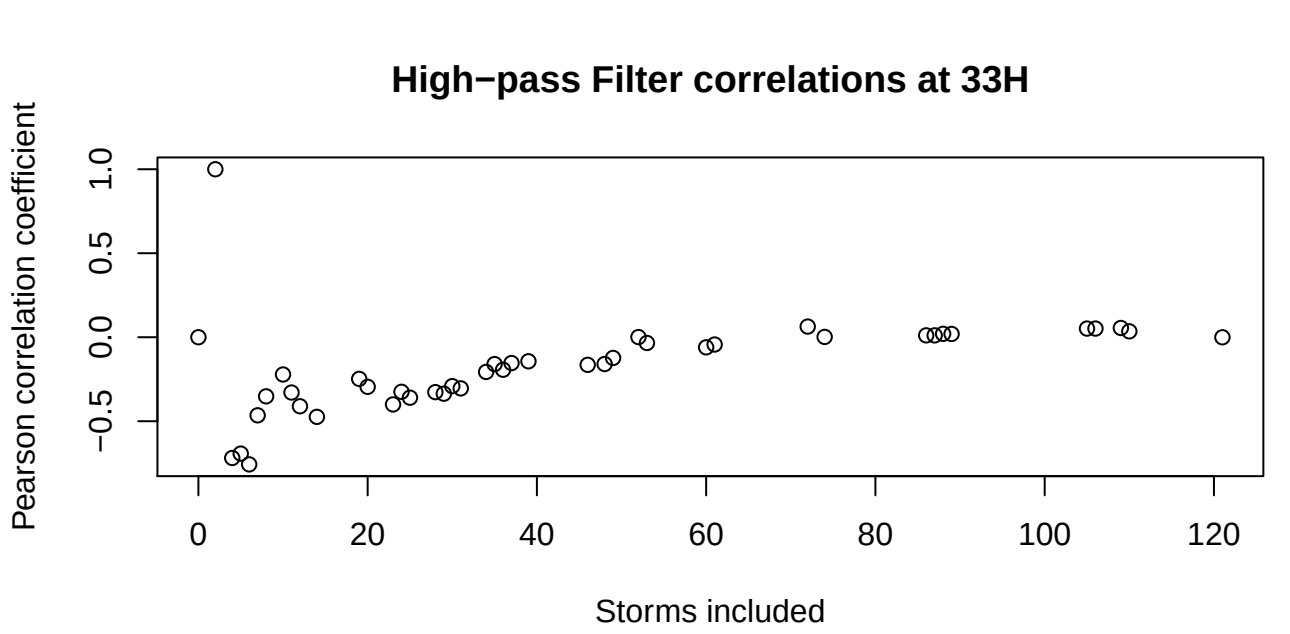
High−pass Filter correlations at 33H
Pearson correlation coefficient
1.0
0.5
0.0
−0.5
0
20
40
60
80
100
120
Storms included

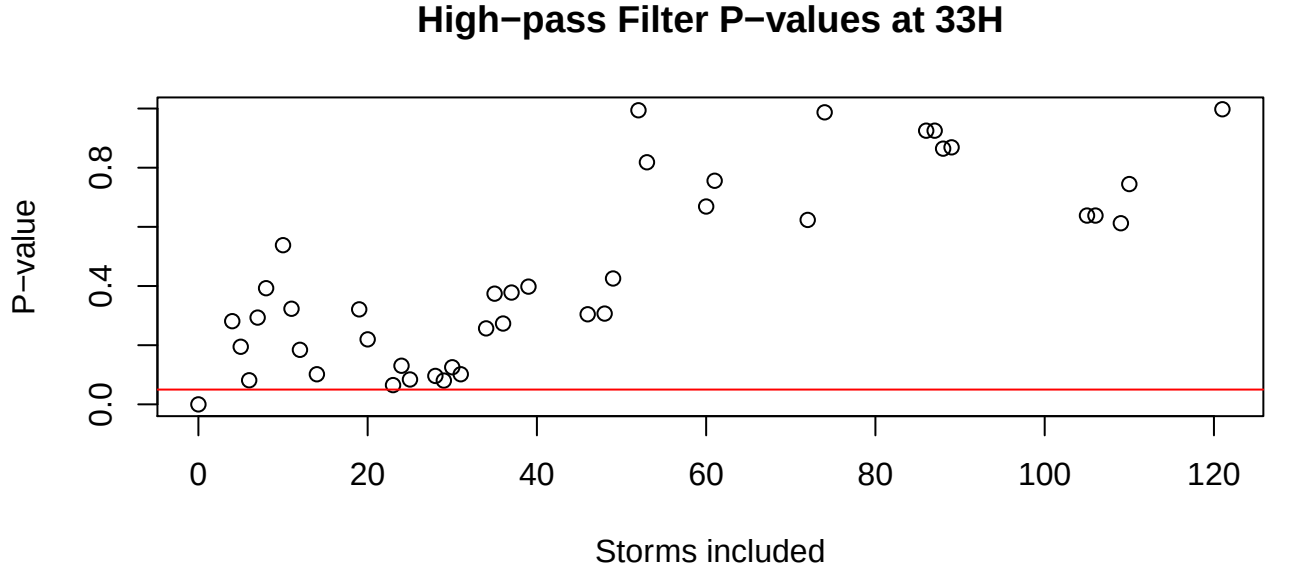
High−pass Filter P−values at 33H
P−value
0.8
0.4
0.0
0
20
40
60
80
100
120
Storms included

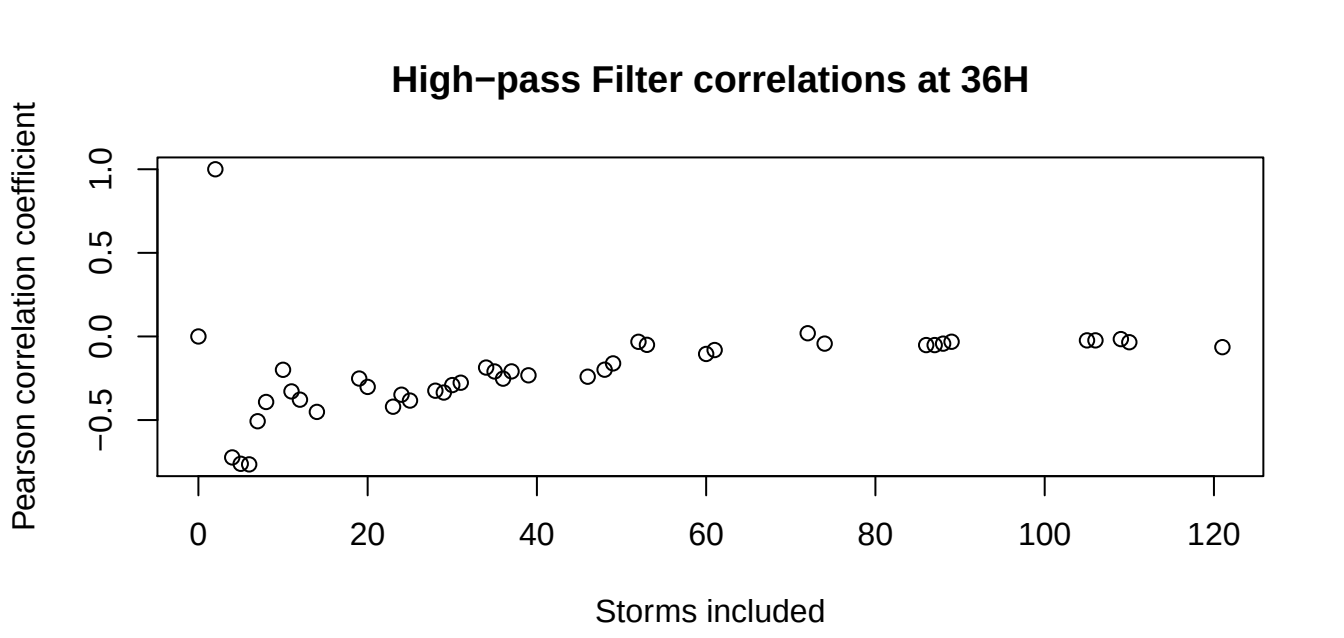
High−pass Filter correlations at 36H
Pearson correlation coefficient
−0.5
0.0
0.5
1.0
0
20
40
60
80
100
120
Storms included

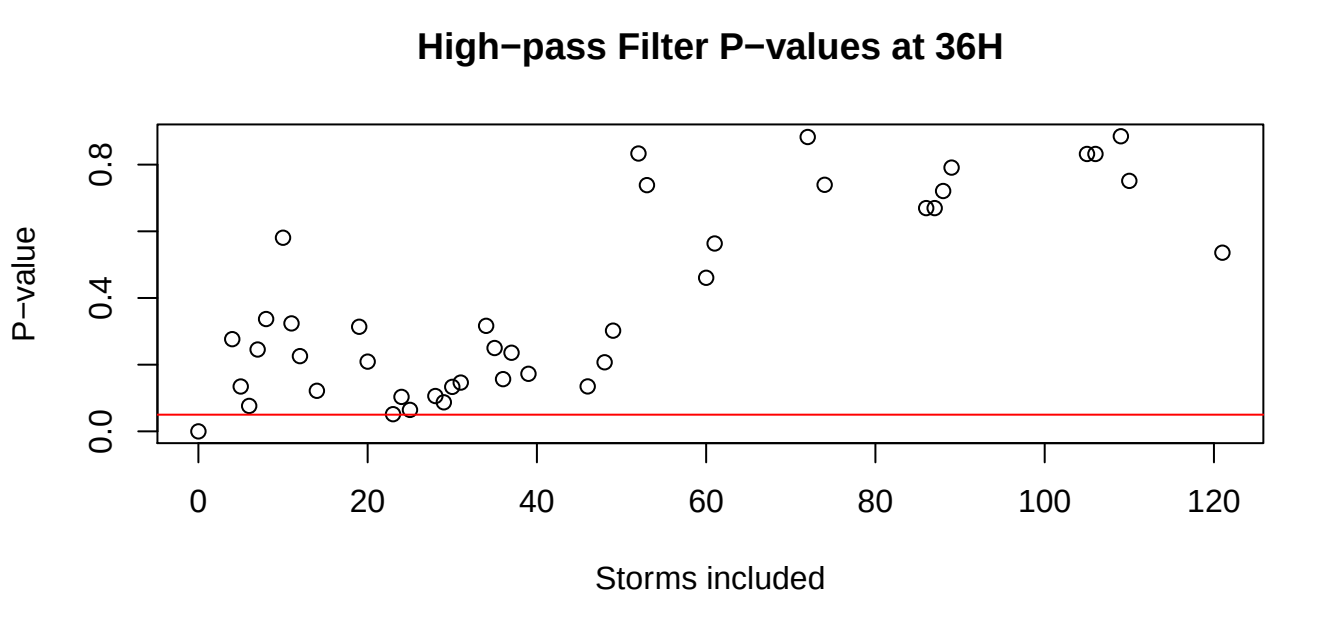
High−pass Filter P−values at 36H
P−value
0.0
0.4
0.8
0
20
40
60
80
100
120
Storms included

# LOW-PASS STATISTICS BY TIME INTERVAL

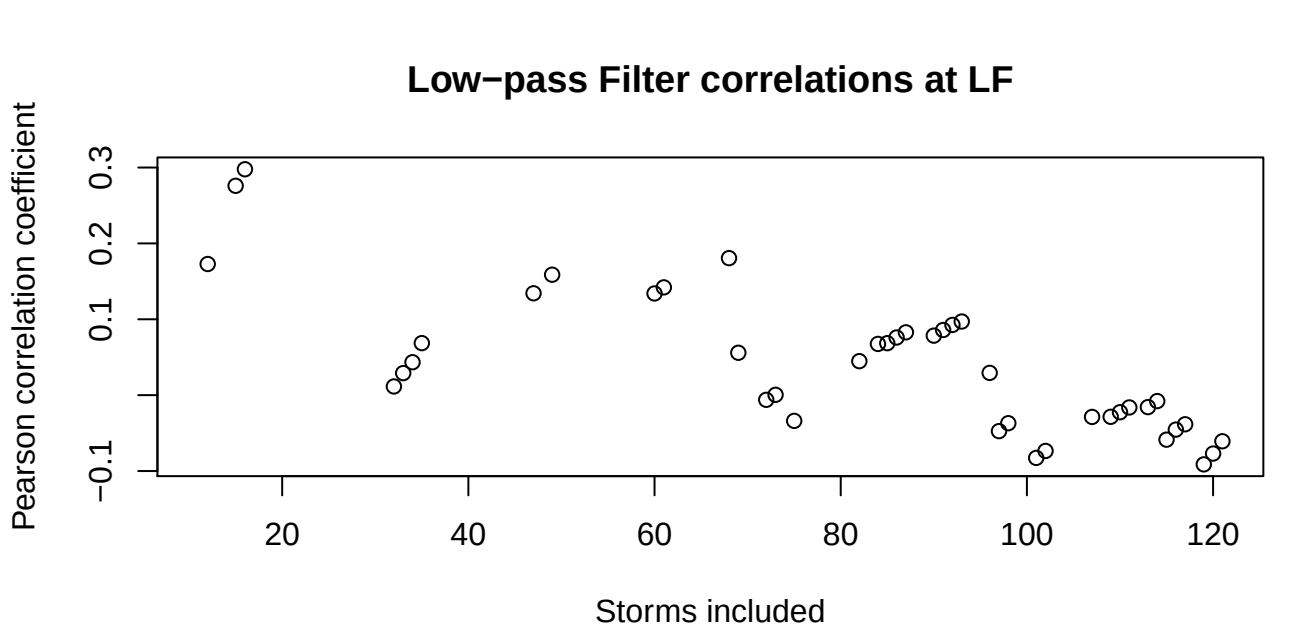
Low−pass Filter correlations at LF
Pearson correlation coefficient
−0.1
0.1
0.2
0.3
20
40
60
80
100
120
Storms included

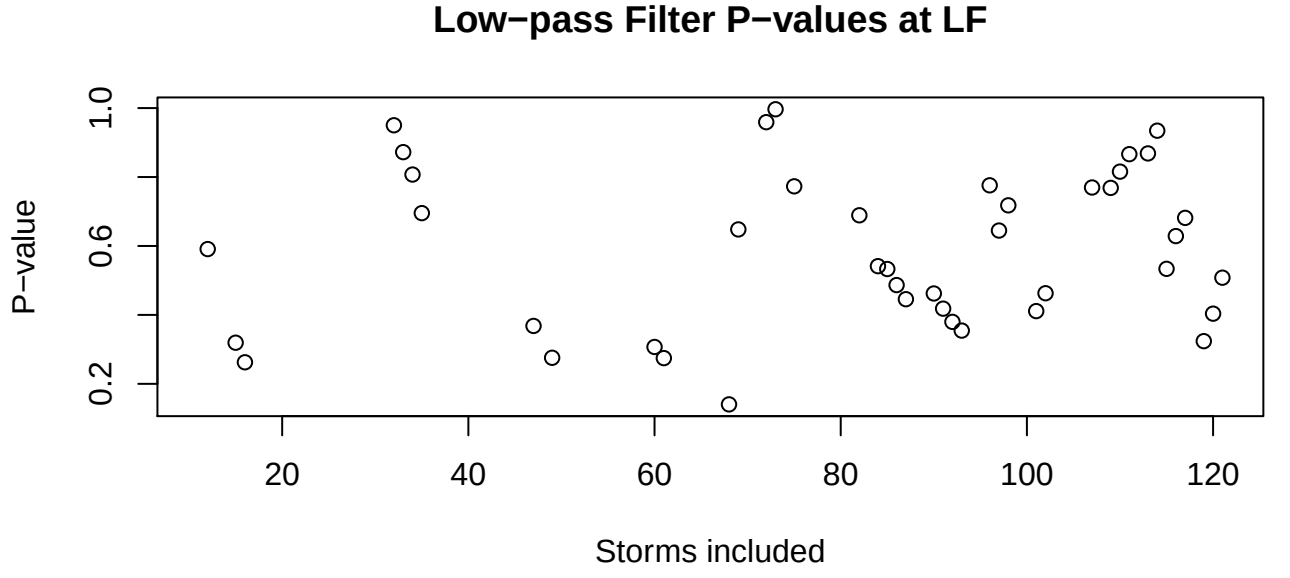
Low−pass Filter P−values at LF
P−value
0.2
0.6
1.0
20
40
60
80
100
120
Storms included

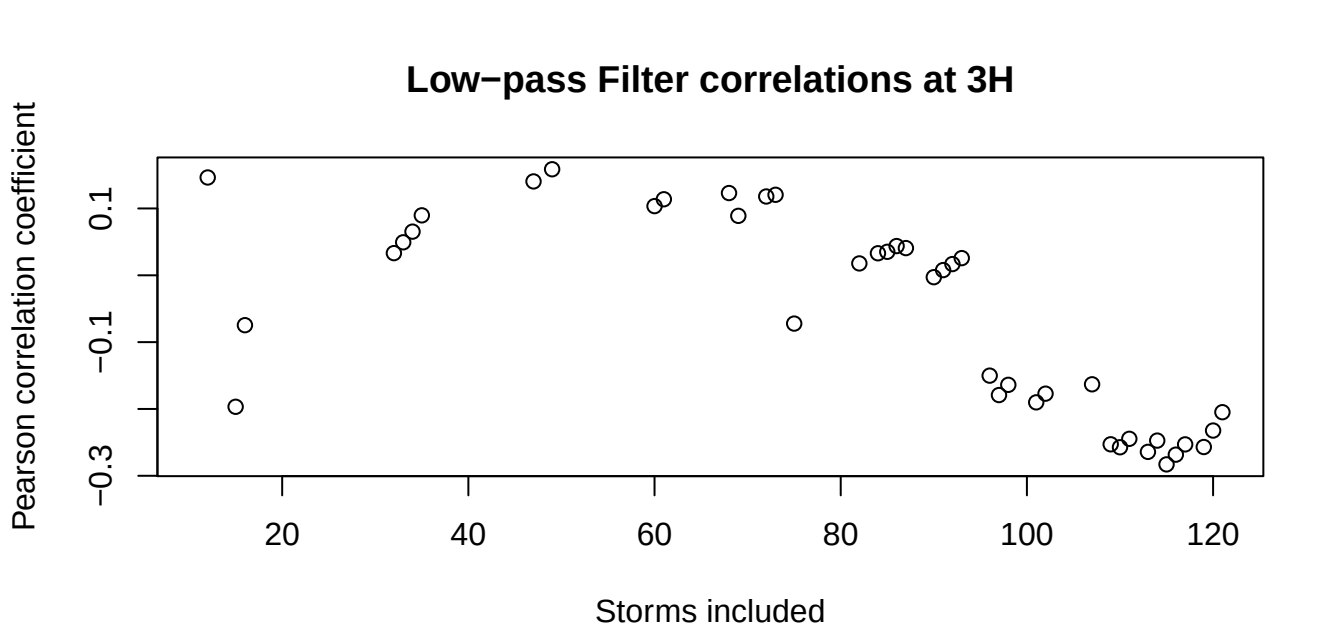
Low−pass Filter correlations at 3H
Pearson correlation coefficient
0.1
−0.1
−0.3
20
40
60
80
100
120
Storms included

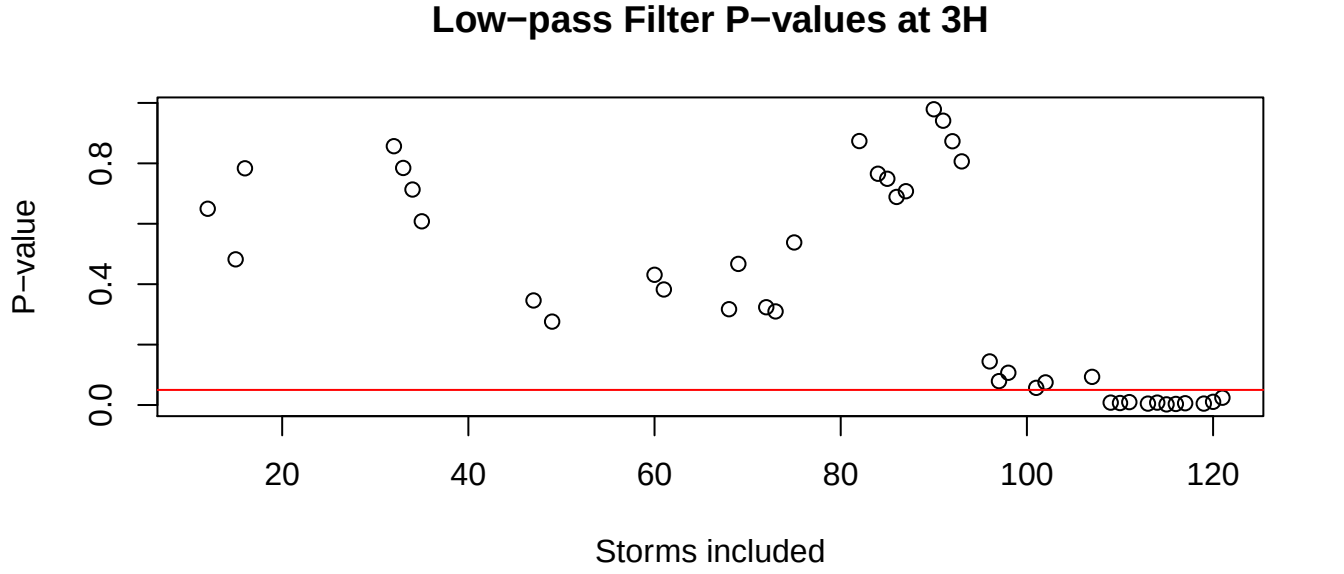
Low−pass Filter P−values at 3H
P−value
0.0
0.4
0.8
20
40
60
80
100
120
Storms included

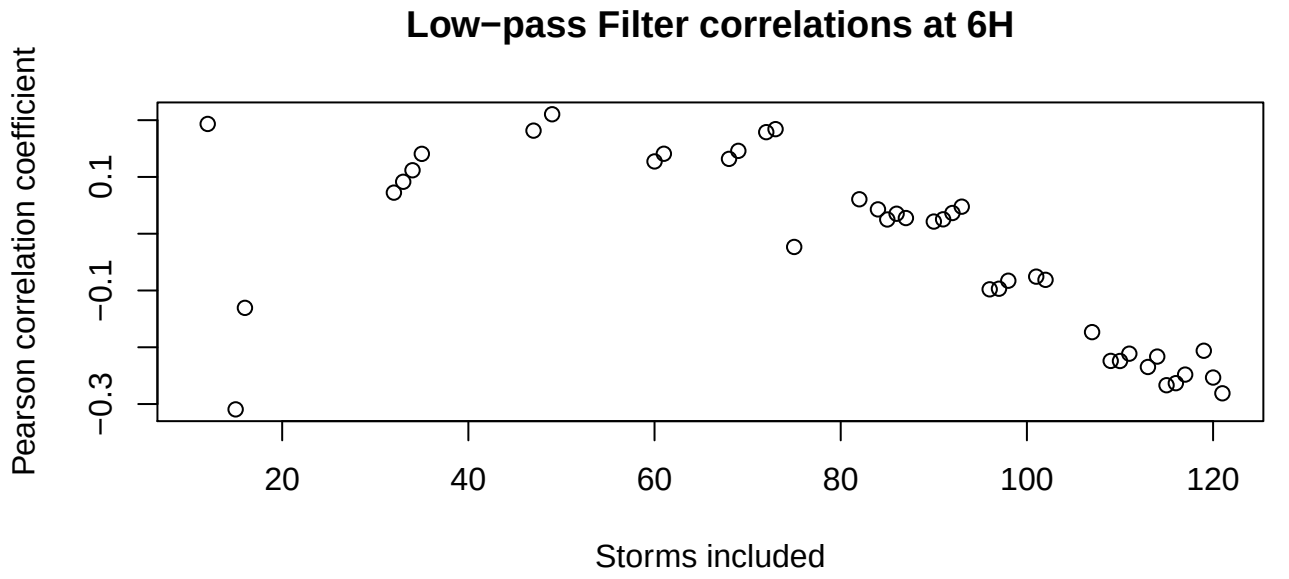
Low−pass Filter correlations at 6H
Pearson correlation coefficient
−0.3
−0.1
0.1
20
40
60
80
100
120
Storms included

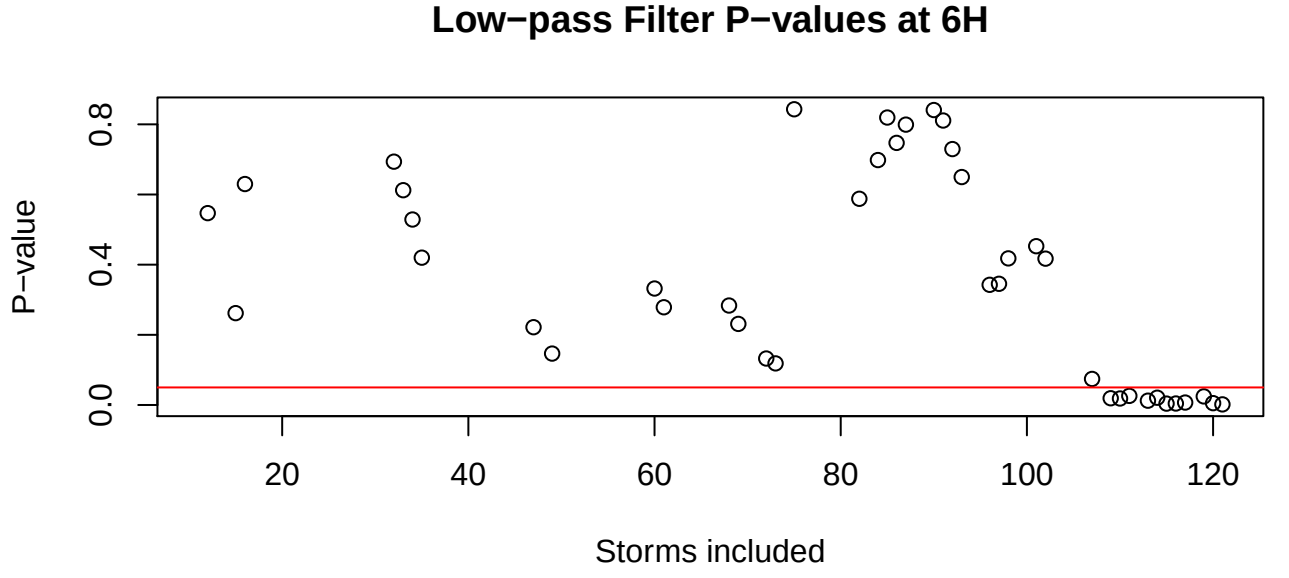
Low−pass Filter P−values at 6H
P−value
0.0
0.4
0.8
20
40
60
80
100
120
Storms included

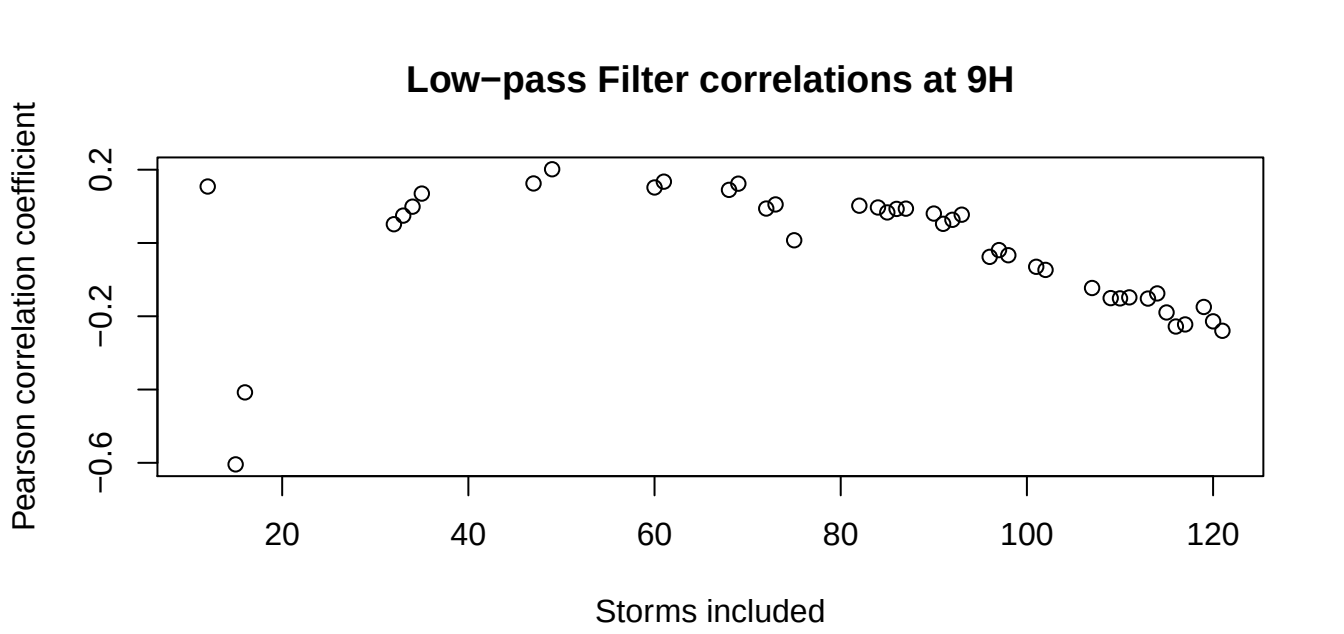
Low−pass Filter correlations at 9H
Pearson correlation coefficient
0.2
−0.2
−0.6
20
40
60
80
100
120
Storms included

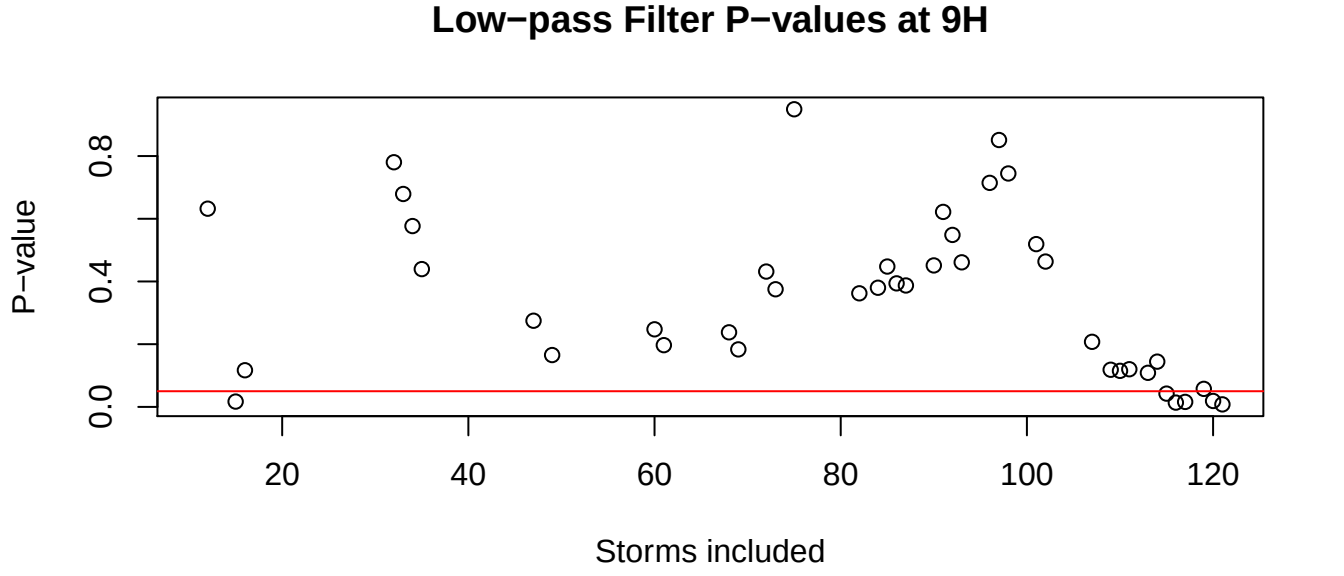
Low−pass Filter P−values at 9H
P−value
0.0
0.4
0.8
20
40
60
80
100
120
Storms included

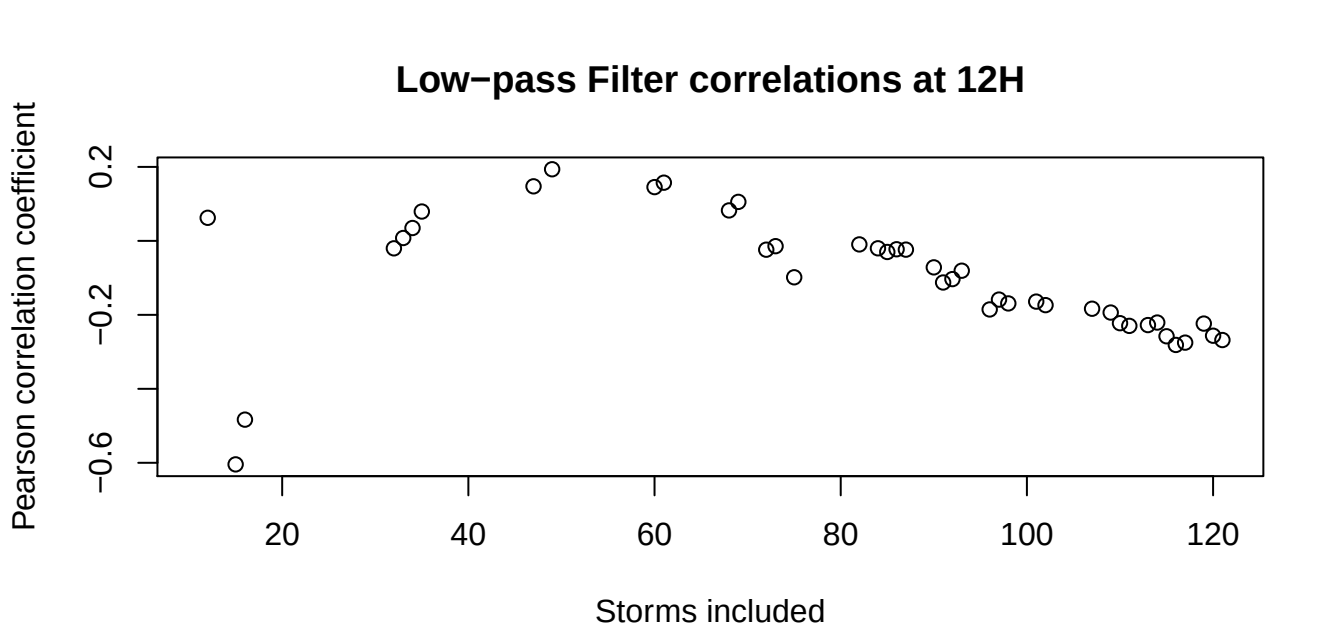
Low−pass Filter correlations at 12H
Pearson correlation coefficient
0.2
−0.2
−0.6
20
40
60
80
100
120
Storms included

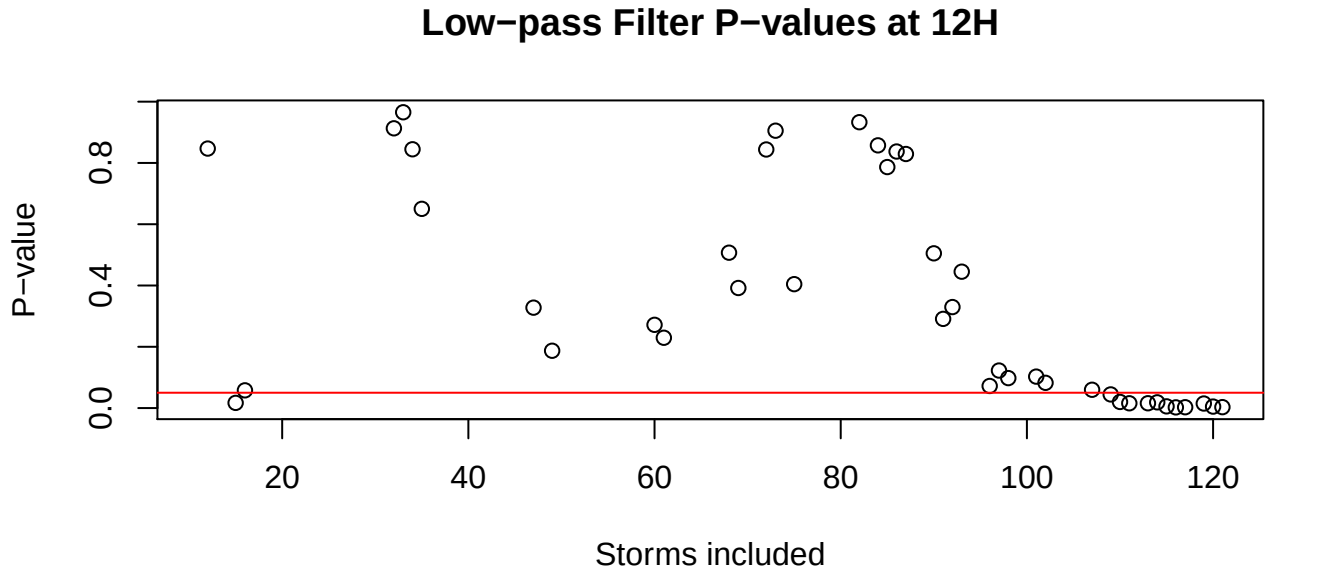
Low−pass Filter P−values at 12H
P−value
0.0
0.4
0.8
20
40
60
80
100
120
Storms included

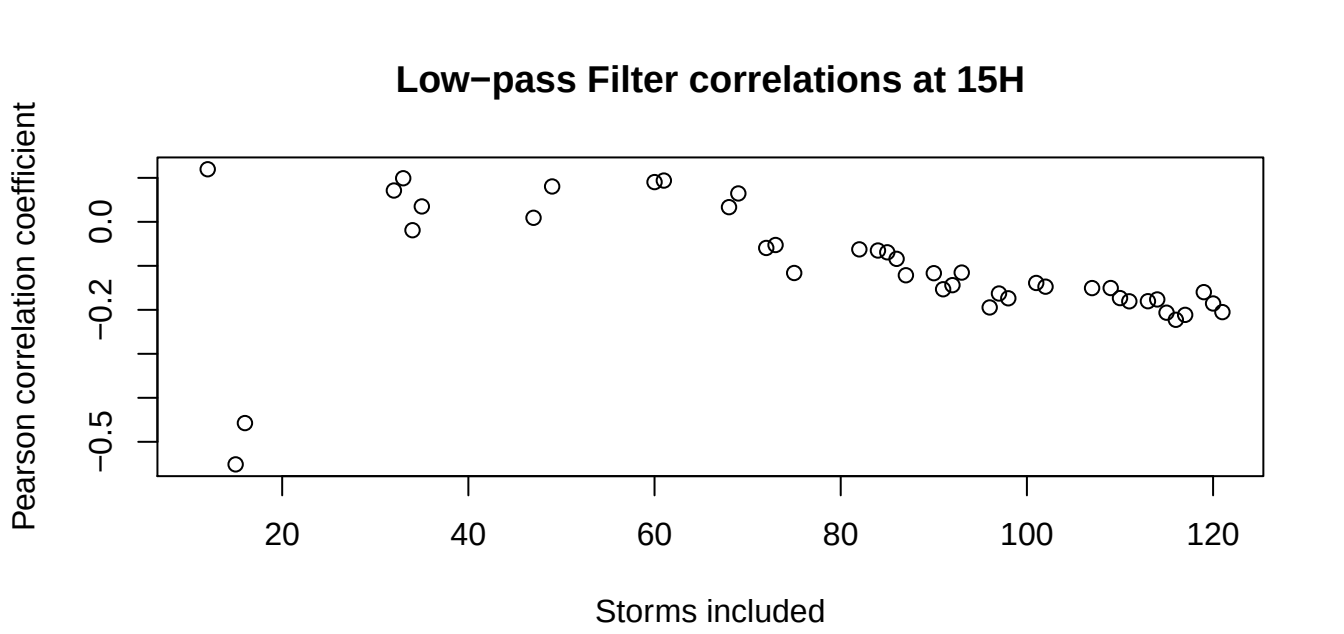
Low−pass Filter correlations at 15H
Pearson correlation coefficient
−0.5
−0.2
0.0
20
40
60
80
100
120
Storms included

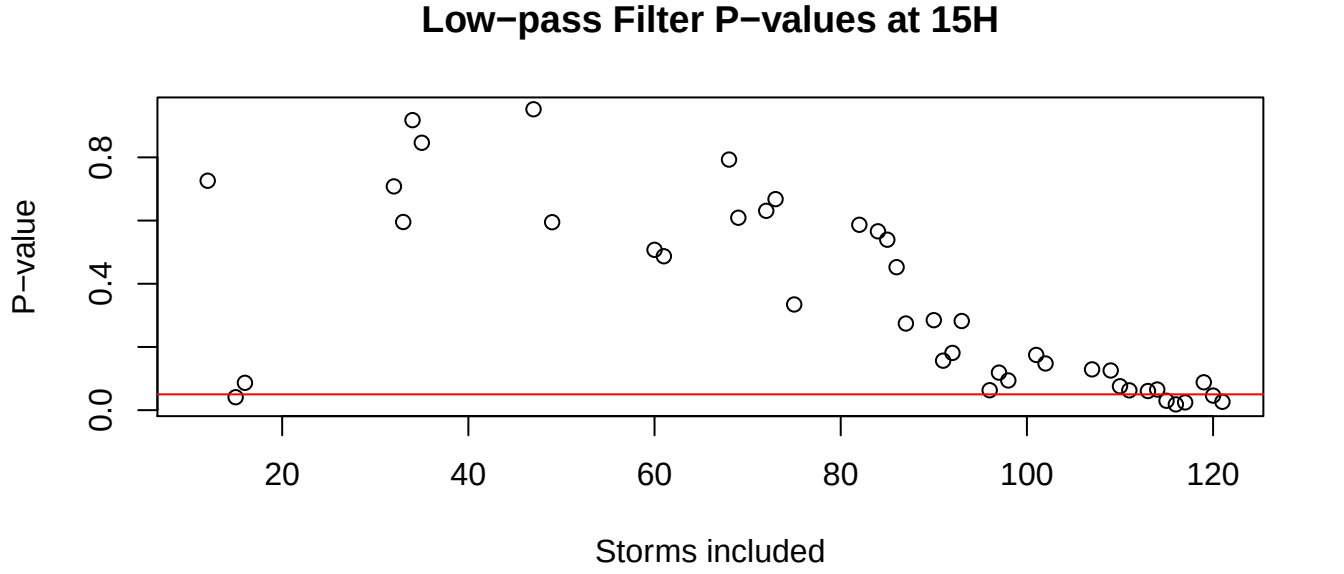
Low−pass Filter P−values at 15H
P−value
0.0
0.4
0.8
20
40
60
80
100
120
Storms included

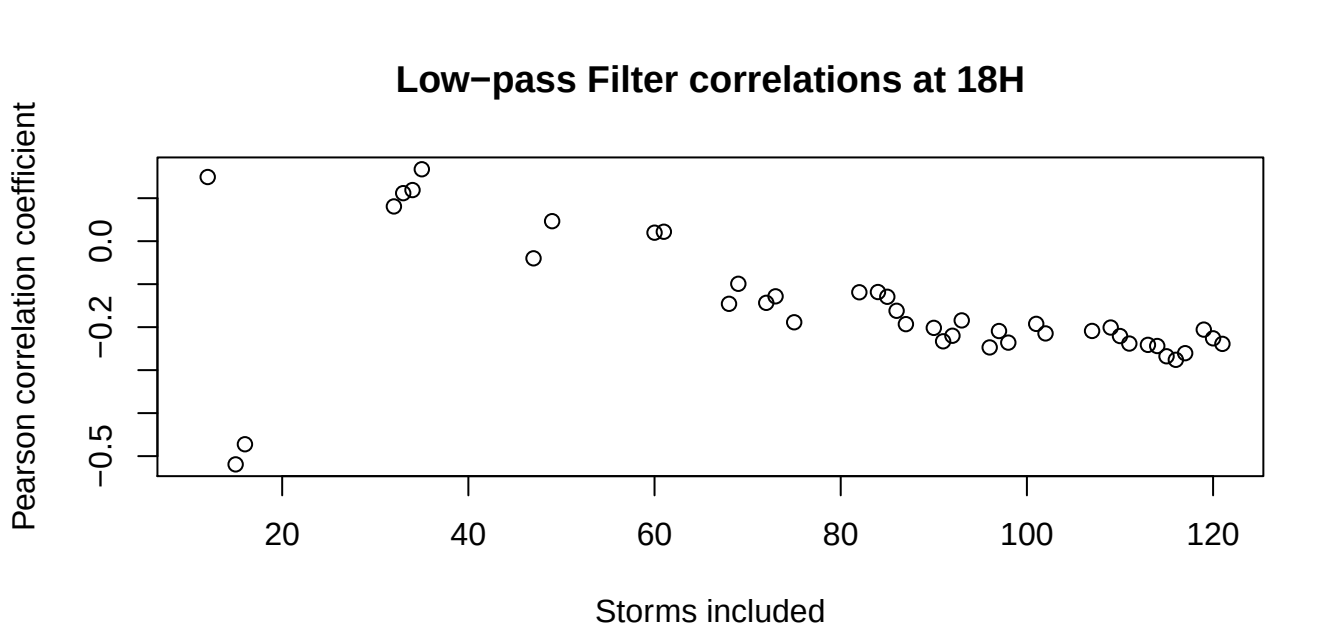
Low−pass Filter correlations at 18H
Pearson correlation coefficient
−0.5
−0.2
0.0
20
40
60
80
100
120
Storms included

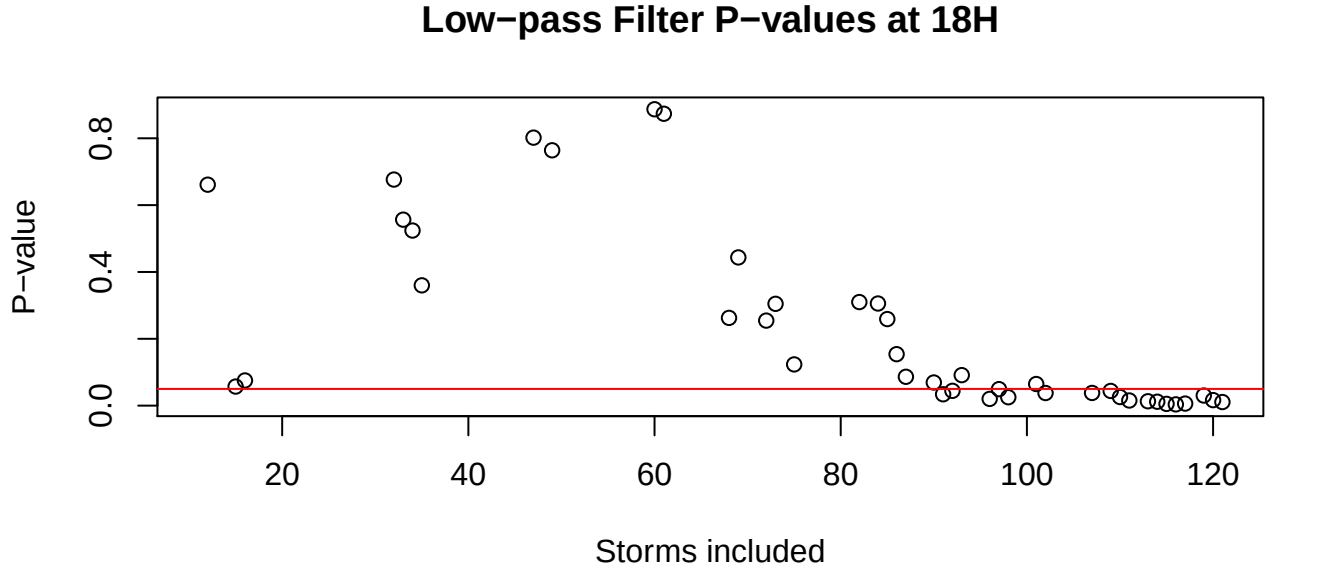
Low−pass Filter P−values at 18H
P−value
0.0
0.4
0.8
20
40
60
80
100
120
Storms included

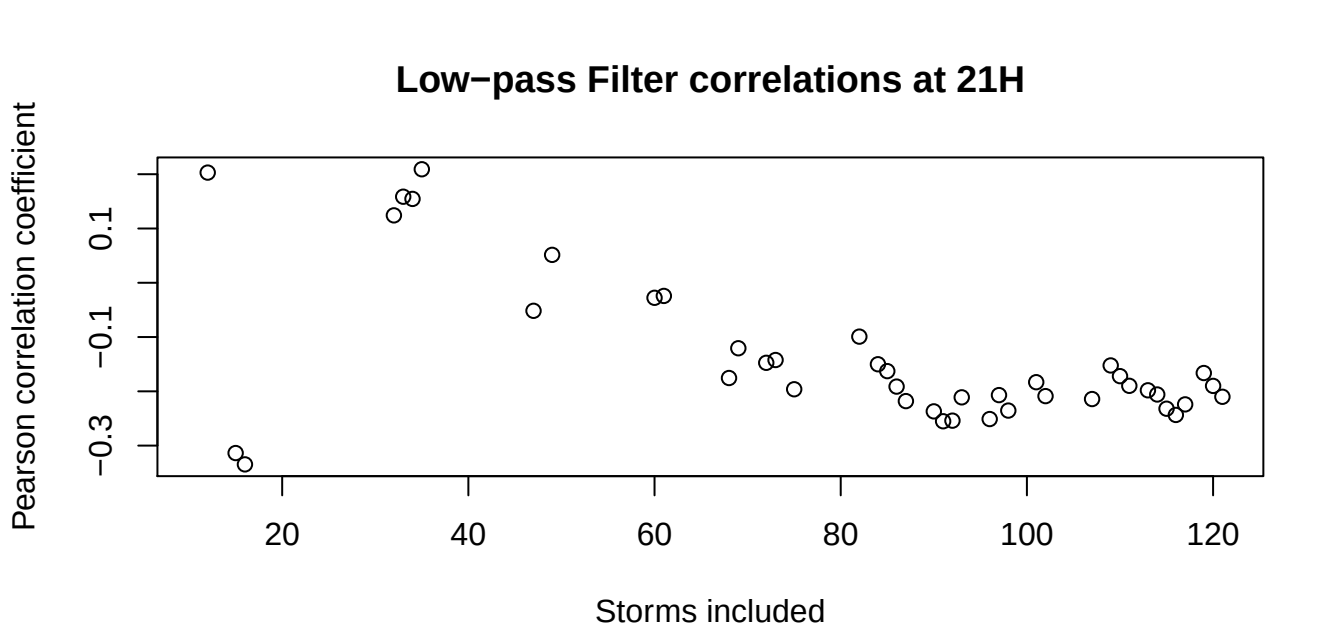
Low−pass Filter correlations at 21H
Pearson correlation coefficient
0.1
−0.1
−0.3
20
40
60
80
100
120
Storms included

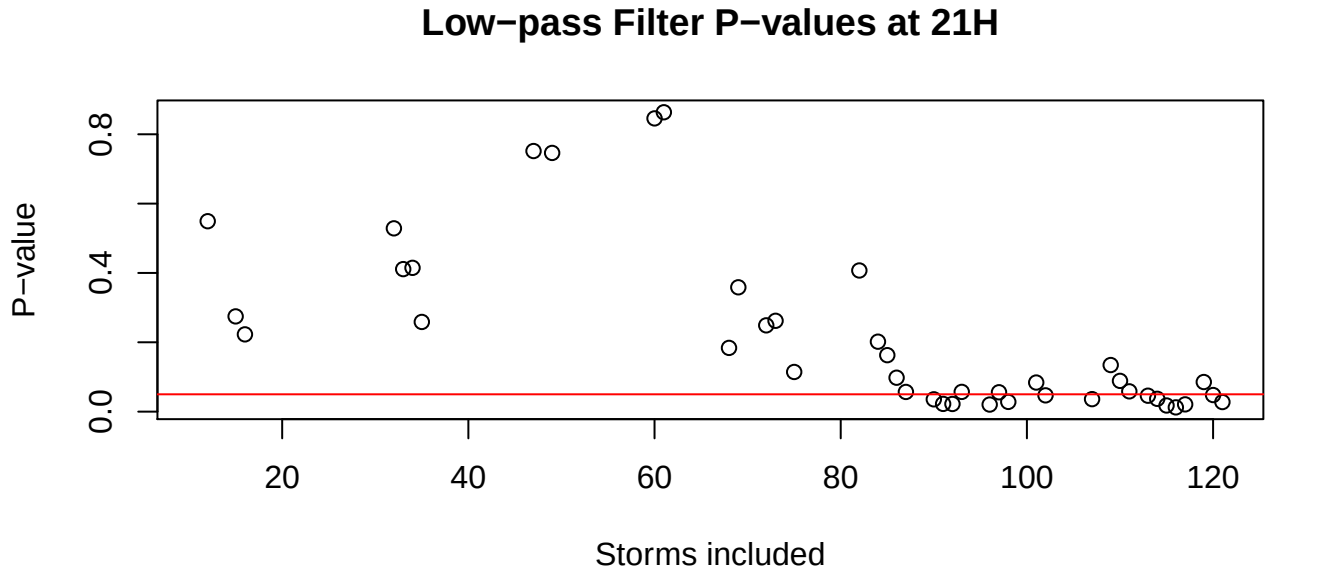
Low−pass Filter P−values at 21H
P−value
0.8
0.4
0.0
20
40
60
80
100
120
Storms included

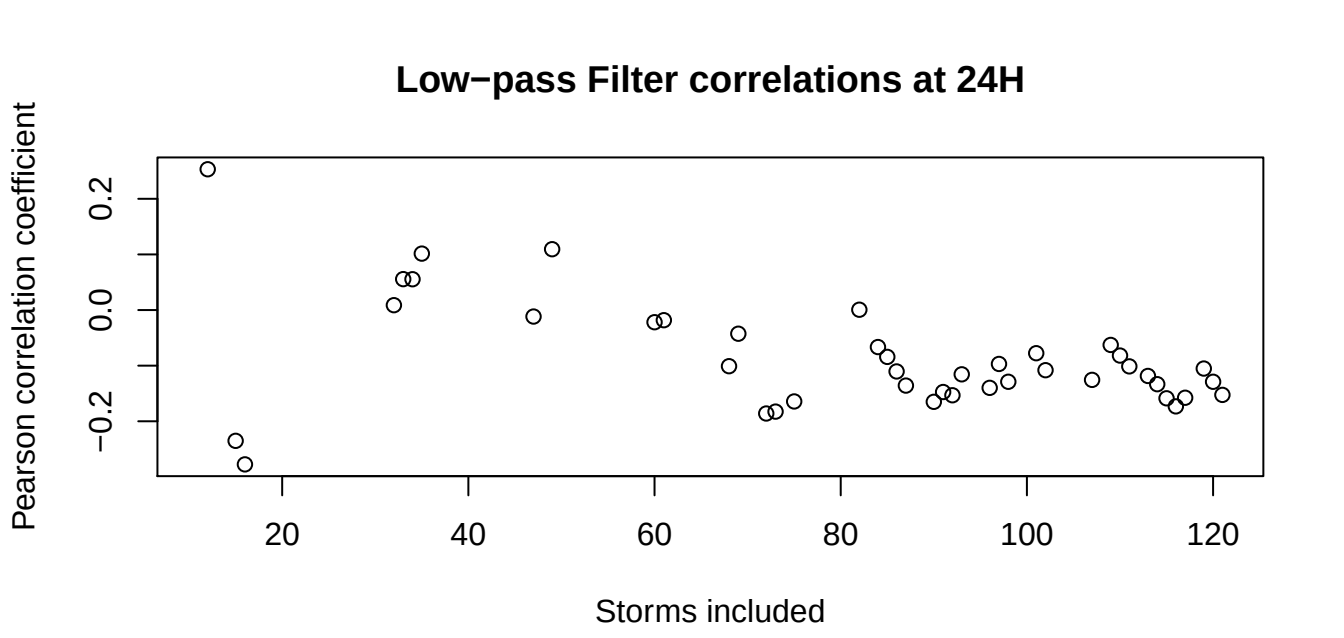
Low−pass Filter correlations at 24H
Pearson correlation coefficient
−0.2
0.0
0.2
20
40
60
80
100
120
Storms included

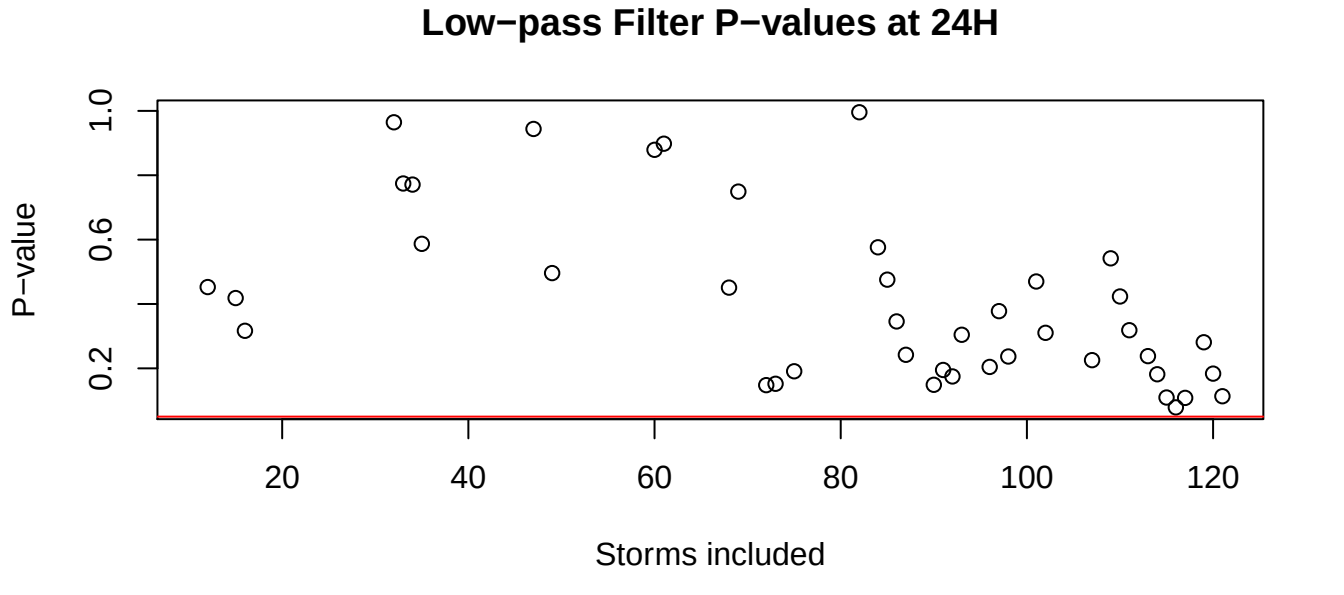
Low−pass Filter P−values at 24H
P−value
0.2
0.6
1.0
20
40
60
80
100
120
Storms included

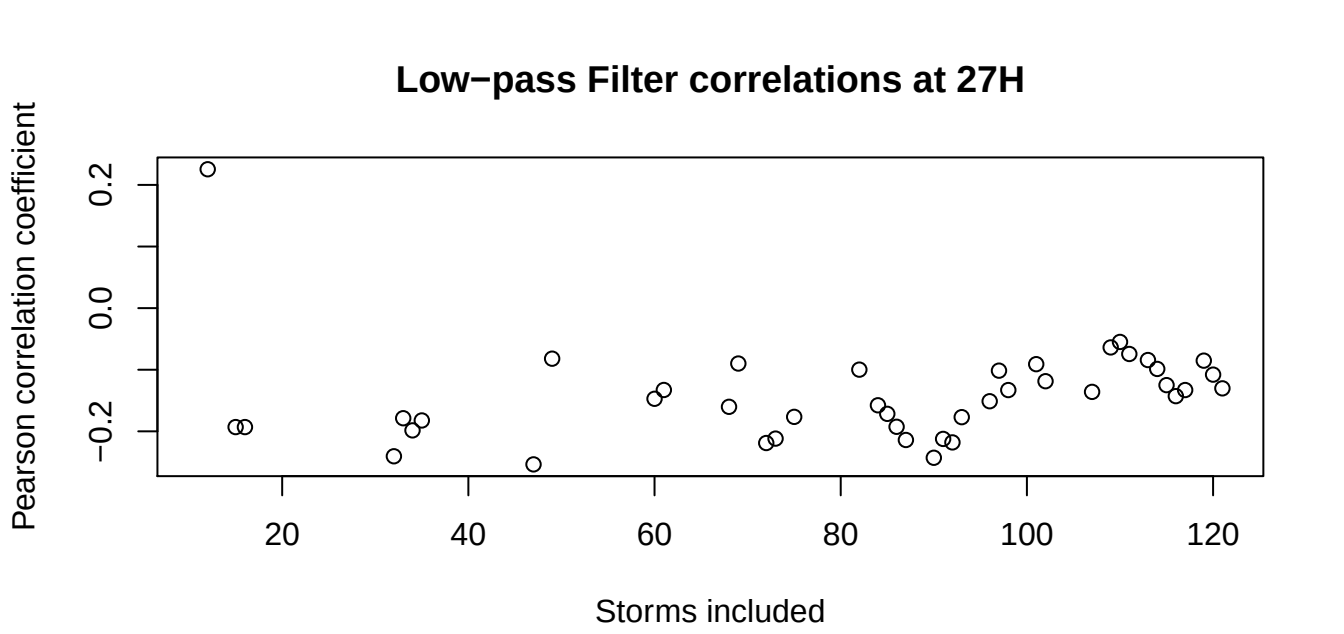
Low−pass Filter correlations at 27H
Pearson correlation coefficient
−0.2
0.0
0.2
20
40
60
80
100
120
Storms included

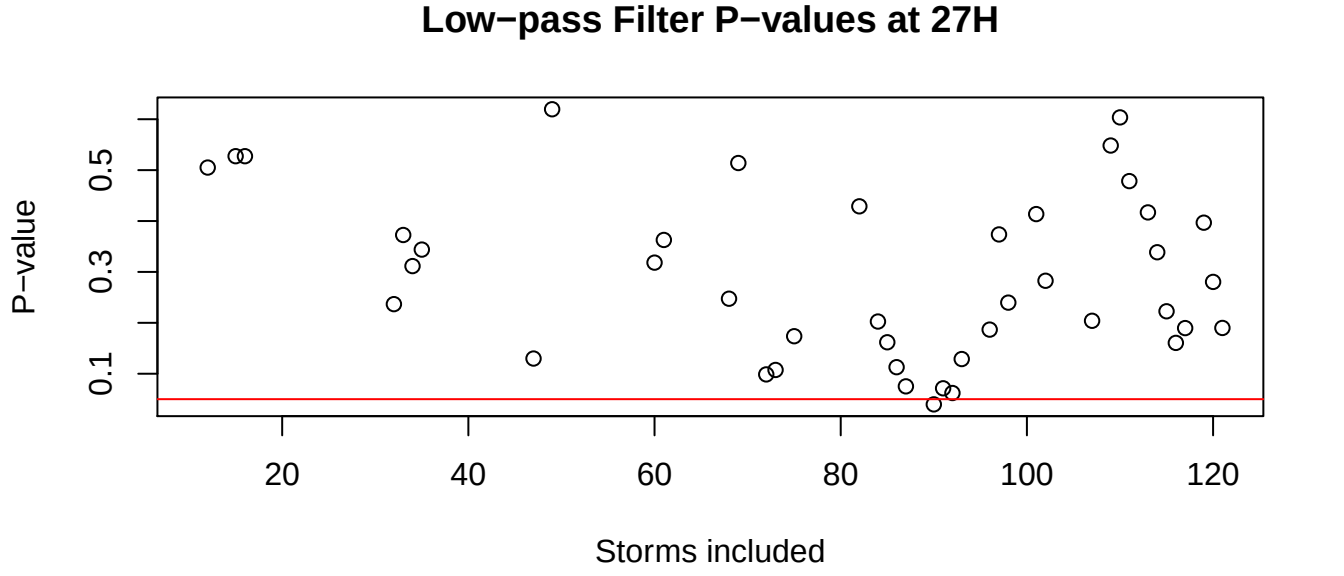
Low−pass Filter P−values at 27H
P−value
0.1
0.3
0.5
20
40
60
80
100
120
Storms included

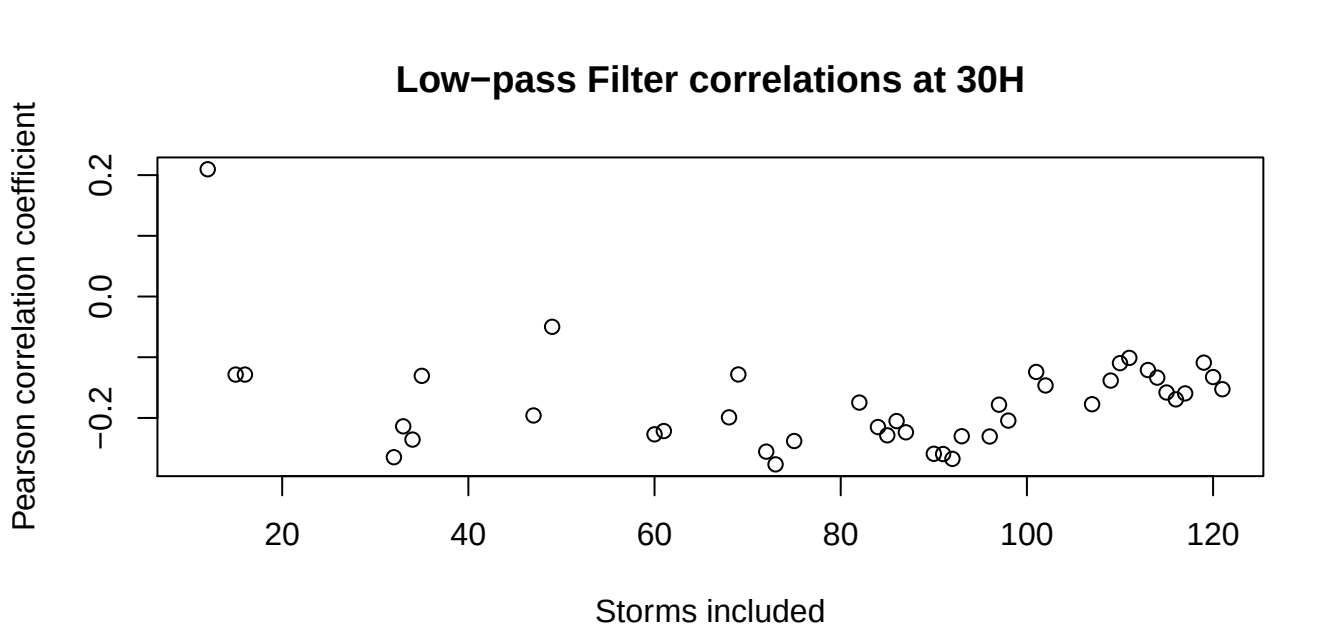
Low−pass Filter correlations at 30H
Pearson correlation coefficient
0.2
0.0
−0.2
20
40
60
80
100
120
Storms included

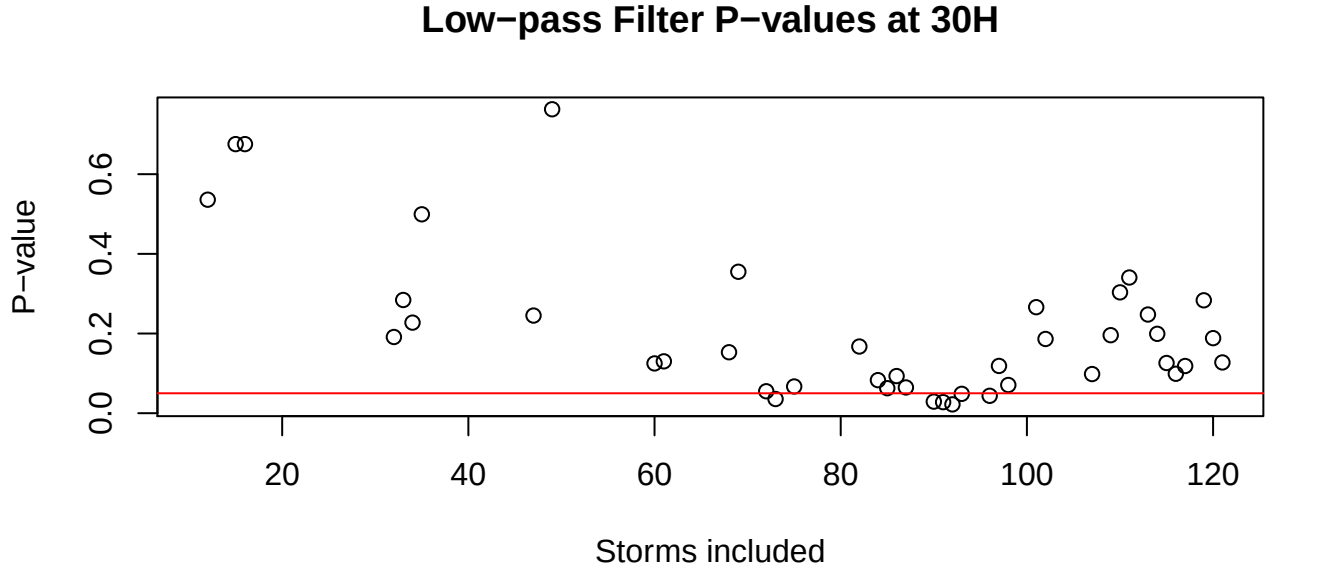
Low−pass Filter P−values at 30H
P−value
0.0
0.2
0.4
0.6
20
40
60
80
100
120
Storms included

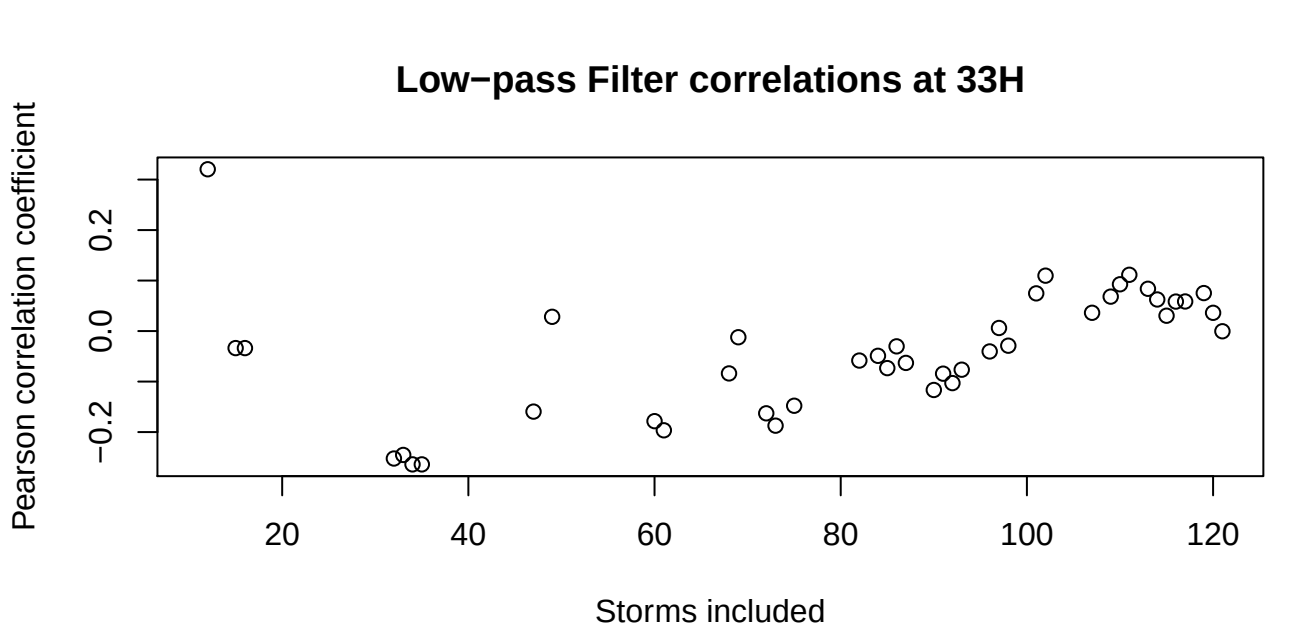
Low−pass Filter correlations at 33H
Pearson correlation coefficient
−0.2
0.0
0.2
20
40
60
80
100
120
Storms included

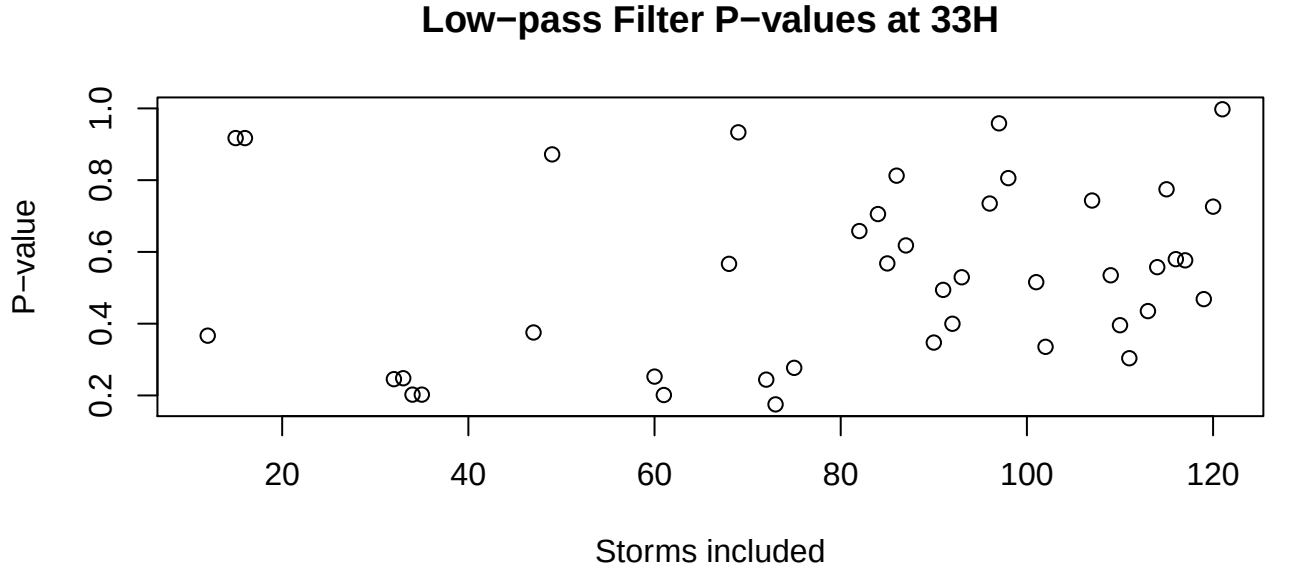
Low−pass Filter P−values at 33H
P−value
0.2
0.4
0.6
0.8
1.0
20
40
60
80
100
120
Storms included

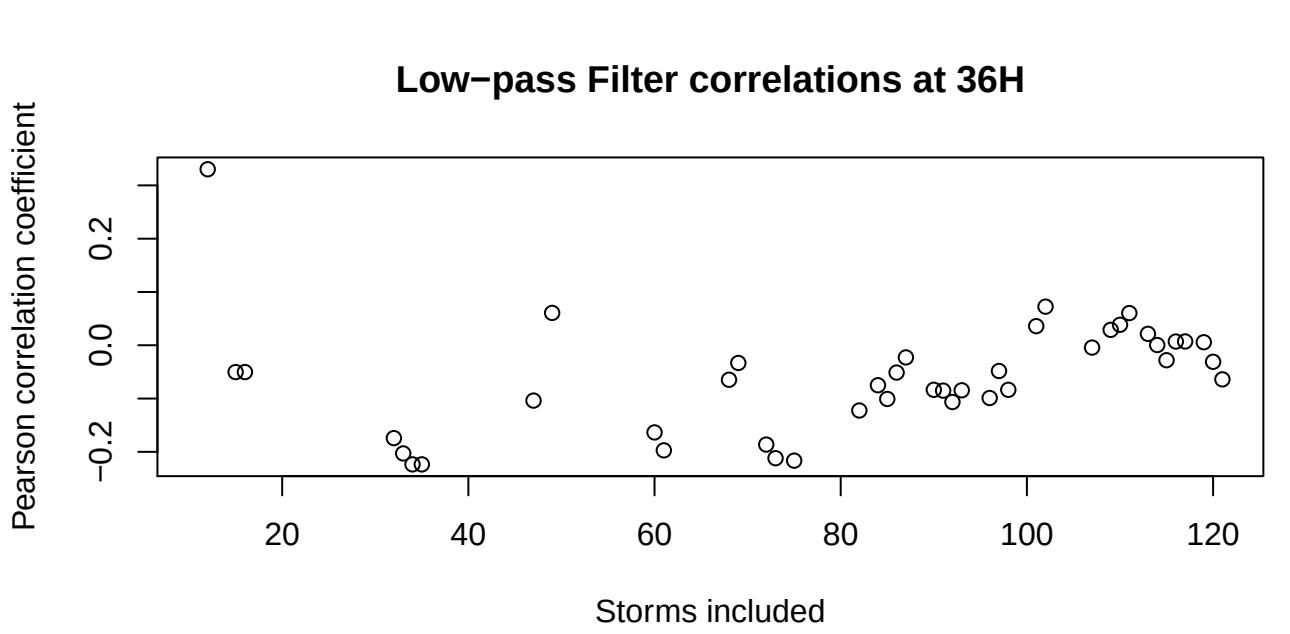
Low−pass Filter correlations at 36H
Pearson correlation coefficient
−0.2
0.0
0.2
20
40
60
80
100
120
Storms included

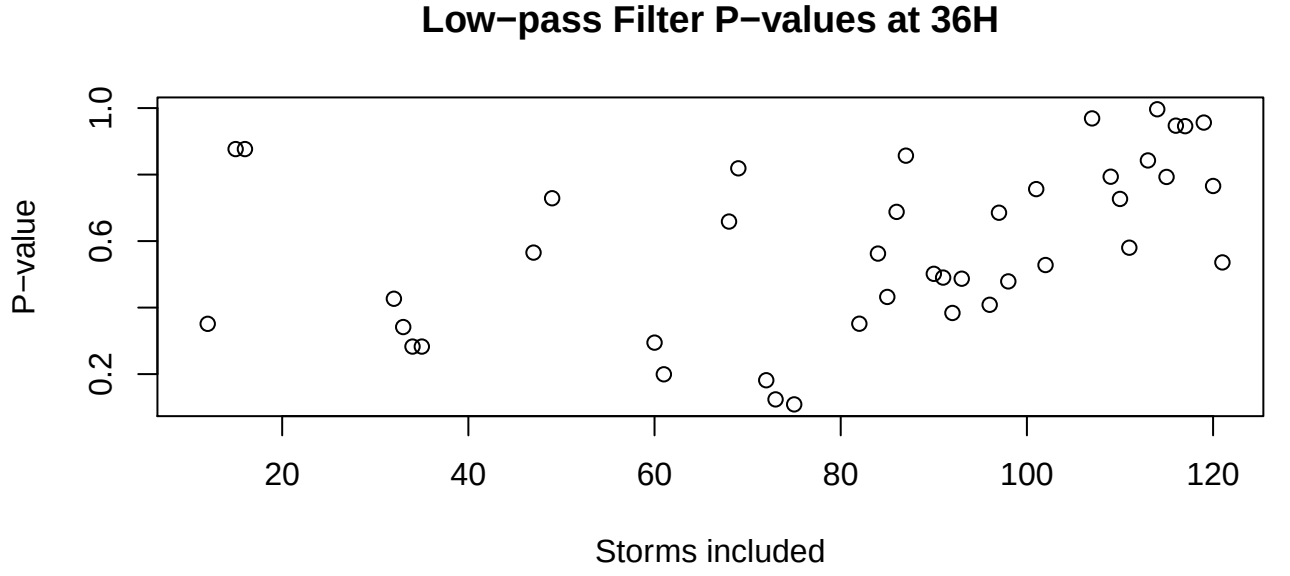
Low−pass Filter P−values at 36H
P−value
0.2
0.6
1.0
20
40
60
80
100
120
Storms included

# OPTIMAL CUTOFF DEPTH GRAPH AND STATISTICS

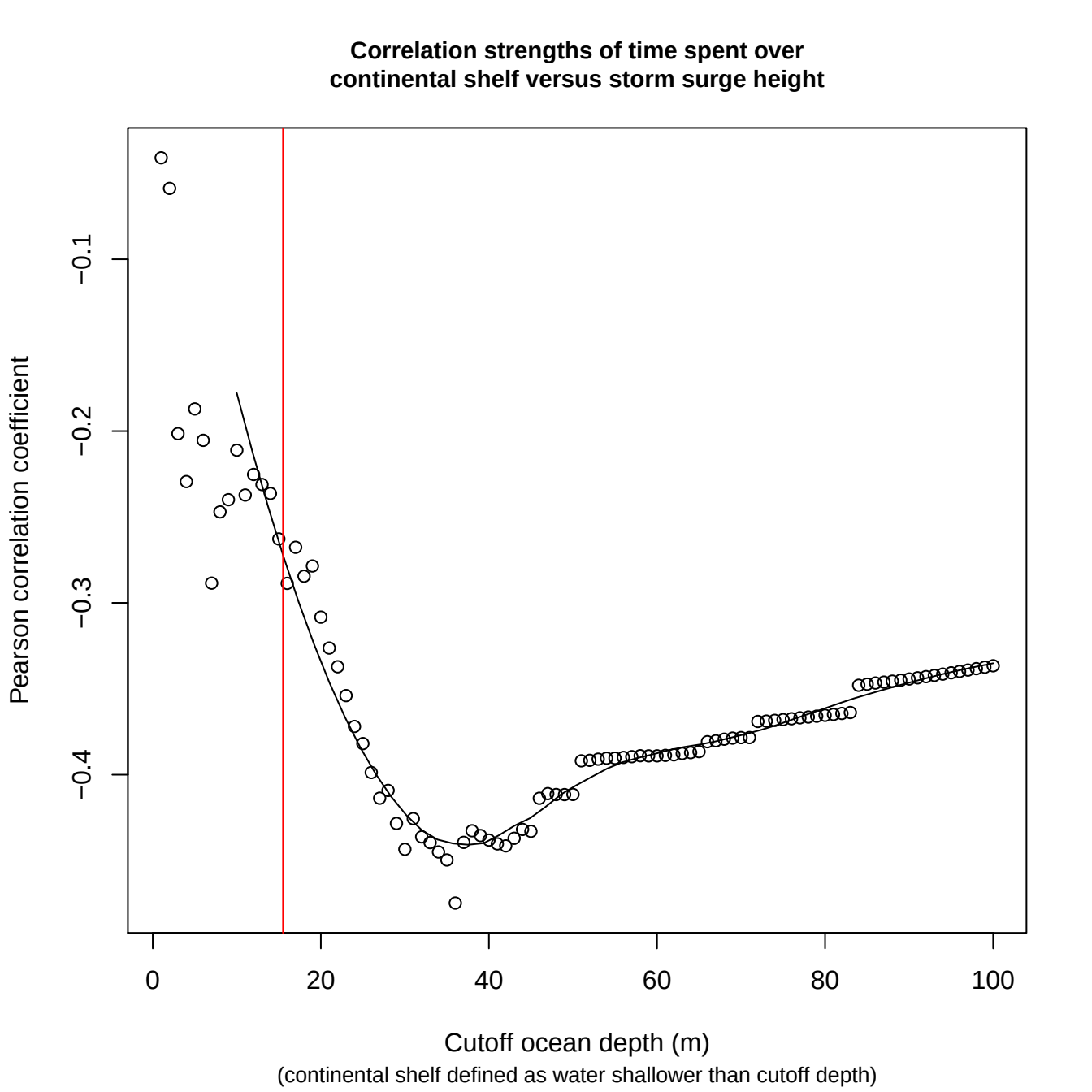
Correlation strengths of time spent over
continental shelf versus storm surge height
Pearson correlation coefficient
−0.1
−0.2
−0.3
−0.4
0
20
40
60
80
100
Cutoff ocean depth (m)
(continental shelf defined as water shallower than cutoff depth)

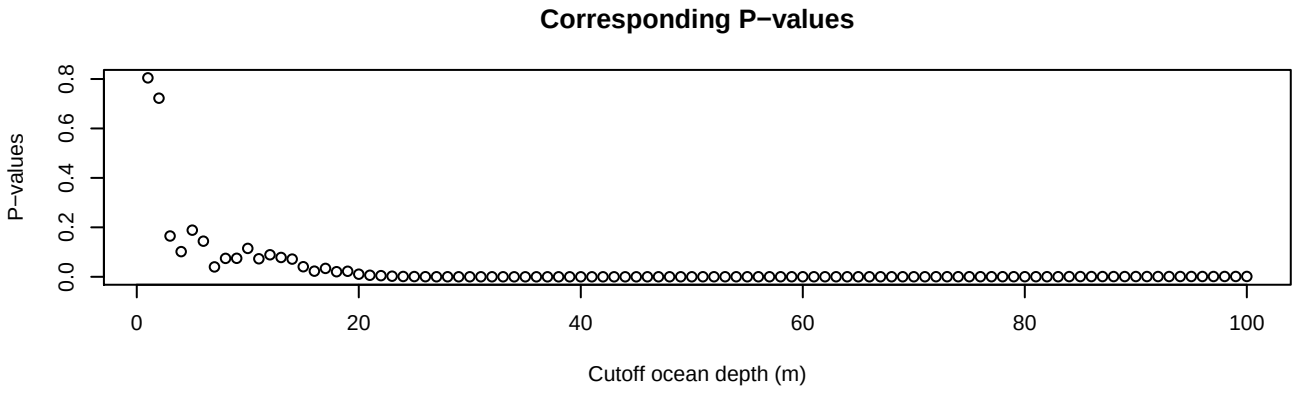
Corresponding P−values
P−values
0.0
0.2
0.4
0.6
0.8
0
20
40
60
80
100
Cutoff ocean depth (m)

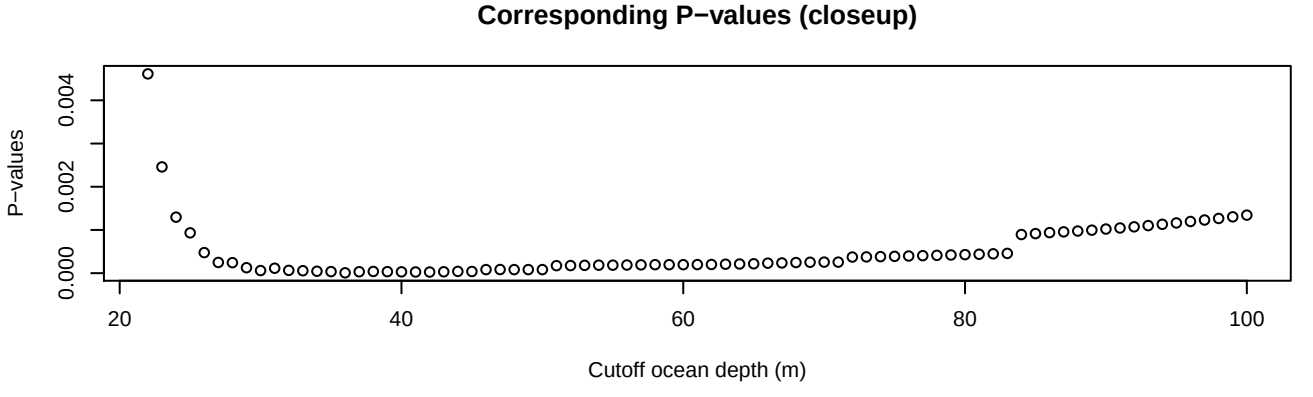
Corresponding P−values (closeup)
P−values
0.000
0.002
0.004
20
40
60
80
100
Cutoff ocean depth (m)

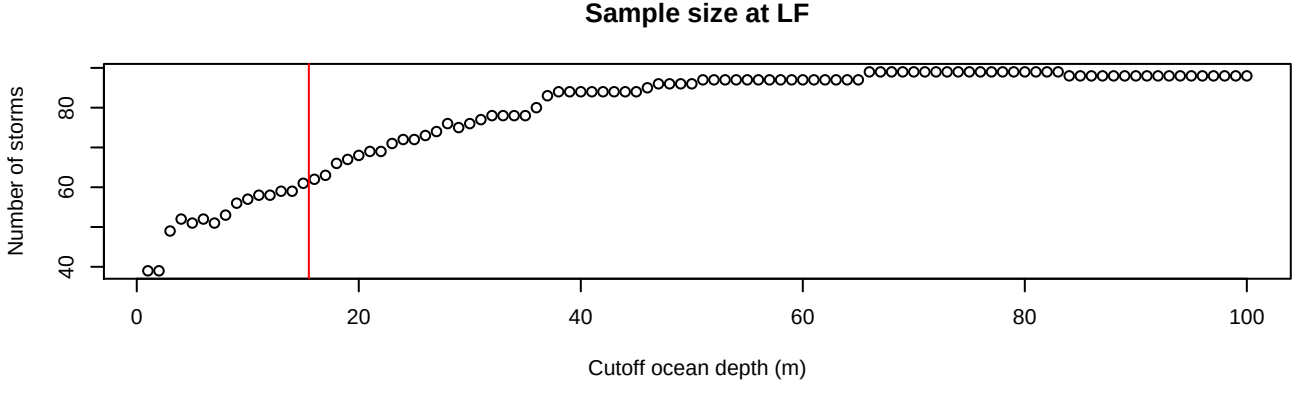
Sample size at LF
Number of storms
40
60
80
0
20
40
60
80
100
Cutoff ocean depth (m)

# CUTOFF DEPTH GRAPHS USING DIFFERENT MAPS

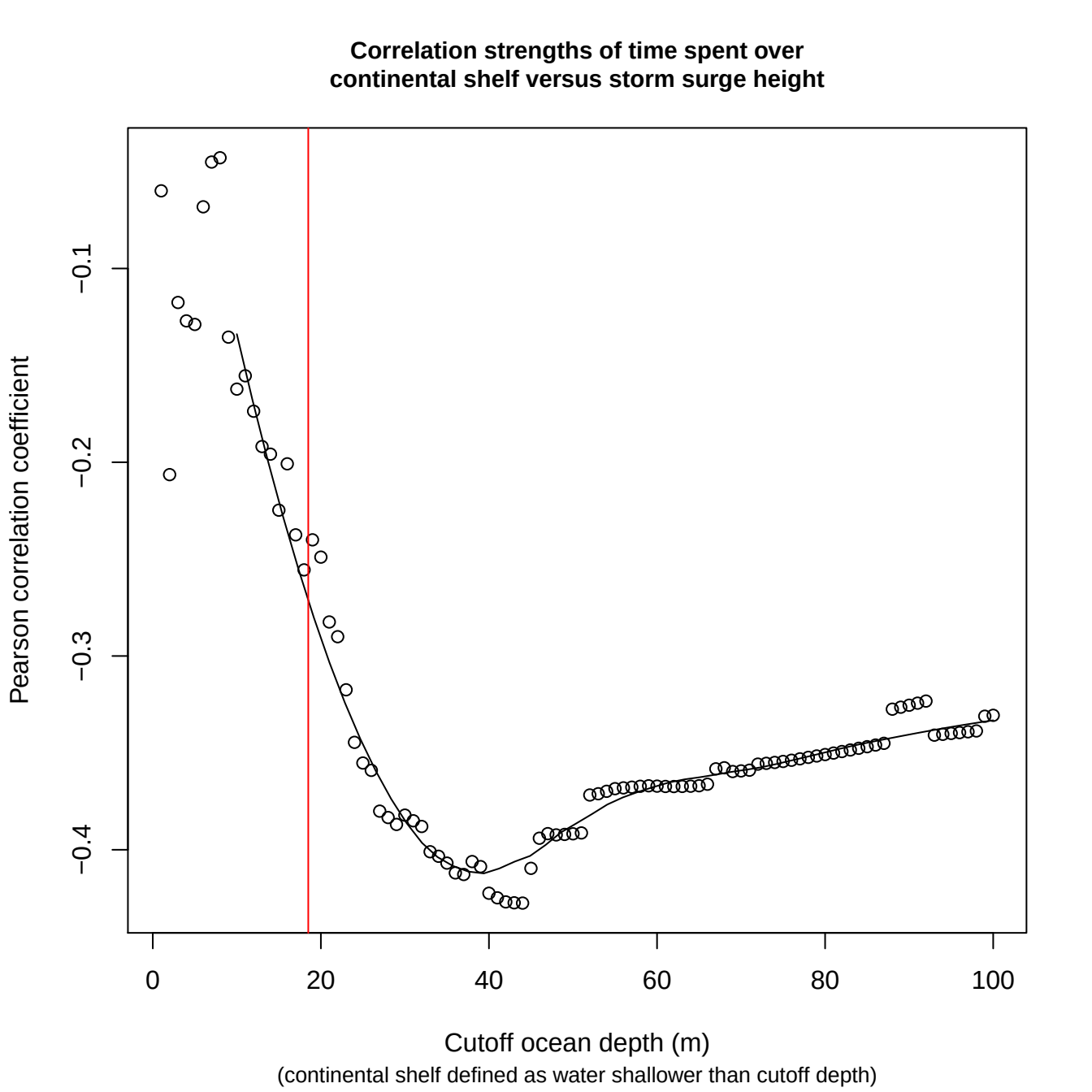
Correlation strengths of time spent over
continental shelf versus storm surge height
Pearson correlation coefficient
−0.1
−0.2
−0.3
−0.4
0
20
40
60
80
100
Cutoff ocean depth (m)
(continental shelf defined as water shallower than cutoff depth)

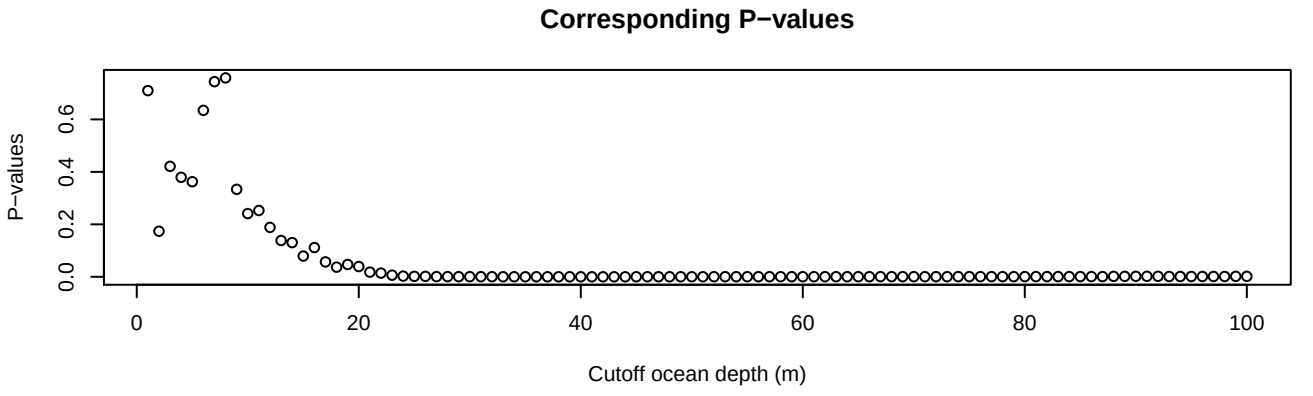
Corresponding P−values
P−values
0.0
0.2
0.4
0.6
0
20
40
60
80
100
Cutoff ocean depth (m)

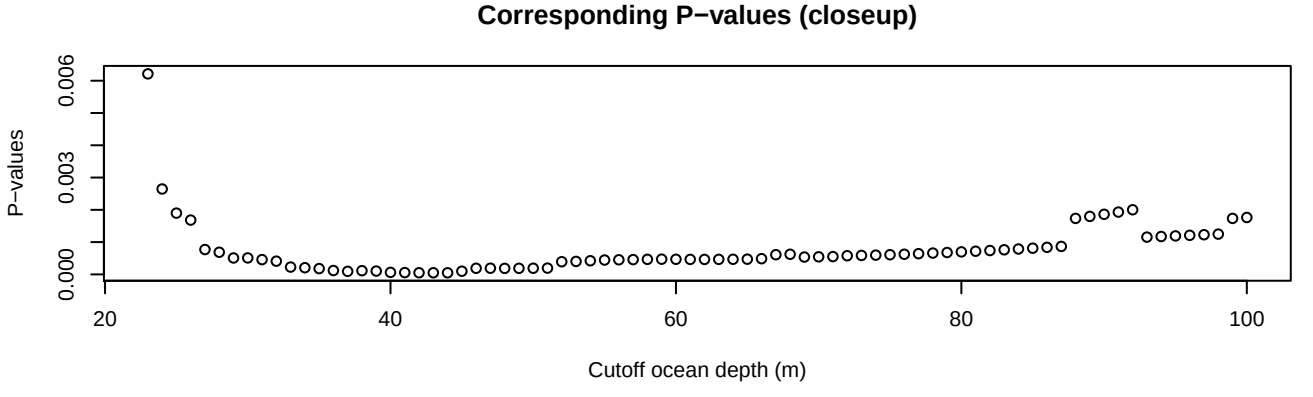
Corresponding P−values (closeup)
P−values
0.000
0.003
0.006
20
40
60
80
100
Cutoff ocean depth (m)

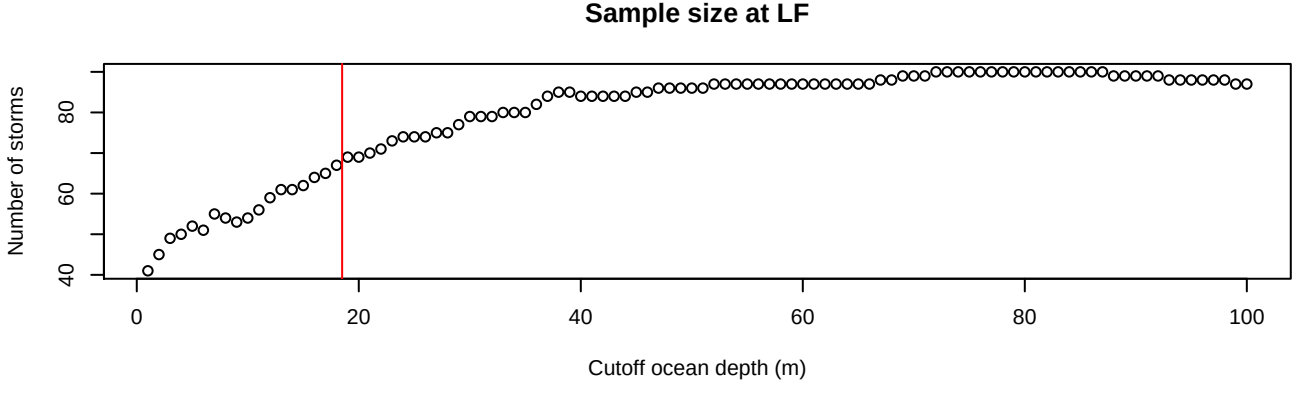
Sample size at LF
Number of storms
40
60
80
0
20
40
60
80
100
Cutoff ocean depth (m)

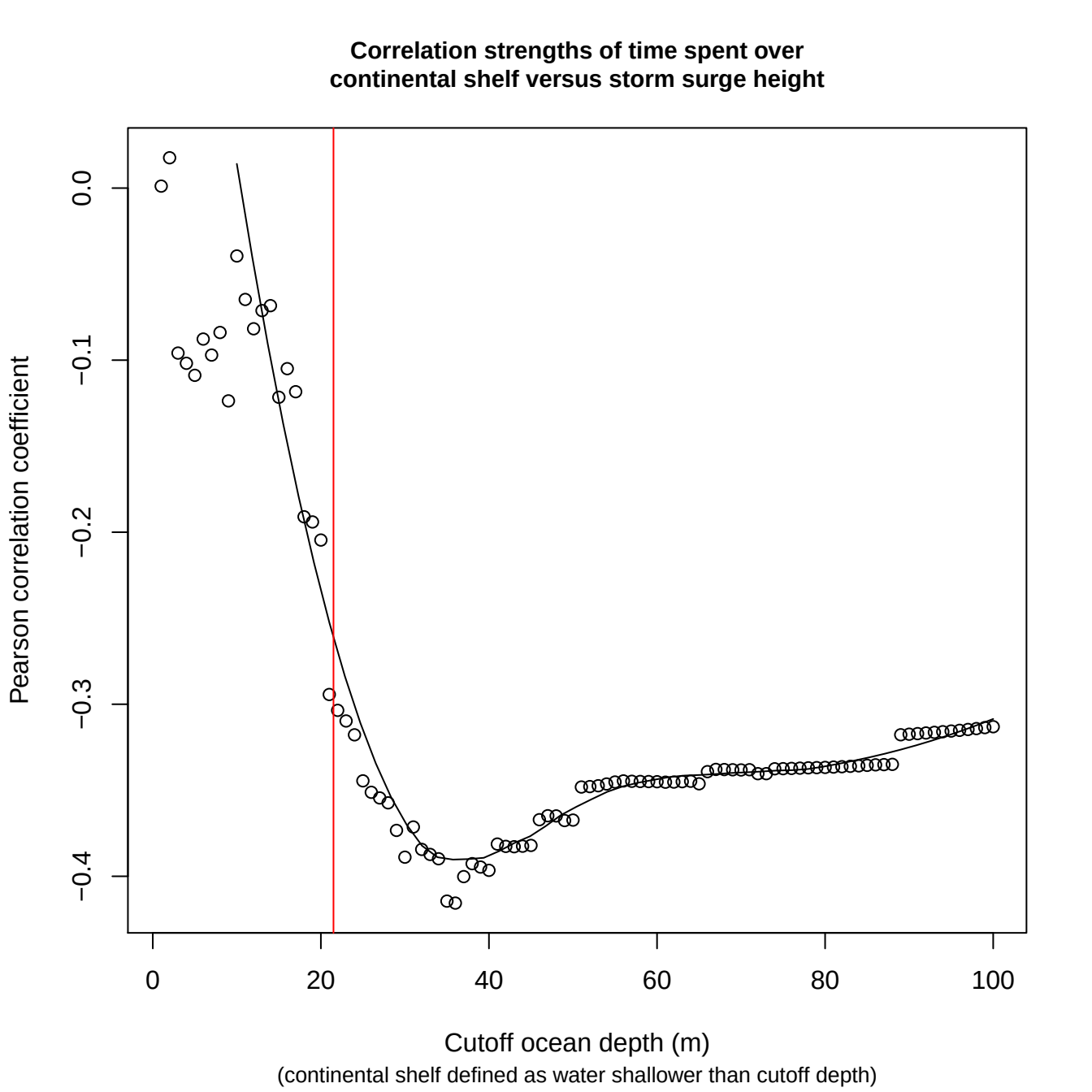
Correlation strengths of time spent over
continental shelf versus storm surge height
Pearson correlation coefficient
0.0
−0.1
−0.2
−0.3
−0.4
0
20
40
60
80
100
Cutoff ocean depth (m)
(continental shelf defined as water shallower than cutoff depth)

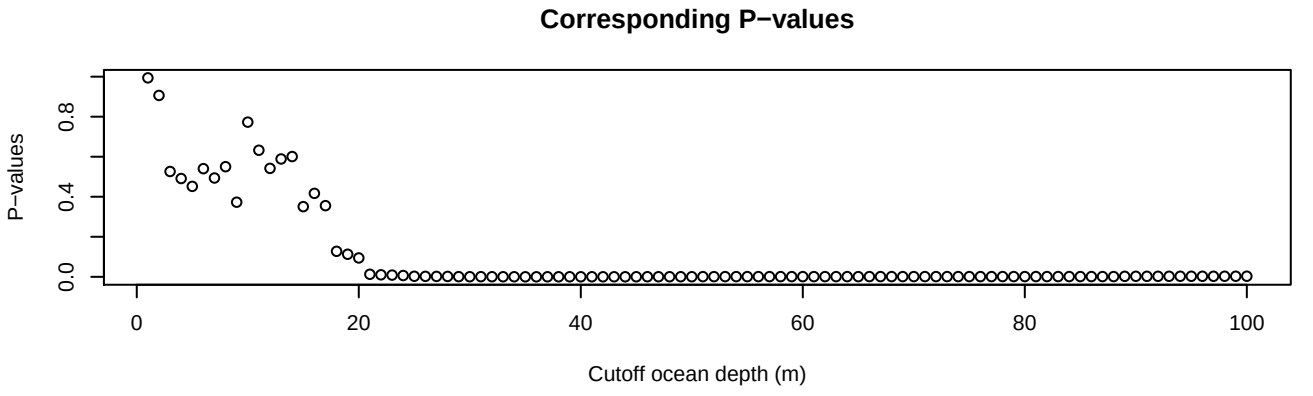
Corresponding P−values
P−values
0.0
0.4
0.8
0
20
40
60
80
100
Cutoff ocean depth (m)

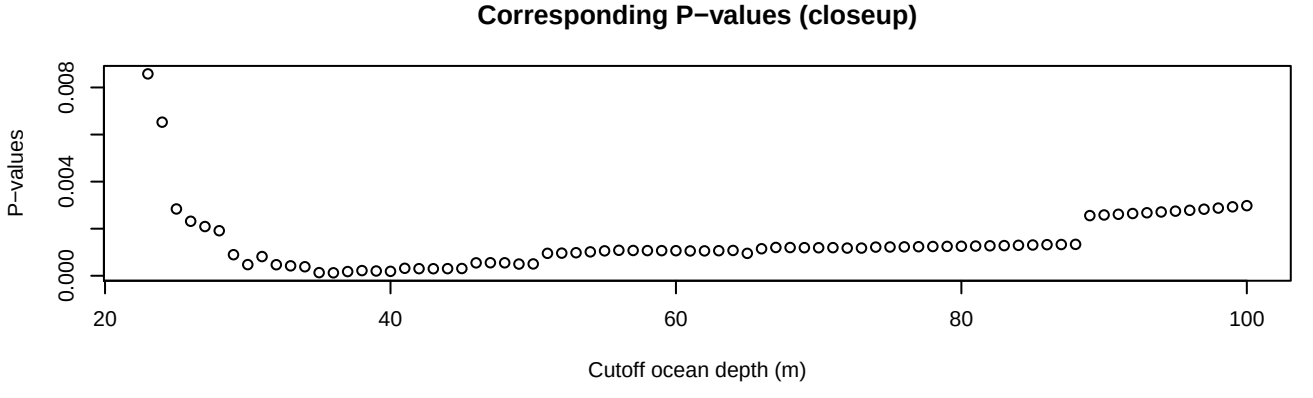
Corresponding P−values (closeup)
P−values
0.000
0.004
0.008
20
40
60
80
100
Cutoff ocean depth (m)

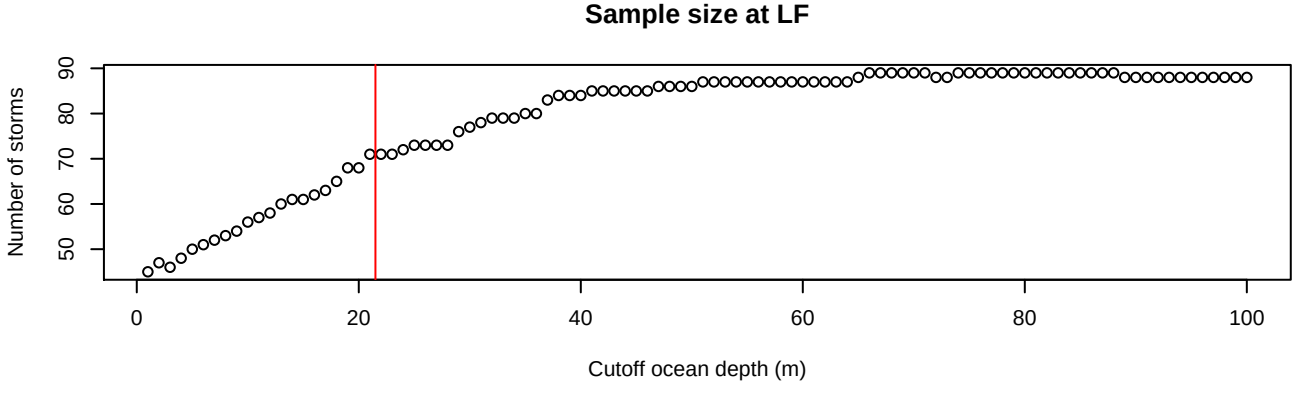
Sample size at LF
Number of storms
50
60
70
80
90
0
20
40
60
80
100
Cutoff ocean depth (m)

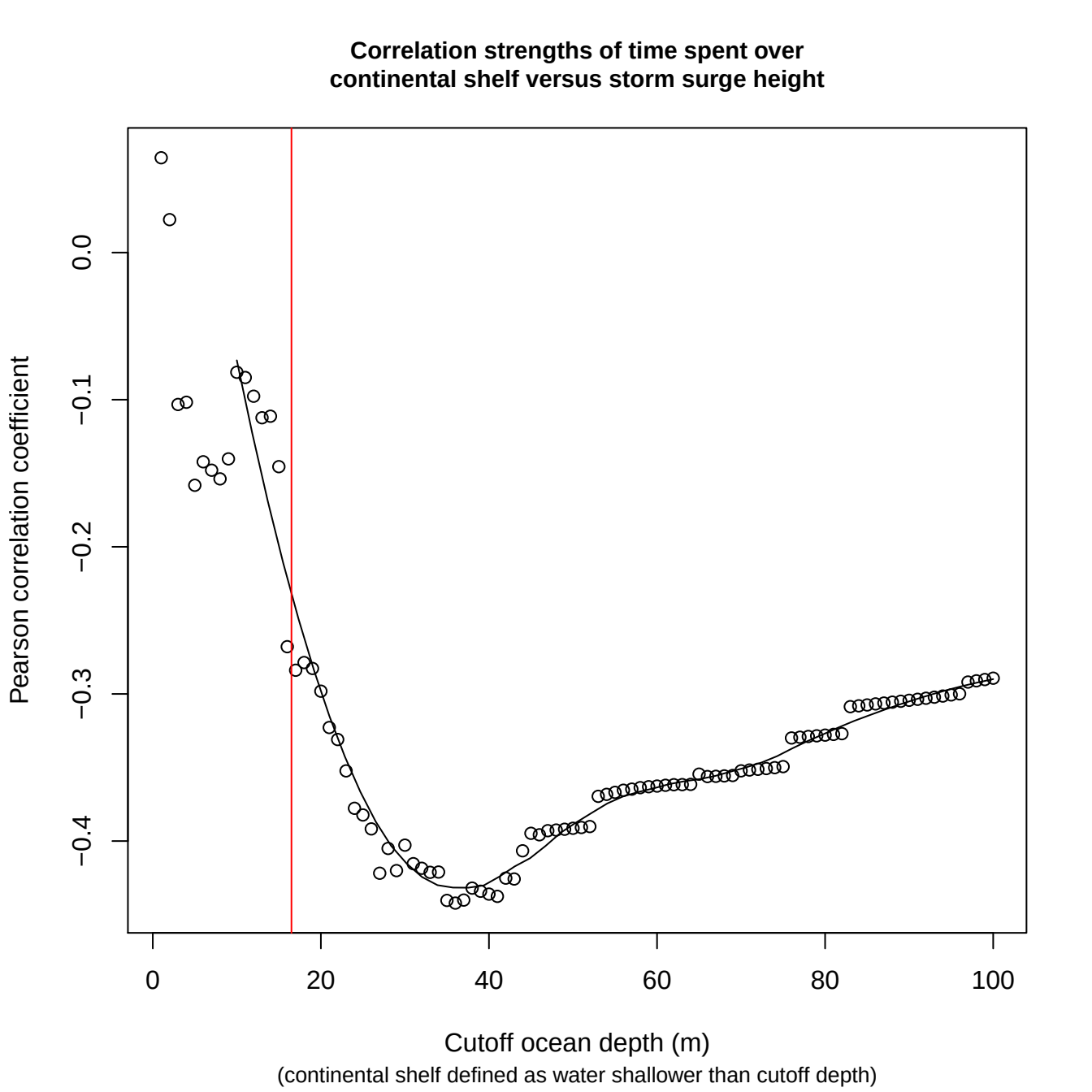
Correlation strengths of time spent over
continental shelf versus storm surge height
Pearson correlation coefficient
0.0
−0.1
−0.2
−0.3
−0.4
0
20
40
60
80
100
Cutoff ocean depth (m)
(continental shelf defined as water shallower than cutoff depth)

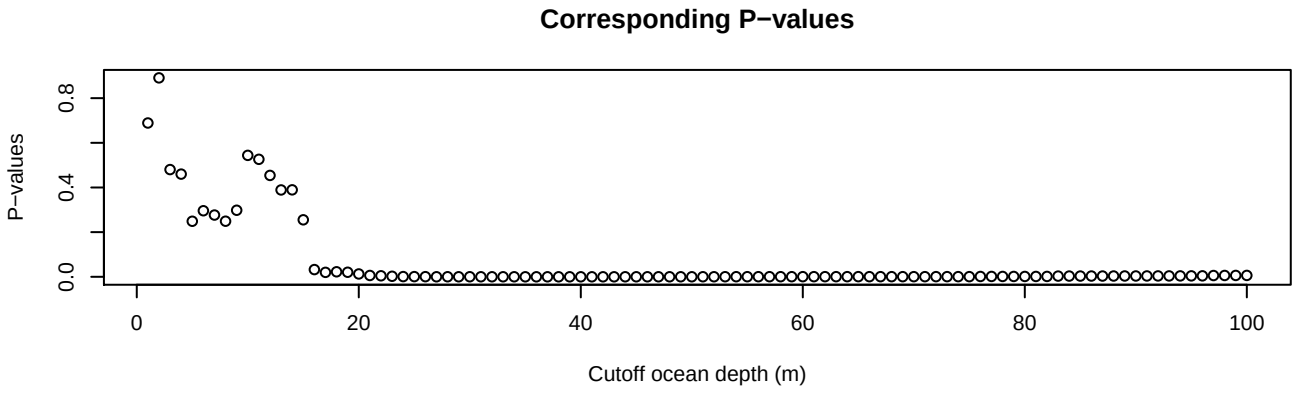
Corresponding P−values
P−values
0.0
0.4
0.8
0
20
40
60
80
100
Cutoff ocean depth (m)

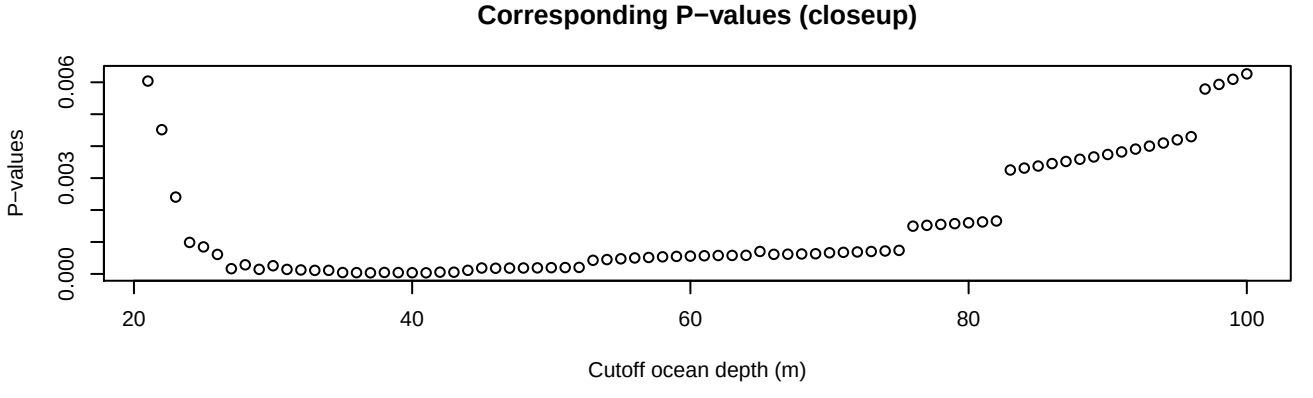
Corresponding P−values (closeup)
P−values
0.000
0.003
0.006
20
40
60
80
100
Cutoff ocean depth (m)

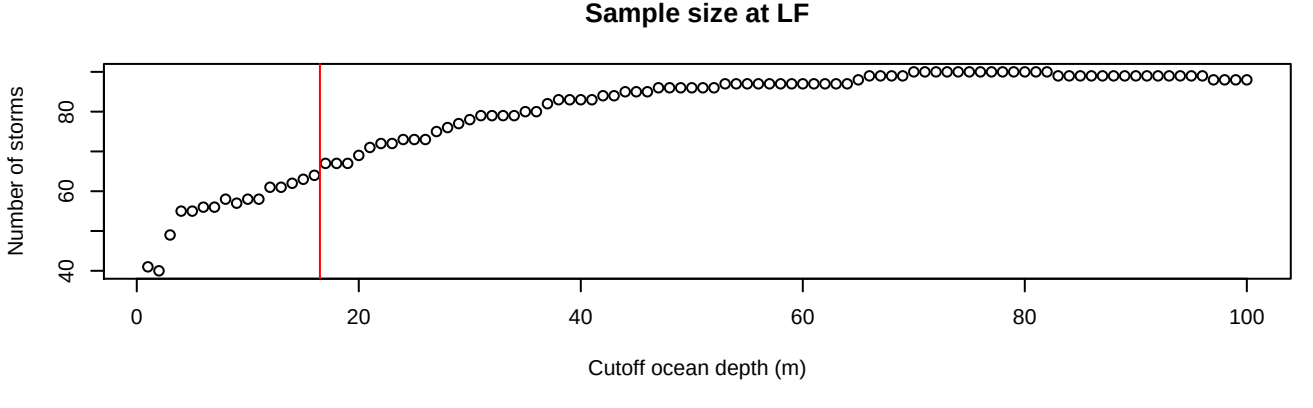
Sample size at LF
Number of storms
40
60
80
0
20
40
60
80
100
Cutoff ocean depth (m)